THE BIOCHEMICAL STUDY IN TUMOR NECROSIS FACTOR-ALPHA-MEDIATED CYTOTOXICITY

By

Ko Samuel, B. Sc. (Hons.), CUHK

A Thesis Submitted in Partial Fulfilment

of the requirement for the degree of

Master of Philosophy

in the Department of Biochemistry

The Chinese University of Hong Kong

June, 1998

Acknowledgements

I would like to thank my supervisor, Prof. S. K. Kong, for his guidance and supervision throughout the project. Without his creative idea, all the work would not be successful.

I also would like to thank Mr. M. C. S. Wong and Ms. J. M. Y. Lai for their help in cell culture techniques. I am grateful to Mr. Y. K. Suen for his kind guidance in flow cytometry technique. Moreover, without the help from Ms. K. Y. Lam, agarose gel electrophoresis would not be complete.

I wish to thank Prof. T. T. Kwok, Prof. K. P. Fung and Prof. H. K. Cheng for providing me the TNF resistant cell lines.

Finally, thanks are also extended to my friends in BMSB room 316 and 310 for their friendship and support.

Abbreviations

%	Percent / Percentage
°C	Degree Celsius
$\Delta\psi_m$	Mitochondrial Membrane Potential
$[Ca^{2+}]_i$	Intracellular Free Calcium Concentration
$[Ca^{2+}]_m$	Mitochondrial Free Calcium Concentration
$[Ca^{2+}]_n$	Nuclear Free Calcium Concentration
1,2-DAG	1,2-Diacylglycerol
4-OH-TEMPO	4-Hydroxy-2,2,6,6-Tetramethylpiperidine-1-oxyl
ADP	Adenosine Diphosphate
AM	Acetoxymethyl
AMD	Actionmycin D
ATP	Adenosine Triphosphate
BAPTA/AM	[1,2-bi(2)aminophenoxy]ethane-N,N,N^1,N^1-tetraacetic, acetoxymethyl ester
BCG	Bacillus Calmette-Guerin
Bcl-2	B-cell leukemia/lymphoma-2 gene
b.p.	Base Pair
Ca^{2+}	Calcium Ions
cAMP	Cyclic Adenosine Monophosphate
cDNA	Complementary Deoxyribonucleic Acid
CLSM	Confocal Laser Scanning Microscopy
$cPLA_2$	Cytosolic Phospholipase A_2
Cu/ZnSOD	Copper/Zinc Dependent Superoxide Dismutase
cyt c	Cytochrome c
DCF	2',7'-Dichlorofluorescin Diacetate
DCFH	2',7'-Dichlorofluorescin
DED	Death Effector Domain
DMSO	Dimethylsuphoxide

DNA	Deoxyribonucleic Acid
DNP	2,4-Dinitrophenol
EDTA	Ethylenediaminetetraacetic acid
EGTA	Ethylene glycol-bis(β-aminoethyl ether) N,N,N',N'-tetraacetic acid
ER	Endoplasmic Reticulum
EtBr	Ethdium Bromide
EtOH	Ethanol
expt	Experiment
F	Fluorescence Intensity
FADD	Fas-Associating Protein with Death Domain
FBS	Fetal Bovine Serum
FCM	Flow Cytometry
FSC	Forward Scatter
H_2O_2	Hydrogen Peroxide
HE	Hydroethidine
HEPES	N-[2-hydroxyethyl]piperazine-N'-[2-ethanesulfonic acid]
HLA	Human Leukocyte Antigen
hr	Hour
HuTNF	Human Tumor Necrosis Factor
IFN	Interferon
IL	Interleukin
IP	Inositol Monophosphate
IP_2	Inositol Bisphosphate
IP_3	Inositol Trisphosphate
IP_4	Phosphoinositol 1,3,4,5-tetrakisphosphate
kDa	Kilodalton
LiCl	Lithium Chloride
LPS	Lipopolysaccharide
LT	Lymphotoxin

M phase	Mitotic Phase
μg	Microgram
mg	Milligram
min	Minute
μl	Microliter
ml	Milliliter
μM	Micromolar
mM	Millimolar
MnSOD	Manganese Dependent Superoxide Dismutase
mRNA	Messenger Ribonucleic Acid
mtDNA	Mitochondrial Deoxyribonucleic Acid
MTT	3-[4,5-dimethylthiazol-2-yl]-2,5-diphenyltetrazolium bromide
MuTNF	Murine Tumor Nerosis Factor
mV	Millivolt
n	Number
NAc	N-Acetyl-L-Cysteine
NADH	Reduced form of Nicotinamide Adenine Dinucleotide
Neutral red	3-amino-7-dimethylamino-2-methyl-phenazine hydrochloride
NFκB	Nuclear Factor κB
ng	Nanogram
NH_4Cl	Ammonium Chloride
nm	Nanometer
nM	Nanomolar
$O_2^{\bullet -}$	Superoxide Radical
O.D.	Optical Density
p	P Value
PBS	Phosphate Buffered Saline
PC-PLC	Phosphatidylcholine-Specific Phospholipase C

PCR	Polymerase Chain Reaction
PDE	Phosphodiesterase
PI	Propidium iodide
PIP_2	Phosphatidylinositol 4,5-Bisphosphate
PKA	Protein Kinase A
PKC	Protein Kinase C
PLA_2	Phospholipase A_2
PMA	4-β-phorbol-1, 2β-myristate-13α-acetate
PMT	Photomultiplier Tube
Q	Ubiquinone
R	Region
r.p.m.	Revolution Per Minute
rHuTNF	Recombinant Human Tumor Necrosis Factor
RIP	Receptor Interacting Protein
rL929	Resistant L929
rMuTNF	Recombinant Murine Tumor Necrosis Factor
RNaseA	Ribonuclease A
ROS	Reactive Oxygen Species
RPMI-1640	Roswell Park Memorial Institute tissue culture medium 1640
S.D.	Standard Deviation
SDS	Sodium Dodecyl Sulfate
sec	Second
SM	Sphingomyelin
SMase	Sphingomyelinase
SNARF-1/AM	Carboxy-seminaphthorhodafluor-1, Acetoxymethyl Ester
SSC	Side Scatter
sTNFR	Soluble Tumor Necrosis Factor Receptor
TCA Cycle	Tricarboxylic Acid Cycle
TG	Thapsigargin

Thimersol	Sodium Ethylmercurithio-Salicylate
TNF	Tumor Necrosis Factor
TRADD	Tumor Necrosis Factor Receptor 1-Associated Death Domain Protein
TRAF2	Tumor Necrosis Factor-Associated Factor 2
TTFA	4,4,4-trifluoro-1-[2-thienyl]-1,2-butanedione
U	Unit
UV	Ultraviolet
v/v	Volume by Volume
w/v	Weight by Volume

Abstract

Tumor necrosis factor-alpha (TNF) is one of the pleiotropic cytokines that is primarily produced by activated macrophages and lymphocytes. It elicits a wide range of immunological events such as fever, inflammation and tumor killing. Recently, it was found that TNF increased the release of reactive oxygen species (ROS) such as superoxide radical ($O_2\bullet^-$) and hydrogen peroxide (H_2O_2) inside the cells. Moreover, some findings indicate that TNF produces the increase in the intracellular free calcium concentration ($[Ca^{2+}]_i$).

High concentration of ROS induces lipid peroxidation and DNA damage. High $[Ca^{2+}]$ inside the cell activates phospholipases, proteases and/or endonucleases. In this connection, ROS and Ca^{2+} have been suggested to be the messengers that lead to a form of cell death known as apoptosis. However, the relationship between ROS and Ca^{2+} is still unknown. Therefore, the objective of my research project is to investigate the role and the relationship between the ROS and Ca^{2+} in the TNF-mediated cytotoxicity in a TNF-sensitive cell line, L929 cells. Techniques such as agarose gel electrophoresis, confocal laser scanning microscopy, flow cytometry and cytotoxicity assay were applied.

Results from my experiments indicate that TNF induces DNA fragmentation, a hallmark of apoptosis, as observed by agarose gel electrophoresis. Moreover, in the cell cycle study with flow cytometry, TNF produced a hypodiploid peak next to the G0/G1 phase suggesting the presence of apoptotic cells and apoptotic bodies. On the other hand,

TNF caused a slow rise in ROS and $[Ca^{2+}]_i$ in L929 cells. The release of ROS could be suppressed by enzymatic antioxidants such as catalase or manganese dependent superoxide dismutase (MnSOD), and the non-enzymatic antioxidants such as N-acetylcysteine or 4-hydroxy-TEMPO. Application of mitochondrial electron transport chain inhibitors such as rotenone and antimycin A indicates that TNF caused the release of ROS from the mitochondria mainly at the ubiquinone site (complex III). The use of dinitrophenol indicates that the TNF-mediated cell death was an energy dependent process. Application of antioxidants and mitochondrial electron transport chain inhibitors could suppress or enhance the TNF-mediated cytotoxicity.

Similar to the ROS formation, TNF did not produce an immediate increase but a slow rise of $[Ca^{2+}]_i$ in L929 cells. This was confirmed by the use of thapsigargin, an ATPase inhibitor. In the presence of thapsigargin, the $[Ca^{2+}]_i$ was significant increased by TNF. Addition of calcium-inducing agent such as thimerosal produced a higher TNF-mediated cytotoxicity. In contrast, application of calcium chelator such as BAPTA/AM suppressed both the redox rate and the cytotoxicity in TNF-treated cells. In the experiments with the use of mitochondrial Ca^{2+} cycling inhibitors such as ruthenium red and diltiazem, the possible source of Ca^{2+} for the TNF-effect was found to be mitochondria. These results suggest that $[Ca^{2+}]_i$ might induce the release of ROS in TNF-treated L929 cells.

In addition, TNF did not change the intracellular pH in the early phase of treatment. Moreover, there was no change in the mitochondrial membrane potential ($\Delta\psi_m$) in TNF-treated L929 cells.

The differences between TNF-sensitive cell line L929 and TNF-resistant cell lines, rL929, rL929-11E and rL929-4F were also examined. It was found that (1) TNF induced cytotoxicity in the sensitive cell line but not in the resistant cell lines; (2) TNF induced apoptosis in L929 cells but not in rL929; (3) TNF induced the release of ROS and Ca^{2+} in the sensitive cell line while no similar response was observed in resistant cell lines. These observations thus suggest that both ROS and $[Ca^{2+}]_i$ play an important role in the TNF-mediated cell killing.

論文題目: 癌細胞壞死因子所引致的細胞死亡的生化研究

學生姓名: 高翰森

導師姓名: 江紹佳教授

修業學位: 哲學碩士

學系: 生物化學

肄業日期: 一九九八年七月

摘要:

癌細胞壞死因子(Tumor Necrosis Factor)是一種多效性的細胞因子(Cytokine)。它主要由激活的巨噬細胞(Macrophage)及淋巴細胞(Lymphocyte)所分泌。癌細胞壞死因子擁有多種免疫功能,包括引致發熱(Fever)、炎症(Inflammation)和癌細胞死亡等。最近的研究發現它能夠令細胞釋放出過氧化物(Reactive oxygen species),包括過氧化物自由基(Superoxide radical)和過氧化氫(Hydrogen peroxide)等。再者,它亦能夠令細胞釋放出鈣離子(Calcium ion)。

高濃度的過氧化物能引致脂肪的過氧化(Lipid peroxidation)反應及去氧核糖核酸(Deoxyribonucleic acid, DNA)的破壞。高濃度的鈣離子能激活磷脂酶(Phospholipase),蛋白酶(Protease)及核酸內切酶(Endonuclease)等酵素。以上所述的破壞及酶的激活能引致細胞有秩序地死亡(Apoptosis)。因此,研究細胞內的過氧化物及鈣離子的濃度的關係是很重要的,而科學家對它們的關係所知的仍然很少。因此,這項研究的目的旨在發掘癌細胞壞死因子引致細胞死亡的機理,

將焦點集中在過氧化物及鈣離子的相互關係。癌細胞壞死因子敏感的細胞 L929 會作爲研究的對象。本研究利用瓊脂糖凝膠電泳法(Agarose gel electrophoresis)，共聚焦顯微鏡技術(Confocal Microscopy)，流式細胞光度術(Flow cytometry)及細胞死亡測定(Cytotoxicity assay)等技術來探討癌細胞壞死因子的生化機理。

本研究發現癌細胞壞死因子能引致去氧核糖核酸的斷裂，這現象爲細胞有秩序地死亡的特徵。細胞周期(Cell cycle)的研究發現癌細胞壞死因子能引致 G0/G1 期旁邊有一尖端，證明了去氧核糖核酸的斷裂。再者，它令到過氧化物及鈣離子在細胞內慢慢地釋放。過氧化氫酶(Catalase)、錳離子-過氧化物歧化酶(MnSOD)、 N-乙酰半胱氨酸(N-acetylcysteine)和四-氫氧-二,二,六,六-四甲基六氫吡啶-一-氧(4-OH-TEMPO)等抗氧化劑(Antioxidant)能夠阻止過氧化物的釋出。魚滕酮(Rotenone)及抗霉素 A(Antimycin A)等電子傳遞鏈抑制物(Electron transport chain inhibitor)的應用證明癌細胞壞死因子作用於輔酶 Q(Coenzyme Q)，並引致更多過氧化物的釋放。利用二硝基苯酚(2,4-Dinitrophenol)，我們發現癌細胞壞死因子所導致的細胞死亡是需要能量的。抗氧化劑和電子傳遞鏈抑制物的應用能增加或降低癌細胞壞死因子所引致的細胞死亡。

癌細胞壞死因子引起細胞內鈣離子慢慢地釋放。三磷酸腺苷酶(ATPase)的抑制物 Thapsigargin 能增加癌細胞壞死因子引致的鈣離子的釋出。鈣離子釋放物如硫柳汞(Thimerosal)能增加癌細胞壞死因子引致的死亡的嚴重性。相反地，鈣離子的螯合物如 BAPTA/AM 能降低癌細胞壞死因子引致的細胞死亡及過氧化物的釋出。利用粒線體的鈣離子循環(Mitochondrial calcium cycling)的抑制物如鍕紅(Ruthenium Red)和地爾硫草(Diltiazem)證明癌細胞壞死因子引致的鈣離子釋

物的釋出。利用粒線體的鈣離子循環(Mitochondrial calcium cycling)的抑制物如鍺紅(Ruthenium Red)和地爾硫草(Diltiazem)證明癌細胞壞死因子引致的鈣離子釋放的源頭可能來自粒線體。綜合以上各實驗的結果，經過癌細胞壞死因子的處理，細胞內的鈣離子能引致過氧化物的釋出。

癌細胞壞死因子不會即時改變細胞內的氫離子當量濃度指數(pH)。再者，粒線體膜的電位(Mitochondrial membrane potential)也不會受到癌細胞壞死因子所影響。

本研究亦曾比較癌細胞壞死因子敏感的細胞如 L929 ，及有抗性的細胞如 rL929, rL929-11E 和 rL929-4F 等的反應。結果發現如下: (一)癌細胞壞死因子不會引起抗性細胞的死亡; (二)癌細胞壞死因子不會引發抗性細胞有秩序地死亡; (三)癌細胞壞死因子不會引致抗性細胞放出過氧化物及鈣離子。以上發現均證明過氧化物及鈣離子在癌細胞壞死因子引致的細胞死亡擔當了重要的角色。

List of Figures

List of Tables

Publication

Lui, P. P. Y., Lee, M. M. F., Ko, S., Lee, C. Y., and Kong, S. K. (1997) Practical considerations in acquiring biological signals from confocal microscope: II. Laser-induced rise of fluorescence and effect of agonist droplet application. *Biol. Signals* **6**:45-51

Chapter 1

General Introduction

Chapter 1. General Introduction

1.1 Tumor Necrosis Factor

1.1.1 History of Tumor Necrosis Factor

The tumor necrotic effects of bacterial endotoxins have been known for a long time and are mediated by tumor necrosis factor (TNF). The story of the discovery of TNF properly begins with Willam B. Coley. In the late 19th century, he and a few other physicians had some successes in treating cancer patients by infecting them with vaccines of killed bacteria, and the mixture of *Streptococcus pyogenes* and *Serratia marcescens* which came to be known as Coley's toxins (Coley, 1891). Gratia and Linz in 1931 (Gratia and Linz, 1931) and Shear and colleagues in 1943 (Shear *et al.*, 1943) demonstrated that endotoxins can induce hemorrhagic necrosis of certain transplanted tumors in mice. However, endotoxins are not directly cytotoxic to tumor cells *in vitro*. In 1975 Carswell and colleagues showed that serum from mice infected with Bacillus Calmette-Guerin (BCG) and subsequently treated with endotoxin contained a substance capable of inducing tumor necrosis in certain transplantable tumors in mice (Carswell *et al.*, 1975). They called this substance "tumor necrosis factor". They developed a hypothesis that endotoxin-induced tumor necrosis was mediated by the release of TNF from activated macrophages.

1.1.2 TNF Subtypes and Their Purification

There are two types of TNF, TNF-α (generally called TNF or cachectin) and TNF-β (previously known as lymphotoxin (LT)).

Cachexia is a profound loss of weight and wasting of muscle which sometimes occurs in patients with chronic bacterial infection or parasitic infestation. Cachectin is a molecule which was first isolated from the culture supernatants of endotoxin-treated mouse macrophages, that caused cachexia when injected into normal mice (Beutler *et al.*, 1985a; Beutler *et al.*, 1985b). Extensive biochemical analysis of this molecule has revealed its identity as TNF-α (Beutler and Cerami, 1986).

Actually, the initiation of the TNF field can be assigned back to 1967 when Ruddle and his colleagues (Ruddle and Waksman, 1967) studied delayed-type hypersensitivity. They found that lymphocytes from immunized rats, when cultured in the presence of specific antigen, killed syngeneic fibroblasts. This killing was due to a "cytotoxic factor" released from lymphocytes. Later, Granger and his colleagues showed that mitogen-activated spleen cells could produce such a soluble cytotoxic factor that they called "lymphotoxin" (Granger and Williams, 1968).

In summary, TNF-α can be obtained from endotoxin-treated macrophage cell lines whereas TNF-β can be obtained from lectin-stimulated T-lymphocytes. Moreover, some researchers demonstrated that TNF-α is produced not only by macrophages but by several other cell types, including monocytes, natural killer cells, T-lymphocytes and glial cells.

The production of TNF-β, however, seems to be restricted to lymphocytes. A report indicates that myeloma cells may also be a source of TNF-β (Garrett *et al.*, 1987).

Adherent cells isolated from human peripheral blood mononuclear cells stimulated with BCG and endotoxin produced a factor with tumor necrosis activity (Pennica *et al.*, 1984). This factor named human TNF-α (HuTNF-α) showed *in vivo* activities similar to those of murine TNF originally discovered in the sera of mice injected with BCG and subsequently treated with endotoxin (Carswell *et al.*, 1975). Measurable levels of HuTNF-α were detectable after 4-β-phorbol-1, 2β-myristate-13α-acetate (PMA) stimulation of HL-60 cells. Therefore this cell line was used for both the protein purification and the cDNA isolation (Pennica *et al.*, 1984). The mature polypeptide consists of 157 amino acids. The NH_2-terminal amino acid sequence of natural HuTNF-α, however, consists of 233 amino acids. A segment of 76 residues preceded in natural HuTNF-α is probably involved in TNF secretion as it is not observed on mature HuTNF-α (Pennica *et al.*, 1984). From the cDNA sequence, a relative molecular weight of 17,000 was calculated for the mature protein.

The accessibility of a cDNA probe for recombinant HuTNF-α (rHuTNF-α) permitted the isolation of the cDNA for Murine TNF-α (MuTNF-α). It was found that PU5-1.8 cell line with PMA stimulation secreted the highest levels of MuTNF activity (Pennica *et al.*, 1985). The isolated MuTNF-α cDNA encoded a polypeptide consisting of

a 79-amino-acid presequence region followed by a sequence for mature MuTNF-α of 156 amino acids and with a relative molecular weight of approximately 16,000 to 18,000.

The human TNF-β (HuTNF-β) was successfully purified from supernatants of PMA-stimulated RPMI-1788 B-lymphoblastoid cells grown in serum-free RPMI-1640 medium (Aggarwal *et al.*, 1984). Recombinant TNF-β was determined to be a glycoprotein with 171 amino acid residues in length with a relative molecular weight of approximately 25,000. An N-linked glycosylation probably accounted for the increased size.

The gene for murine TNF-β (MuTNF-β) was cloned in 1987 (Ruddle *et al.*, 1987). The number of amino acids in mature protein is 169 with a molecular weight of approximately 18,000. There are 33 residues in the signal peptide.

The characteristics of TNFs isolated from human and murine is shown in Table 1.1 (review: Aggarwal and Vilcek, 1992; Pennica *et al.*, 1987; Ruddle *et al.*, 1987). Figure 1.1 shows the comparison of rHuTNF-α, rMuTNF-α and rHuTNF-β sequences (Pennica *et al.*, 1987). Table 1.2 shows the summary of discovery of TNF (modified from Palladino *et al.*, 1987).

In this thesis, the actions of TNF-α will be focused in more detail and TNF-α will be abbreviated as "TNF" in the following sections.

Table 1.1
Characteristics of TNFs isolated from human and murine.

	Human TNF-α	**Murine TNF-α**	**Human TNF-β**	**Murine TNF-β**
Source	HL-60	PU5-1.8	RPMI-1788	T lymphocyte
Molecular weight (kDa)	17	16-18	25	18
Glycoslation	No	Yes	Yes	Yes
Cysteine residues	2	2	None	1
Amino acid length	157	156	171	169
Signal peptide	76	79	34	33
Chromosome assignment	6	17	6	17
Homology	79 %		72 %	

(Modified from Aggarwal and Vilcek, 1992; Pennica *et al.*, 1987; Ruddle *et al.*, 1987)

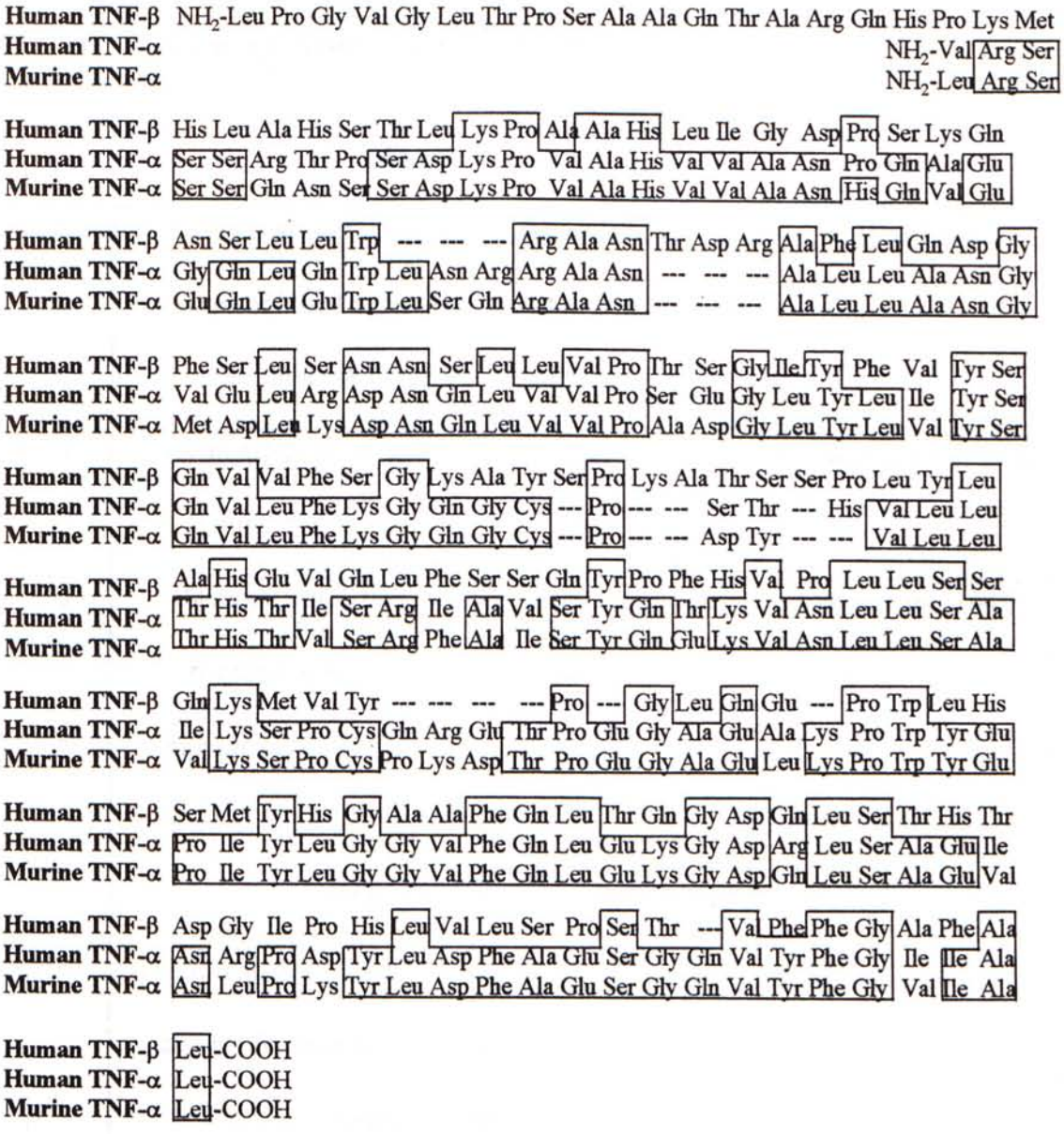

Figure 1.1

Comparison of rHuTNF-α, rMuTNF-α and rHuTNF-β sequences. Identical amino acids are boxed. Broken lines indicate amino acid deletions in the sequences (Modified from Gillis, 1987).

Table 1.2
Summary of discovery of tumor necrosis factor.

Date	Event	Reference
1891	Coley treated human cancer patients with mixtures of killed Streptococcus pyrogenes and Serratia marcescens preparations	Coley, 1891
1931	Demonstration of hemorrhagic necrosis of animal tumors after injection of bacterial filtrates	Gratia and Linz, 1931
1943	Bacterial agent that induces hemorrhagic necrosis identified as a polysaccharide	Shear *et al.*, 1943
1968	Lymphotoxin (TNF-β) produced by antigen- or mitogen-stimulated lymphocytes shown to cause target cell lysis	Ruddle and Waksman 1987 Granger and Williams 1968
1975	Factor capable of inducing tumor necrosis and distinct from endotoxin characterized from mouse serum	Carswell *et al.*, 1975
1984	Human tumor necrosis factor-β (lymphotoxin) cDNA cloned	Aggarwal *et al.*, 1984
1984	Human tumor necrosis factor-α (cachectin) cDNA cloned	Pennica *et al.*, 1984

(Modified from Palladino *et al.*, 1987)

1.1.3 Release of TNF

The release of TNF is divided into two stages, priming and triggering. Figure 1.2 shows the possible mechanism of priming and triggering of TNF-α production in macrophage (Kitahara-Tanabe *et al.*, 1991; Kriegler *et al.*, 1988). The primers such as BCG and *Corynebacterium parvum* can prime on TNF production in macrophages. The inducers such as lipopolysaccharide (LPS), phorbol esters and cytokines can trigger the release of TNF from activated macrophage. Proteolysis of membrane-associated TNF produces soluble TNF. The proteolysis is mediated by a membrane enzyme, metalloproteinase (Gearing *et al.*, 1994).

1.1.4 Biological Actions of TNF

The native TNF is a trimer. Results from X-ray small-angle scattering spectra indicated that the TNF trimer has a molecular weight between 50,000 and 53,000 (Lewit-Bentley *et al.*, 1988). In another study, Smith and his colleagues showed that treating TNF with a nonionic detergent such as triton X-100 and by gel filtration produced, in addition to the trimer peak, another peak which is believed to be contributed by monomeric TNF. Monomeric TNF had a lower specific biological activitiy (Smith and Baglioni, 1987).

TNF is almost not species specific. Human TNF is capable of producing biological effects on murine cells, and vice versa (Kramer *et al.*, 1988).However, when measured the cytotoxicity of murine L929 cells, the specific activity of MuTNF is about threefold higher than that mediated by HuTNF.

Primed stage

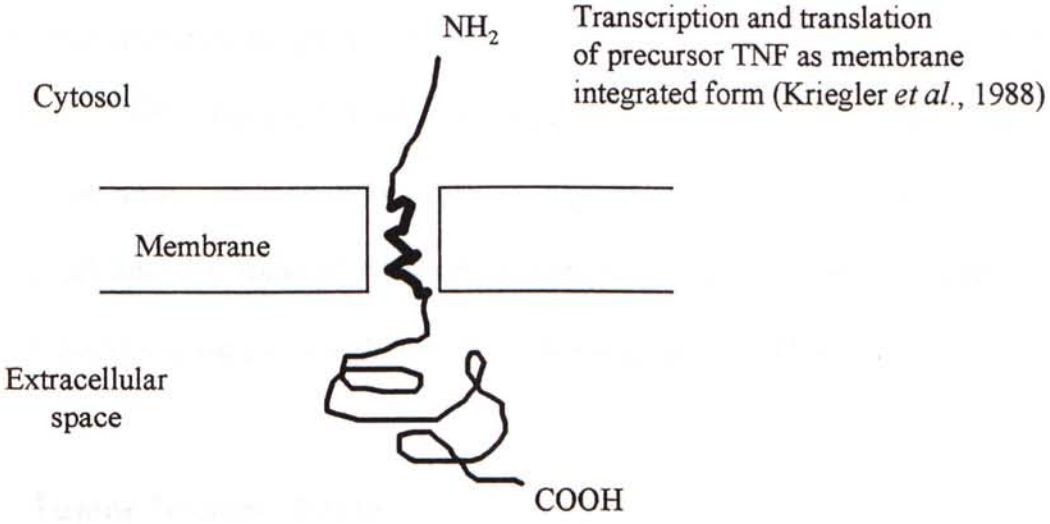

Triggered stage

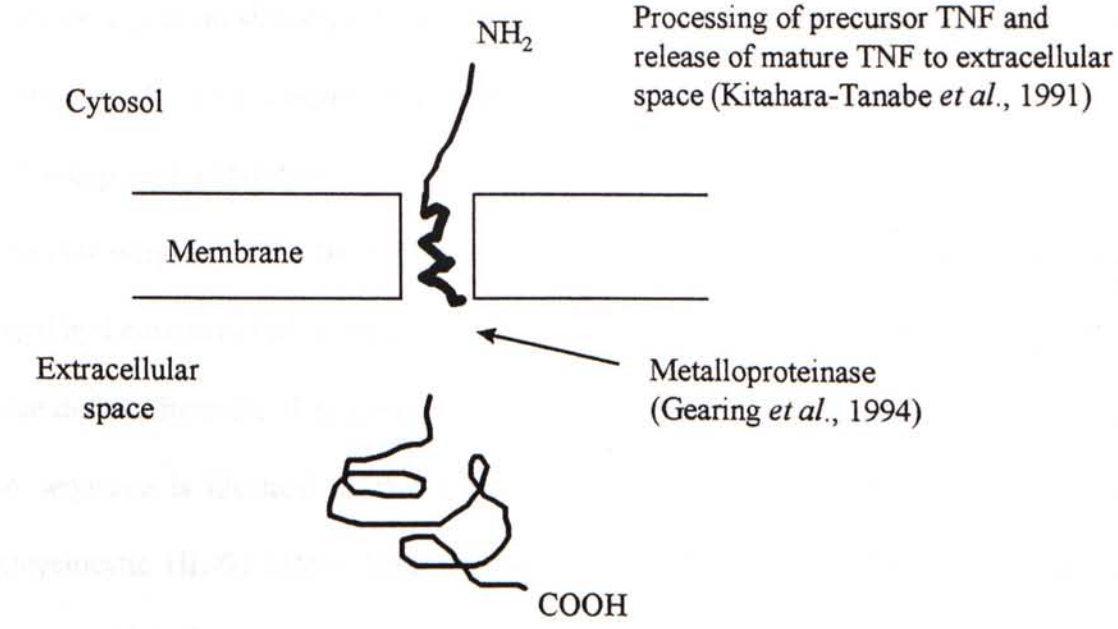

Figure 1.2
Possible mechanism of priming and triggering on TNF production in macrophage.

TNF is a pleiotropic cytokine that elicits a wide range of biological events. It gives effect on hematopoietic system (review: Trinchieri, 1992) and immunomodulation (review: Bonavida, 1992). Table 1.3 shows the biological activities of TNF. Sugarman *et al.* have conducted an extensive *in vitro* screen on a panel of 23 human tumors and 12 murine tumor cell lines and some of the results are shown in Table 1.4 (Sugarman *et al.*, 1985). Their results suggest that not all tumor cells are susceptible to TNF.

1.2 Tumor Necrosis Factor Receptor

1.2.1 Purification of TNF Receptor

To exerts its biological actions, TNF must first bind to cell surface receptors. TNF receptors appear on virtually all somatic cells (Beutler and Cerami, 1989). TNF receptors channel signals to the cytoplasm and nucleus. There are two types of surface receptors, TNF receptor 1 (TNFR1) and TNF receptor 2 (TNFR2). TNFR1 and TNFR2 have a molecular weight of 55 kDa and 75 kDa, respectively. In 1990, the TNF receptor was cloned by Leotscher *et al.* from a human placental lambda gt11 cDNA library using a PCR probe derived from the N-terminus of the 55 kDa TNF receptor (Leotscher *et al.*, 1990). The sequence is identical to that cloned by Schall *et al.* (from both plancental and premyelocytic HL-60 cDNA libraries) using probes derived from TNF-binding protein sequences (Schall *et al.*, 1990).

TNFR1 is composed of 455 amino acids that can be subdivided into four domains: (1) a signal sequence; (2) a 182 residues extracellular cysteine-rich domain; (3) a 20-22

Table 1.3
Biological activities of TNF.

Activity	**Reference**
Induces hemorrhagic necrosis of tumors	Pennica *et al.*, 1984
Induces IL-1 production	Torti *et al.*, 1985
Activates neutrophil functions	Gamble *et al.*, 1985
Growth-stimulatory action (e.g. murine thymocytes)	Ranges *et al.*, 1988
Antiviral activity	Wong and Goeddel, 1986
Antiparasitic effect	Review: Playfair and Taverne, 1987
Gene expression (e.g. c-fos, c-myc)	Lin and Vilcek, 1987

Table 1.4
Summary of responses of human and murine cell lines to rHuTNF-α *in vitro*.

Human cell line	**Origin**	***In vitro* sensitivity**
A549	Lung carcinoma	-
BT-20	Breast carcinoma	+
Calu-3	Lung carcinoma	-
G-361	Melanoma	-
HeLa	Cervical carcinoma	-
KB	Oral epidermoid carcinoma	-
LS174T	Colon carcinoma	-
MCF-7	Breast carcinoma	+
Saos-2	Osteogenic sarcoma	-
SD-MEL-109	Melanoma	+
T24	Bladder carcinoma	-
WIDR	Colon carcinoma	+
Murine cell line	**Origin**	***In vitro* sensitivity**
B16F10	Melanoma	-
CMS4	Chemically induced sarcoma	+
L929	Fibroblast	+
Meth A	Chemically induced sarcoma	+
S49	Lymphoma	-
WEHI164	Sarcoma	+

(-) Represents < 25 % cytostasis/cytotoxicity.

(+) Represents > 25 % cytostasis/cytotoxicity.

residues transmembrane helical segment; and (4) a 221-223 residues intracellular domain. Smith *et al.* discovered a very different breed of TNF receptor by expression screening a human lung fibroblast cDNA library and classified as TNFR2. This receptor is composed of 461 amino acids. It comprises signal, cysteine-rich, transmembrane and cytoplasmic domains. TNFR1 and TNFR2 show 40 % homology in their extracellular domains, but virtually none in their intracellular domains (Smith *et al.*, 1990a; Tartaglia and Goeddel, 1992).

1.2.2 Regulation of TNF Receptor

A large number of examples of receptor regulation by homologous or heterologous ligands have been reported (review: Tsujimoto and Oku, 1992). These reports suggested that the regulation of receptor number or affinity might be a prevalent mechanism of cellular regulation. The biological significance of receptor regulation might be related to synergistic or inhibitory effects.

Up-regulation of TNF receptors

In some tumor cell lines, TNF and IFNs were shown to exert a synergistic cytotoxic action (Williamson *et al.*, 1983). Pretreatment of various tumor cells with IFN-γ resulted in an increase of TNF binding (Tsujimoto *et al.*, 1986a). Resting T cells do not express surface receptors for TNF. However, treatment of lymphocytes with IL-2 resulted in specific TNF binding to the surface of lympocytes (Owen-Schaub *et al.*, 1989). Moreover, exposure of human cervical carcinoma cell line ME-180 to some lectins, such

as concanavalin A and wheat germ agglutinin, caused an increase in TNF receptors without significant change in their affinity constant (Aggarwal *et al.*, 1986).

Down-regulation of TNF receptors

Aggarwal and Eessalu reported that phorbol esters such as PMA, that are known to bind and activate protein kinase C (PKC), reduced the total receptor number without any significant change in the affinity constant of the receptors in U937 cells (Aggarwal and Eessalu, 1987). Treatment of SV80 cells or FS-11 cells with IL-1 resulted in a decrease of TNF binding to cell surface receptors (Holtmann and Wallach, 1987). Recently, it was found that blockade of mitochondrial respiration down-regulated tumor necrosis receptors (Sanchez-Alcazar *et al.*, 1995). This down-regulation could be simply a side effect of mitochondrial dysfunction, secondary to the loss of cellular energy. Moreover, LPS and glucocorticoids as well as TNF may down-regulate TNF receptors (Ding *et al.*, 1989; Kull, 1988; Tsujimoto and Vilcek, 1987).

1.2.3 Functions of TNF Receptor 1 , Receptor 2 and Soluble TNF Receptors

TNF interacts with its specific receptor and is then internalized. The internalization of the receptor-ligand complex, through receptor-mediated endocytosis, and the eventual degradation of the ligand by lysosomal hydrolases (Tsujimoto *et al.*, 1985).

TNFR1

The cross-linking of TNFR1 is an important component of the activation process. TNFR1 was shown to be responsible for inducing nuclear factor κB (NFκB),

accumulation of c-fos, IL-6, and manganous superoxide dismutase mRNA, prostaglandin E_2, IL-2 receptor, HLA class I and II cell surface antigen expression, growth inhibition and cytotoxicity (Brakebusch *et al.*, 1992; Engelmann *et al.*, 1990b; Espevik *et al.*, 1990; Hohmann *et al.*, 1990; Kruppa *et al.*, 1992; Naume *et al.*, 1991; Shalaby *et al.*, 1990; Tartaglia *et al.*, 1991; Thoma *et al.*, 1990). The actions of TNFR1-mediated signaling transduction and cytotoxicity will be discussed later.

TNFR2

Proliferation of mouse thymocytes and the murine cytotoxic T-cell line CT-6 is stimulated by murine TNF (Tartaglia *et al.*, 1991). Polyclonal antibodies directed against TNFR2 induced proliferation in both of these cell types, whereas polyclonal antibodies directed against TNFR1 had no effect. In contrast, cytotoxicity in murine L-M cells was induced by antibodies against TNFR1 but not by antibodies against TNFR2. These results suggest that TNFR2 initiates signals for the proliferation of thymocytes and cytotoxic T cells, whereas TNFR1 stimulates signals for cytotoxicity. However, TNF-induced proliferation may not be mediated by TNFR2 in all cell types. Engelmann *et al.* have shown that polyclonal antibodies against human TNFR1 can stimulate proliferation of human FS11 fibroblasts (Engelmann *et al.*, 1990a).

Soluble TNFR

The soluble forms of TNF receptors (sTNFR) have been identified in the serum, urine, ascites, and synovial and cerebrospinal fluids of humans. The urinary sTNFR are structurally related to the cell surface TNF receptors. Comparison of their amino acid

sequences with those of the TNFR1 and TNFR2 revealed that they are in fact the shed form of the extracellular part of the TNFR1 (Nophar *et al.*, 1990). The mechanism of the release of these receptors is not understood. It has been shown that treatment of U937 cells with PMA could induce the shedding of TNFRs (Kohno *et al.*, 1990), suggesting a role for PKC. The possible physiological roles of the sTNFR may serve as: (1) TNF buffers by inhibiting the acute and potentially harmful effects of high TNF concentrations; (2) a slow release pool for TNF; (3) TNF carrier proteins between body compartments; and (4) stabilizers of TNF bioactivity. It was observed that, at physiological concentrations, the trimeric bioactive TNF molecule dissociates irreversibly into inactive monomers which subsequently form inactive high molecular weight TNF multimers. Therefore, sTNFR may prevent trimeric TNF from dissociating into monomers and then to form multimers (Aderka *et al.*, 1992).

1.3 Possible Signal Transductions of Tumor Necrosis Factor-Alpha

The feature of TNF action is the striking diversity of many cellular responses. Nowadays, no specific biological activity of TNF could be defined that is in common to all TNF-responsive cells. Based on the limited structural heterogeneity of specific TNF receptors, the multitude of biological activities inducible by TNF must depend on a diversification of postreceptor signaling mechanisms. In general, the first event in triggering a cellular response is specific high-affinity interaction of TNF with membrane receptor molecules, thereby initiating a cascade of signal transfer reaction inside the cell. The most direct way of the signaling mechanism is found with receptors that themselves

possess intrinsic tyrosine kinase activity in their intracellular domains. However, there is no induction for tyrosine kinase activity of TNF receptors (Waterman and Sha'afi, 1995). A report from Smith *et al.* shows that cytotoxic activity of microinjected TNF was a receptor-independent intracellular function of the ligand itself (Smith *et al.*, 1990b). According to this report, TNF membrane receptors would serve as a ligand transporter and a signal transmitter in the membrane.

TNF induces the activation of five possible cascades inside the cells: (1) phospholipase A_2; (2) phospholipase C; (3) sphingomyelin; (4) protein kinase; and (5) death domain.

1.3.1 Activation of Phospholipase A_2 Cascade

TNF induces the activation of phospholipase A_2 (PLA_2) in human neutrophils (Bauldry *et al.*, 1991) and can be inhibited by glucocorticoids in human epithelial carcinoma cell line Hep-2 (Goppelt-Struebe and Rehfeldt, 1992). Recently, it was found that TNF induces the 85 kDa cytosolic PLA_2 ($cPLA_2$) gene expression in human bronchial epithelial cells, BEAS 2B (Wu *et al.*, 1996). PLA_2 has been demonstrated to be coupled by G-proteins to membrane receptors (Silk *et al.*, 1989). The PLA_2 activation mediated by TNF in different cell types induces the production of arachidonic acid (Gustafson-Svard *et al.*, 1993). The arachidonic acid metabolites such as prostaglandins and leukotrienes exhibit gene regulatory activity such as the induction of c-fos gene (Haliday, *et al.*, 1991) and are important mediators of cytotoxicity (Hayakawa *et al.*, 1993; Neale *et al.*, 1988). In fact, the TNF-induced cytotoxicity can be reduced by inhibitors of PLA_2, such as

quinacrine (Suffys *et al.*, 1987). However, Robaye and Dumont found that PLA_2 activity is not involved in the TNF-triggered cell death in bovine aortic endothelial cells (Robaye and Dumont, 1992). Recently, it was found that TNF-induced apoptosis (programmed cell death that will be discussed later) is mediated by caspases, the cysteine proteases related to interleukin 1β-converting enzyme, that results in the cleavage and activation of $cPLA_2$, which in turn elicits to apoptosis (Wissing *et al.*, 1997).

1.3.2 Activation of Phospholipase C Pathway

The second major signaling pathway of TNF-mediated cell responses involves specific phospholipases. However, release of Ca^{2+} from internal stores and increase in intracellular inositol trisphosphate (IP_3) levels have not been detectable in U937 cell line (Schutze *et al.*, 1992a). TNF stimulates the production of 1,2-diacylglycerol (1,2-DAG) by activation of phosphatidylcholine-specific phospholipase C (PC-PLC) in the absence of changes in intracellular calcium concentration ($[Ca^{2+}]_i$). The 1,2-DAG formation in response to TNF is a very rapid and transient event (Schutze *et al.*, 1992a). In contrast, Beyaert *et al.* found that lithium chloride (LiCl), an inhibitor of phosphoinositide metabolism and cycling, increases the cytotoxic activity of TNF towards some transformed cell lines such as L929. Treatment of these cell lines with the combination of TNF and LiCl leads to the prolonged accumulation of inositol monophosphate (IP), inositol bisphosphate (IP_2), and inositol trisphosphate (IP_3), whereas treatment with TNF or LiCl alone did not (Beyaert *et al.*, 1993). Both TNF-mediated cytotoxicity and -induced accumulation of inositol phosphates were blocked by neomycin, a phospholipase inhibitor. The increase in IP_3 after treating cells with TNF and LiCl suggests a role of

$[Ca^{2+}]_i$ in TNF action. Moreover, several agents that lower the $[Ca^{2+}]_i$ inhibited TNF cytotoxicity (Beyaert *et al.*, 1993). In conclusion, TNF-induced production of IP_3 or $[Ca^{2+}]_i$ is still controversial.

1.3.3 Activation of Sphingomyelin Pathway

TNF signaling may involve sphingomyelin (SM) hydrolysis to ceramide by sphingomyelinase (SMase) (Figure 1.3). In a cell-free system, TNF induced a rapid reduction in membrane sphingomyelin content and a quantitative elevation in ceramide concentration (Dressler *et al.*, 1992). There are two types of SMase, the acidic and the neutral forms, that exert different functions. The SMases belong to a family of C type phospholipases that hydrolyze SM to produce phosphorylcholine and ceramide. The latter is viewed as a second messenger-like molecule. SMases are widely distributed in various tissues and exhibit characteristic cellular compartmentation. Acidic SMase is an intracellular, compartmentalized glycoprotein with an optimal pH of 4.5 and a molecular size of 72 kDa (Quintern *et al.*, 1987). Activation of the acidic SMase has been shown to require 1,2-DAG (Kolesnick, 1987). Schutze *et al.* found that TNF-responsive PC-PLC via 1,2-DAG couples to an acidic SMase, resulting in the generation of ceramide, with eventually triggers rapid induction of nuclear NFκB activity that controls the expression of a variety of cellular genes (Schutze *et al.*, 1992b; review: Kolesnick and Golde, 1994). The finding indicates that 1,2-DAG activates an acidic SMase that hydrolyzes SM to produce ceramide in U937 and Jurkat cells. The second messenger-like molecule ceramide is found to display a potent, NFκB-inducing capacity (Schutze *et al.*, 1992b). In contrast, neutral SMase has been implicated in mediating TNF-induced differentiation of HL-60

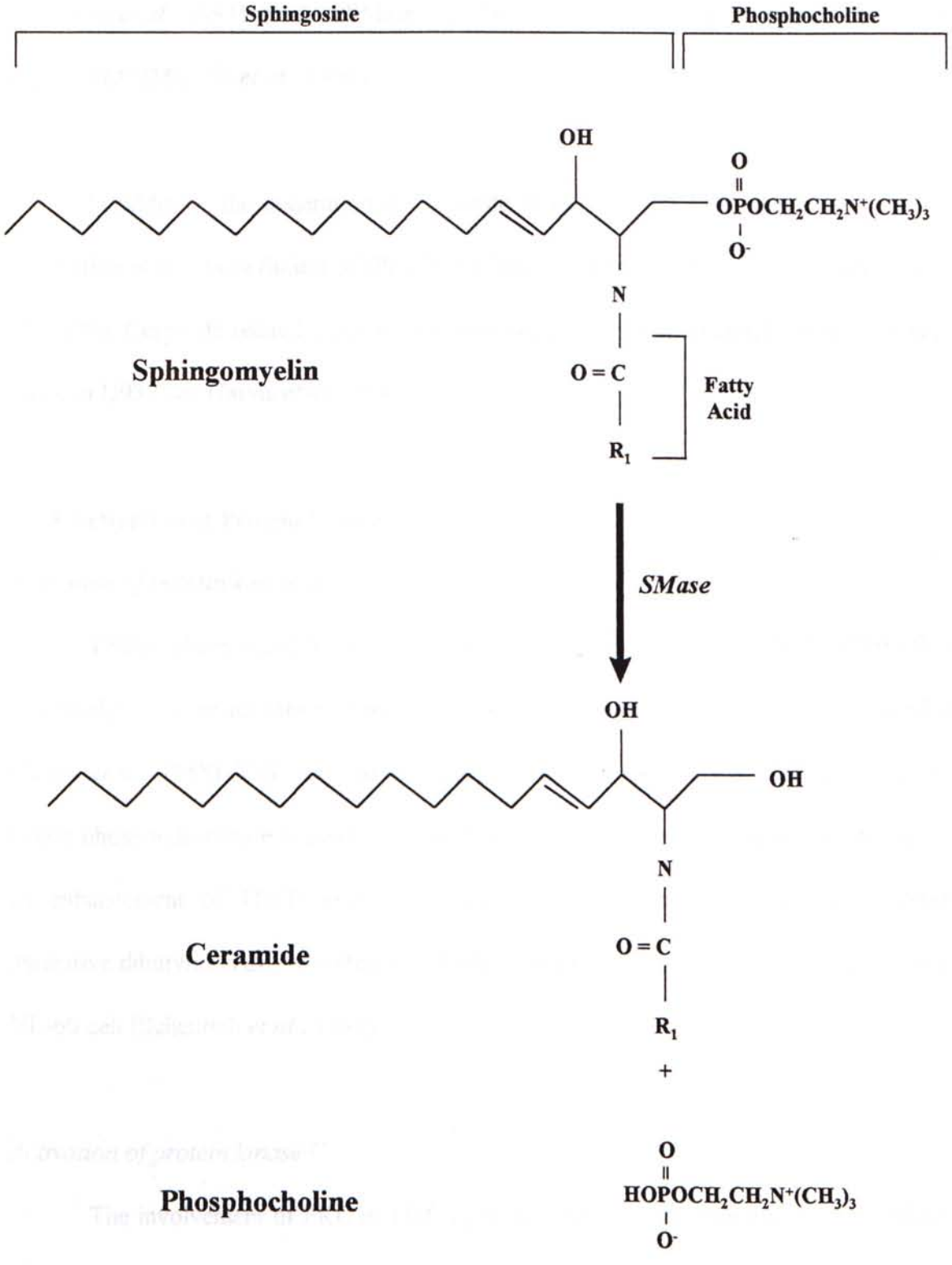

Figure 1.3

Sphingomyelin hydrolysis to ceramide mediated by sphingomyelinase. Sphingomyelin is comprised of a phosphocholine headgroup, a long chain or very long chain saturated or monounsaturated fatty acid and a sphingoid base backbone, predominantly sphingosine.

cells (Kim *et al.*, 1991). Neutral SMase was shown to activate a protein kinase but did not require PLC (Mathias *et al.*, 1991).

In addition, the generation of ceramide in response to TNF may play a role in stimulation of the transcription of cPLA2 and cyclooxygenase 2 in L929 cell (Hayakawa *et al.*, 1996). Ceramide-related signaling processes in the induction of apoptosis by TNF was found in U937 cell (Jarvis *et al.*, 1994).

1.3.4 Activation of Protein Kinase

Activation of protein kinase A

TNF has been noted to rapidly increase the production of cyclic AMP (cAMP) that potentially results in activation of protein kinase A (PKA) in human diploid fibroblast FS-4 (Zhang *et al.*, 1988). TNF may either directly activate adenylate cyclase via G-proteins or inhibit phosphodiesterase activity. Scheurich *et al.* found that activation of PKA results in an enhancement of TNFR expression. Addition of the membrane-permeable cAMP derivative dibutyric-cAMP resulted in a drastic enhancement of TNF binding capacities in HL-60 cell (Scheurich *et al.*, 1989).

Activation of protein kinase C

The involvement of PKC in TNF signaling pathways was monitored by the effects of TNF on the PKC activity in U937 and K562 cell lines (Schutze *et al.*, 1990). TNF treatment resulted in activation of PKC associated with a translocation from the cytosol to the cell membrane. The molecular mechanism of TNF-induced PKC activation is likely

related to 1,2-DAG that generated by PC-specific PLC. Moreover, it has been shown that unsaturated fatty acids, such as arachidonic acid, can activate PKC independently of Ca^{2+} and phospholipids (Murakami and Routtenberg, 1985). Therefore, TNF activation of PKC may occur through stimulation of either phospholipase C, leading to increased levels of 1,2-DAG, or phospholipase A_2, elevating arachidonic acid. As mentioned before, activation of PKC may down-regulate TNFR expression cells (Aggarwal and Eessalu, 1987).

Activation of serine/threonine protein kinases

Treatment of Swiss 3T3 and L929 cells with TNF leads to the rapid stimulation of several cytosolic serine/threonine kinases active toward a number of peptide and protein substrates, such as myelin basic protein (Van Lint *et al.*, 1992). This confirms the hypothesis that kinases other than PKA and PKC may be involved in the TNF signal transduction.

1.3.5 Activation of the Cascade of Death Domain

The cytoplasmic regions of TNFR1 is responsible for transducing the death signal. Subsequent mutational analyses in TNFR1 indicated that this domain has been designated a death domain (Figure 1.4) (Tartaglia *et al.*, 1993, review: Nagata, 1997). The death domain contains protein TRADD (TNFR1-associated death domain protein) that binds to TNFR1 (Hsu *et al.*, 1995). TRADD binds to FADD (Fas-associating protein with death domain) or MORT1 (FADD/MORT1) via interactions between their death domains (Hsu et al., 1996b). FADD/MORT1 then activates caspase-8, that carries two death effector

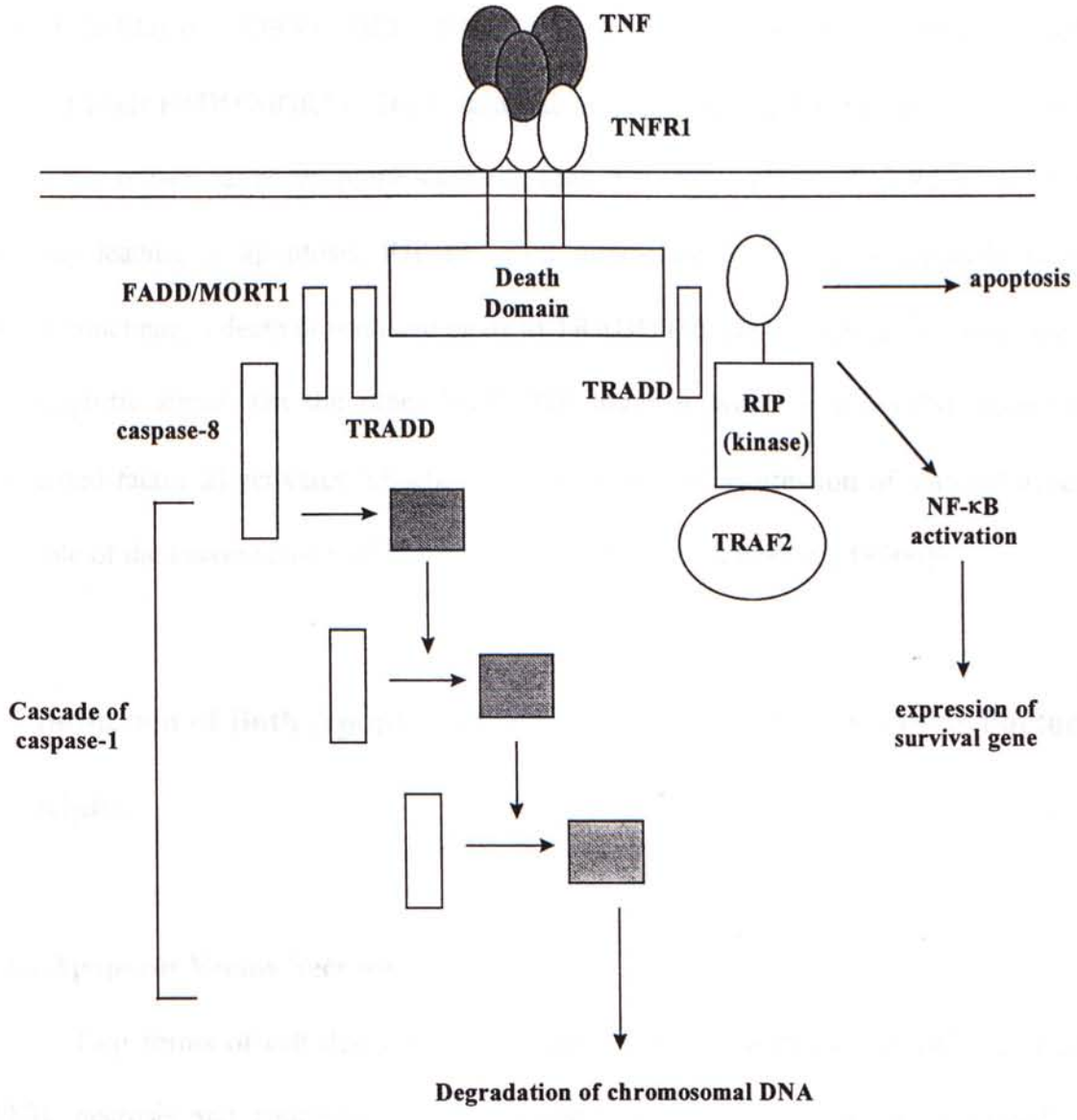

Figure 1.4

TNF induced a cascade of death domain. TNF binds to TNFR1, and the trimerized receptor recruits TRADD via interactions between death domains. The death domain of TRADD then recruits FADD/MORT1 in one pathway to activate caspase-8. In another pathway, RIP binds to TRADD and transduces an apoptotic signal through the death domain. In addition, RIP together with TRAF2 activates NF-κB, which may induce the expression of survival genes.

domain (DED) or MORT1 (DED/MORT1) domains at the N-terminal region, through which it binds FADD/MORT1. The C-terminal region of caspase-8 is related to caspase-1 family that transduces an apoptotic signal. In addition to this pathway, TNFR1 has another pathway leading to apoptosis. RIP (receptor interacting protein) is a serine/threonine kinase containing a death domain and binds to TRADD (Hsu *et al.*, 1996a) and transduces an apoptotic signal. On the other hand, RIP together with TRAF2 (TNF receptor-associated factor 2) activates NF-κB, that may induce the expression of survival genes. The role of the kinase activity of RIP is currently unknown (Liu *et al.*, 1996b).

1.4 Induction of Both Apoptosis and Necrosis by Tumor Necrosis Factor-Alpha

1.4.1 Apoptosis Versus Necrosis

Two forms of cell death have been recognized by Wyllie *et al.* (Wyllie *et al.*, 1980), necrosis and apoptosis (or programmed cell death) that are distinguished by morphological characteristics (review: Kerr *et al.*, 1995).

Cellular necrosis is defined by electron-lucent cytoplasm, mitochondrial swelling, loss of plasma membrane integrity without drastic morphological changes in nuclei. Necrosis has been considered as a passive degenerative phenomenon induced by direct toxic or physical injuries, which most often occurs accidentally (Hawkins *et al.*, 1972). Nuclear DNA is randomly cleaved as a consequence of cellular degeneration. Leakage of

the cytoplasm through plasma membrane disruption induces cellular inflammatory responses. Necrotic cells in tissues tend to retain their shape until removed by mononuclear phagocytes. In cultures, on the other hand, disintegration results in the production of amorphous debris (Kerr *et al.*, 1995).

Apoptosis was originally distinguished from necrosis on the basis of its ultrasturcture (Kerr *et al.*, 1972). Apoptosis is characterized by chromatin condensation, nuclear fragmentation and formation of apoptotic bodies (Wyllie *et al.*, 1980). Apoptosis is tightly regulated by molecular mechanisms. In most but not all forms of apoptosis, nuclear DNA is cleaved at internucleosomal sites that produces 180 base pairs fragments. In tissues, apoptotic bodies are often found in clusters, but scattered single bodies are also common (Kerr *et al.*, 1995). Apoptosis can be induced by various stimuli such as ceramide (Obeid *et al.*, 1993), cytochrome c (Liu *et al.*, 1996a), Ca^{2+} (Park *et al.*, 1996) and hydrogen peroxide (Gardner *et al.*, 1997a). On the other hand, apoptosis can be suppressed by Bcl-2 (B-cell leukemia/lymphoma-2 gene, is a proto-oncogene first identified by its association with B cell malignancies (Reed, 1994)) (Hockenbery *et al.*, 1990). Apoptosis is important in animal development such as sculpting, deleting unwanted structures, controlling cell numbers and eliminating nonfunctional, harmful, abnormal, or misplaced cells (review: Jacobson *et al.*, 1997).

Recently, the intracellular ATP levels have been implicated both *in vitro* and *in vivo* as a determinant of the cell's decision to die by apoptosis or necrosis (review: Tsujimoto 1997). It was found that necrosis did not require intracellular ATP. In contrast,

depletion of intracellular ATP by incubating cells in glucose-free medium to halt glycolysis, in the presence of the mitochondrial F_0-F_1-ATPase inhibitor oligomycin, completely blocked apoptosis induced by Ca^{2+} ionophore and ATP supplied through either glycolysis or mitochondrial oxidative phosphorylation restored the apoptotic cell death pathway. These results indicate that apoptosis is ATP-dependent (review: Nicotera and Leist, 1997).

1.4.2 TNF Can Induce Both Apoptosis and Necrosis

Laster *et al.* found that TNF can induce both apoptotic and necrotic forms of cell lysis that depends on cell type (Laster *et al.*, 1988). In TNF-sensitive target, an adenovirus E1 transformant F17 undergoes DNA fragmentation when it dies. This suggested that in F17 cells, TNF triggers apoptosis. However, L-M cells die in a completely different manner. Unlike F17 cells, L-M cells undergo necrotic form of cell death after TNF treatment.

1.5 Possible Mechanisms of Tumor Necrosis Factor-Alpha-Mediated Cytotoxicity

TNF is cytotoxic to some cell lines, but not all tumor cells (Table 1.4). The exact mechanism for TNF cytotoxicity is still unknown. In this section, several possible mechanisms will be introduced.

1.5.1 Release of Reactive Oxygen Species

Review of reactive oxygen species

Reactive Oxygen Species (ROS), a reduced form of oxygen, are unstable. For examples, superoxide radical ($O_2\bullet^-$), hydrogen peroxide (H_2O_2), hydroxyl radical (OH•), nitric oxide (NO•), semiquinone (SQ•), peroxyl and alkoxyl radicals (ROO• and RO•) (review: Dawson and Dawson, 1996) are the ROS found in the cytosol. The normal background level for H_2O_2 is about micromolar range (μM) and there is about nanomolar (nM) range for $O_2\bullet^-$, OH• and NO•. Mitochondria are considered to be the major site of ROS production whereas the primary source is from the electron transport chain. Therefore, ROS are generated continuously in respiring cells. Figure 1.5 shows the metabolic pathways for the generation of $O_2\bullet^-$, H_2O_2 and OH•. NADH that come from glycolysis or TCA cycle, donates electron to ubiquinone (UQ) and then pass through a cascade, finally to the electron acceptor, molecular oxygen. Almost all electrons pass through this pathway. However, about 1-3 % of electrons leak out from inner mitochondrial membrane and react with molecular oxygen directly, and $O_2\bullet^-$ is formed (Dawson and Dawson, 1996). Then, $O_2\bullet^-$ is converted into H_2O_2 or water, depends on the catalytic pathway. Excessive production of ROS may cause cell death.

ROS attack different targets inside the cells. Proteins, lipids, DNA and RNA are the major targets. ROS cause modification of thiol groups on mitochondrial membrane, therefore, increase the $[Ca^{2+}]_i$ level by releasing the mitochondrial Ca^{2+} into cytosol (review: Vercesi, 1993). ROS cause lipids peroxidation that increase the membrane

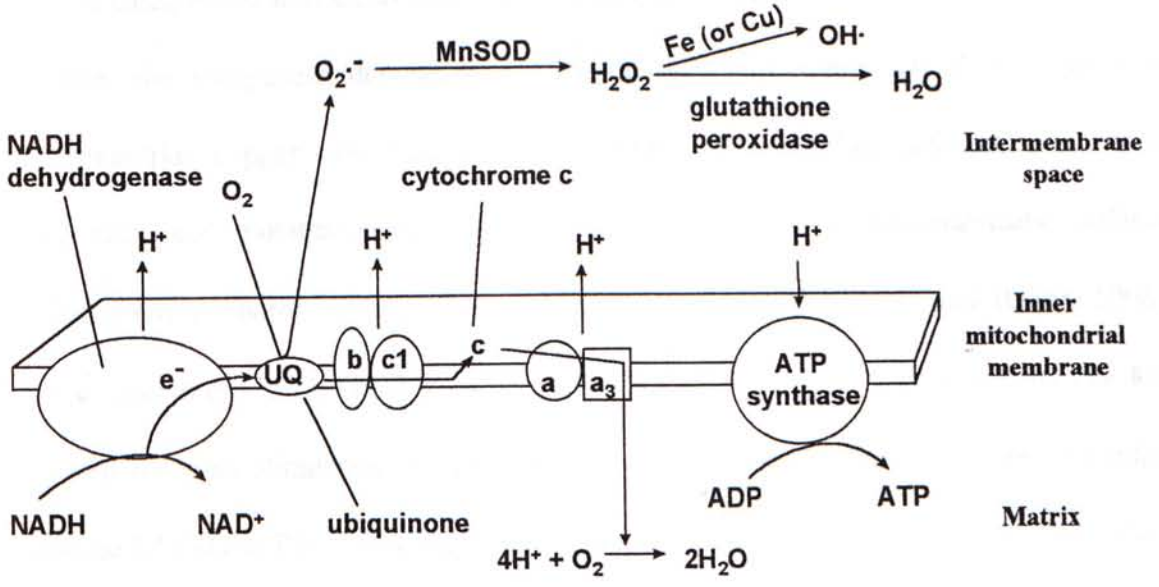

Figure 1.5
Metabolic pathways for the generation of $O_2\bullet^-$, H_2O_2 and OH• in the inner mitochondrial membrane.

permeability (Radi *et al.*, 1991). ROS may induce base damage on DNA or RNA (Park *et al.*, 1998; Wiseman and Halliwell, 1996). Consequently, protein synthesis is inhibited.

There are two main defence mechanisms for removing ROS inside the cells. They can be categorized into enzymatic and non-enzymatic defences. The enzymatic defence includes the manganese dependent superoxide dismutase (MnSOD) that localized in mitochondria; copper and zinc dependent SOD (Cu/ZnSOD), catalase, glutathione peroxidase and glutathione reductase system in cytosol. The non-enzymatic defence includes α-tocopherol, ascorbic acid and β-carotene (review: Briehl and Baker, 1996). The excessive production of ROS impairs the antioxidant system. It is interesting that low level of oxidants stimulates cell proliferation. Different concentrations of redox-cycling quinone DMNQ in RINm5F cells induce different responses. At low concentration about 10 μM, DMNQ induces cell proliferation. At medium concentration about 30 μM, it inhibits cell growth and induces apoptosis. At high concentration such as 100 μM, it causes glutathione and ATP depletion, Ca^{2+} overload and acute necrosis (Dypbukt *et al.*, unpublished data).

Release of ROS after TNF treatment

Tsujimoto *et al.* found that TNF provokes $O_2\bullet^-$ generation from human neutrophils (Tsujimoto *et al.*, 1986b). Treatment of murine tumor cells such as L929, P388 and Pan-02 with rHuTNF induces oxidative damage *in vitro* (Zimmerman *et al.*, 1989). Wong and Goeddel found that TNF induced the production of MnSOD mRNA in all cell lines and normal cells *in vitro* and in various organs of mice *in vivo* (Wong and

Goeddel, 1988). Moreover, the antioxidants desferrioxamine and butylated hydroxyanisol inhibited TNF-induced apoptosis in L929 cells. However, enforced expression of Bcl-2 had no effect against TNF-induced apoptosis (Gardner *et al.*, 1997b).

1.5.2 Release of Intracellular Calcium

Review of Ca^{2+} homeostatsis

There are many signaling pathways in cells. Phosphoinositide cycle (Figure 1.6) is one of these pathways and it regulates the mobilization of calcium ion (Ca^{2+}) (Berridge, 1985). Cytosolic Ca^{2+} is important in the regulation of many cellular activities. For instance, secretory cell requires Ca^{2+} as the regulator for secretion. Nuclear calcium $(Ca^{2+})_n$ is important in the regulation of a number of nuclear activities such as DNA replication (Jindal *et al.*, 1991), gene transcription (Morgan and Curran, 1986), DNA repair (Bachs *et al.*, 1994) and apoptosis (Jones *et al.*, 1989). In general, the concentration of Ca^{2+} in extracellular medium is in the range of mM level while the intracellular one is as low as nM. Moreover, Ca^{2+} cannot be synthesized or degraded, hence, the fine tune of Ca^{2+} concentration is very important. If the concentration of Ca^{2+} is too high, it may induce apoptosis or programmed cell death (Nicotera *et al.*, 1994).

In general, there are three transporting systems for Ca^{2+} influx from extracellular medium into cytosol. They include receptor-operated channel, voltage-operated channel and Na^{+}/Ca^{2+} exchanger. On the other hand, Ca^{2+} efflux is regulated by Ca^{2+}-ATPase (Figure 1.6a). Ca^{2+} is sequestered by intracellular Ca^{2+} stores such as nucleus and endoplasmic reticulum and mediated by Ca^{2+}-ATPase (Figure 1.6b). Ca^{2+} efflux can be

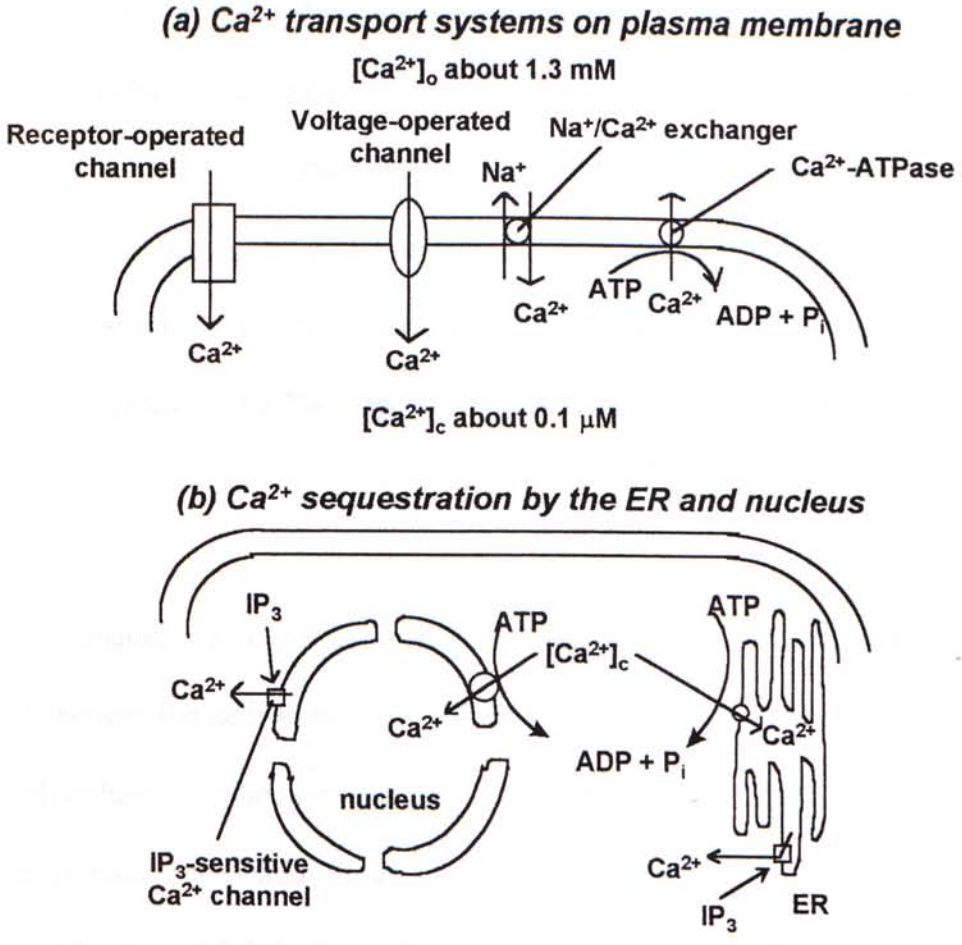

Figure 1.6

Calcium homeostatsis inside a cell. (a) Ca^{2+} transport systems on plasma membrane, (b) Ca^{2+} sequestration by the ER and nucleus and (c) Ca^{2+} cycling in a mitochondrion.

regulated by inositol 1,4,5-trisphosphate (IP_3). The binding of IP_3 to IP_3-sensitive Ca^{2+} channel induces Ca^{2+} release from Ca^{2+} stores (review: Berridge, 1993). Moreover, Ca^{2+} cycling exists in mitochondrion. The uniporter on inner mitochondrial membrane for Ca^{2+} transport is regulated by mitochondrial membrane potential ($\Delta\psi_m$) (Figure 1.6c). The membrane potential of mitochondria is about -180 mV inside. The mitochondrial Ca^{2+} efflux is mediated by Na^+-dependent and Na^+-independent exchanger (review: Vercesi, 1993).

Figure 1.7 shows the phosphoinositide cycle. At first, agonist binds to receptor that induces the activation of G protein which in turn acts on phosphatidylinositol 4,5-bisphosphate phosphodiesterase (PDE), or phospholipase Cβ (PLCβ). PLCβ is an enzyme that degrades phosphatidylinositol 4,5-bisphosphate (PIP_2) into two products, IP_3 and 1,2-diacylglycerol (1,2-DAG). 1,2-DAG acts on inactive form of Ca^{2+}-dependent protein kinase (PKC) and changes it to an active form. The active form of PKC is very important for various functions and also for mitogenesis (Berridge, 1993). On the other hand, IP_3 binds to the IP_3-sensitive receptor that induces the release of Ca^{2+}. In general, IP_3 receptors localize on the cytosolic endoplasmic reticulum. To date, several lines of evidence show that nuclear membrane may have IP_3 receptor (Hennager *et al.*, 1995; Malviya, 1994). Therefore, endoplasmic reticulum and perinuclear space are both Ca^{2+} pools that contain 10^{-6} M Ca^{2+} inside. Moreover, IP_3 is phosphorylated to phosphoinositol 1,3,4,5-tetrakisphosphate (IP_4) by the enzyme, IP_3-3 kinase. IP_4 binds to its receptor, which localized on the plasma membrane and also on the nuclear membrane (Hennager *et al.*, 1995). IP_4 receptor itself is a Ca^{2+} channel that permits Ca^{2+} influx from the external

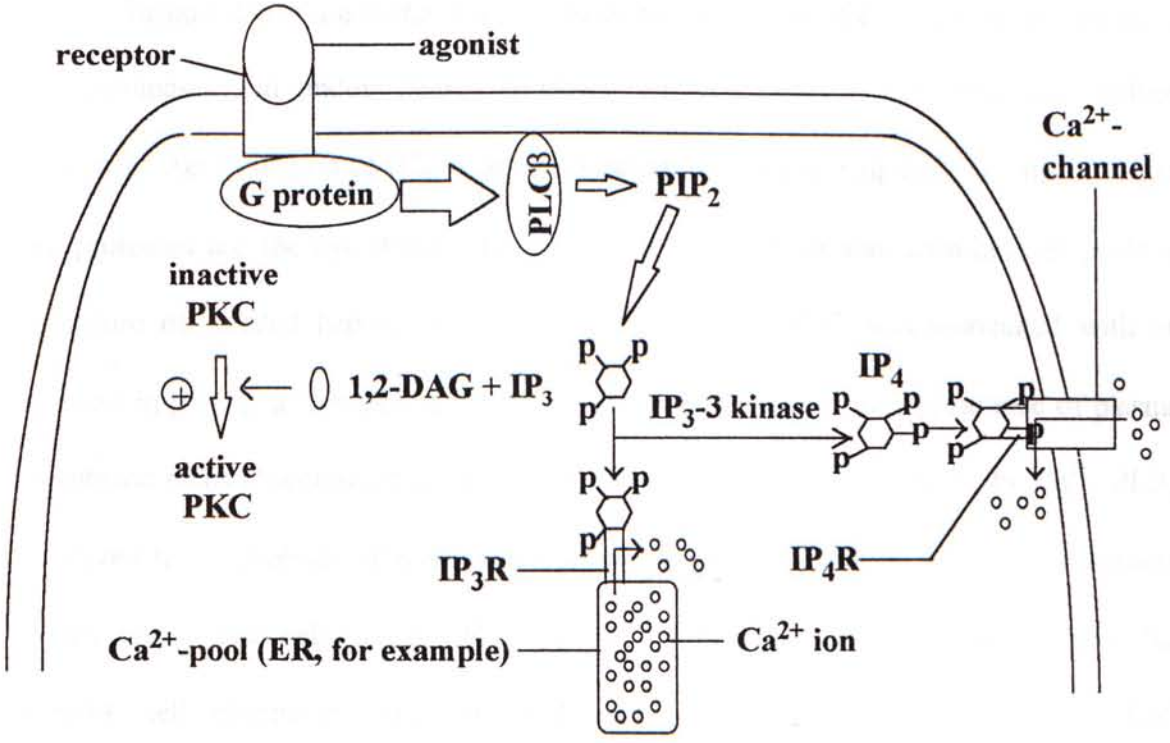

Figure 1.7

The phosphoinositide cycle. The first messenger binds to its specific receptor, activating a G protein that in turn stimulates phospholipase Cβ (PLCβ). Phospholipase Cβ cleaves phosphatidylinositol 4,5-bisphosphate (PIP_2) into two products, inositol 1,4,5-trisphosphate (IP_3) and 1,2-diacylglycerol (1,2-DAG). IP_3 binds to the IP_3 receptor on the Ca^{2+} pool and releases Ca^{2+} into cytosol. 1,2-DAG acts on inactive PKC and produces activated PKC. Both Ca^{2+} and PKC act on other cellular effector molecules.

medium into the cytosol. After finishing the mobilization of Ca^{2+} from Ca^{2+}-pool, IP_3 was degraded (Berridge, 1985).

Sustained increase in the $[Ca^{2+}]_i$ induces the activation of Ca^{2+}-dependent protease, phospholipases and endonucleases (review: Orrenius *et al.*, 1989) that may induce apoptosis. Accumulation of $[Ca^{2+}]_i$ activates proteases such as calpains. The major target for proteases are the cytoskeletal proteins such as α-actinin and actin-binding protein. Exposure of isolated hepatocytes to Ca^{2+} ionophore A23187 was associated with an increase in $[Ca^{2+}]_i$, a stimulation of intracellular proteolysis and the appearance of plasma membrane blebs (Nicotera *et al.*, 1986). Phospholipases can be activated by Ca^{2+}. PLA_2 catalyzes the hydrolysis of membrane phospholipids that requires Ca^{2+} for activation, which could cause cell damage (Chien *et al.*, 1979). Ca^{2+} activates endonucleases that cleaves cell chromatin into oligonucleosomal fragments. Accumulation of Ca^{2+} concentration induced DNA fragmentation in rat liver nuclei (Jones *et al.*, 1989).

Release of calcium after TNF treatment

It is still controversial that TNF does affect the $[Ca^{2+}]_i$ level and involves in cytotoxicity. TNF induces a rapid release of $[Ca^{2+}]_i$ in human neutrophils (Schumann *et al.*, 1993). Moreover, several reports found that TNF induces a slow rise in $[Ca^{2+}]_i$ level in mammary adenocarcinoma cells BT-20 (Bellomo *et al.*, 1992), glial cells (Koller *et al.*, 1996), and L929 cells (Kong *et al.*, 1997). In contrast, Hasegawa and Bonavida reported that human peripheral blood lymphocytes shows a Ca^{2+}-independent pathway of TNF-mediated lysis (Hasegawa and Bonavida, 1989).

1.5.3 Miscellaneous Mechanisms

Other mechanisms may be involved in the cytotoxic effects of TNF. TNF-mediated cytotoxic action involves ADP-ribosylation in target cells. ADP-ribosylation induces NAD^+ and ATP depletion that causes cell death (Weilckens *et al.*, 1982). Agarwal *et al.* found that ADP-ribosylation in TNF-treated L929 cells increases in a time- and dose-dependent manner and the inhibitors of ADP-ribosyl transferase, such as 3-aminobenzamide and nicotinamide, block TNF-mediated cytotoxicity (Agarwal *et al.*, 1988). Reports of the synergistic effects of other cytokines IFN-γ (Fransen *et al.*, 1986) and inhibitors of DNA topoisomerases (Utsugi *et al.*, 1990) may uncover other mechanisms of TNF cytotoxicity. Moreover, the potentiation of TNF cytotoxicity by increased temperatures has been reported (Dubois *et al.*, 1989).

1.6 Objectives of Study

As mentioned before, TNF induces cytotoxic effect in some cell lines. The mechanisms involve the release of ROS and Ca^{2+}. However, their relationship is still unknown. Therefore, the objectives of this study is to investigate the effects of TNF on the release of ROS and Ca^{2+} in L929 cells. Moreover, the relationship between ROS and Ca^{2+} will be examined. The role of Ca^{2+} and ROS in the TNF-induced cytotoxicity will also be investigated. In this connection, the release of ROS and Ca^{2+} were investigated. The effects of antioxidants, mitochondrial inhibitors, and Ca^{2+} chelating agent were studied also. Moreover, the mitochondrial membrane potential, pH and cell cycle were explored.

L929 cells are one of the TNF-sensitive cell lines that is widely used in the field of TNF studies. In fact, cytotoxicity of TNF on L929 cells was first described by Carswell *et al.* in 1975 (Carswel *et al.*, 1975). In this study, L929 cells were chosen as a model since L929 cells is well studied in many reports. The data obtained in this project can be easily compared with others. Moreover, in this study, the effects of TNF on resistant-L929 (rL929) cells were investigated as well. The differences between TNF-sensitive and resistant cell lines and the possible mechanisms account for the resistance to TNF were examined in this project. The effect of TNF on the (1) cytotoxicity, (2) release of ROS, (3) release of Ca^{2+}, and (4) cell cycle were investigated and the responses to TNF in both sensitive and resistant L929 cells were compared.

As described before, the specific activity of MuTNF is about threefold higher than HuTNF on the cytotoxicity of L929 cells. Fiers *et al.* have repeatedly reported on the considerable difference in response *in vivo* between MuTNF and HuTNF (Brouckaert *et al.*, 1986). In normal mice, HuTNF is about 50-fold less toxic than MuTNF (Brouckaert *et al.*, 1992). Therefore, in this study, the effects of recombinant murine TNF (rMuTNF) was selected.

Several approaches were used for studying the effects of TNF on L929 cells. For instance, agarose gel electrophoresis and cytotoxicity assay were used for investigating cell death. Confocal laser scanning microscopy and flow cytometry were used for exploring the release of ROS and Ca^{2+}, pH, mitochondrial membrane potential and cell cycle after TNF treatment.

Chapter 2

Materials and Methods

Chapter 2. Materials and Methods

2.1 Materials

Table 2.1 shows a summary of the common name, chemical name, formula, formula weight and source of chemicals.

2.1.1 Buffer

Preparation of buffer

Buffer was prepared from dissolving chemicals in distilled water and titrated to suitable pH with either HCl or NaOH except specified.

Calcium-free buffer was composed of 130 mM NaCl, 5 mM KCl, 1 mM $MgSO_4$-$7H_2O$, 1 mM Na_2HPO_4-$2H_2O$, 10 mM Tris-HEPES, 0.3 % (w/v) glucose and 5 mM EGTA. Tris-HEPES was prepared from dissolving HEPES into water and titrated to pH 7.4 with Tris-base. Calcium-free buffer was titrated to pH 7.4 by Tris-base. Subsequently, buffer was filtered by bottle-top filter (0.22 μm cellulose acetate membrane, 7111, Falcon, Becton Dickinson, NJ, USA). Buffer was stored at 4 °C.

Lysis buffer for agarose gel electrophoresis was composed of 5 mM Tris, 100 mM EDTA and 1 % SDS (w/v). pH was adjusted to 8.0. Buffer was stored at 4 °C.

Table 2.1
Table of the common name, chemical name, formula, formula weight and source of chemicals used in this project.

Common Name, Chemical name and formula	*Formula Weight*	*Source*
Actinomycin D	1255.4	Sigma Chemical Co., St. Louis, MO, USA
Agarose	—	Sigma Chemical Co., St. Louis, MO, USA
Ammonium chloride (NH_4Cl)	53.49	Riedel-de Haen, AG, Germany
Antimycin A (a mixture of $C_{28}H_{40}N_2O_9$ $C_{27}H_{38}N_2O_9$ $C_{26}H_{36}N_2O_9$ $C_{25}H_{34}N_2O_9$)	548.6 534.6 520.6 506.6	Sigma Chemical Co., St. Louis, MO, USA
BAPTA/AM ([1,2-bis(2)aminophenoxy]ethane-N,N,N^1,N^1-tetra-acetic, acetoxymethyl ester)	764.69	Molecular Probes, Eugene, Oregon, USA
Boric acid (H_3BO_3)	61.83	Riedel-de Haen, AG, Germany
Calcium chloride-2-hydrate ($CaCl_2$-$2H_2O$)	147.02	Riedel-de Haen, AG, Germany
Catalase (from bovine liver) (2000U/mg protein)	—	Sigma Chemical Co., St. Louis, MO, USA
Chloroform ($CHCl_3$)	119.38	Merck, Germany
DCF (2',7'-dichlorofluorescin diacetate) (H_2DCFDA)	487.29	Molecular Probes, Eugene, Oregon, USA
Diltiazem ($C_{22}H_{26}N_2O_4S$)	451	Sigma Chemical Co., St. Louis, MO, USA
2,4-Dinitrophenol (DNP) ($C_6H_4O_5N_2$)	184.1	Sigma Chemical Co., St. Louis, MO, USA
DMSO (dimethylsulphoxide) (CH_3SOCH_3)	78.13	BDH Chemicals Ltd., Poole, England
DNA marker (100 base pair)	—	Pharmacia Biotech, USA
Ethanol (EtOH) (C_2H_5OH)	46.07	BDH Chemicals Ltd., Poole, England
Ethdium bromide (EtBr)	394	Molecular Probes, Eugene, Oregon, USA

Continue **Table 2.1**

Ethylenediaminetetraacetic acid (EDTA) ($C_{10}H_{16}N_2O_8$)	292.2	Sigma Chemical Co., St. Louis, MO, USA
Ethylene glycol-bis(β-aminoethyl ether) N,N,N',N'-tetraacetic acid (EGTA) ($C_{14}H_{24}N_2O_{10}$)	380.4	Sigma Chemical Co., St. Louis, MO, USA
Fetal bovine serum (FBS)	—	GibcoBRL, Life Technologies Inc.
Fluo-3/AM (Fluo-3, acetoxymethyl ester)	1129.86	Molecular Probes, Eugene, Oregon, USA
Fura-red/AM (Fura-red, acetoxymethyl ester)	1089	Molecular Probes, Eugene, Oregon, USA
Gel loading dye (bromphenol blue and glycerol)	—	Kindly provided by Prof. K. P. Fung
Glucose ($C_6H_{12}O_6$)	180.2	Sigma Chemical Co., St. Louis, MO, USA
HEPES (N-[2-hydroxyethyl]piperazine-N'-[2-ethanesulfonic acid])	238.3	Sigma Chemical Co., St. Louis, MO, USA
Hydrochloric acid (HCl)	36.45	BDH Chemicals Ltd., Poole, England
Hydroethidine (HE)	315	Molecular Probes, Eugene, Oregon, USA
Hydrogen peroxide (H_2O_2) (perhydrol 30 % H_2O_2)	34.01	Merck, Darmstadt, Germany
4-Hydroxy-TEMPO (4-OH-TEMPO) ($C_9H_{18}NO_2$)	172.2	Sigma Chemical Co., St. Louis, MO, USA
Ionomycin ($C_{41}H_{72}O_9$)	709	Calbiochem, CA, USA
Isopropanol ($(CH_3)_2CHOH$)	60.1	BDH Chemicals Ltd., Poole, England
Isoamyl alcohol (3-methyl butanol-(1)) ($C_5H_{12}O$)	88.15	Riedel-de Haen, AG, Germany
Magnesium sulfate-7-hydrate ($MgSO_4$-$7H_2O$)	246.48	BDH Chemicals Ltd., Poole, England
MTT (3-[4,5-dimethylthiazol-2-yl]-2,5-diphenyltetrazolium bromide; thiazolyl blue) ($C_{18}H_{16}N_5SBr$)	414.3	Sigma Chemical Co., St. Louis, MO, USA
Molecular sieve (Potassium, Sodium alumino-silicate) (nominal pore diameter: 3 angstrom)	—	Sigma Chemical Co., St. Louis, MO, USA
N-acetyl-L-cysteine (NAc) ($C_5H_9NO_3S$)	163.2	Sigma Chemical Co., St. Louis, MO, USA

Continue **Table 2.1**

Neutral red (3-amino-7-dimethylamino-2-methyl-phenazine hydrochloride) ($C_{15}H_{16}N_4$)	288.8	Sigma Chemical Co., St. Louis, MO, USA
Penicillin-streptomycin (penicillin: 5000U/ml protein streptomycin: 5000μg/ml)	—	GibcoBRL, Life Technologies Inc.
Phenol (C_6H_5OH)	94.11	USB (United States Biochemical), Cleveland, OH, USA
Potassium chloride (KCl)	74.55	Sigma Chemical Co., St. Louis, MO, USA
Potassium phosphate (monobasic anhydrous) (KH_2PO_4)	136.1	Sigma Chemical Co., St. Louis, MO, USA
Propidium iodide (PI)	668.4	Sigma Chemical Co., St. Louis, MO, USA
Proteinase K (from tritirachium album) (16 U/mg protein)	—	Sigma Chemical Co., St. Louis, MO, USA
Rhodamine 123	381	Molecular Probes, Eugene, Oregon, USA
Ribonuclease A (RNase A) (102 U/mg protein)	—	Sigma Chemical Co., St. Louis, MO, USA
Rotenone ($C_{23}H_{22}O_6$)	384.4	Sigma Chemical Co., St. Louis, MO, USA
RPMI (with phenol red)	—	GibcoBRL, Life Technologies Inc.
RPMI (without phenol red)	—	GibcoBRL, Life Technologies Inc.
Ruthenium red	786.35	Sigma Chemical Co., St. Louis, MO, USA
SDS (sodium dodecyl sulfate) ($CH_3(CH_2)_{11}SO_4Na$)	288.38	USB (United States Biochemical), Cleveland, OH, USA
Sheath fluid	—	Becton Dickinson, NJ, USA
SNARF-1/AM (carboxy-seminaphthorhodafluor-1, acetoxymethyl ester)	568	Molecular Probes, Eugene, Oregon, USA
Sodium chloride (NaCl)	58.44	Riedel-de Haen, AG, Germany
Sodium hydrogen carbonate ($NaHCO_3$)	84.01	Riedel-de Haen, AG, Germany

Continue **Table 2.1**

Sodium hydrogen phosphate (Na_2HPO_4)	141.96	Riedel-de Haen, AG, Germany
Super oxide dismutase (manganese-containing) (MnSOD) (4400U/mg protein)	—	Sigma Chemical Co., St. Louis, MO, USA
Thapsigargin	650.76	Molecular Probes, Eugene, Oregon, USA
Thenoyltrifluoroacetone (TTFA) (4,4,4-trifluoro-1-[2-thienyl]-1,3-butanedione) ($C_8H_5F_3O_2S$)	222.2	Sigma Chemical Co., St. Louis, MO, USA
Thimersol (sodium ethylmercurithio-salicylate; mercury-[(o-carboxyphenyl)thio] ethyl sodium salt) ($C_9H_9HgO_2SNa$)	404.8	Sigma Chemical Co., St. Louis, MO, USA
TNF (recombinant murine tumor necrosis factor-alpha)	—	Boehringer Mannheim, Germany
Tris ($NH_2C(CH_2OH)_3$)	121.14	USB (United States Biochemical), Cleveland, OH, USA
Trypsin-EDTA (0.25 % trypsin, 1 mM EDTA)	—	GibcoBRL, Life Technologies Inc.

Phosphate buffered saline (PBS) was composed of 136 mM NaCl, 2.7 mM KCl, 1.5 mM KH_2PO_4 and 8 mM Na_2HPO_4. PBS was titrated to pH 7.4 and sterilized by autoclave. PBS was stored at room temperature.

Sodium-HEPES buffer was composed of 130 mM NaCl, 5 mM KCl, 1 mM $MgSO_4$-$7H_2O$, 1.2 mM Na_2HPO_4, 10 mM Tris-HEPES, 0.3 % (w/v) glucose and 1 mM $CaCl_2$-$2H_2O$. Buffer was titrated to pH 7.4 with Tris-base and filtered by bottle-top filter. Buffer was store at 4 °C.

TBE buffer was composed of 890 mM Tris, 890 mM boric acid and 20 mM EDTA. Buffer was adjusted to pH 7.4. TBE buffer was stored at room temperature.

TE buffer was composed of 10 mM Tris and 0.5 mM EDTA. Buffer was adjusted to pH 7.4. Buffer was stored at room temperature.

2.1.2 Culture Media

Roswell Park Memorial Institute tissue culture medium 1640 (RPMI 1640 medium) was used for cell culture. Each pack of the powder of RPMI 1640 medium with phenol red, L-glutamine and 0.5 mM HEPES was dissolved in 1 liter of dH_2O. The medium was supplemented with 24 mM $NaHCO_3$. The pH of the medium was adjusted to 7.4. Finally, medium was filtered by bottle-top filter. The complete RPMI 1640 medium was supplemented with 1 % penicillin-streptomycin (v/v) and 10 % FBS (v/v). In some experiments, phenol red-free RPMI 1640 medium was used. Colorless RPMI 1640

medium was prepared by dissolving each pack of the powder of RPMI 1640 medium, without phenol red but with L-glutamine, in 1 liter of dH_2O. The medium was supplemented with 24 mM $NaHCO_3$ and 25 mM HEPES. The pH of medium was adjusted to 7.4. The medium was filtered by bottle-top filtered. The serum-free, colorless RPMI 1640 medium was supplemented with 1 % penicillin-streptomycin only. Culture media were stored at 4 °C.

2.1.3 Chemicals

Antioxidants such as NAc, 4-OH-TEMPO, catalase and MnSOD were used. All of them were dissolved in culture medium. Antioxidants should be prepared freshly except MnSOD (stock concentration was 6.25 mg/ml) that was stored at -70 °C after dissolving in medium. NAc was acidic after dissolving in medium, therefore, pH should be adjusted to 7.4.

Calcium-chelator such as BAPTA/AM was used. It was dissolved in DMSO (excess water was absorbed by molecular sieve). The stock concentration was 2.5 mM and it was stored at 4 °C.

Calcium-inducing agents such as thapsigargin, ionomycin and thimersol were used. Thapsigargin and ionomycin were dissolved in DMSO whereas the stock concentration were 0.5 mM and 2 mg/ml, respectively. Thimersol was dissolved in dH_2O and the stock concentration were 5 mM. Thapsigargin and thimersol were stored at 4 °C whereas ionomycin was store at -70 °C.

Dye for cytotoxicity assay such as neutral red and MTT were prepared. 0.5 g neutral red powder was dissolved in 100 ml 0.9 % NaCl (normal saline). The final percentage of neutral red was 0.5 % (w/v) and it was stored at room temperature. The precipitate of neutral red was filtered by filter paper (Whatman). 5 mg/ml MTT was prepared by dissolving MTT powder in PBS and filtered by filter paper. MTT solution was stored at 4 °C.

Fluorescence dye such as fluo-3/AM, fura-red/AM, DCF, HE, SNARF-1/AM, rhodamine 123 and PI were used. The fluorescence dyes for Ca^{2+} studies include fluo-3/AM and fura-red/AM. The fluorescence dyes for ROS were DCF and HE. All of them were dissolved in DMSO and the stock concentration was 2.5 mM. The fluorescence indicators for pH was SNARF-1/AM. SNARF-1/AM was dissolved in DMSO and the stock concentrations was 2.5 mM. Rhodamine 123 is the indicator for mitochondrial membrane potential. It was dissolved in absolute EtOH and the stock concentration was 0.5 mM. DNA chelating dye such as PI was prepared. PI was dissolved in PBS. The stock concentration of PI was 2 mg/ml. Except rhodamine 123 that was stored at -20 °C, all fluorescence dyes were kept at 4 °C.

Lysis buffer for cytotoxicity assay such as 1 % SDS (w/v) in dH_2O and 0.04 N HCl in isopropanol were prepared. Both SDS and acidified isopropanol were stored at room temperature.

Mitochondrial-calcium-cycling inhibitors such as ruthenium red and diltiazem were used. Ruthenium red and diltiazem were dissolved in Na^+-HEPES buffer and dH_2O respectively. The stock concentration of ruthenium red was 5 mM and diltiazem was 50 mM. They were stored at 4 °C.

Mitochondrial inhibitors include rotenone, TTFA, antimycin A and DNP. Rotenone was dissolved in DMSO. TTFA, antimycin A and DNP were dissolved in absolute EtOH. The stock concentration of rotenone, antimycin A and DNP were 5 mM whereas TTFA was 50 mM. All mitochondrial inhibitors were kept at 4 °C.

Protein inhibitor such as actinomycin D was used. The powder of actinomycin D was dissolved in serum-free RPMI and the stock concentration was 1 mg/ml. It was stored at -20 °C.

Recombinant murine TNF-α is produced from *Escherichia coli* and purified by standard chromatographic techniques (Manuel from Boehringer Mannheim, Germany). It was dissolved in PBS. The specific activity is $\cong 6.0 \times 10^7$ U/mg. One unit is defined as the amount of TNF that is required to mediate half-maximal cytotoxicity with L929 cells in the presence of actinomycin D. The stock concentration of TNF was 5μg/ml. TNF was aliquot and stored at -70 °C. Repeated freezing and thawing should be avoided.

Preparation of other chemicals such as $MnCl_2$, NH_4Cl, agarose, proteinase K, RNase A and EtBr were used. $MnCl_2$ was dissolved in Ca^{2+}-free buffer and the stock

concentration was 1 M. NH_4Cl was dissolved in dH_2O and stock concentration was 3.75 M. Both $MnCl_2$ and NH_4Cl were kept at 4 °C. The powder of agarose was dissolved in TBE buffer and final percentage was 1.5 % (w/v). Proteinase K and EtBr was dissolved in dH_2O and the stock concentrations were 20 mg/ml and 0.5 μg/ml, respectively. RNase A was prepared from dissolving in TE buffer and the stock concentration was 10 mg/ml. Proteinase K and RNase A were stored at -20 °C whereas EtBr was kept at room temperature.

Chemicals such as H_2O_2, phenol, chloroform, isoamyl alcohol, gel loading dye, DNA marker, trypsin and sheath fluid were also applied. H_2O_2 should be freshly diluted from stock (9.8 M).

2.1.4 Culture of Cells

2.1.4.1 Tumor Necrosis Factor-Alpha-Sensitive Cell Line, L929

L929 cells were purchased from American Type Culture Collection (ATCC, Rockville, MD, USA). They were derived from transformed fibroblasts in C3H mice. They were maintained in RPMI 1640 medium and supplemented with 10 % FBS and 1 % Penicillin-streptomycin (complete RPMI). L929 cells were kept at 37 °C, 5 % CO_2 incubator (SHEL LAB) with humidified atmosphere. Cells were cultured in 25 cm^2, 75 cm^2 or 150 cm^2 culture flask (Corning) and were kept the passage every 3 or 4 days. For every passage, medium was discarded and washed once with PBS. Cells were trypsinized by the application of trypsin. The cells suspension was collected by addition of complete

RPMI and was centrifuged at 1500 r.p.m. for 3 min. Cells were then resuspended in complete RPMI and passaged to a new flask.

2.1.4.2 Tumor Necrosis Factor-Alpha-Resistant Cell Line, rL929, rL929-11E and rL929-4F

rL929, rL929-11E and rL929-4F were kindly provided by Prof. K. P. Fung and H. K. Cheng (Department of Biochemistry, CUHK). The isolation of TNF-resistant variants of L929 cells were according to the methods described by Zimmerman *et al.* with modifications (Zimmerman *et al.*, 1989). The modified methods were described by Kwan (Kwan, 1995). Briefly, L929 cells were subcultured into 25 cm^2 culture flasks and 20 units/ml TNF was added into medium. The cells were maintained in this medium for a period of two weeks with a change of fresh medium every 3 days. Dead cells were washed away and living cells were allowed to grow to confluence again. TNF concentration was then increased to 50, 100, 200, 1000, and 2000 units/ml in a stepwise manner. Finally, three cell clones, rL929, rL929-11E and rL929-4F, were isolated. Resistant cells were kept at 37 °C, 5 % CO_2 incubator. The method of passage was the same as that of L929.

2.2 Methods

2.2.1 Agarose Gel Electrophoresis

The DNA fragmentation resulting from apoptosis was investigated with electrophoresis of DNA extracts according to Park *et al.* with modifications (Park *et al.*, 1996).

One million of L929 cells in complete RPMI 1640 medium were seeded in 6-well plate (Corning) and incubated at 37 °C, 5 % CO_2 overnight until confluence. Cells were then treated with TNF for various time intervals. The suspension of dead cells were collected. The adherent cells were washed with PBS and trypsinized. L929 cells were resuspended in lysis buffer and proteinase K (200 μg) and incubated at 37 °C overnight. DNA was extracted by phenol-chloroform:isoamyl alcohol (24:1) method and spun by centrifuge (MSE, MicroCentaur, Sanyo) at 10,000 r.p.m. for 1 min. After centrifugation, the aqueous layer was extracted, mixed with chloroform:isoamyl alcohol and centrifuged at 10,000 r.p.m. for 1 min. The aqueous layer was extracted and was mixed with 5 M ice-cold NaCl and absolute ice-cold EtOH, and stored at -20 °C overnight. Mixture was spun at 10,000 r.p.m. by using Heraeus Centrifuge (Sepatech Biofuge B, Heraeus) for 5 min and then centrifuged at 14,000 r.p.m., 4 °C by Eppendorf Centrifuge (5402, Eppendorf) for 25 min. EtOH was drained away and air-dry overnight. 20 μg RNase A and TE buffer were added, and incubated at 37 °C for 2 hr. The DNA content in the final preparation was estimated by spectrophotometer (U-2000, Hitachi) at O.D. 260. DNA solution was diluted so that O.D. 260 of the 4 μl-to-0.5 ml DNA solution become 0.1. 10 μl of the diluted DNA solution was mixed with 2 μl gel loading dye and DNA marker (100 b.p.), and loaded in 1.5 % agarose gel in TBE. DNA was run for 2 hr at 60 volts. DNA was stained with EtBr for 30 min and washed twice with dH_2O. The image of the gel was taken by photographing with polaroid film (type 667, Polaroid (U.K.) Ltd., England) under UV illumination.

2.2.2 Cytotoxicity Assay

The viability of cells can be determined by various assays such as neutral red assay, [^{3}H]thymidine release assay, crystal violet assay (Flick and Gifford, 1984) and MTT assay (Schulze-Osthoff *et al.*, 1992). In this study, neutral red and MTT assays were used for determining cell viability since both of them are easier to be applied.

Neutral red assay

L929 cells were seeded at 3 x 10^4/well in 100 µl of complete RPMI 1640 medium in 96-well flat bottom microtiter plates (Corning) and incubated for 20 hr at 37 °C, 5 % CO_2 incubator until confluence. Spent medium was removed. Cells were washed twice by serum-free RPMI medium and 100 µl of diluted TNF of various concentrations and drugs in serum-free RPMI medium were added to wells. Control wells contained serum-free medium only. Plates were re-incubated at 37°C, 5 % CO_2 for another 20 hr. After incubation, cells were washed twice with PBS. 50 µl/well 0.5 % neutral red (w/v) was added to each well and incubated for 1 hr at 37 °C, 5 % CO_2. Subsequently, dye was removed and the wells were washed twice with PBS. Plates were air-dry in oven overnight. The cells were lyzed with 1 % SDS (w/v). Absorbance of wells at 540 nm was determined by using microplate reader (BIO-RAD). 1 % SDS was used as blank.

MTT assay

The procedure for MTT assay is similar to that of neutral red assay. Briefly, L929 cells were seeded at 3 x 10^4/well in a 96-well plate and were treated with various concentrations of TNF and drugs in serum-free medium. After incubation, medium was

discarded. 100 µl serum-free RPMI and 20 µl MTT were added per well. Plates were incubated at 37 °C, 5 % CO_2 incubator for 2 hr. MTT solution was discarded and 100 µl/well of acidified isopropanol was added to each well. Plates were incubated at 37 °C for 15 min. Absorbance of wells at 540 nm was determined by using microplate reader. Acidified isopropanol was used as blank.

Statistical calculations

Samples were tested in triplicate or septuplicate in each plate. Percentage cytotoxicity is means ± standard deviation (S.D.). Percentage cytotoxicity is defined as follows:

$$\text{Percentage cytotoxicity} = 100\ \% \times (\text{O.D. control} - \text{O.D. test}) / (\text{O.D. control})$$

whereas control cells were incubated with medium only. Statistical significance was claimed only at p-value less than 0.05 or 0.005. The smaller the p-value is, the more the significance for the test.

2.2.3 Confocal Laser Scanning Microscopy

Introduction

Confocal laser scanning microscopy (CLSM) allows 3-D measurements of biological structures with little blur and high spatial contrast (review: Schild, 1996; Lichtman, 1994). CLSM achieves high resolution of a selected plane in a specimen by means of three basic steps (Figure 2.1). First, light is focused by an objective lens into an

hourglass-shaped beam so that the beam strikes one spot at some chosen depth in a specimen (Figure 2.1). Next, light reflected from that spot is focused to a point and allowed to pass in its entirety through a pinhole aperture in a mask positioned in front of a detecting device such as photomultiplier tube (PMT). Meanwhile the opaque regions around the pinhole block out most of the rays that would tend to obscure the resulting image, those reflected by illuminated parts of the specimen lying above and below the plane of interest. Finally, the light is moved rapidly from point to point in the specimen until the entire plane has been scanned.

Procedure for detecting cell activity by CLSM

About 2,000 L929 cells were seeded on a round cover glass with complete RPMI 1640 medium and incubated at 37 °C, 5 % CO_2 for 3 or 4 days.

Detection of $[Ca^{2+}]_i$ by CLSM: During the experiment, cover glass was mounted on a home-made holder. Cells were then washed twice with Na^+-HEPES buffer and loaded with fluo-3/AM (final concentration: 10 μM) at room temperature for 1 hr. After loading of dye, cells were washed twice with Na^+-HEPES buffer or Ca^{2+}-free buffer. The final volume of buffer was 0.5 ml in all experiments since change of volume of buffer during the experiment will affect the position of the confocal plane (Lui *et al.*, 1997). Cells were then observed under CLSM at room temperature and TNF was added during scanning. At various time intervals, x-y images of cells were acquired on a system of CLSM (Multiprobe 2001, Molecular Dynamics (MD)), or InSight Plus, (Meridian, Miss., USA) that fitted with an argon laser (6 mW at excitation for CLSM-MD, 5 mW at

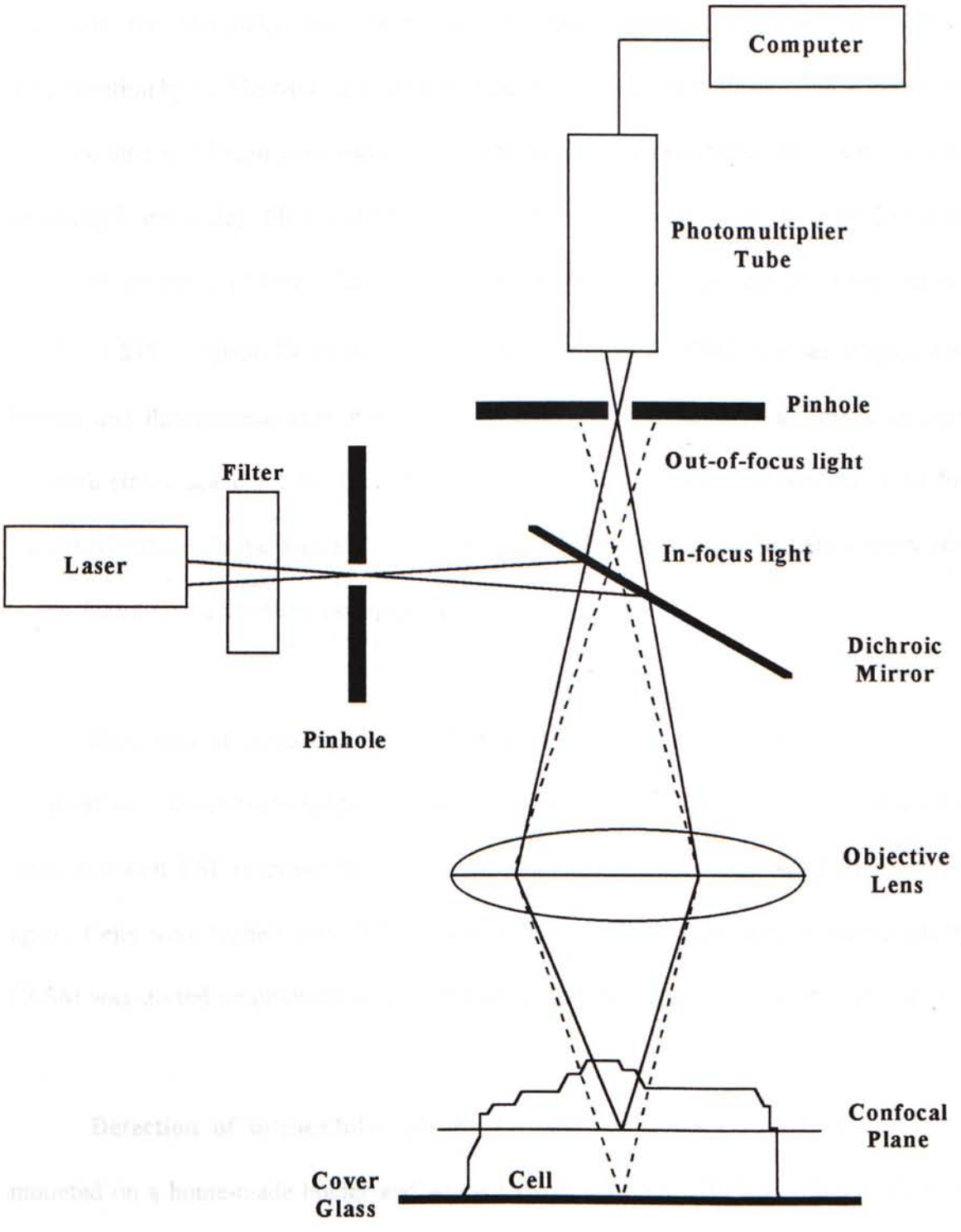

Figure 2.1
Principle of CLSM.

excitation for Meridian) and Nikon diaphot inverted microscope. For fluorescence determination by CLSM-MD, an excitation filter with 488 nm wavelength and a long-pass emission filter of 510 nm were used. For CLSM-Meridian, an excitation filter with 488 nm wavelength and a clear filter was used. L929 cells were scanned by using a 60X (Nikon PlanApo) or 100X (Nikon, Fluor) oil objectives with low-fluorescence immersion oil ($\eta^{23°C}$ = 1.515, Stephens Scientifics, USA). The voltage of the PMT was set at optimum. Images and fluorescence intensities were processed and averaged by an image analysis software (Imagespace 3.1 for CLSM-MD, or Insight IQ Master Program ver. 1.12 for CLSM-Meridian). In the pseudo-color images, cool and warm colors indicate a lower and higher fluorescence intensity, respectively.

Detection of intracellular ROS by CLSM: Cover glass with L929 cells was mounted on a home-made holder and washed twice with Na^+-HEPES buffer. Cells were incubated with TNF or drugs for 15 min and then washed twice with Na^+-HEPES buffer again. Cells were loaded with DCF or HE in Na^+-HEPES buffer and measurement by CLSM was started simultaneously. The setting of detection was similar to that of $[Ca^{2+}]_i$.

Detection of intracellular pH by CLSM: Cover glass with L929 cells was mounted on a home-made holder and washed twice with Na^+-HEPES buffer. Cells were then loaded with SNARF-1/AM in Na^+-HEPES buffer (final concentration: 10 μM) for 1 hr at room temperature. After loading, cells were washed twice with Na^+-HEPES buffer. Cells were then observed by CLSM and the setting of detection was similar to that of $[Ca^{2+}]_i$.

2.2.4 Flow Cytometry

Introduction

Flow cytometry (FCM) has been used extensively to analyze various biological properties of cells (Ormerod, 1994). FCM is the measurement of cells in a flow system that has been designed to deliver particles in single file past a point of measurement. A basic flow cytometer consists of a source of light such as laser beam, a flow cell, optical components to focus light of different colors on to the detectors, electronics to amplify and process the resulting signals and a computer (Figure 2.2). The flow cell is to deliver cells singly to a specific point by hydrodynamic focusing at which the source of light is focused. This is achieved by injection of the sample into the center of a stream of liquid called the sheath fluid. Light source strikes on the cells and the emission of light is collected by detectors. Image analysis by computer was then made to study the distribution of light signals emitting from a population of cells.

Procedure for detecting cell activity by FCM

One million of L929 cells in complete RPMI 1640 medium were seeded in a 6-well plate and incubated at 37 °C, 5 % CO_2 overnight until confluence. Cells were then treated with TNF and different drugs for various time intervals. The procedure for detecting Ca^{2+}, ROS, mitochondrial membrane potential (ψ_m) and cell cycle are different.

Detection of $[Ca^{2+}]_i$ by FCM: After incubation with TNF or drugs, cells were washed twice with serum-free RPMI 1640 medium for removing non-adherent cells. The adherent cells were loaded with fluo-3/AM and fura-red/AM in serum-free RPMI medium

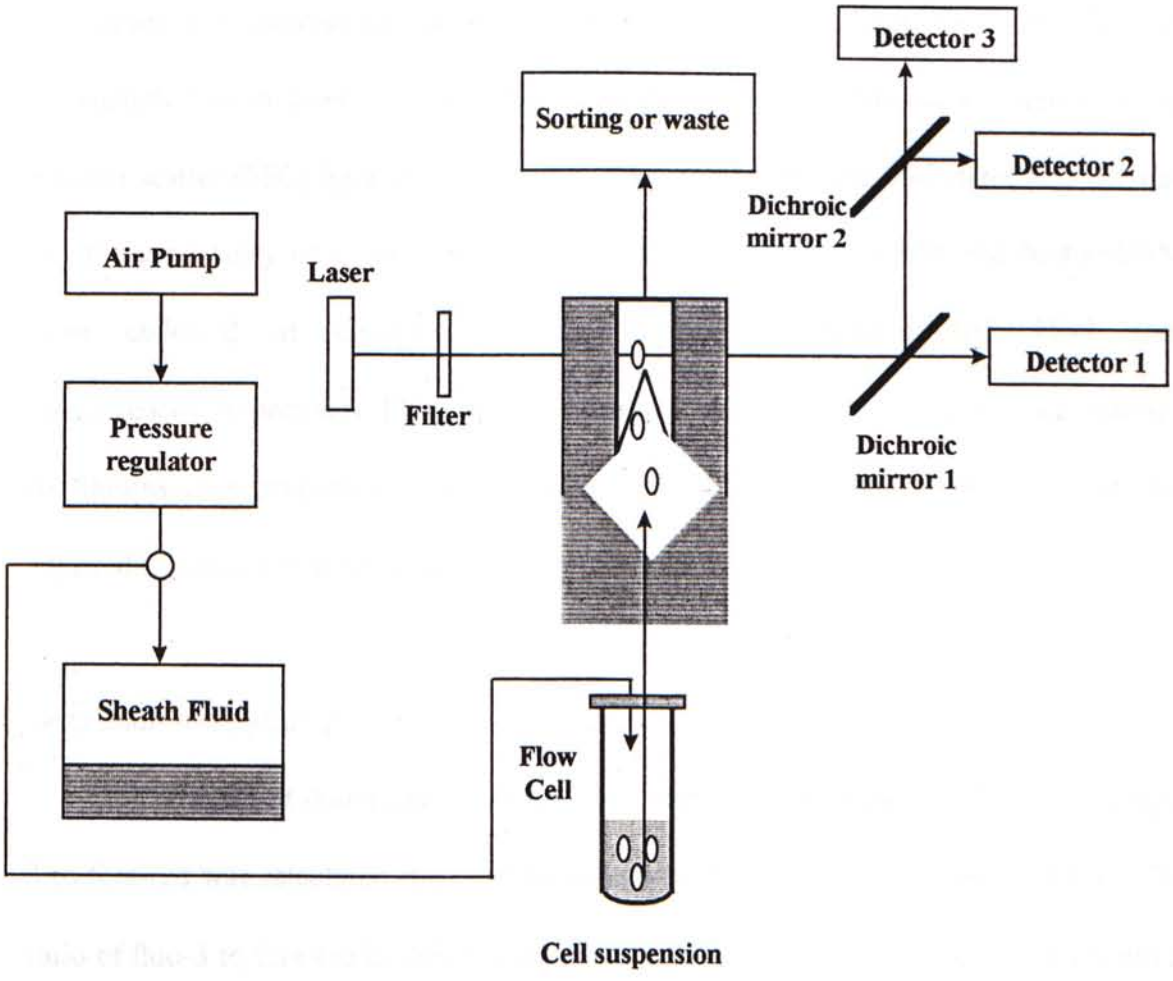

Figure 2.2
Principle of FCM (Becton Dickinson, FacSort model).

for 1 hr. Only the adherent cells were loaded with fluorescence dyes. Cells were then trypsinized and washed twice with Na^+-HEPES buffer. L929 cells were suspended in Na^+-HEPES buffer. Cells were acquired on a system of FACSort flow cytometer (Becton Dickinson). The acquisition of cells were analyzed by lysys II program (Becton Dickinson). For fluorescence determination by FCM, an excitation filter with 488 nm wavelength (argon laser) was selected. The population of cells were determined by forward scatter (FSC) light and side scatter (SSC) light. FSC and SSC determine the size and the granularity of a cell, respectively. The signals of fluo-3/AM and fura-red/AM were collected at channels of FL-1 (green fluorescence) and FL-3 (red fluorescence), respectively. FL-1 and FL-3 were set at linear scale. For one single analysis, the fluorescence properties of 10,000 cells were collected. The sample flow rate was adjusted to about 1,000 cells/sec.

Data analysis of $[Ca^{2+}]_i$

The mean of fluorescence of fluo-3 and fura-red were collected. The ratio of fluo-3 to fura-red was calculated and used for comparing the extent of the release of Ca^{2+}. The ratio of fluo-3 to fura-red in different treatments was compared with that of control group and presented in percentage of control. Furthermore, the dot plots of fluo-3 against fura-red was analyzed. Each dot represented one cell. The dot plot was divided by a diagonal line into two regions, R1 and R2 (Figure 2.3). Number of dots in both R1 and R2 were recorded. Addition of ionomycin (40 μg/ml) for 10 min induced Ca^{2+} release and was used for positive control. When the $[Ca^{2+}]_i$ level increased, fluorescence of fluo-3 increased

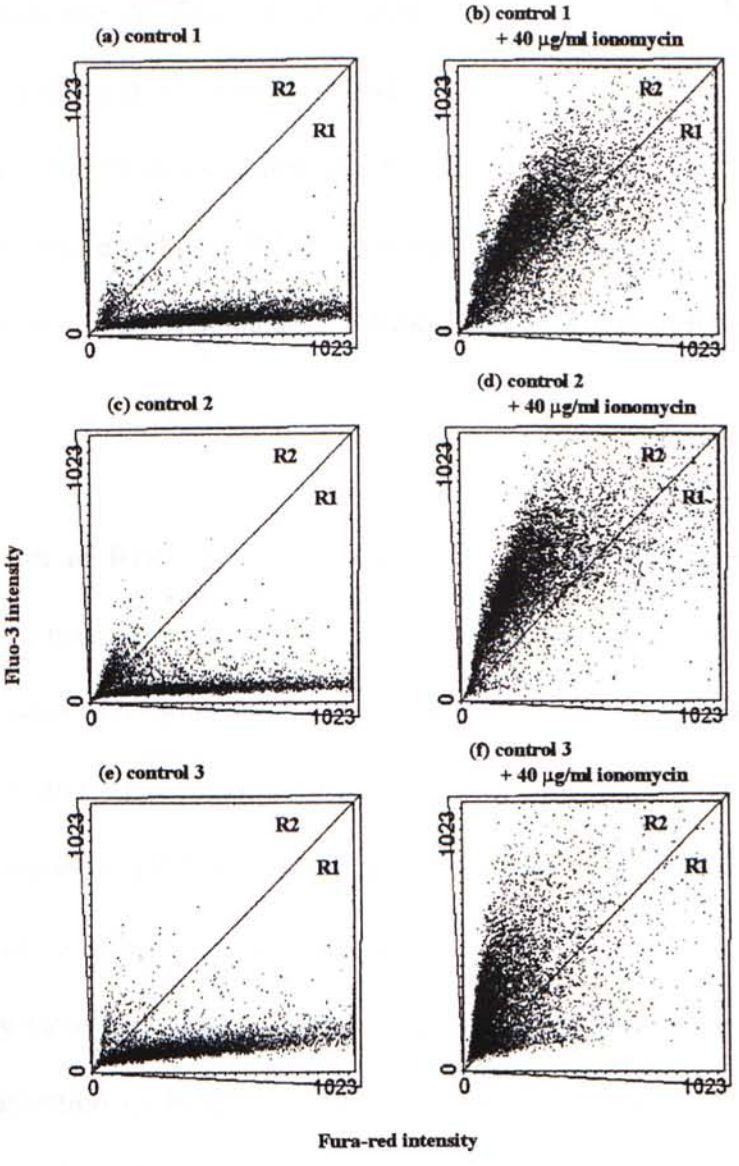

Figure 2.3

Analysis of $[Ca^{2+}]_i$ changes by the use of fluo-3 and fura-red. L929 cells (10^6/ml) were seeded in a 6-well plate and were incubated overnight at 37 °C, 5 % CO_2. Cells were loaded with 10 μM fluo-3/AM and 10 μM fura-red/AM for another hr. Cells were then trypsinized. After washing, cells were re-suspended in the Na^+-HEPES buffer and the fluorescence of fluo-3 and fura-red were determined by FCM with an argon laser. Y-axis represents the fluorescence intensity of fluo-3 whereas x-axis represents the fluorescence intensity of fura-red. Panels (a), (c) and (e) are control group from different experiments. Panels (b), (d) and (f) are three experiments in which L929 cells were treated with 40 μg/ml ionomycin 10 min before measurement. Note that a shift in the cell population at the upper-left in panels (b), (d) and (f) indicates an increase in fluo-3 fluorescence with a decrease in fura-red. These imply an increase in $[Ca^{2+}]_i$. Dot plots were divided arbitrarily by a diagonal line into two regions, R1 and R2. And the % of cells in each region was calculated.

whereas fluorescence of fura-red decreased, the cell population shifted to the upper-left (Figure 2.3). If the $[Ca^{2+}]_i$ level was high in L929 cells, more dots should occur in R1 and vice versa in R2. Table 2.2 summarizes the results from Figure 2.3. The summation of the number of dots in R1 and R2 was 10,000, that was the total number of cells in analysis. Addition of ionomycin induced a drastic shift of dots from R1 to R2 (Figure 2.3b, d and f).

Detection of ROS and cell death by FCM: After incubation with TNF and drugs, cells were washed twice with serum-free RPMI 1640 medium and trypsinized. Cells were washed twice with serum-free medium and re-suspended. DCF, DCF with PI, or HE was added to the suspension and measurement was started simultaneously. The fluorescence signals of DCF and PI/HE were collected at channels of FL-1 and FL-3, respectively. FL-1 and FL-3 were set at log scale. HE and PI cannot be applied simultaneously since they have the same emission wavelength (collected at FL-3). Other settings for detection of ROS was similar to that of $[Ca^{2+}]_i$. The mean of DCF was collected and used for determining the extent of ROS release in different treatments and compared to control group.

Data analysis of cell death

The proportion of dead cells could be analyzed by the dot plots of PI against DCF (Figure 2.4). Dot plot was divided into three regions, R1, R2 and R3. Population R1 with PI-negative fluorescence properties, indicating viable cells. Population R2 with PI-positive fluorescence properties, indicating dying cells population. Population R3 with PI-positive

Table 2.2
Ionomycin induced Ca^{2+} release.

Treatment	control 1	+ 40 μg/ml ionomycin	control 2	+ 40 μg/ml ionomycin	control 3	+ 40 μg/ml ionomycin
Fluo-3 intensity (arbitrary unit)	74.68	395.34	65.15	455.11	89.49	285.34
Fura-red intensity (arbitrary unit)	406.65	303.30	274.39	281.27	304.80	174.81
Fluo-3 /Fura-red	0.18	1.30	0.24	1.62	0.29	1.63
% of control * (%)	722		675		562	
Number of cells in R1	9684	2285	9176	1286	9550	1883
Number of cells in R2	316	7715	824	8714	450	8117

Results from Figure 2.3 were summarized and the peak fluorescences at the x- and y-axis were acquired. The ratio of fluo-3 to fura-red was then calculated and the % of control was obtained according to the following formula:

* % of control (%)

= [fluo-3 / fura-red (TNF treatment)] / [fluo-3 / fura-red (control)] x 100 %

Moreover, the number of dots in R1 and R2 were determined.

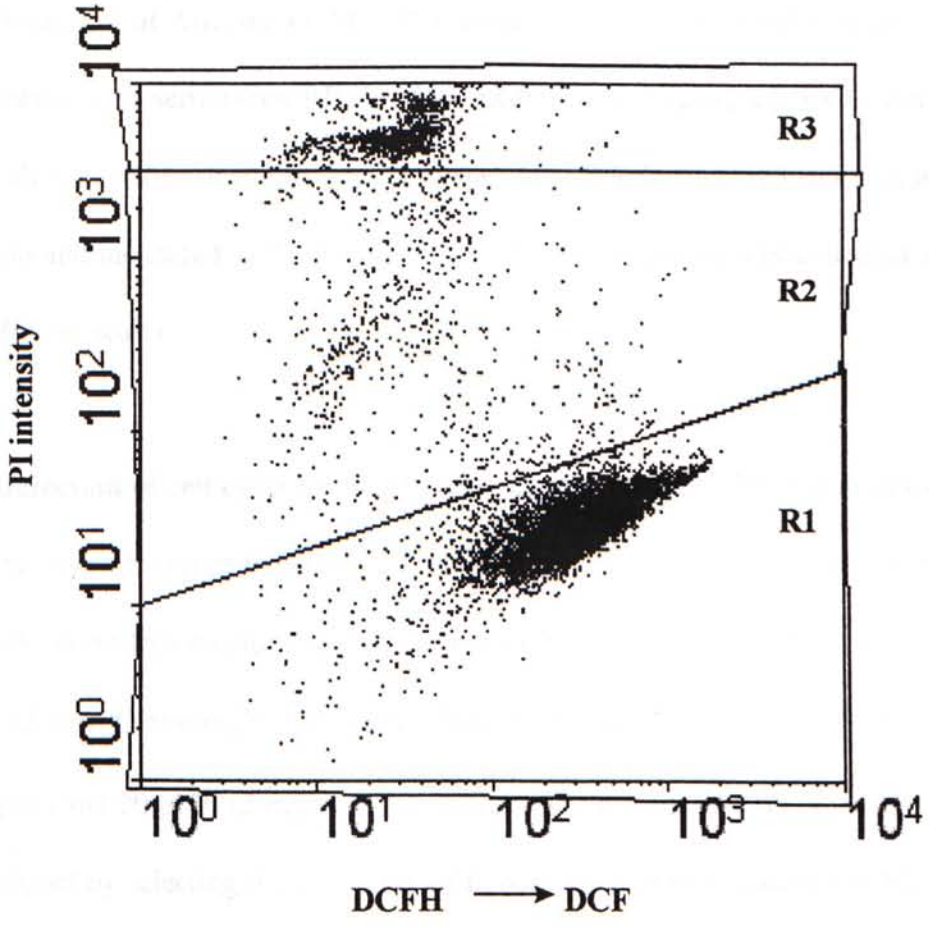

Figure 2.4

Dot plots of PI against DCF. L929 cells (10^6/ml) were seeded in a 6-well plate and were incubated overnight at 37 °C, 5 % CO_2. Cells were then trypsinized and were re-suspended in the serum-free RPMI. Cells were then loaded with 10 μM DCF and 8 μg/ml PI. Measurement was made by FCM. Y-axis represents the fluorescence intensity of PI whereas x-axis represents the fluorescence intensity of DCF. The dot plot was divided by two line into three regions, R1, R2 and R3. The % of cells in each region was also calculated.

fluorescence properties, indicating dead cells. Number of dots in the three regions were recorded.

Detection of $\Delta\psi_m$ by FCM: After incubation with TNF and/or drugs, cells were washed twice with serum-free RPMI 1640 medium and trypsinized. Cells were washed twice with serum-free medium and re-suspended. Rhodamine 123 was added to the suspension and incubated at 37 °C for 15 min. The fluorescence was collected at channel of FL-1 (linear scale).

Detection of cell cycle by FCM: After incubation with TNF and drugs, cells were washed twice with serum-free RPMI 1640 medium and trypsinized. Cells were washed twice with serum-free medium and re-suspended in ice-cold 70 % EtOH. Cell suspension was stored at 4 °C overnight. Cells were then re-suspended in 800 μl PBS, 100 μl RNase A (1 mg/ml) and 20 μl PI (2 mg/ml). The mixture was incubated at 37 °C for 30 min. Cells were analyzed by selecting the collection of fluorescence of PI at channel of FL-2A (linear scale) and/or FL-2H (log scale).

All data from FCM were analyzed by WinMDI version 2.6 that was downloaded from internet (www site: 'http://facs.scripps.edu/software.html').

Chapter 3

Results

Chapter 3. Results

3.1 Tumor Necrosis Factor-Alpha Induced Apoptosis in L929 Cells

3.1.1 Introduction

Carswell *et al.* firstly described that L929 cells are sensitive to TNF action (Carswell *et al.*, 1975). Since then, L929 cells are widely used as a model to study the mechanisms of cytotoxicity mediated by TNF.

For determining cell viability, two assays were used in this project, the MTT and the neutral red assay. MTT is a pale yellow substrate that produces a dark blue formazan product. MTT is cleaved to form formazan by active mitochondria in all living, metabolically active cells but not dead cells. MTT is converted into formazan derivative via mitochondrial dehydrogenase activity by viable cells (Pagliacci *et al.*, 1993). The MTT formazan reaction product is partially soluble in medium, and so an alcohol such as acidified isopropanol is used to dissolve the formazan and produce a homogeneous solution suitable for measurement of optical density. The amount of formazan generated is therefore directly proportional to the number of viable cells (Mosmann, 1983). On the other hand, neutral red is a dye that is commonly used for staining viable cells. Neutral red is taken up by viable cells but not by dead cells. The uptake is an energy-dependent process. The stained cells are solublized by SDS and a homogeneous colored solution is produced for the measurement of color intensity.

L929 cells were seeded in a 96-well plate and the optimal cell density of L929 cells was determined. Figure 3.1 and Figure 3.2 show the relationship between the optical density (O.D.) at 540 nm and the cell density of L929 cells by the MTT and neutral red assays, respectively. It was found that the density of cell at or below 3 x 10^4/well was an optimum for MTT assay since the slope of the curve is almost linear in this region. As the density of cell increased, the O.D. 540 nm for neutral red assay increased also. Similar result was obtained by neutral red assay. Moreover, L929 cells reached confluence in a 96-well plate 20 hr after seeding with a cell density of 3 x 10^4/well. Therefore, the density of L929 cells was set at 3 x 10^4/well in cytotoxicity assays.

Figure 3.3a shows that TNF induced cell death by using neutral red assay. Similar results were obtained by using MTT assay (Figure 3.3b). It was found that the cytotoxicity of TNF-treated L929 cells is concentration dependent. As TNF concentration increased, cytotoxicity increased also. In a 20-hr treatment, the LC_{50} of TNF on L929 cells was less than 5 ng/ml (with cell density: 3 x 10^5/ml) (Figure 3.3a and 3.3b). As the cell density of experiments of FCM was 1 million/ml, higher concentration of TNF should be used and the concentration of TNF was arbitrarily set as 50 ng/ml.

3.1.2 TNF Induced DNA Fragmentation in L929 cells

To determine whether TNF induces apoptosis or necrosis in L929 cells, gel electrophoretic analysis of DNA fragmentation was applied.

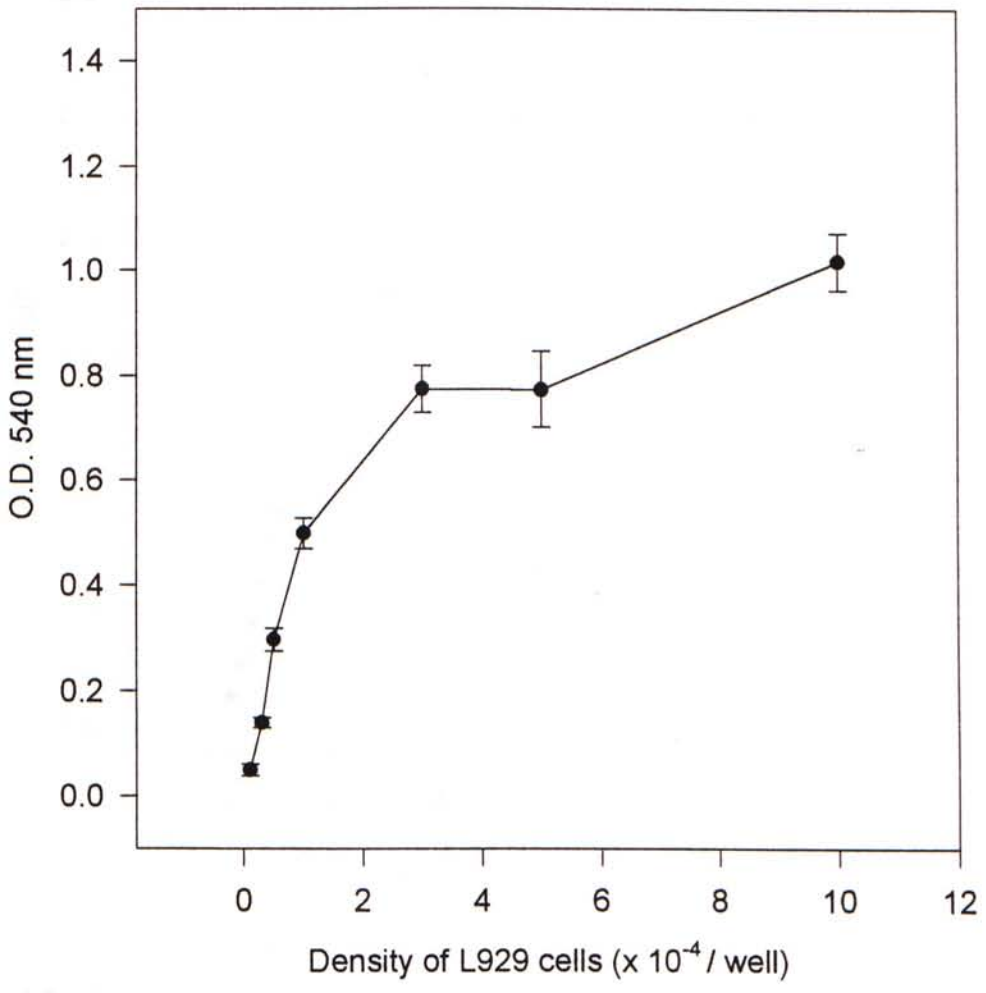

Figure 3.1

Optical density (O.D.) 540 nm was proportional to the cell density of L929 cells in MTT assay. As described in materials and methods, L929 cells were seeded at different density (10^3 - 10^5/well) in complete RPMI 1640 medium and incubated for 20 hr at 37 °C, 5 % CO_2. After incubation, spent medium was discarded and washed twice by serum-free medium. 100 µl of serum-free medium was added to each well and incubated for 20 hr at 37 °C, 5 % CO_2. MTT assay was then applied and O.D. 540 nm was read by a microplate reader (n = 5, expt = 2).

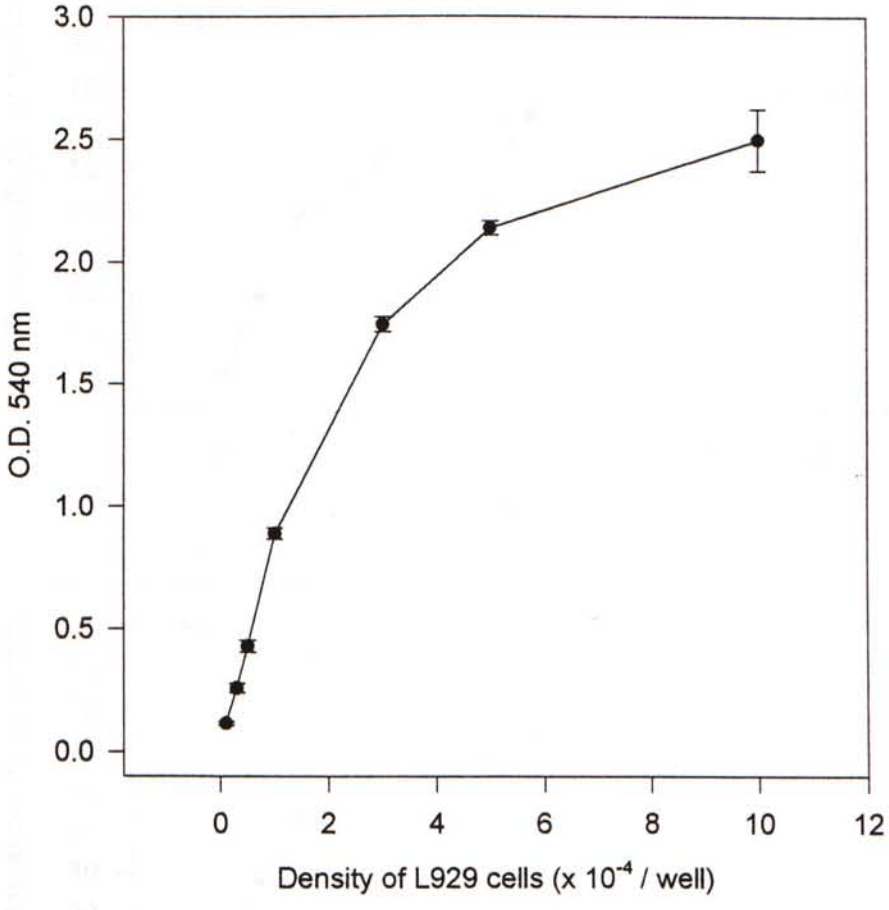

Figure 3.2
Optical density (O.D.) 540 was proportional to the cell density of L929 cells in neutral red assay. L929 cells were seeded at different density (10^3 - 10^5/well) in complete RPMI 1640 medium and incubated for 20 hr at 37 °C, 5 % CO_2. After incubation, spent medium was discarded and washed twice by serum-free medium. 100 µl of serum-free medium was added to each well and incubated for 20 hr at 37 °C, 5 % CO_2. Neutral red assay was then applied and O.D. 540 nm was read by a microplate reader (n = 5, expt = 2).

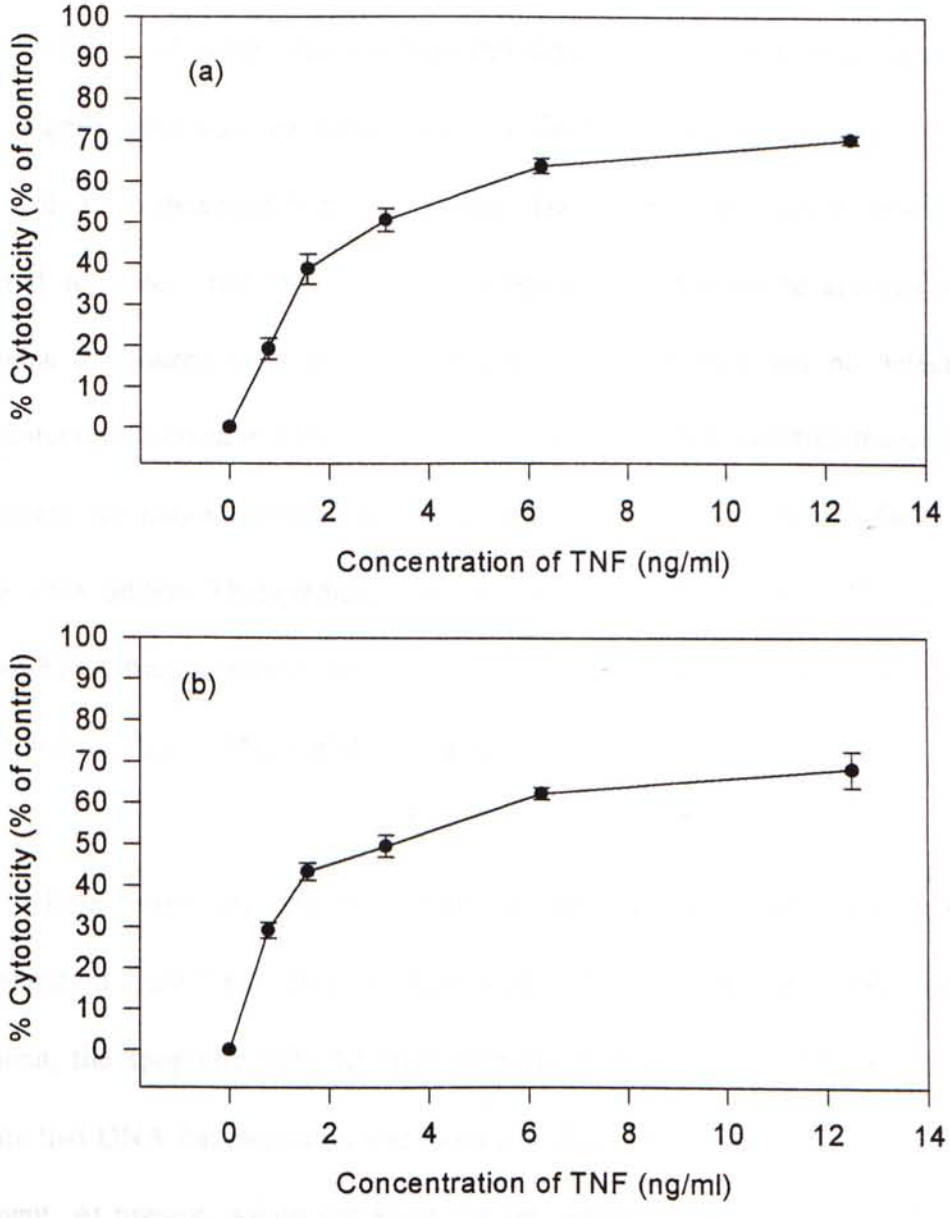

Figure 3.3

TNF induced cytotoxicity in L929 cells in a concentration dependent manner. L929 cells were seeded at 3 x 10^4/well in complete RPMI 1640 medium and incubated for 20 hr at 37 °C, 5 % CO_2. After incubation, spent medium was discarded and washed twice by serum-free medium. 100 µl of serum-free medium with various concentrations of TNF as indicated was added to each well and incubated for 20 hr at 37 °C, 5 % CO_2. (a) Neutral red assay (n = 7, expt = 4), and (b) MTT assay (n = 7, expt = 2) were then applied and the % of cytotoxicity was then calculated.

Figure 3.4 shows the result of DNA fragmentation by agarose gel electrophoresis. It was found that in the absence of serum, L929 cells treated with 50 ng/ml TNF for 3 hr did not induce cell death since no dead cell detached from the bottom of plate and no DNA fragmentation was detectable. However, for the 6 and 10 hr treatment of TNF, some L929 cells were detached from the bottom. The adherent and non-adherent cells were collected separately and DNA were extracted for electrophoretic analysis in order to determine the source of DNA fragmentation. It can be seen that no detectable DNA fragmentation occurred in adherent cells with 3 hr TNF (50 ng/ml) treatment (Figure 3.4). In contrast, the non-adherent cells from 6 or 10 hr treatment showed a faint, but clearly visible DNA ladders. These indicate that incubation of L929 cells with TNF for 6 or 10 hr induced DNA fragmentation. Moreover, DNA fragmentation progressively increased as the incubation time of TNF with L929 cells was increased.

These results are consistent with the previous report that TNF induced DNA fragmentation in L929 cells (review: Kerr *et al.*, 1995). It seems very likely that after TNF treatment, the apoptotic cells detached from the bottom of plate. Moreover, our results indicate that DNA fragmentation was more significant in the non-adherent cells after TNF treatment. At present, we do not know the relationship between the DNA fragmentation and matrix adherence. However, recent reports have shown that surface adherence is an important factor to keep cell survival (Chen *et al.*, 1998).

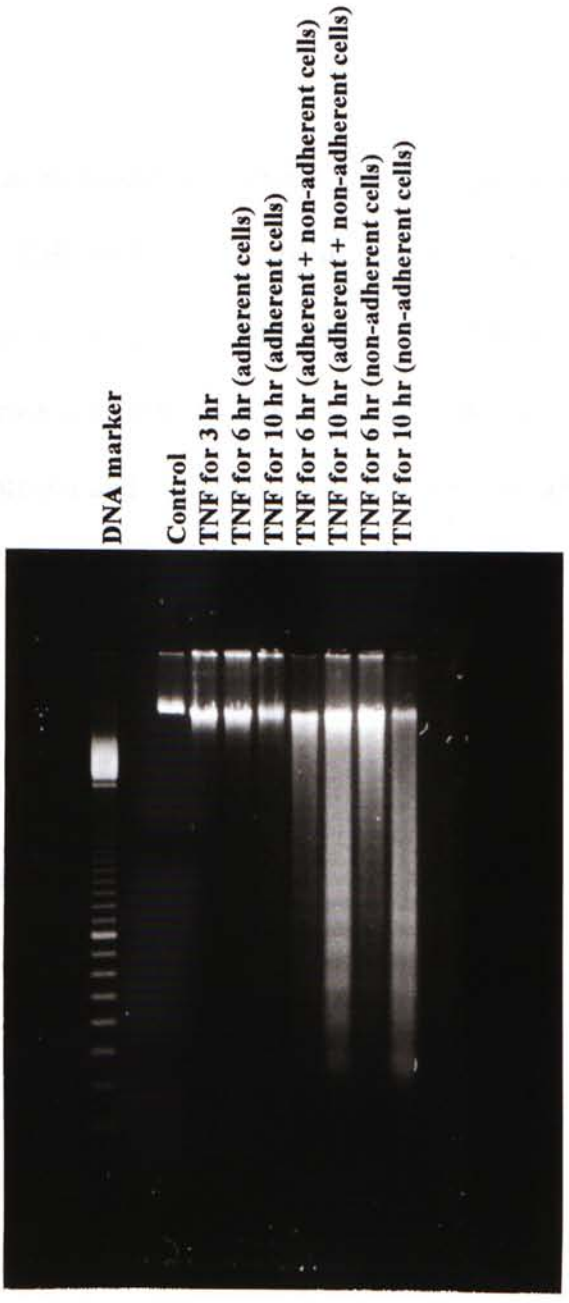

Figure 3.4

Agarose gel electrophoresis of DNA extracted from TNF-treated L929 cells. In the serum-free condition, there was no DNA fragmentation for 3 hour-treatment with 50 ng/ml TNF. Moreover, for 6 and 10 hr incubation, the adherent cells did not show DNA fragmentation. In contrast, DNA fragmentation occurred only in non-adherent cells after TNF treatment for 6 or 10 hr.

3.2 Effect of Tumor Necrosis Factor-Alpha on Cell Cycle

3.2.1 Introduction

The cell cycle can be divided into several phases (Figure 3.5). A non-cycling cell is said to be in G0 phase. Cells in G1 phase are sitting around either just recovering from division or preparing for the initiation of another cycle. Cells are said to be in S phase when they are in the process of making new DNA. Cells in the G2 phase are those that have finished DNA synthesis and therefore possess double the normal amount of DNA. Cells in M phase are undergoing the chromosome condensation and organization of mitosis that occur immediately prior to cytokinesis with the production of two daughter cells.

One of the most common application of FCM is the measurement of DNA to give a picture of the cell cycle by showing the DNA histogram (Figure 3.5). By measuring the DNA content, it can be determined whether a cell is in G0/G1, S or G2/M phases of the cycle. Any change in cell cycle parameters will be reflected in the appearance of the DNA histogram. Changes in the DNA histogram are used to study the mechanism of action of cytotoxic drugs since such compounds generally disrupt the cell cycle. The most widely used dye to determine the DNA content is propridium iodide (PI) (Sherwood and Schimke, 1995). It intercalates into double-stranded nucleic acids, is excited by the 488 nm line of an argon-ion laser and fluoresces red. Since it is excluded by viable cells, cells must be fixed or permeabilized before adding the dye.

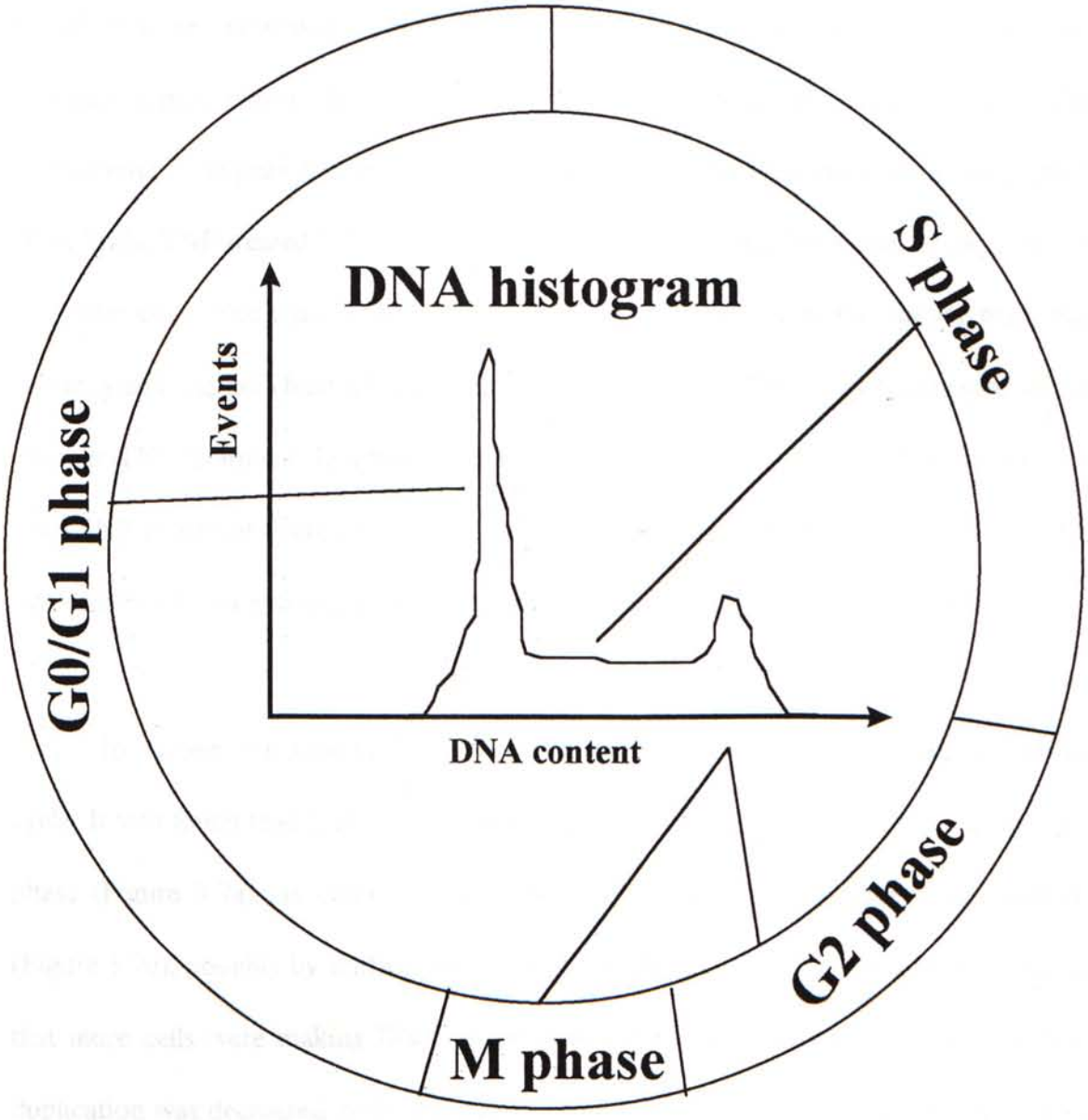

Figure 3.5
The cell cycle and DNA content of the cell.

3.2.2 Effect of TNF on Cell Cycle

Figure 3.6 shows the DNA histogram of TNF-treated L929 cells. It was found that addition of 50 ng/ml TNF for 15 min, 3 or 6 hr did not cause any significant change in the G0/G1, S or G2/M phases as compared to control. However, addition of TNF for 10 hr produced a peak before the G0/G1 phase (Figure 3.6e). Since the x-axis represents the DNA content, the peak before the G0/G1 phase implied that there were some fragmented DNA in the TNF-treated L929 cell population. The fragmented DNA may come from the apoptotic cells. The data from the cell cycle are consistent with the results from our previous agarose gel electrophoresis study (Figure 3.4) that DNA was fragmented in the 10-hour-TNF treatment. In addition, the number of cells in the G0/G1 and S phase in 10-hour-TNF treatment decreased. Therefore, cells in S phase were more susceptible to TNF since the % of cells in S phase dropped significantly with the 10-hour-TNF treatment.

In another experiment, the presence of serum affected the TNF effect on the cell cycle. It was found that in the control group, addition of serum caused more cells in the S phase (Figure 3.7a), as compared with the control group in the serum-free condition (Figure 3.7e), possibly by shifting cells from the G0/G1 phase to the S phase. This implies that more cells were making DNA in the presence of serum whereas the rate of DNA duplication was decreased in the absence of serum. Furthermore, serum might affect the S phase in TNF-treated cells. In the presence of serum, the adherent cells show DNA fragmentation as indicated in Figure 3.7b. The combination of adherent and non-adherent cells produced a higher proportion in the DNA fragmentation (Figure 3.7c).

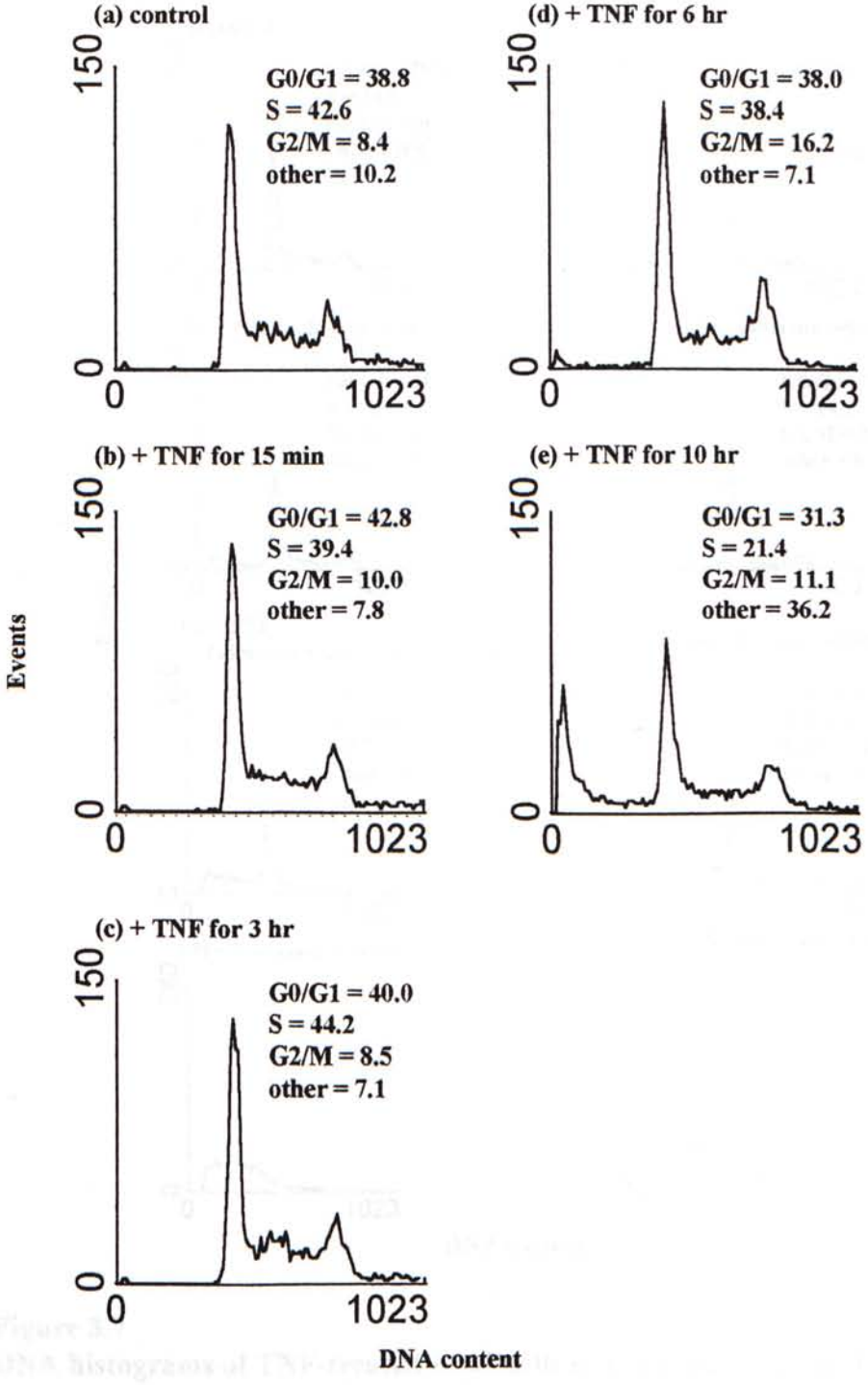

Figure 3.6

DNA histograms of TNF-treated L929 cells. L929 cells (1 x 10^6/ml) were seeded in a 6-well plate and incubated at 37 °C and 5 % CO_2 overnight. Cells were then treated with (a) complete RPMI medium alone; 50 ng/ml TNF for (b) 15 min, (c) 3 hr, (d) 6 hr and (e) 10 hr. Cells were then trypsinized and fixed with 70 % ethanol overnight. Cells were then stained with 43 µg/ml PI for 30 min and the cell cycle was determined by FCM.

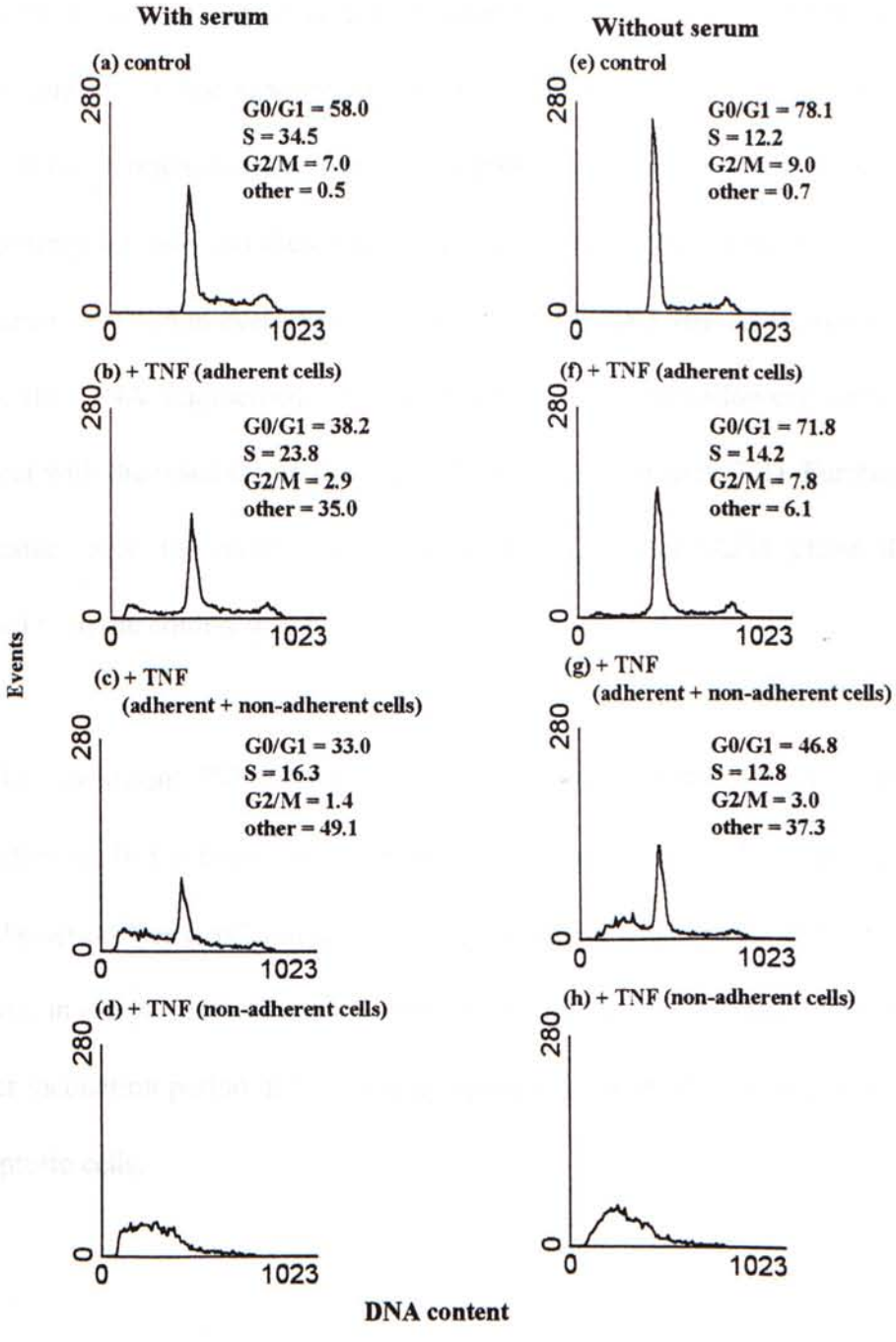

Figure 3.7

DNA histograms of TNF-treated L929 cells in the presence and absence of serum for 10 hours. L929 cells (1 x 10^6/ml) were seeded in a 6-well plate and incubated at 37 °C and 5 % CO_2 overnight. Cells were then treated with (a) complete RPMI. L929 cells were treated with complete RPMI plus 50 ng/ml TNF for 10 hr and (b) adherent cells (c) adherent and non-adherent cells and (d) non-adherent cells were collected. In addition, cells treated with (e) serum-free RPMI, adherent cells after incubaiton with serum-free RPMI plus 50 ng/ml TNF for 10 hr (f) adherent and non-adherent cells (g) and non-adherent cells (h) with TNF treatment were also collected.

Figure 3.7d shows that almost all non-adherent cells were mainly in the DNA fragmented state. In contrast, in the absence of serum, the adherent cells did not produce a large amount of DNA fragmentation. Serum is a good source of growth factors that provides enough energy for cells and therefore, apoptosis (an ATP-dependent process) might occur in the presence of serum even in the adherent cells (Figure 3.7b). As shown in Figure 3.71f - 3.71h, the DNA fragmented cells were all from the non-adherent cells which is in agreement with the results from DNA gel electrophoresis (Figure 3.4). Furthermore, in the TNF-treated cells, the number of cells in G0/G1, S and G2/M phase decreased as compared with the control group.

In conclusion, TNF induced apoptosis by examining the pattern of cell cycle after TNF treatment. In the presence of serum, the number of cells in S phase was higher than that in the serum-free condition and the cells might shift from G0/G1 phase to the S phase. Moreover, in the presence of serum, addition of TNF for 10 hr induced apoptosis whereas a shorter incubation period did not induce apoptosis. Most of the non-adherent cells were the apoptotic cells.

3.3 Release of Reactive Oxygen Species in Tumor Necrosis Factor-Alpha Treated Cells

3.3.1 Introduction

It was found that one of the mechanisms of cytotoxicity after TNF treatment on murine cells involved the release of ROS such as H_2O_2 or $O_2\bullet^-$ (Zimmerman *et al.*, 1989). However, the mechanism and the triggering messengers in this regard are not clear. In this project, the release of ROS from L929 cells after treatment with rMuTNF was examined. For investigating ROS inside the cells, two fluorescent dyes, the diacetate form of dichlorofluorescin and hydroethidine, were applied.

The diacetate form of dichlorofluorescin (DCF-DA) was employed for detecting the formation of H_2O_2 (Figure 3.8a). The DCF assay for the quantification of intracellular H_2O_2 was described previously (Cathcart *et al.*, 1983). The principle is that DCF-DA diffuses into the cell and is converted into the non-fluorescent intermediate dichlorofluorescin (DCFH) by hydrolysis. The non-fluorescent form of DCFH is then converted into fluorescent form of dichlorofluorescein (DCF) by cellular H_2O_2. It was found that 1:1 stoichiometry is observed between H_2O_2 and dichlorofluoroscein (Cathcart *et al.*, 1983).

On the other hand, $O_2\bullet^-$ can be detected by hydroethidine (HE). The HE assay for the quantification of intracellular $O_2\bullet^-$ has been described (Gorman *et al.*, 1997). HE is

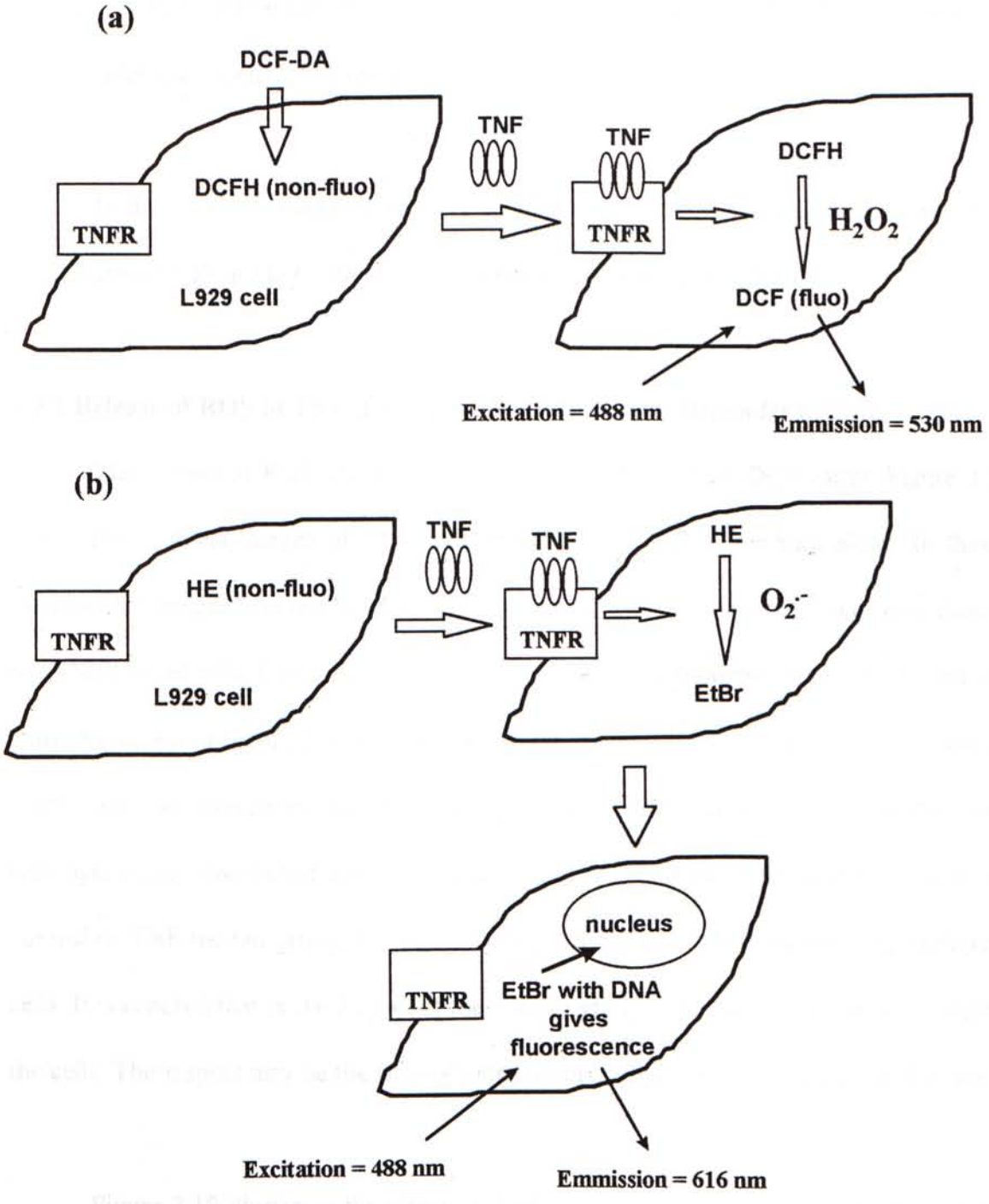

Figure 3.8
Detection of intracellular H_2O_2 and $O_2\bullet^-$ by fluorescence dyes dichlorofluorescin diacetate and hydroethidine. (a) Detection of H_2O_2: non-fluorescent form of DCFH can be oxidized to fluorescent form of DCF by H_2O_2. (b) Detection of $O_2\bullet^-$: non-fluorescent form of HE can be oxidized to fluorescent form of EtBr by $O_2\bullet^-$.

oxidized by $O_2\bullet^-$ within the cell to produce ethidium bromide, which emits fluorescence when it intercalates into DNA (Figure 3.8b).

In this section, several techniques such as CLSM, FCM were applied to monitor the release of ROS inside L929 cells in the presence or absence of TNF.

3.3.2 Release of ROS in TNF-Treated L929 Cells is Time Dependent

The release of ROS can be monitored by CLSM and the DCF assay. Figure 3.9 shows the confocal images of L929 cells treated with TNF or medium alone. In these pseudocolor images, the upper panel shows the control cells while the lower one shows the TNF-treated cells. Confocal scannings were made at the time indicated (15, 30 and 45 min). As shown in Figure 3.9, TNF caused an increase in the rate of H_2O_2 production in L929 cells as compared to the control group. The fluorescence intensity was heterogeneously distributed inside the cells. Moreover, it was also found that either in control or TNF-treated group, the rate of release of H_2O_2 was heterogeneous in different cells. It was noted that in the 30 min of the control group, some hot spots occurred inside the cells. These spots may be the sites of mitochondria since redox rate is high in that site.

Figure 3.10 illustrates the effect of TNF on the $O_2\bullet^-$ production in L929 cells by using the HE assay. Similar to the results from DCF assay, TNF caused an increase in the rate of $O_2\bullet^-$ production in L929 cells as compared to the control group. Since HE can be converted into EtBr by $O_2\bullet^-$, the emission of fluorescence of EtBr-chelated DNA clearly shows the location of nucleus.

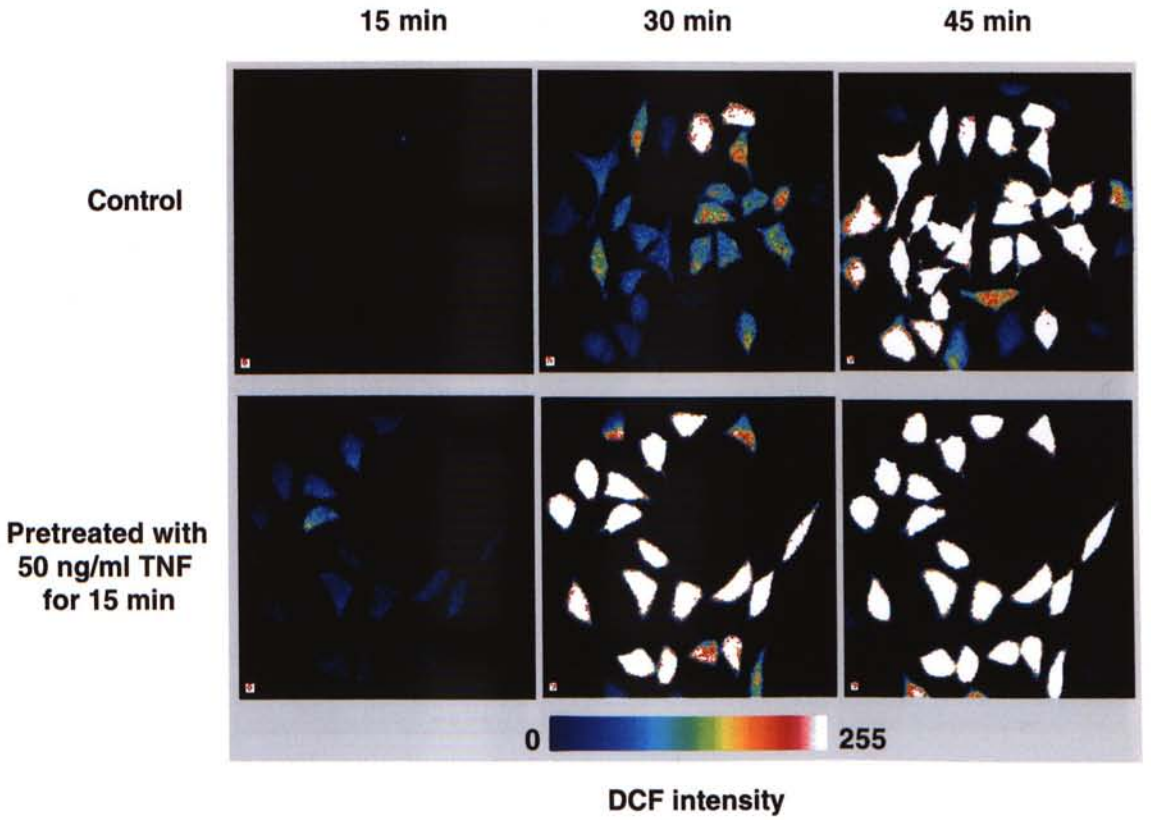

Figure 3.9
TNF caused an increase in the rate of H_2O_2 production in L929 cells. The upper panel shows the control cells and the lower panel shows the TNF-treated cells at the time indicated. L929 cells (2 x 10^3/ml) were seeded on a cover glass and incubated at 37 ℃, 5 % CO_2 for 3 days. TNF (50 ng/ml) was then applied to L929 cells. 15 min after the addition of TNF, DCF (final concentration 10 μM) was added at time zero and measurement (CLSM-MD) was made at room temperature. Cells were scanned at a 5-minute-interval. The cool and the warm color indicate the lower and the higher fluorescence intensity, respectively. Note that TNF caused an increase in the rate of H_2O_2 production in L929 cells when compared to the control group (expt = 9).

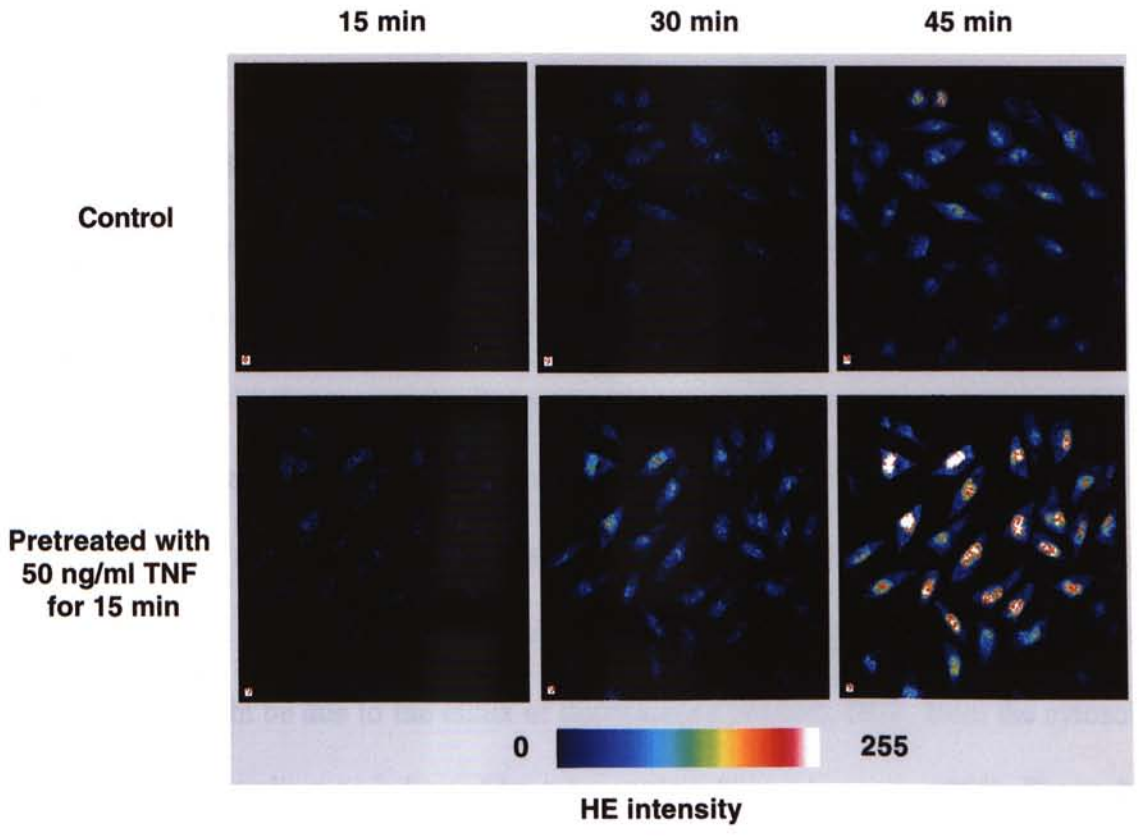

Figure 3.10
TNF caused an increase in the rate of $O_2\bullet^-$ production in L929 cells. The upper panel shows the control cells and the lower panel shows the TNF-treated cells at the time indicated. L929 cells (2 x 10^3/ml) were seeded on a cover glass and incubated at 37 ℃, 5 % CO_2 for 3 days. TNF (50 ng/ml) was then applied to L929 cells. 15 min after the addition of TNF, HE (final concentration 10 μM) was added at time zero and measurement (CLSM-MD) was made at room temperature. Cells were scanned at a 5-minute-interval. The cool and the warm color indicate the lower and the higher fluorescence intensity, respectively. Note that TNF caused an increase in the rate of $O_2\bullet^-$ production in L929 cells when compared to the control group (expt = 6). EtBr-chelated DNA presented in the cells.

For a longer time measurement, the release of ROS can be monitored by FCM. Figure 3.11 shows the results from FCM. In general, as time increases, DCF (Figure 3.11a) and HE (Figure 3.11b) fluorescence intensities increase. These results indicate that H_2O_2 and $O_2\bullet^-$ are produced in cells continuously even in the absence of TNF stimulation.

Next, the effect of TNF on the release of ROS was investigated. Incubation of L929 cells with 50 ng/ml TNF for 15 min (Figure 3.12a) or 3 hr (Figure 3.12b) did not cause more H_2O_2 production. Interestingly, when cells were treated with TNF (50 ng/ml) for 6 or 10 hr, a significant increase in H_2O_2 production was observed (Figure 3.13). It is clear in Figure 3.13 that two peaks (two populations of cells) were seen in terms of DCF fluorescence. These results again suggest that the response of cells was heterogeneous. Moreover, in the control and TNF-treated group, the large population shifted to the right and then to the left, that is, the fluorescence intensity of DCF increased and then decreased. It might be due to the efflux of fluorescence product, DCF, from the cytosol to the extracellular medium as indicated by other groups (Gorman *et al.*, 1997). Figure 3.14 summaries the above results. It can be seen that the amount of H_2O_2 produced in L929 cells upon TNF treatment was dependent on the incubation time.

After monitoring the production of H_2O_2 by TNF, the release of $O_2\bullet^-$ was also examined by applying fluorescence dye, HE. It was found that incubation of cells with 50 ng/ml TNF for 15 min, 3 or 6 hr, did not cause more production of $O_2\bullet^-$ (Figure 3.15). However, there was no significant changes as compared to the control group even L929 cells were incubated with 50 ng/ml TNF for 6 hr (Figure 3.15c). Only a small

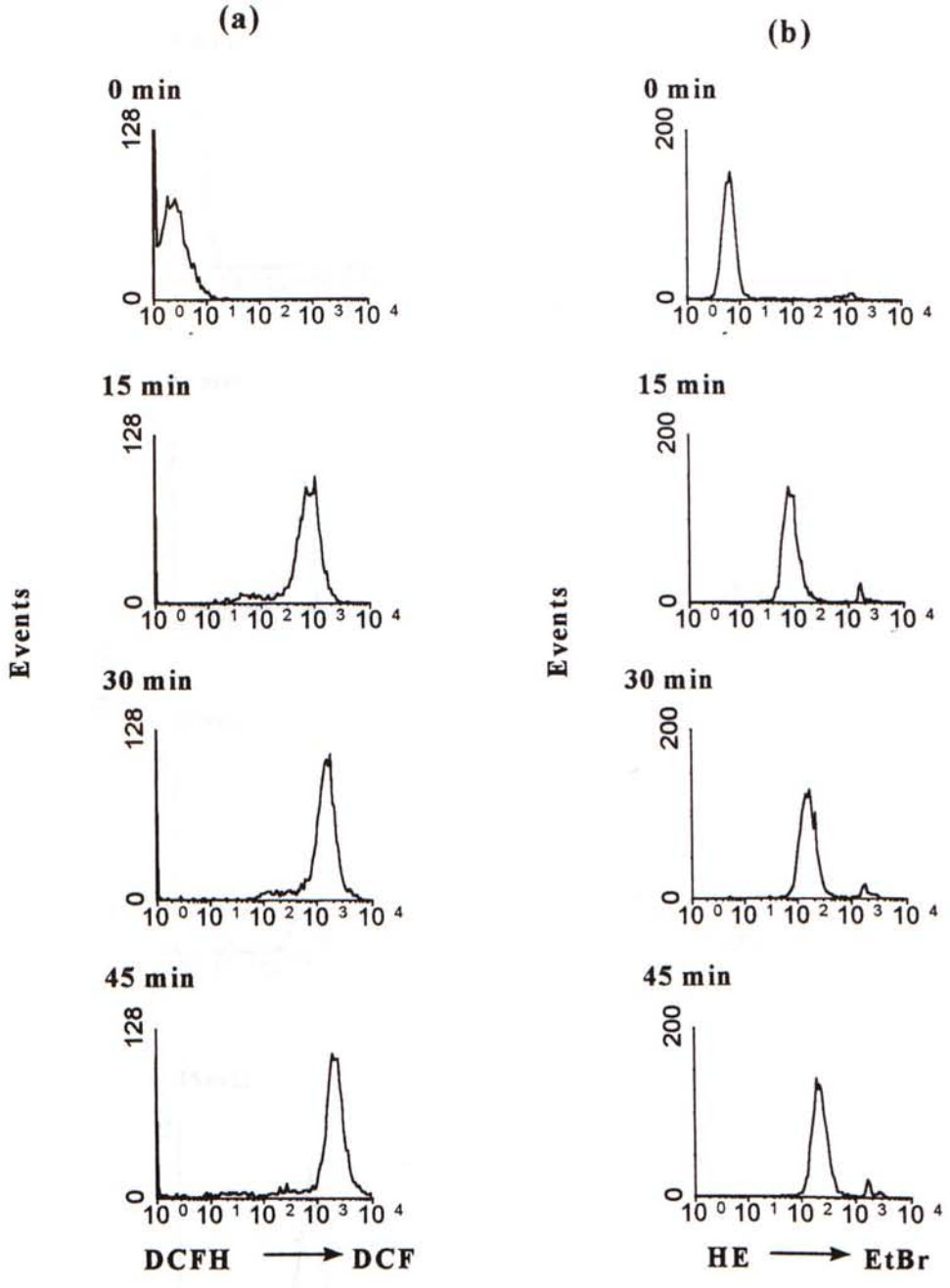

Figure 3.11

Time-dependent conversion of non-fluorescent indicators into fluorescent ones. L929 cells (1 x 10^6/ml) were seeded in a 6-well plate and were incubated overnight at 37 °C, 5 % CO_2. Cells were then trypsinized. After washing, DCF (10 μM) (a) or HE (10 μM) (b) was added and measurement was made at the time indicated. Y-axis represents the number of events (total = 10,000) whereas x-axis represents the fluorescence intensity. Note the shifting of the population from left to right indicating the time-dependent conversion of non-fluorescent indicators to the fluorescent one (expt > 10).

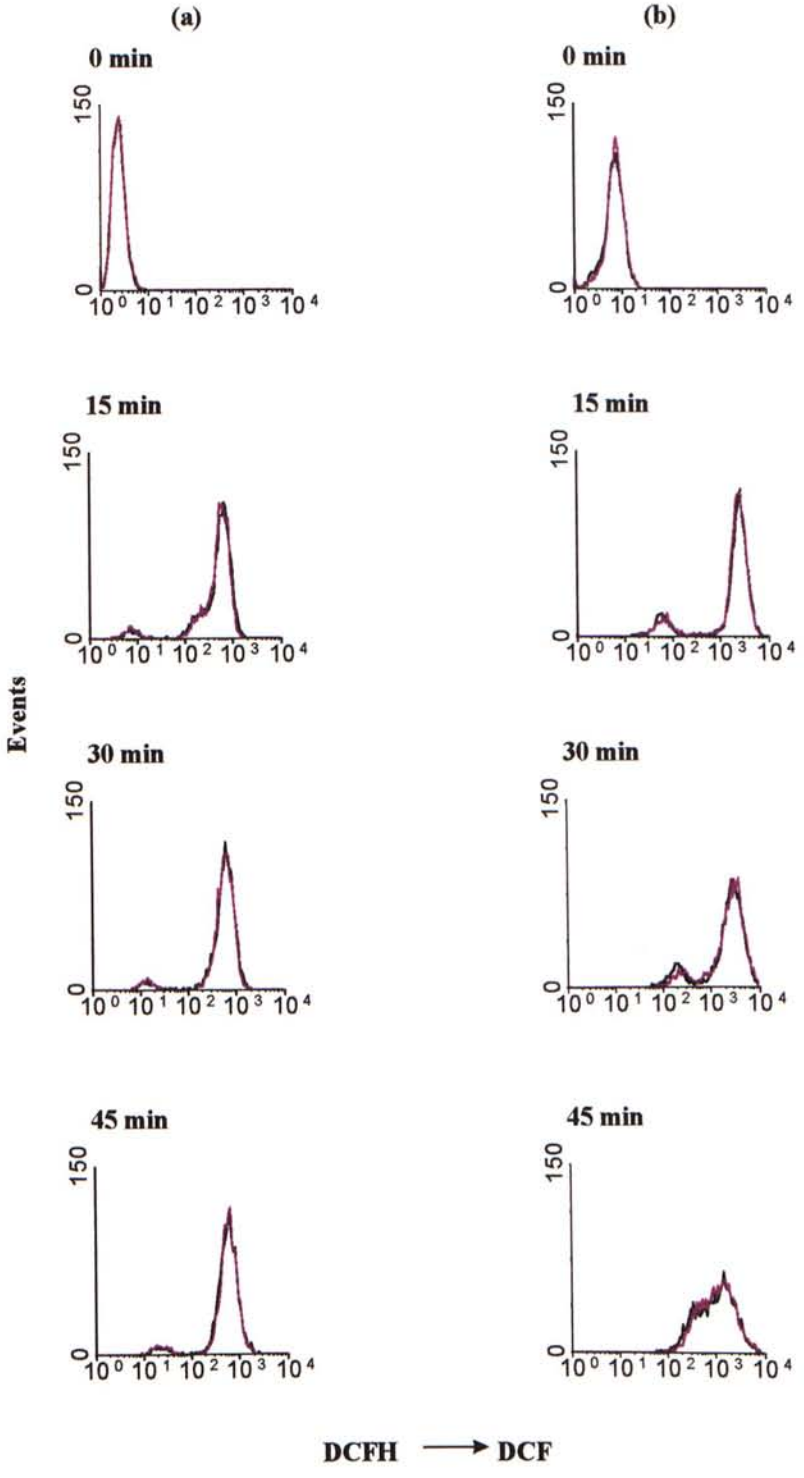

Figure 3.12

Incubation of L929 cells with TNF for 15 min or 3 hr did not produce more H_2O_2 production. Incubation of L929 cells with 50 ng/ml TNF (purple line) for (a) 15 min (expt = 9) or (b) 3 hr (expt = 8) did not cause more H_2O_2 production as compared to control group (black line). The time on the left indicates the incubation period of cells with DCF.

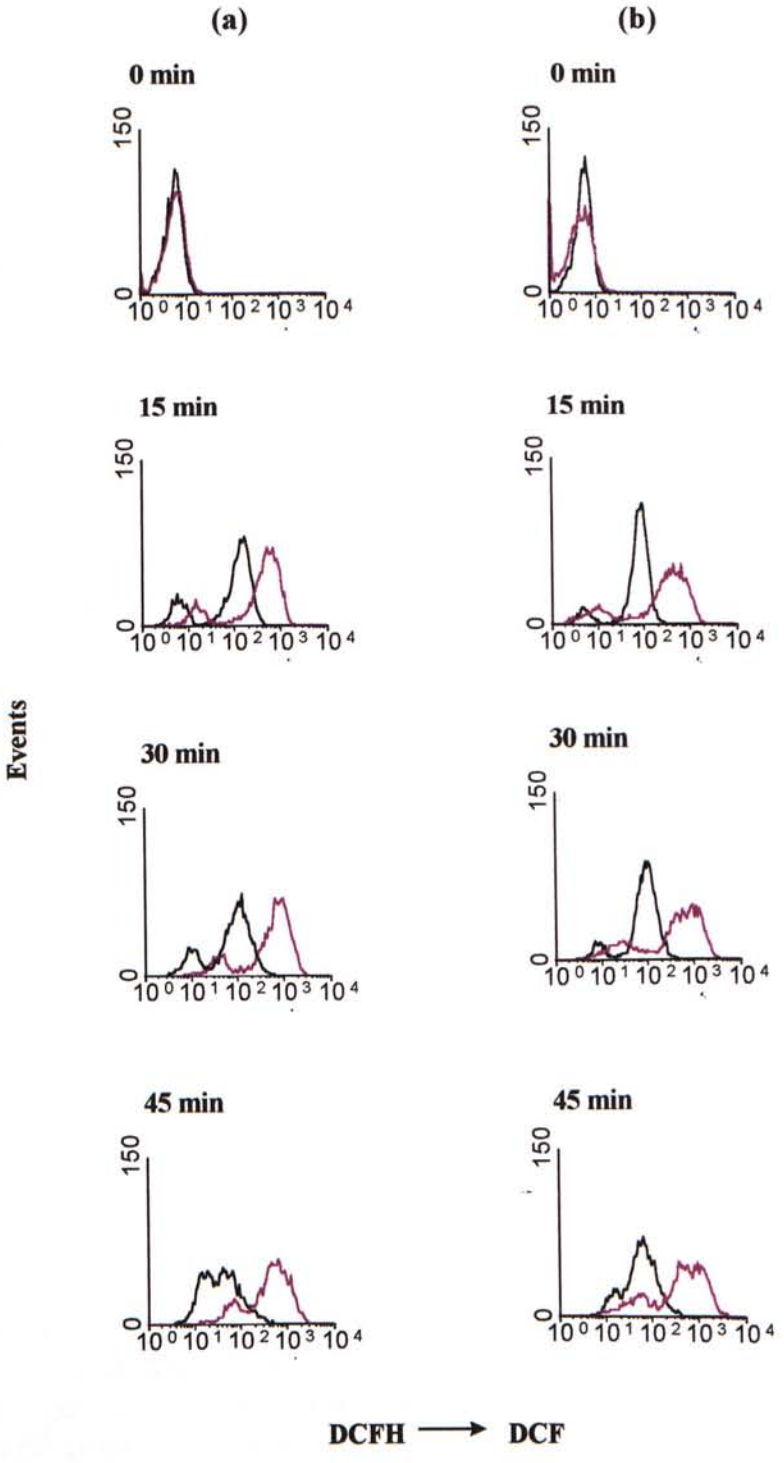

Figure 3.13
Incubation of L929 cells with TNF for 6 or 10 hr produced more H_2O_2 production. Incubation of L929 cells with 50 ng/ml TNF (purple line) for (a) 6 hr (expt > 10) or (b) 10 hr (expt = 3) caused more H_2O_2 production as compared to control group (black line). The time on the left indicates the incubation period of cells with DCF.

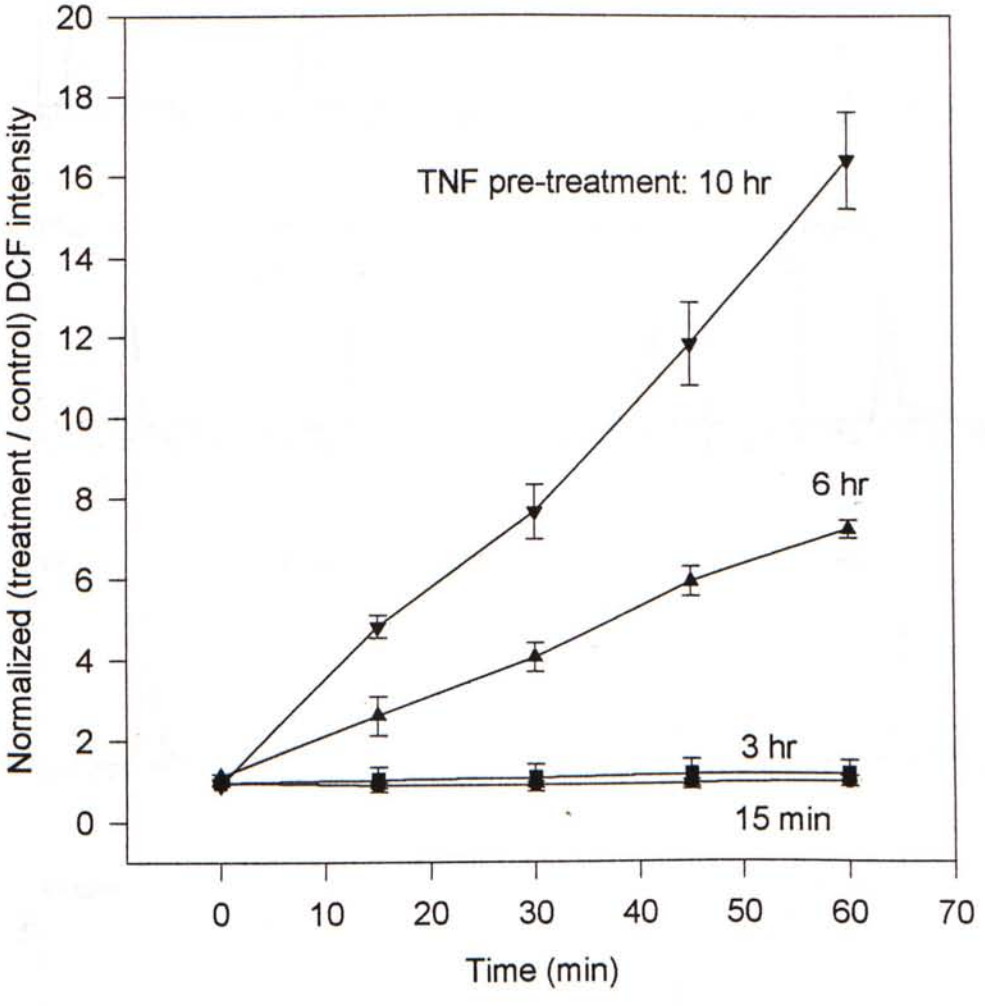

Figure 3.14

The release of H_2O_2 in TNF-treated L929 cells is time dependent. The H_2O_2 production in cells treated with or without TNF (50 ng/ml) for various time intervals as shown in Figure 3.12 and 3.13 were normalized by dividing the peak fluorescence of the TNF-treated group with the one of control group. The x-axis represents the incubation time of cells with DCF. Results are mean ± SD from 3 experiments. Note the increase in the amount of H_2O_2 produced in cells with longer TNF treatment time intervals.

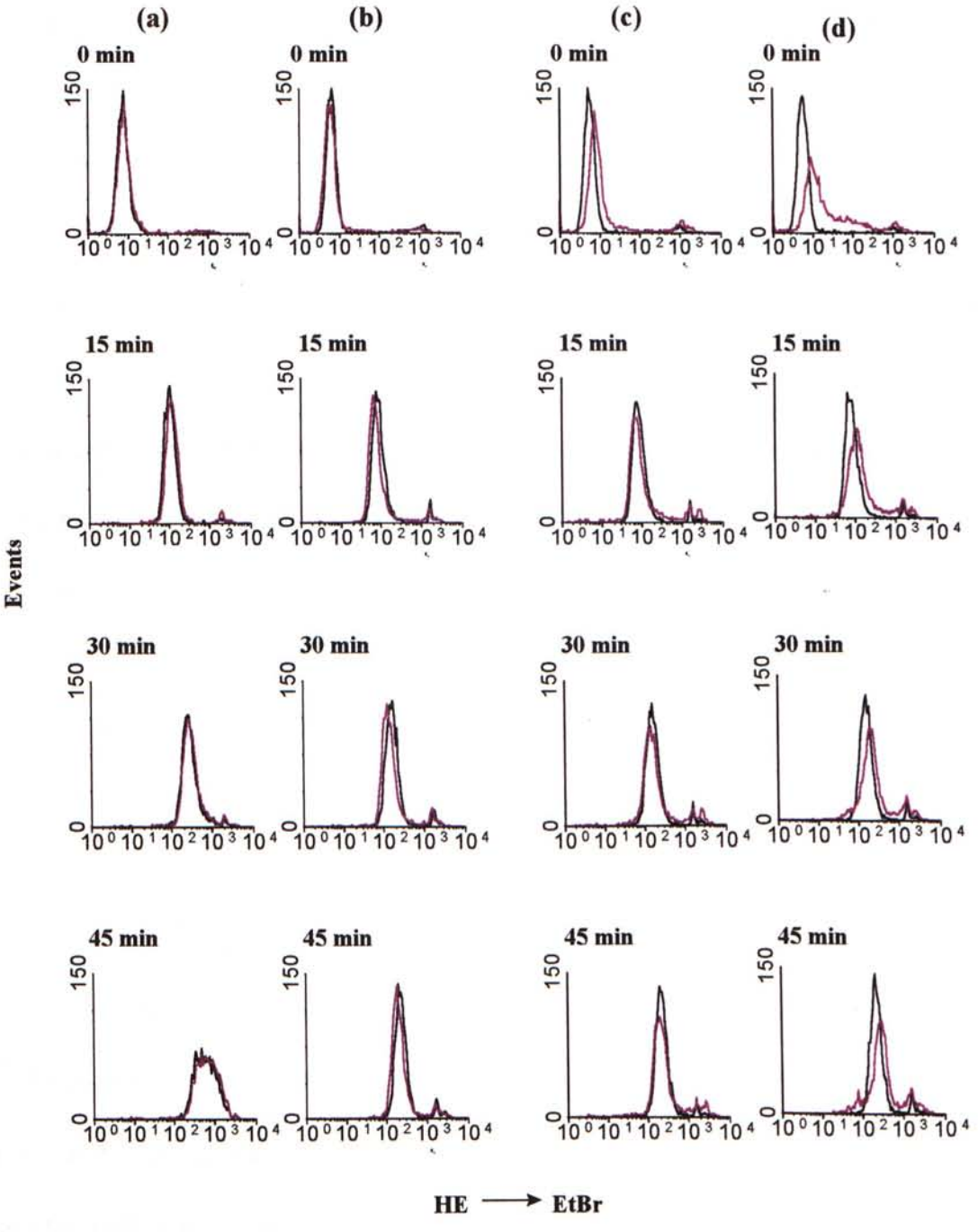

Figure 3.15

Incubation of L929 cells with TNF for 15 min, 3 or 6 hr did not cause more $O_2\bullet^-$ production but produced a small increase in a 10 hr assay. Incubation of L929 cells with 50 ng/ml TNF (purple line) for (a) 15 min (expt = 3), (b) 3 hr (expt = 4) or (c) 6 hr (expt = 3) did not cause more $O_2\bullet^-$ production as compared to control group (black line). In another experiment, Incubation of L929 cells with 50 ng/ml TNF (purple line) for (d) 10 hr caused a small increase in $O_2\bullet^-$ production as compared to control group (black line). The time on the left indicates the incubation period of cells with HE.

increase in $O_2\bullet^-$ production was seen in the group for 10 hr TNF (50 ng/ml) incubation (Figure 3.15d).

L929 cells with TNF for 6- or 10-hour incubation produced more release of H_2O_2 than that of $O_2\bullet^-$. This discrepancy might be due to the protective mechanism inside the cells. As mentioned in section 1.5.1, TNF induced MnSOD mRNA in all cell lines and normal cells (Wong and Goeddel, 1988). As indicated in Figure 1.5, $O_2\bullet^-$ is converted into H_2O_2 by MnSOD inside mitochondria. Therefore, addition of metabolic inhibitor such as actinomycin D (AMD), a transcriptase blocker that blocks transcription (Ostrove and Gifford, 1979), should reduce the expression of MnSOD mRNA (Wong and Goeddel, 1988). This explains why the sensitivity of TNF cytotoxicity assay is markedly increased when cells were incubated with TNF in the presence of AMD.

In light of this, cells were treated with TNF in the presence of AMD (2μg/ml). It can be seen that there was no response in the 15-minute-incubation of cells with TNF and AMD (Figure 3.16). However, Figure 3.17 shows that addition of TNF plus AMD did increase the rate of $O_2\bullet^-$ production after incubation for 3 or 6 hr. Moreover, It was found that the response of cells was heterogeneous in TNF plus AMD treatment. There were two populations of cells, the fast and the slow responding cells. Since cells incubated with TNF plus AMD for 10 hr induced cell death (most of the cells were detached from the bottom of the plate) and $O_2\bullet^-$ level was not measured (data not shown).

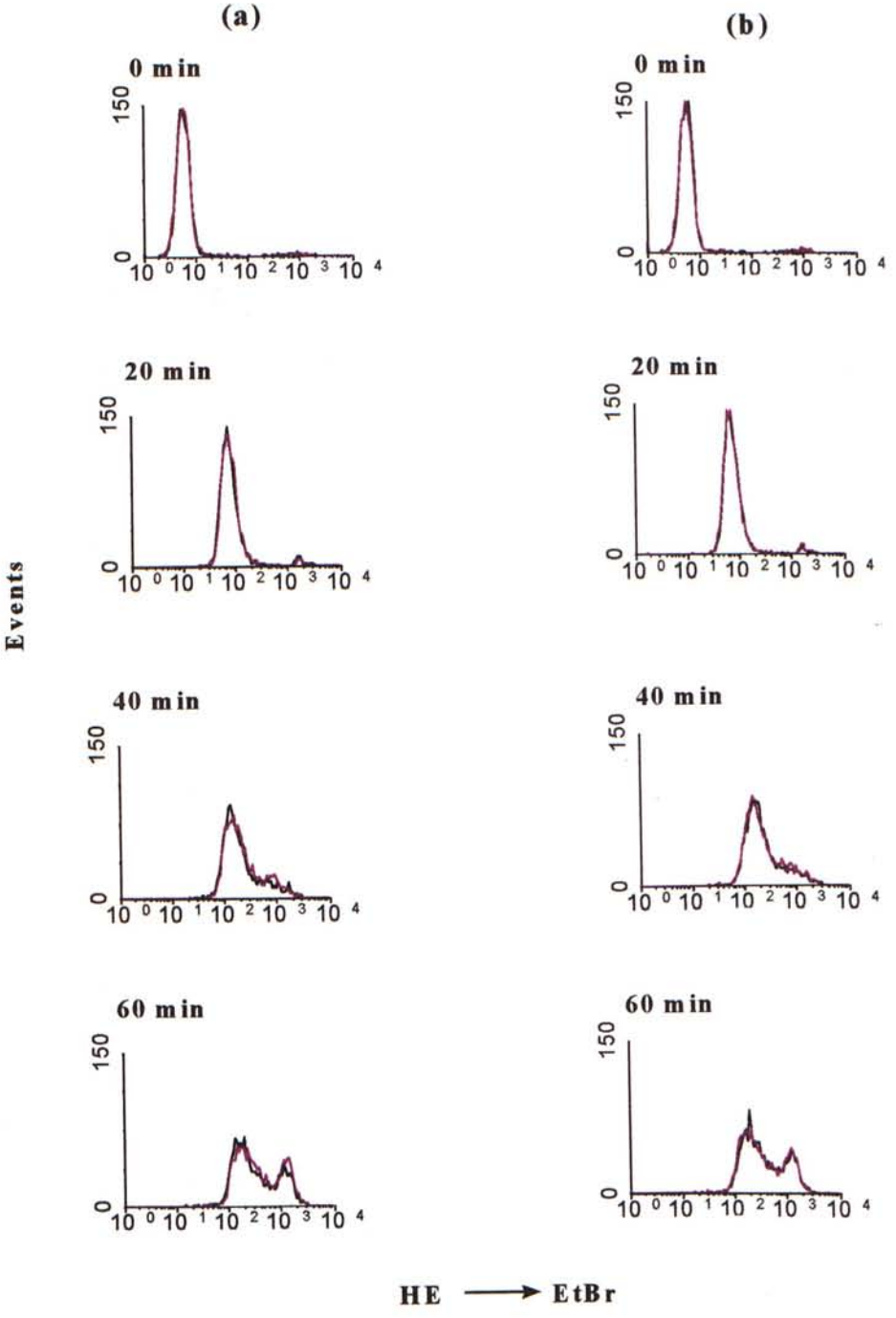

Figure 3.16

Incubation of TNF with or without AMD for 15 min did not cause more $O_2\bullet^-$ production in L929 cells. L929 cells (1 x 10^6/ml) were seeded in a 6-well plate and were incubated overnight at 37 °C, 5 % CO_2. Cells were pre-treated with 50 ng/ml TNF (purple line) with or without 2 μg/ml AMD for 15 min. Cells were then trypsinized. 10 μM HE was added and measurement was made at the time indicated. It was found that cells incubated with TNF (a) in the absence of AMD (expt = 3) or (b) presence of AMD (expt = 2) for 15 min did not cause $O_2\bullet^-$ release as compared to control (black line).

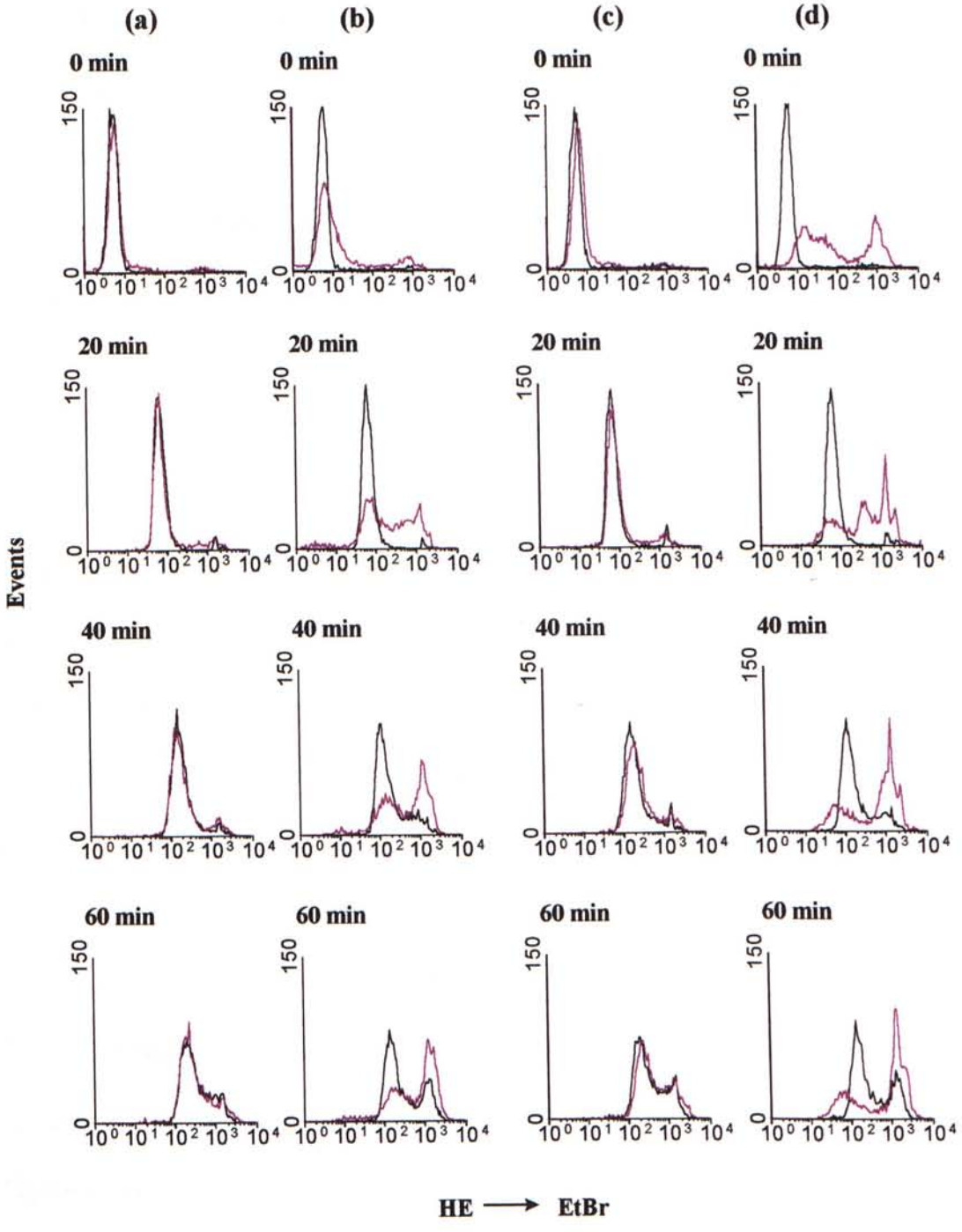

Figure 3.17

Incubation of TNF with AMD for 3 or 6 hr produced more $O_2\bullet^-$ release in L929 cells. It was found that cells incubated with 50 ng/ml TNF in the absence of AMD (a) did not increase $O_2\bullet^-$ production (expt = 4), (b) in the presence of AMD (2 μg/ml), L929 cells incubated with 50 ng/ml TNF for 3 hr produced more $O_2\bullet^-$ release (expt = 3). Incubation of TNF in the absence of AMD (c) did not increase $O_2\bullet^-$ production (expt = 3) whereas (d) TNF plus AMD produced more $O_2\bullet^-$ release in 6-hour treatment (expt = 3).

3.3.3 Effect of Antioxidants on TNF-Mediated Cytotoxicity

As described earlier, our data indicate that treatment of L929 with TNF produces oxidative damage. In this section, the effect of antioxidants such as catalase, MnSOD, NAc and 4-OH-TEMPO on the rMuTNF induced cytotoxicity of L929 cells was examined.

It is well known that catalase removes H_2O_2 by the formation of water and molecular oxygen whereas SOD removes $O_2\bullet^-$ to form H_2O_2 (Briehl and Baker, 1996). Therefore, catalase and MnSOD are considered to be an antioxidant. Other antioxidants such as NAc and 4-OH-TEMPO were applied in this project as well. The actions of NAc involve: (1) replenishment of GSH stores; (2) scavenging of ROS; and (3) prevention of mitochondrial membrane depolarization (Cossarizza *et al.*, 1995). 4-OH-TEMPO is a low molecular weight SOD analogue that removes excess $O_2\bullet^-$ inside the cells. Moreover, it prevents lipid hydroperoxide formation (Reddan *et al.*, 1993).

The data from FCM indicated that addition of catalase, NAc and 4-OH-TEMPO did reduce the rate of TNF-mediated H_2O_2 release in an assay with 6-hour-incubation (Figure 3.18).

From the cytotoxicity assay, it was found that addition of antioxidants partially reduced TNF-mediated cytotoxicity. Addition of 1000 U/ml catalase with 50 ng/ml TNF reduced about 10 % in cytotoxicity (Figure 3.19). The hydrogen peroxide-scavenging enzyme, catalase converts two molecules of H_2O_2 into two molecules of water and one of

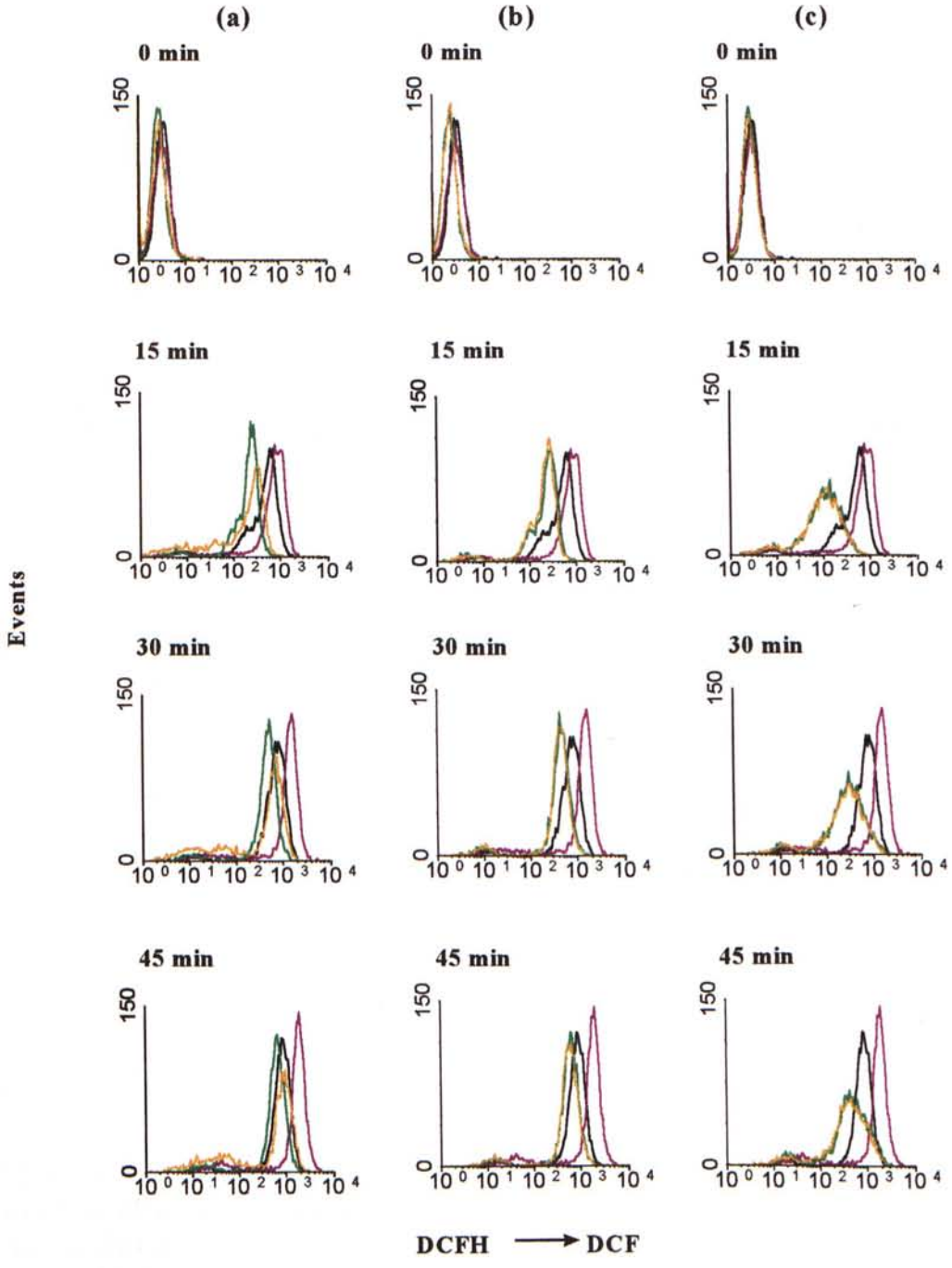

Figure 3.18

Addition of antioxidants reduced the amount of TNF-mediated H_2O_2 release in L929 cells. L929 cells (1 x 10^6/ml) were seeded in a 6-well plate and were incubated overnight at 37 °C, 5 % CO_2. Cells were then treated with medium only (black line), 50 ng/ml TNF (purple line), antioxidants only (green line), and TNF (50 ng/ml) plus antioxidants (orange line) for 6 hr. The dose of the antioxidants are: (a) 2000 U/ml catalase, (b) 10 mM NAc and (c) 20 mM TEMPO. Subsequently, cells were assayed with DCF by FCM. Note the antioxidants reduced the amount of H_2O_2 production.

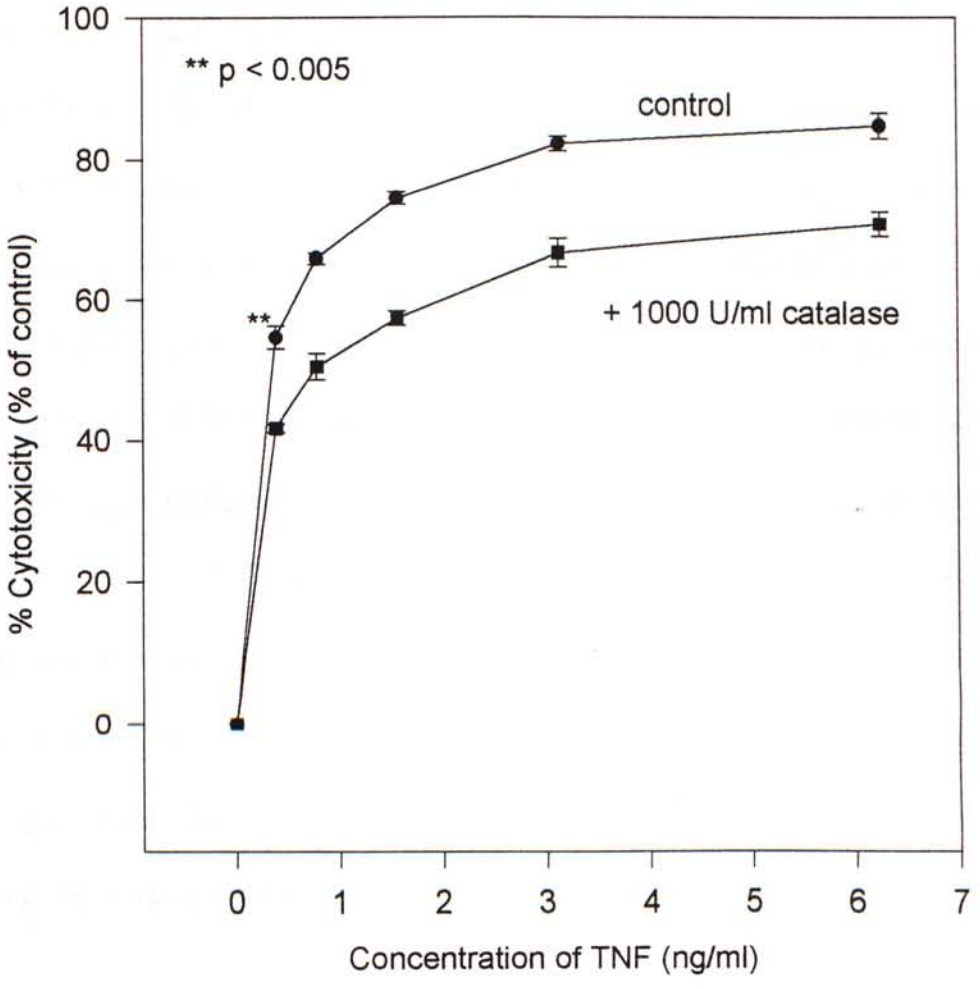

Figure 3.19

Addition of catalase reduced TNF-mediated cytotoxicity in L929 cells. L929 cells were seeded at 3 x 10^4/well in complete RPMI 1640 medium in a 96-well plate and incubated for 20 hr at 37 °C, 5 % CO_2. After incubation, spent medium was discarded and washed twice by serum-free medium. 100 µl of TNF of various concentrations in the presence (■) or absence (●) of catalase (1000 U/ml) in serum-free medium was added and incubated for 20 hr at 37 °C, 5 % CO_2. MTT assay was then applied and O.D. at 540 nm was read by a microplate reader (n = 7). ** $p < 0.005$ indicates that there was a significant difference between control group and the treatment group.

oxygen. Catalase is not cell-permeable whereas H_2O_2 is freely permeable to the cell (Gorman *et al.*, 1997). The antioxidant effect of catalase that acts on L929 cells might probably due to the removal of H_2O_2 from the culture medium that would promote the exit of H_2O_2 from the cellular cytoplasm to the extracellular environment, and therefore, reduced TNF-mediated cytotoxicity. Application of MnSOD (25 μg/ml) also reduced TNF-mediated cytotoxicity by about 5 - 10 % (Figure 3.20). MnSOD is a relatively large molecule that is membrane-impermeable (Mitchell *et al.*, 1990). The mechanism of the antioxidant effect of MnSOD was similar to that of catalase. The effect of MnSOD on L929 cells might probably due to the removal of $O_2\bullet^-$ from the culture medium that promoted the efflux of $O_2\bullet^-$ from the cytoplasm. Addition of 20 mM NAc suppressed the TNF-mediated cytotoxicity (about 5 - 10 %) (Figure 3.21). Furthermore, addition of 5 mM 4-OH-TEMPO produced a lower TNF-mediated cytotoxicity (reduced about 20 - 40 %) (Figure 3.22). These results implied that addition of antioxidants was capable of reducing the production of ROS thereby suppressing the cell death.

3.3.4 Effect of Mitochondrial Inhibitors on TNF-Mediated Cytotoxicity

As mentioned before, mitochondria are considered to be the major site of ROS production. The primary source of ROS may come from the electron transport chain. Therefore, the application of mitochondrial inhibitors on electron transport chain may affect the release of ROS and the cytotoxicity of TNF. In this connection, several mitochondrial inhibitors such as rotenone (mitochondrial complex I inhibitor), TTFA (mitochondrial complex II inhibitor), antimycin A (mitochondrial complex III inhibitor)

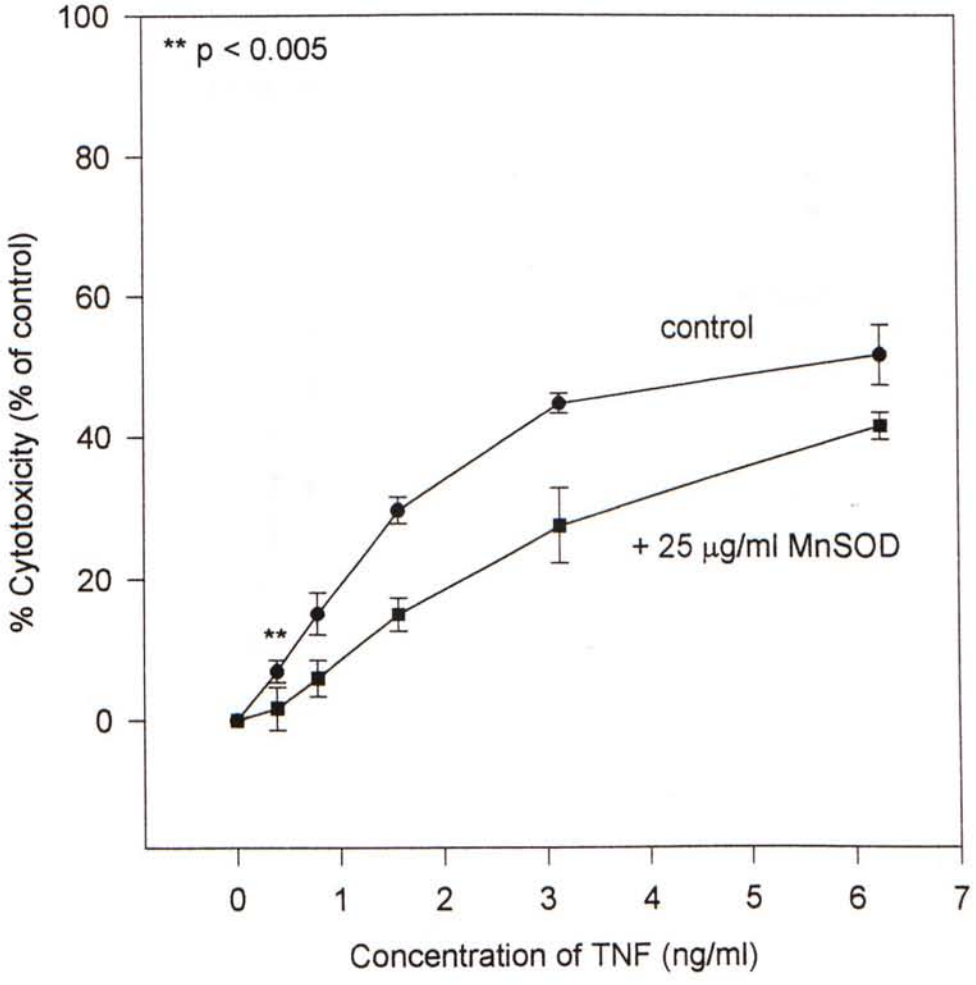

Figure 3.20

Addition of MnSOD reduced TNF-mediated cytotoxicity in L929 cells. L929 cells were seeded at 3 x 10^4/well in complete RPMI 1640 medium in a 96-well plate and incubated for 20 hr at 37 °C, 5 % CO_2. 100 μl TNF of various concentrations in the presence (■) or absence (●) of MnSOD (25 μg/ml) in serum-free medium was added and incubated for 20 hr at 37 °C, 5 % CO_2. Neutral red assay was then applied and O.D. at 540 nm was read by a microplate reader (n = 7). ** $p < 0.005$ indicates that there was a significant difference between control and treatment group.

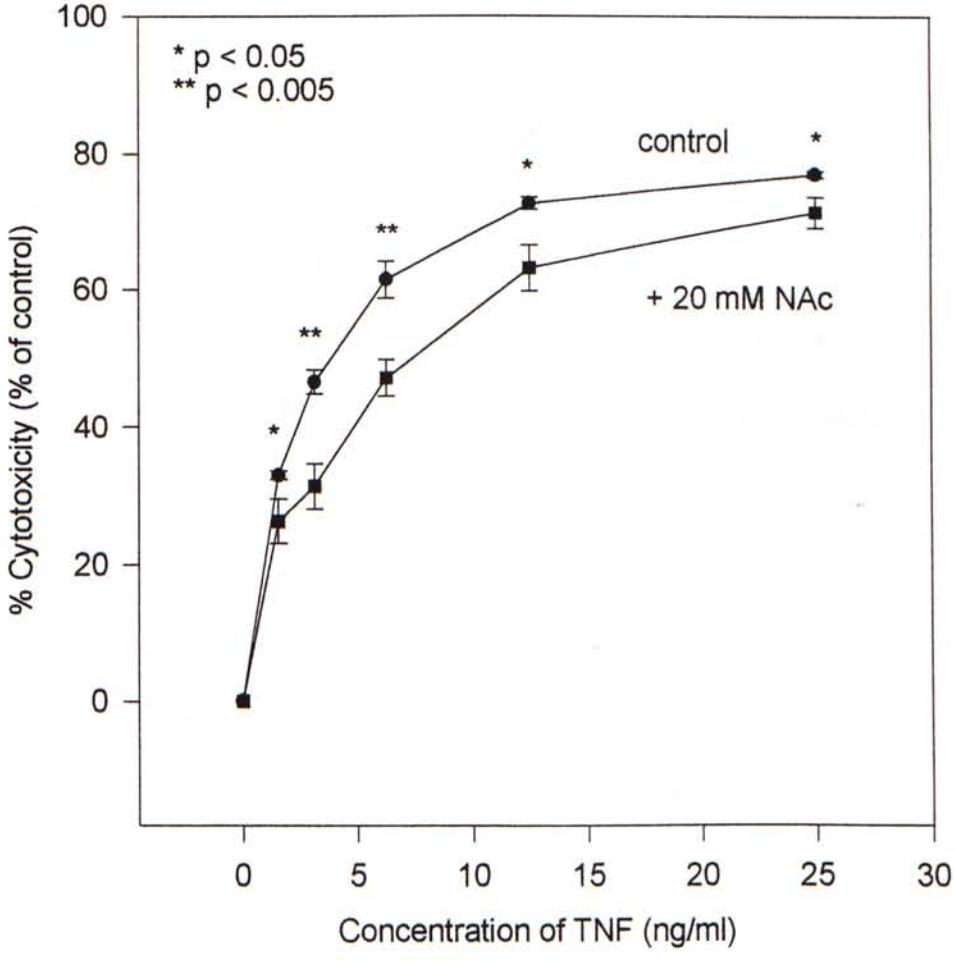

Figure 3.21

Addition of NAc reduced TNF-mediated cytotoxicity in L929 cells. L929 cells were seeded at 3 x 10^4/well in complete RPMI 1640 medium in a 96-well plate and incubated for 20 hr at 37 °C, 5 % CO_2. 100 µl TNF of various concentrations in the presence (■) or absence (●) of NAc (20 mM) in serum-free medium was added and incubated for 20 hr at 37 °C, 5 % CO_2. Neutral red assay was then applied and O.D. at 540 nm was read by a microplate reader (n = 3). * $p < 0.05$ and ** $< p < 0.005$ indicate that there was a significant difference between control and treatment group.

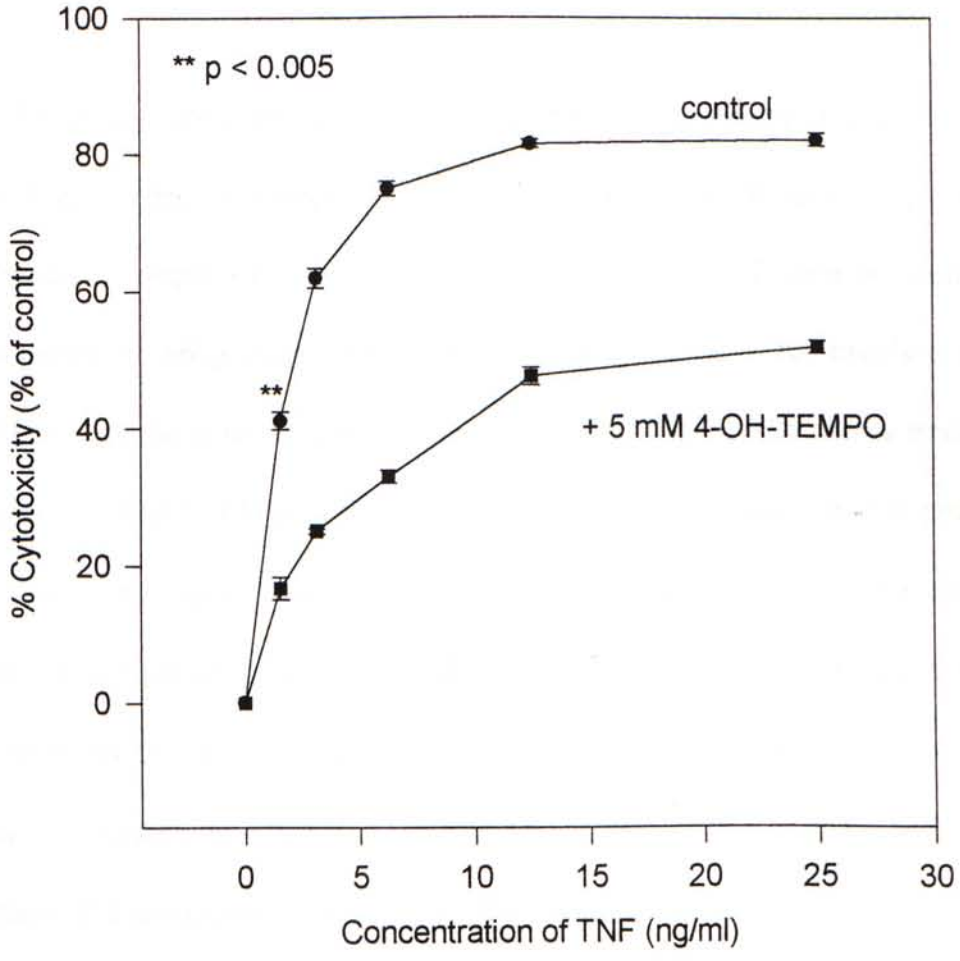

Figure 3.22

Addition of 4-OH-TEMPO reduced TNF-mediated cytotoxicity in L929 cells. L929 cells were seeded at 3 x 10^4/well in complete medium in a 96-well plate and incubated for 20 hr at 37 °C, 5 % CO_2. 100 µl TNF of various concentrations in the presence (■) or absence (●) of 4-OH-TEMPO (5 mM) in serum-free medium was added and incubated for 20 hr at 37 °C, 5 % CO_2. Neutral red assay was then applied and O.D. at 540 nm was read by a microplate reader (n = 3).

and DNP (mitochondrial protonophorous uncoupler of electron flow) were used. Figure 3.23 shows the site of the actions of these mitochondrial inhibitors.

From the cytotoxicity assay, addition of 50 μM rotenone produced a lower TNF-mediated cytotoxicity (reduced 20 - 40 %) (Figure 3.24). Rotenone is one of the mitochondrial complex I inhibitors that blocks the flow of electron from NADH dehydrogenase to ubiquinone (UQ), it reduces $O_2\bullet^-$ production that mainly comes from the UQ site and therefore, it is protective against TNF. Figure 3.25 shows similar results with 250 μM TTFA. TTFA is the mitochondrial complex II inhibitor that prevents the flow of electron from succinate dehydrogenase to UQ and reduces $O_2\bullet^-$ production also. In contrast, application of mitochondrial complex III inhibitor such as antimycin A (25 μM) enhanced the TNF-mediated cytotoxicity (increased about 5 %) (Figure 3.26). Antimycin A blocks the electron flow from UQ to cytochrome c_1 (cyt c_1), that strongly potentiated the production of $O_2\bullet^-$ from the UQ site. This explains why TNF-mediated cell death was enhanced. In summary, TNF increases the release of ROS from mitochondria and the action of TNF may be on mitochondrial complex III.

The data from CLSM further confirmed that rotenone reduced the amount of TNF-mediated $O_2\bullet^-$ production in L929 cells (Figure 3.27 and Figure 3.28). As shown in Figure 3.27, the total fluorescence intensities in TNF-treated group and control group were higher than that of TNF-plus-rotenone group and rotenone-treated group at 45 min. These results indicated that rotenone blocked the electron flow from complex I to UQ, therefore, reduced $O_2\bullet^-$ production. The release of $O_2\bullet^-$ converted HE into EtBr and

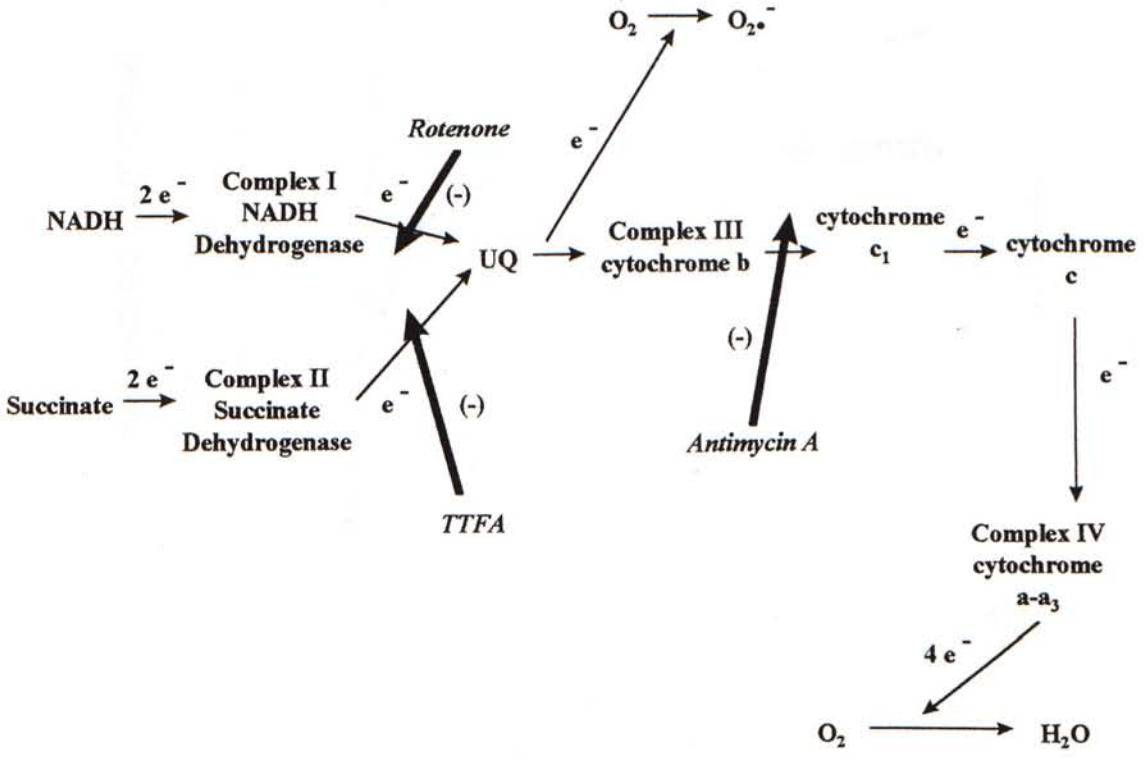

Figure 3.23
The site of the actions of mitochondrial inhibitors.

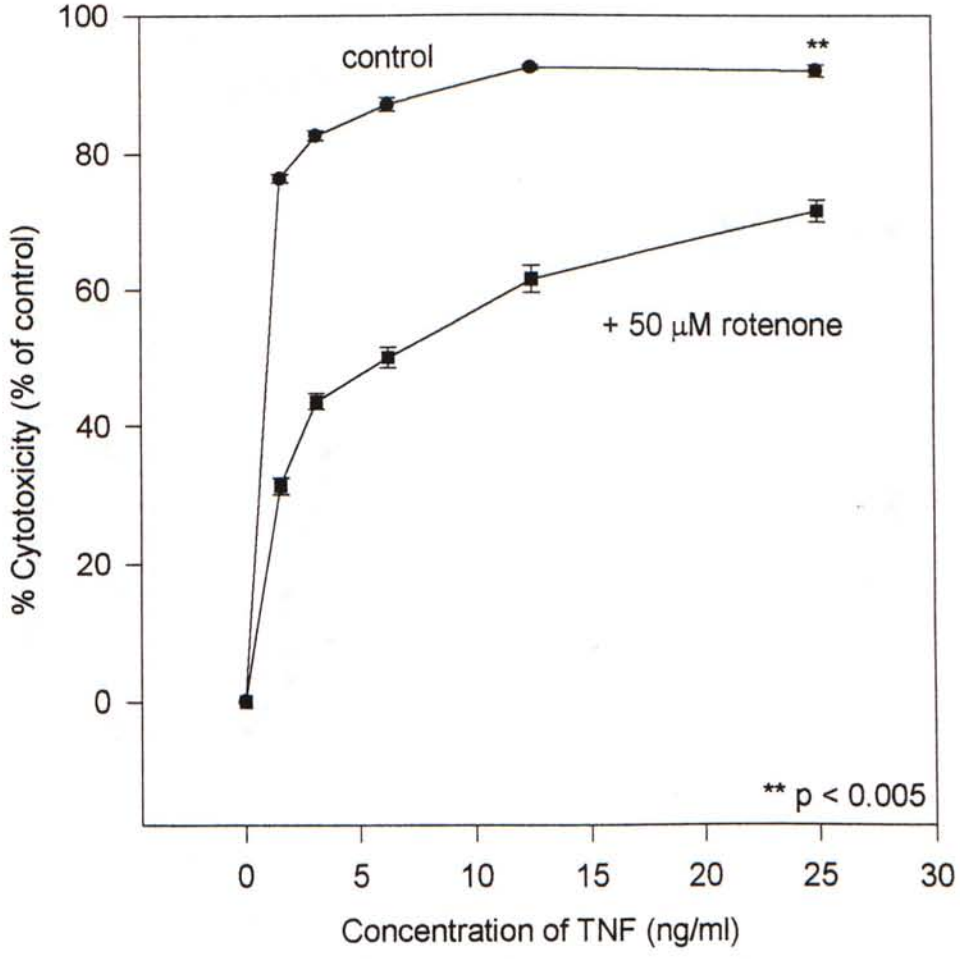

Figure 3.24
Addition of rotenone produced a lower TNF-mediated cytotoxicity in L929 cells. L929 cells were seeded at 3 x 10^4/well in complete medium in a 96-well plate and incubated for 20 hr at 37 °C, 5 % CO_2. 100 μl TNF of various concentrations in the presence (■) or absence (●) of rotenone (50 μM) in serum-free medium was added and incubated for 20 hr at 37 °C, 5 % CO_2. MTT assay was then applied (n = 7, expt = 2). Similar results were obtained in neutral red assay (data not shown).

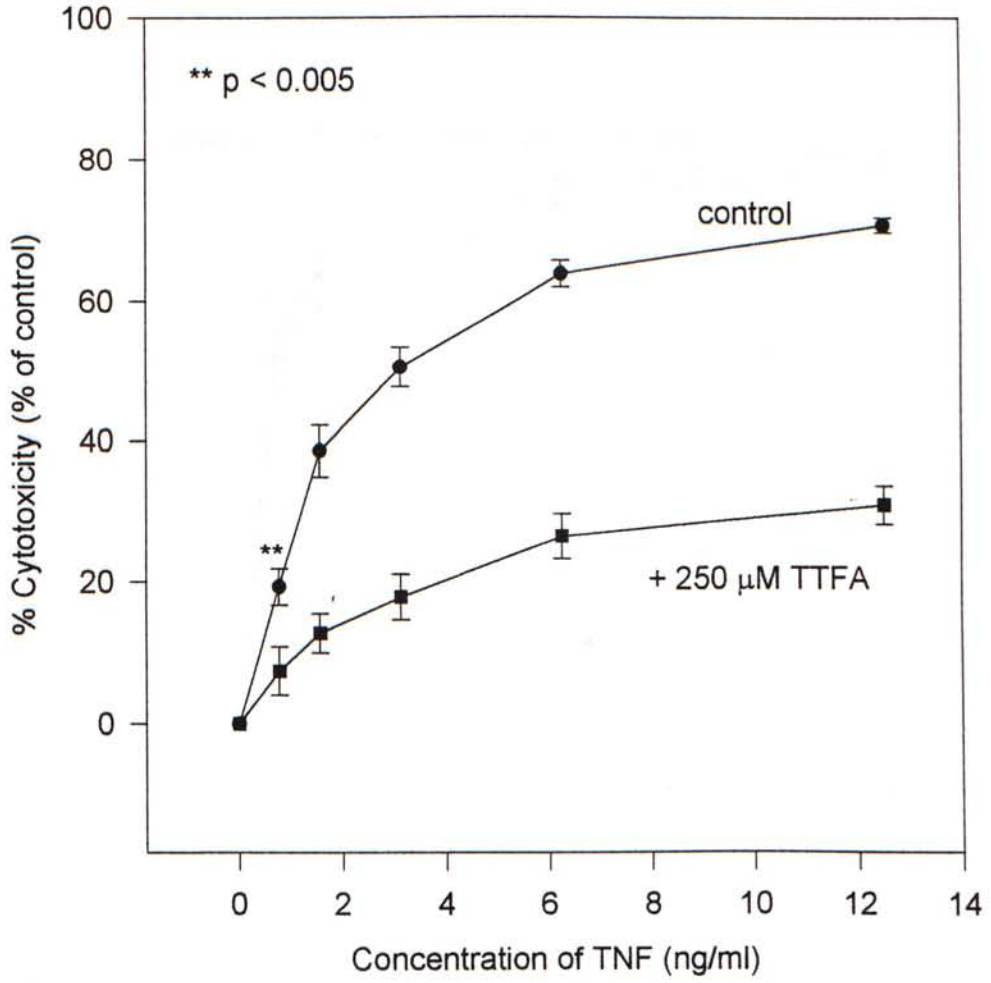

Figure 3.25
Addition of TTFA produced a lower TNF-mediated cytotoxicity in L929 cells. L929 cells were seeded at 3 x 10^4/well in complete medium in a 96-well plate and incubated for 20 hr at 37 °C, 5 % CO_2. 100 μl TNF of various concentrations in the presence (■) or absence (●) of TTFA (250 μM) in serum-free medium was added and incubated for 20 hr at 37 °C, 5 % CO_2. Neutral red assay was then applied (n = 7, expt = 2).

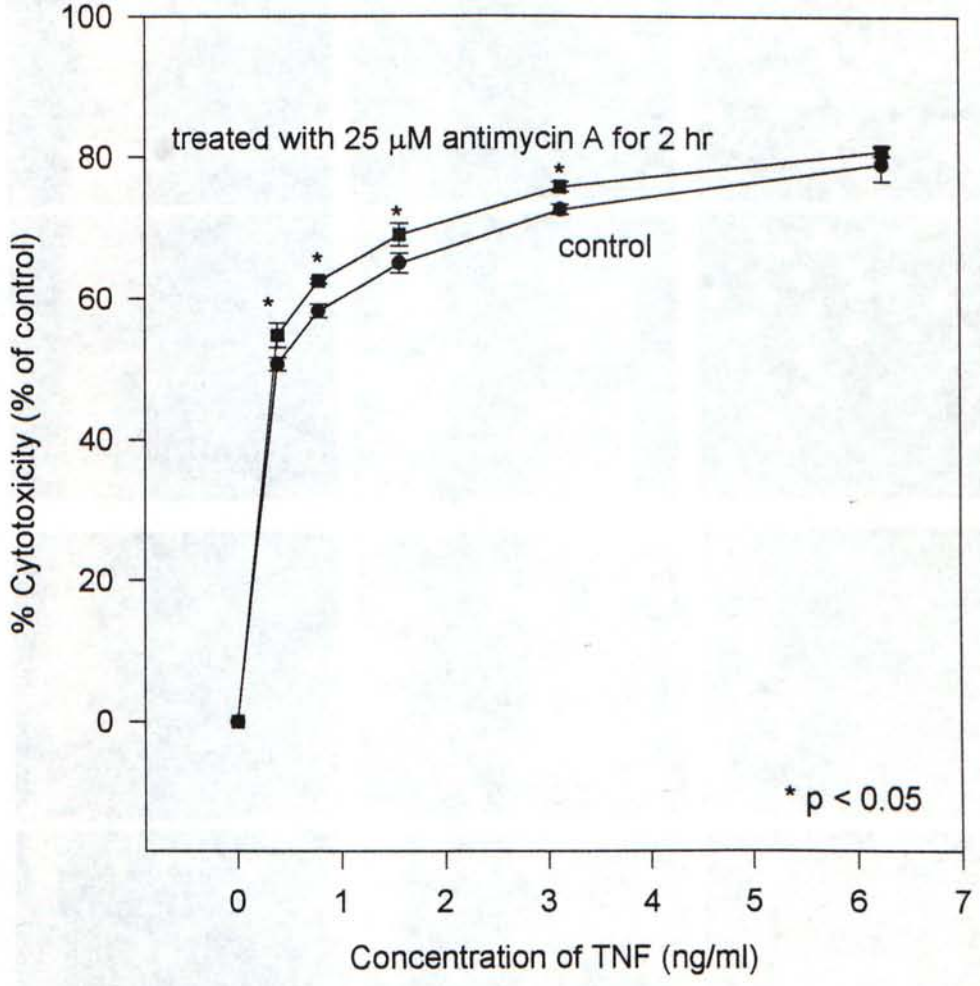

Figure 3.26

Addition of antimycin A enhanced TNF-mediated cytotoxicity in L929 cells. L929 cells were seeded at 3 x 10^4/well in complete medium in a 96-well plate and incubated for 20 hr at 37 °C, 5 % CO_2. 100 μl TNF of various concentrations in the presence (■) or absence (●) of antimycin A (25 μM) in serum-free medium was added and incubated for 20 hr at 37 °C, 5 % CO_2. MTT assay was then applied (n = 7).

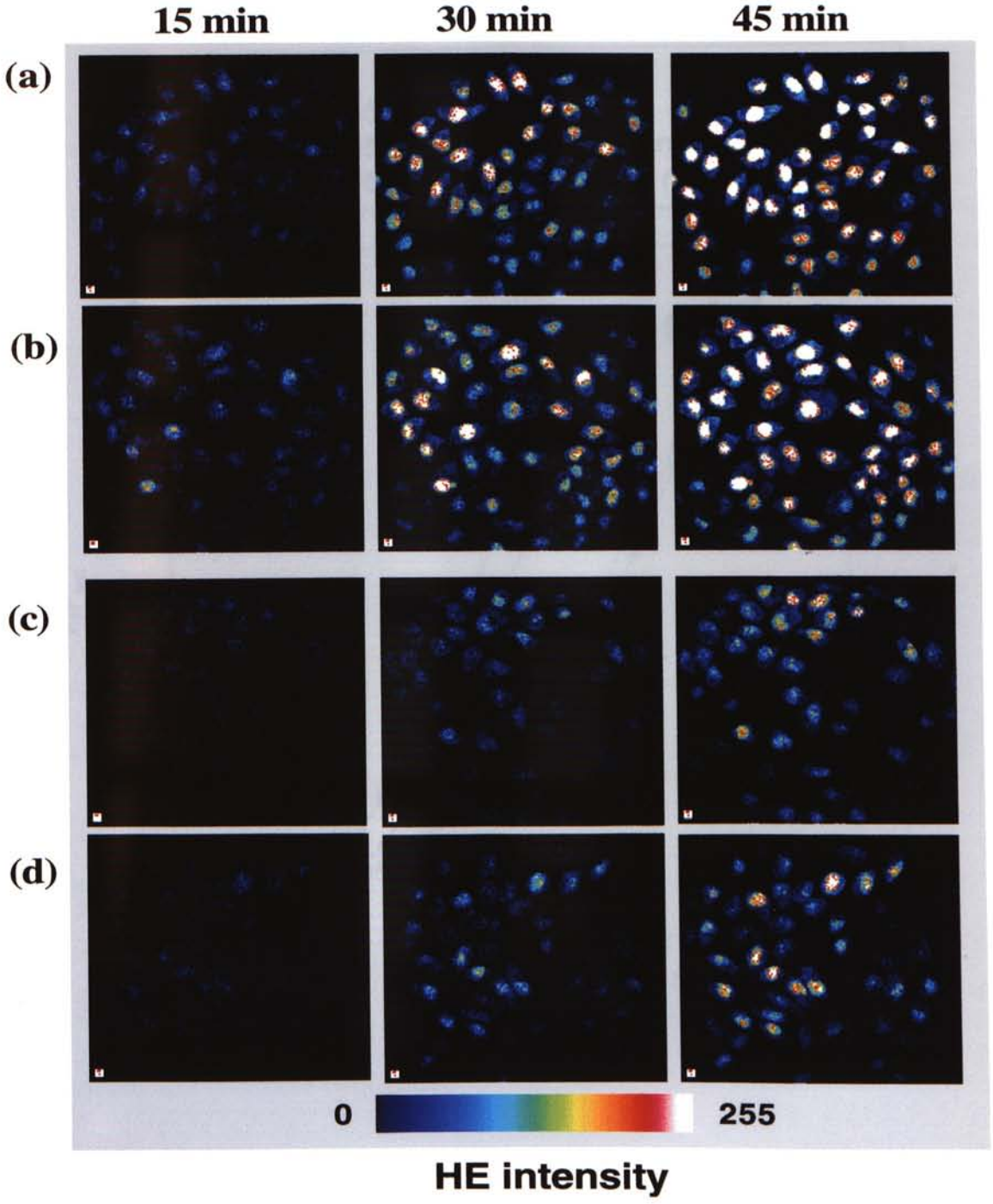

Figure 3.27
The confocal images show that rotenone reduced the amount of TNF-mediated $O_2\bullet^-$ production in L929 cells. L929 cells (2 x 10^3/ml) were seeded on a cover glass and incubated at 37 ℃, 5 % CO_2 for 4 days. Cells were then incubated with Na^+-HEPES buffer (a), 50 ng/ml TNF for 15 min (b), 50 μM rotenone for 15 min (c), and 50 ng/ml TNF and 50 μM rotenone for 15 min (d) at room temperature and the ability of cells to produce $O_2\bullet^-$ was then detected by HE (final concentration 10 μM) with a CLSM-MD at time zero.

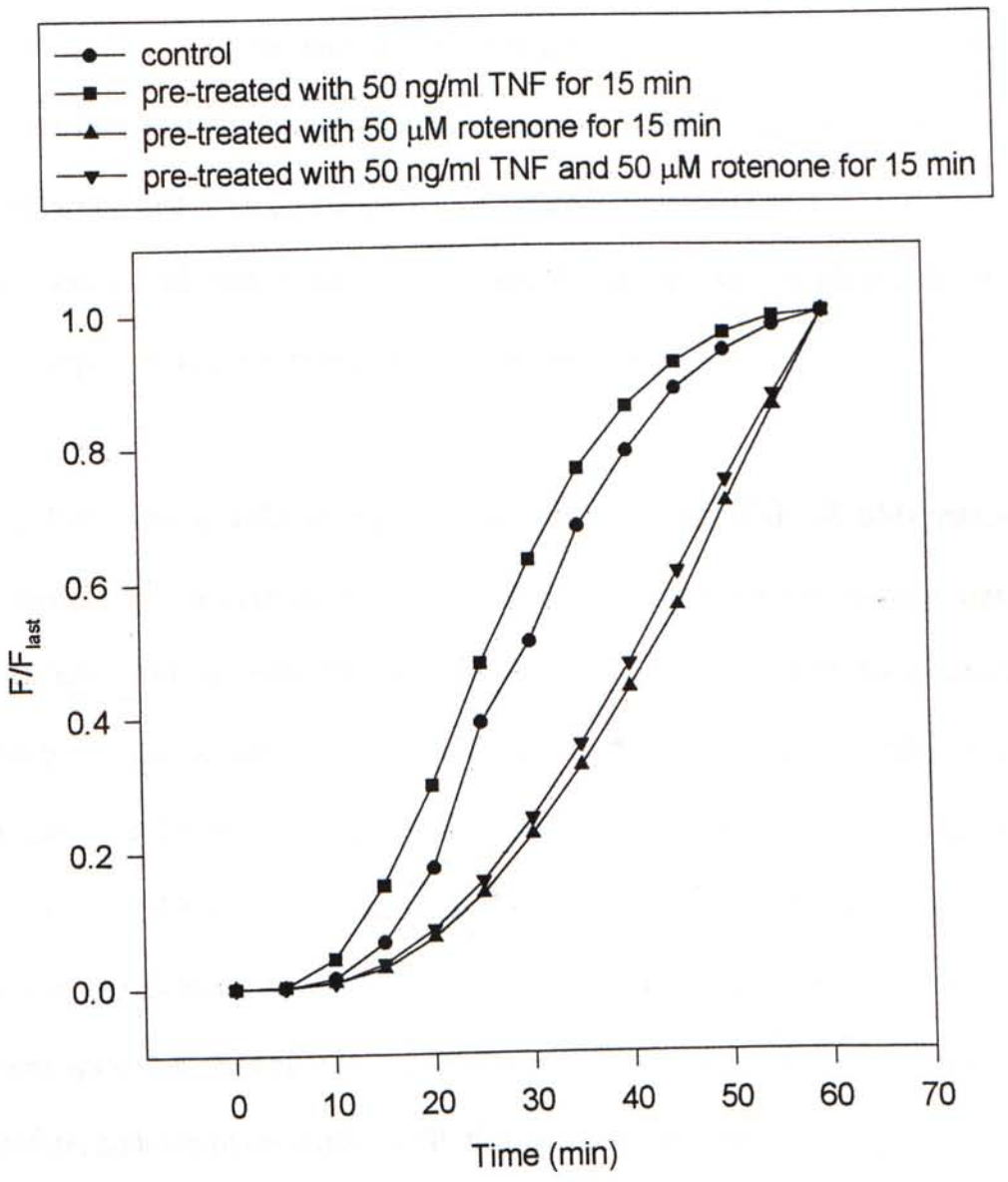

Figure 3.28
Rotenone reduced the rate of TNF-mediated $O_2\bullet^-$ production in L929 cells. This graph summaries the results of the confocal images from figure 3.27. The y-axis, F/F_{last}, represented the summation of fluorescence intensity from all cells at each time interval that was divided by the total fluorescence intensity of the last image.

therefore, it chelated DNA and emitted fluorescence from the nucleus. In contrast, antimycin A enhanced the rate of TNF-mediated $O_2\bullet^-$ production in L929 cells (Figure 3.29 and Figure 3.30). At the 45 min, the total fluorescence intensities in antimycin A-treated group and TNF-plus-antimycin A-treated group were higher than that of TNF-treated group and control group. This implied that antimycin A blocked electron flow from complex III to cyt c_1 that enhanced $O_2\bullet^-$ production.

Furthermore, addition of protonophorous uncoupler DNP (30 μM) reduced TNF-mediated cytotoxicity (about 10 - 30 %) (Figure 3.31). DNP allows electron transport in mitochondria but prevents the phosphorylation of ADP to ATP by uncoupling the essential linkage between electron transport and ATP synthesis. In the presence of uncoupler, the free energy released by electron transport appears as heat rather than as newly made ATP since uncoupling agents greatly increase the permeability of inner membrane to proton. As mentioned in section 1.4.1, depletion of intracellular ATP blocked apoptosis since apoptosis is ATP-dependent (review: Nicotera and Leist, 1997). Therefore, addition of uncoupler DNP, that reduces ATP synthesis, might block apoptosis and reduced TNF-mediated cytotoxicity.

In conclusion, TNF increased the release of ROS such as H_2O_2 and $O_2\bullet^-$ which may involve in cell death. The release of H_2O_2 by TNF was time dependent. As the incubation time of TNF increased, the amount of production of H_2O_2 increased. Addition of metabolic inhibitor such as AMD, that may block TNF-induced MnSOD production, increased the release of $O_2\bullet^-$. Application of antioxidants such as catalase,

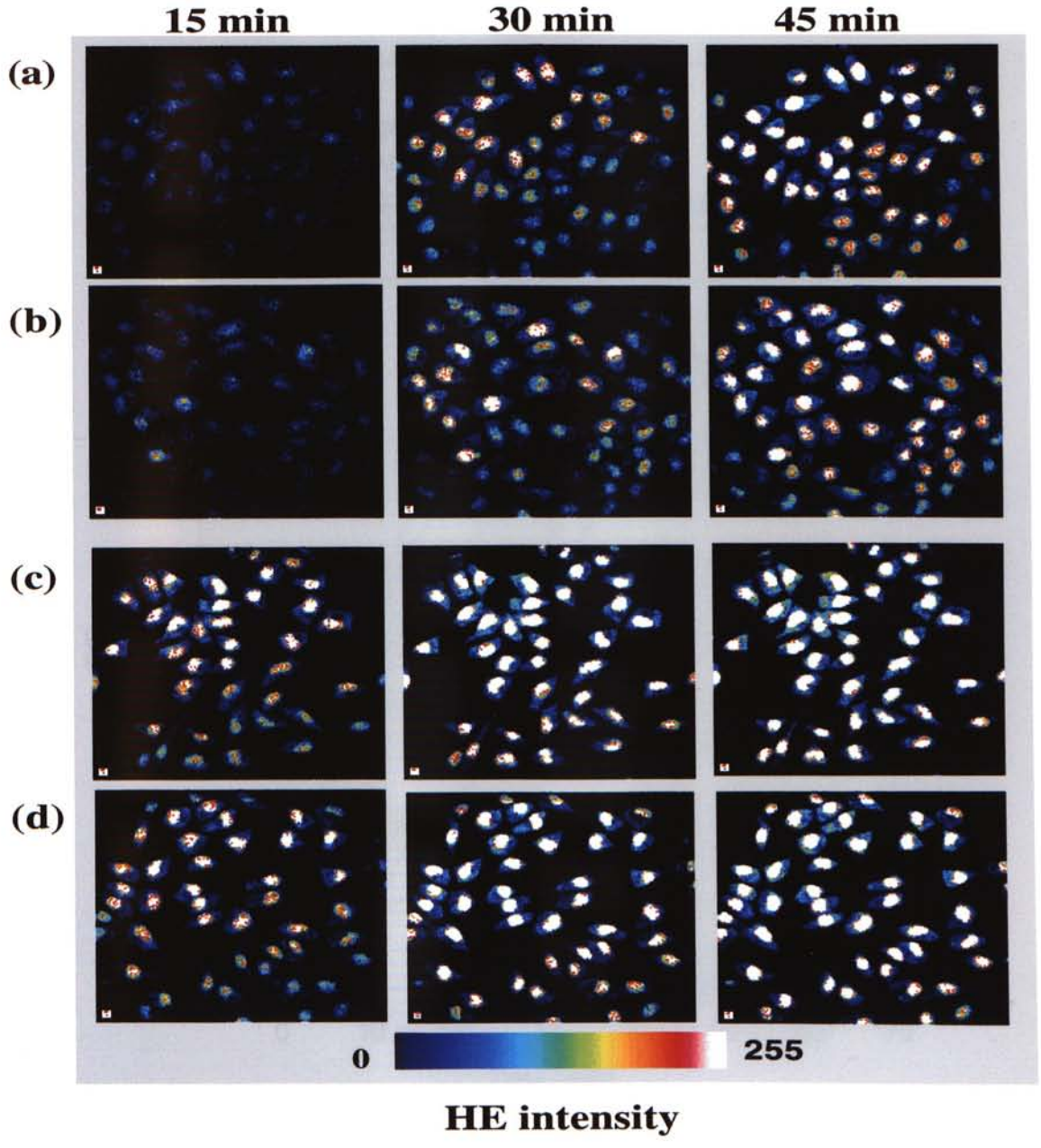

Figure 3.29
The confocal images show that antimycin A enhanced the amount of TNF-mediated $O_2\bullet^-$ production in L929 cells. L929 cells (2 x 10^3/ml) were seeded on a cover glass and incubated at 37 ℃, 5 % CO_2 for 4 days. Cells were then incubated with Na^+-HEPES buffer (a), 50 ng/ml TNF for 15 min (b), 25 μM antimycin A for 15 min (c), and 50 ng/ml TNF and 25 μM antimycin A for 15 min (d) at room temperature and the ability of cells to produce $O_2\bullet^-$ was then detected by HE (final concentration 10 μM) with a CLSM-MD at time zero.

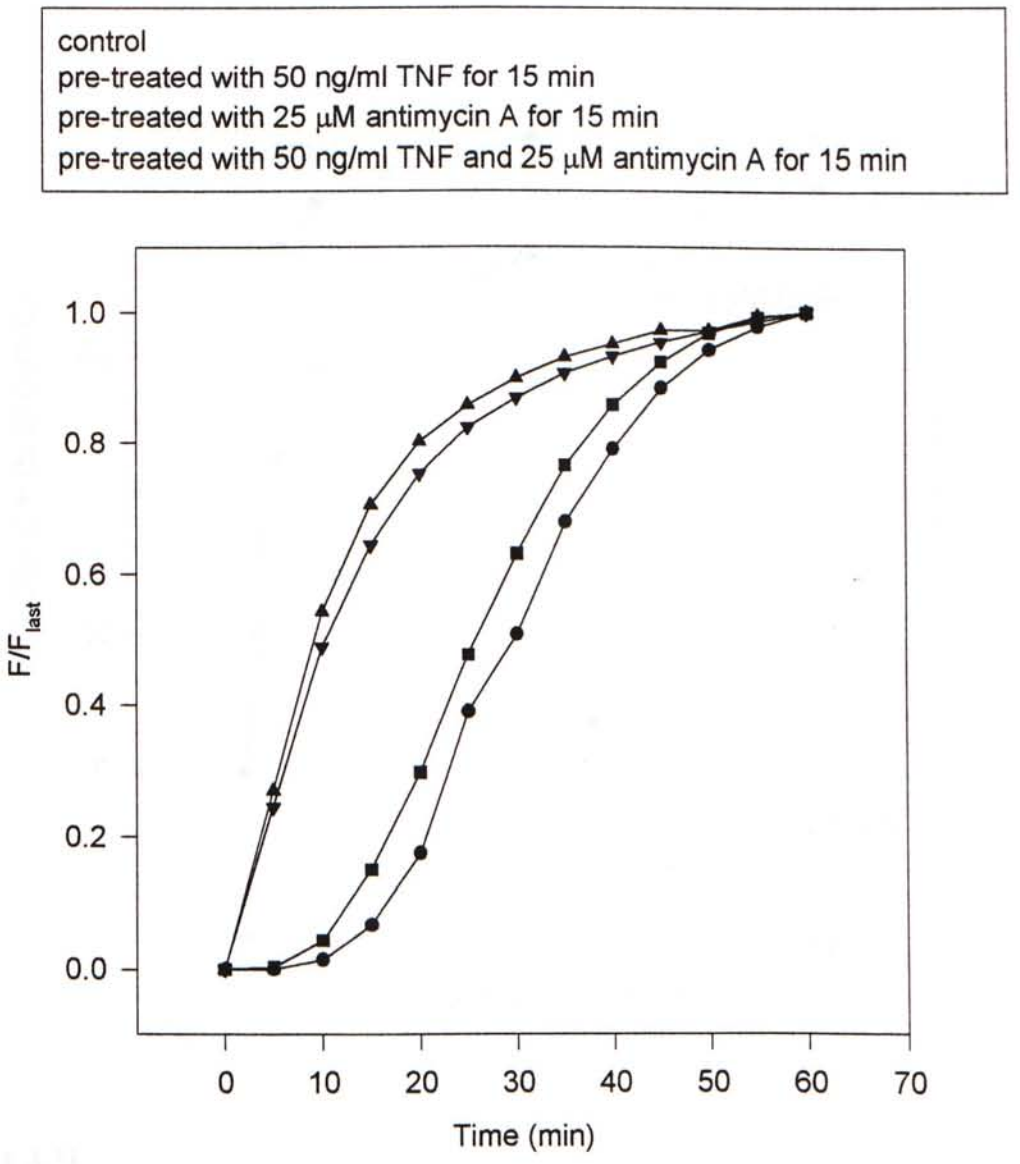

Figure 3.30

Antimycin A enhanced the rate of TNF-mediated $O_2\bullet^-$ production in L929 cells. This graph summaries the results of the confocal images from figure 3.29. The y-axis, F/F_{last}, represented the summation of fluorescence intensity from all cells at each time interval that was divided by the total fluorescence intensity of the last image.

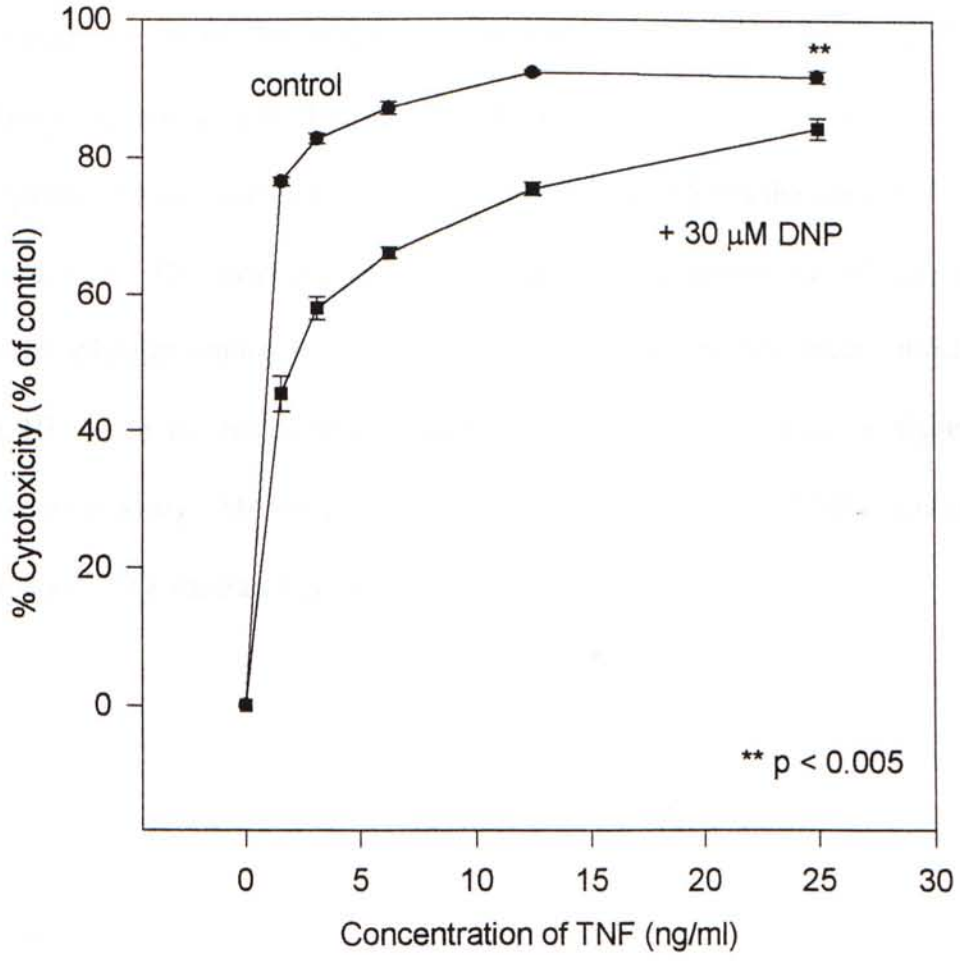

Figure 3.31

Addition of DNP produced a lower TNF-mediated cytotoxicity in L929 cells. L929 cells were seeded at 3 x 10^4/well in complete medium in a 96-well plate and incubated for 20 hr at 37 °C, 5 % CO_2. 100 μl TNF of various concentrations in the presence (■) or absence (●) of DNP (30 μM) in serum-free medium was added and incubated for 20 hr at 37 °C, 5 % CO_2. MTT assay was then applied (n = 7, expt = 2). Similar results were obtained in neutral red assay (data not shown).

MnSOD, NAc and 4-OH-TEMPO reduced TNF-mediated cytotoxicity. Furthermore, TNF potentiated the release of $O_2\bullet^-$ from mitochondria and the action of TNF may be on mitochondrial complex III. The evidence was that addition of mitochondrial complex I and II inhibitors, rotenone and TTFA, that blocked the electron flow from NADH dehydrogenase and succinate dehydrogenase, respectively, reduced the release of $O_2\bullet^-$ and produced a lower TNF-mediated cytotoxicity. In contrast, application of mitochondrial complex III inhibitor antimycin A, that blocked the electron flow from mitochondrial complex III to cyt c_1, enhanced the production of $O_2\bullet^-$ and induced a higher TNF-mediated cytotoxicity. Moreover, the mitochondrial uncoupler DNP reduced ATP production and TNF-mediated cytotoxicity.

3.4 The Role of Calcium in Tumor Necrosis Factor-Alpha Treatment

3.4.1 Introduction

Since $[Ca^{2+}]_i$ plays an important role in cell death, researchers try to consider the relationship between TNF and $[Ca^{2+}]_i$ level. It was found that TNF increases $[Ca^{2+}]_i$ level in L929 cells (Kong *et al.*, 1997). However, Hasegawa and Bonavida reported that TNF-induced cell death was Ca^{2+}-independent in human PBL (Hasegawa and Bonavida, 1989). In this project, the $[Ca^{2+}]_i$ level was examined by different approaches.

Two fluorescence dyes for monitoring $[Ca^{2+}]_i$ level were applied, fluo-3/AM and fura-red/AM. Fluo-3/AM is a commonly used fluorescence indicator for free Ca^{2+} (Merritt *et al.*, 1990). Fluo-3 contains five negative charges and it cannot pass through the plasma membrane. Hence, the uncharged acetoxymethyl (AM) ester form of fluo-3 was employed. The advantage in using fluo-3/AM is that it is distributed rather homogeneously within the cytosol and nucleus (Nicotera *et al.*, 1994). On the other hand, the acetoxymethyl ester form of fura-red was employed for detecting $[Ca^{2+}]_i$ level by chelating free Ca^{2+} also. The difference between fluo-3/AM and fura-red/AM is that the fluorescence intensity of fluo-3/AM increases as $[Ca^{2+}]$ increases whereas the fluorescence intensity of fura-red/AM decreases. Since the emission wavelengths for fluo-3/AM and fura-red/AM are different, they can be loaded and assayed simultaneously that will not interfere with each other.

In this section, several techniques such as CLSM and FCM were applied to monitor the release of $[Ca^{2+}]_i$ inside L929 cells.

3.4.2 Release of Intracellular Calcium in TNF-Treated L929 Cells

$[Ca^{2+}]_i$ was detected by a CLSM (Meridian). Figure 3.32 shows the confocal images. It was found that addition of Ca^{2+}-free buffer did not produce Ca^{2+} release in a short time course (the time interval for each scan was 5 sec). Figure 3.33 shows the change of $[Ca^{2+}]_i$ quantitatively with the replacement of normal buffer by Ca^{2+}-free buffer and the addition of 40 μg/ml ionomycin. It is obviously that addition of ionomycin to cells induced a sharp $[Ca^{2+}]_i$ rise. The increase in $[Ca^{2+}]_i$ by ionomycin confirmed that the Ca^{2+} system did not impair under the experimental conditions and the Ca^{2+} released by ionomycin were from intracellular stores.

Figure 3.34 and Figure 3.35 illustrate that 50 ng/ml TNF did not cause $[Ca^{2+}]_i$ increase in a short incubation time (~ 400 sec) while ionomycin produced an abrupt increase in Ca^{2+} fluorescence intensity. These imply that application of TNF for a short time period did not cause the release of Ca^{2+} from intracellular stores.

For a longer time period, Ca^{2+}-free buffer did not cause an increase in $[Ca^{2+}]_i$ while the addition of ionomycin (40 μg/ml) induced Ca^{2+} release (Figure 3.36 and 3.37). Interestingly, addition of 50 ng/ml TNF caused a slow rise in $[Ca^{2+}]_i$ in Ca^{2+}-free buffer (Figure 3.38). Figure 3.39 summaries the results of Figure 3.38 quantitatively. It is clear that the replacement of Ca^{2+}-containing buffer with a Ca^{2+}-free buffer reduced the fluo-3 fluorescence in the early phase of the experiment. After the addition of TNF (50ng/ml), the $[Ca^{2+}]_i$ increased slowly. This increase was not observed in the Ca^{2+}-free buffer in the absence of TNF (Figure 3.37). These results suggest that TNF could mobilize the Ca^{2+}

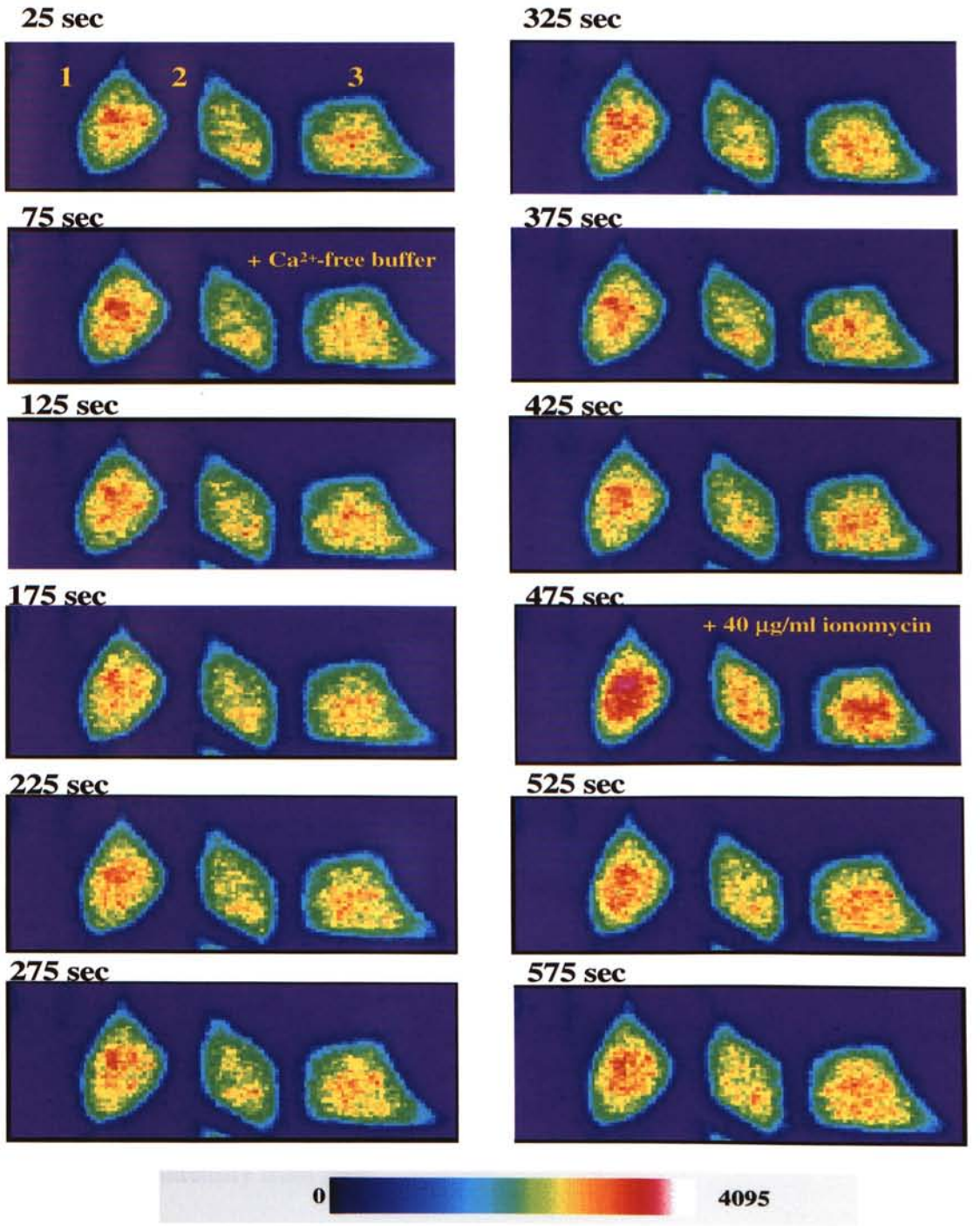

Figure 3.32
The confocal images show that addition of Ca^{2+}-free buffer did not cause Ca^{2+} release in L929 cells in a short time course. L929 cells (2 x 10^3/ml) were seeded on cover glass and incubated at 37 ℃ and 5 % CO_2 for 3 days. Cells were mounted on a home-made holder and washed twice by Na^+-HEPES buffer. Cells were loaded with 10 µM fluo-3/AM for 1 hr and then washed twice by Ca^{2+}-free buffer. Confocal scanning was made with a 5-second-interval at room temperature. Ca^{2+}-free buffer and 40 µg/ml ionomycin were added at the 75th and 475th sec, respectively (n = 3).

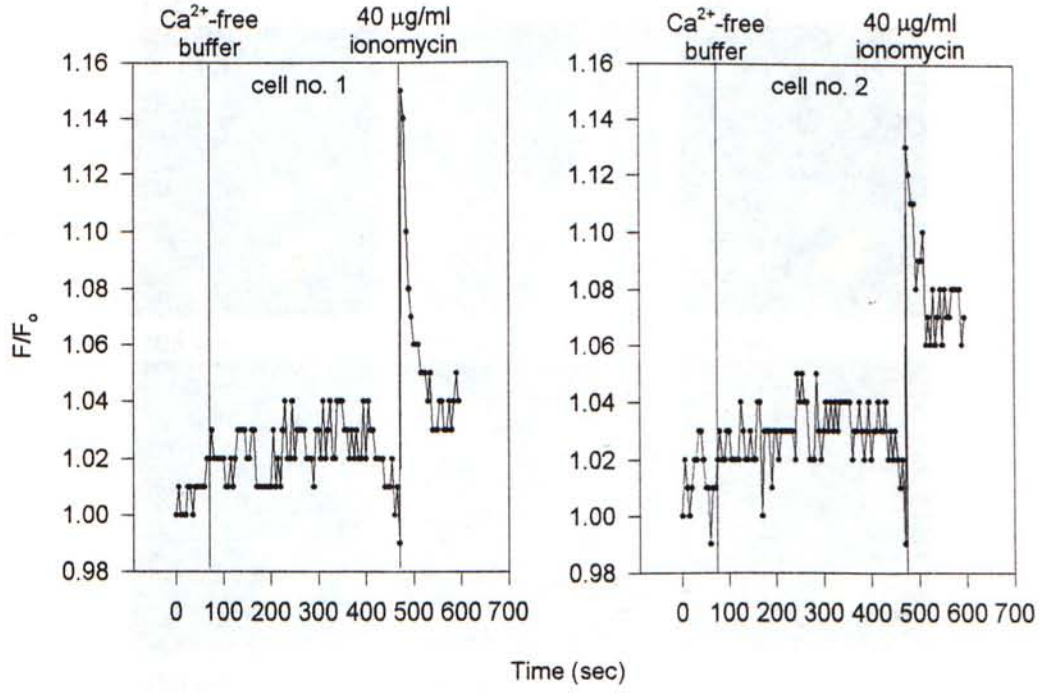

Figure 3.33

Ca^{2+}-free buffer did not cause Ca^{2+} release in L929 cells in a short time course. This graph summaries quantitatively the results of the confocal images of cell number 1 and 2 from figure 3.32. Ca^{2+}-free buffer and ionomycin (40µg/ml) were introduced to the cells at the 1st and 2nd hairline, respectively. The y-axis, F/Fo, represented the normalized fluorescence intensity from cells.

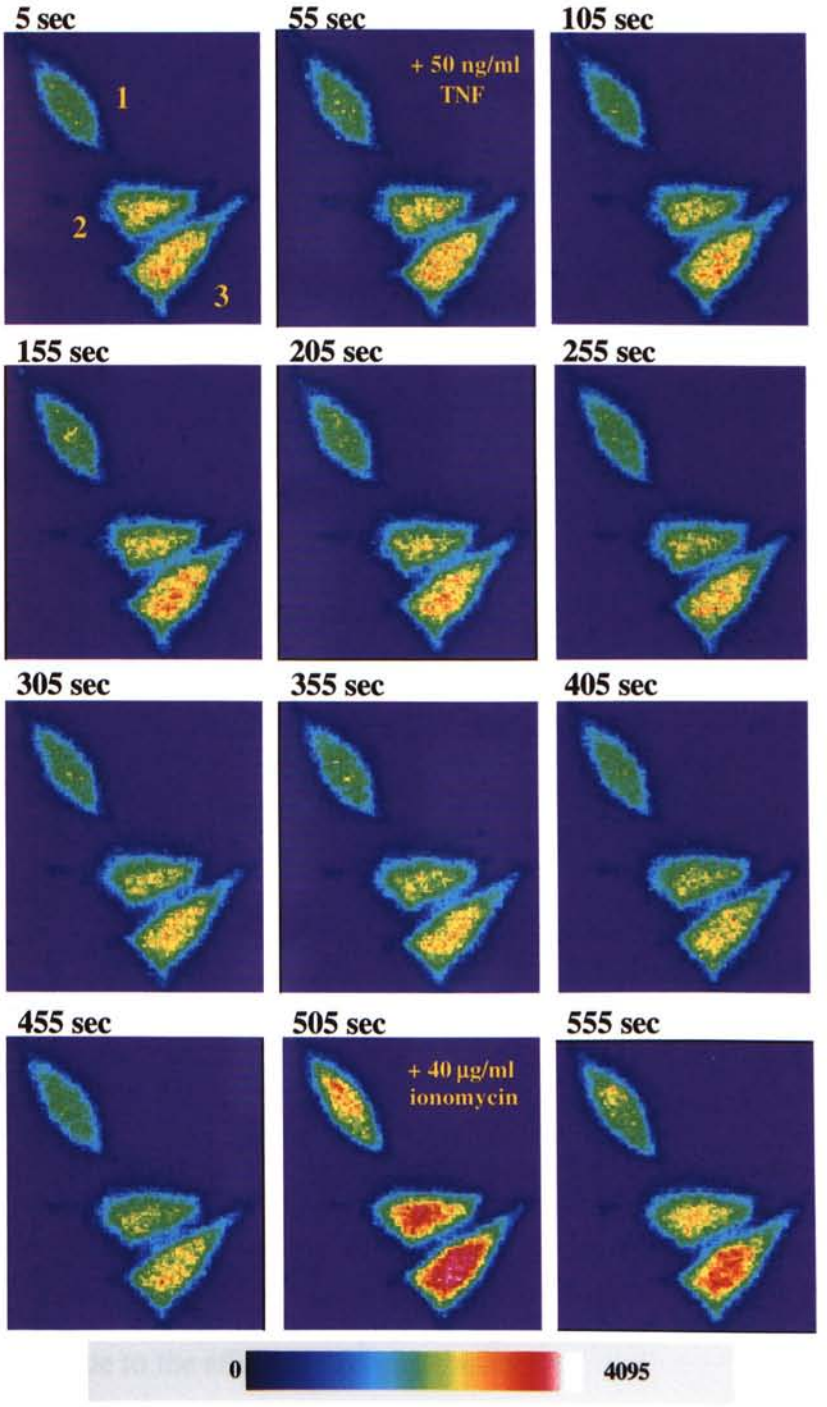

Figure 3.34
The confocal images show that addition of TNF did not cause Ca^{2+} release in L929 cells in a short time course. L929 cells (2 x 10^3/ml)were seeded on cover glass and incubated at 37 ℃ and 5 % CO_2 for 3 days. Cells were mounted on a home-made holder and washed twice by Na^+-HEPES buffer and cells were loaded with 10 µM fluo-3/AM for 1 hr and then washed twice by Ca^{2+}-free buffer. Confocal scanning was made with a 5-second-interval at room temperature. 50 ng/ml TNF in Ca^{2+}-free buffer and 40 µg/ml ionomycin were added at the 55th and 505th sec, respectively (n = 3).

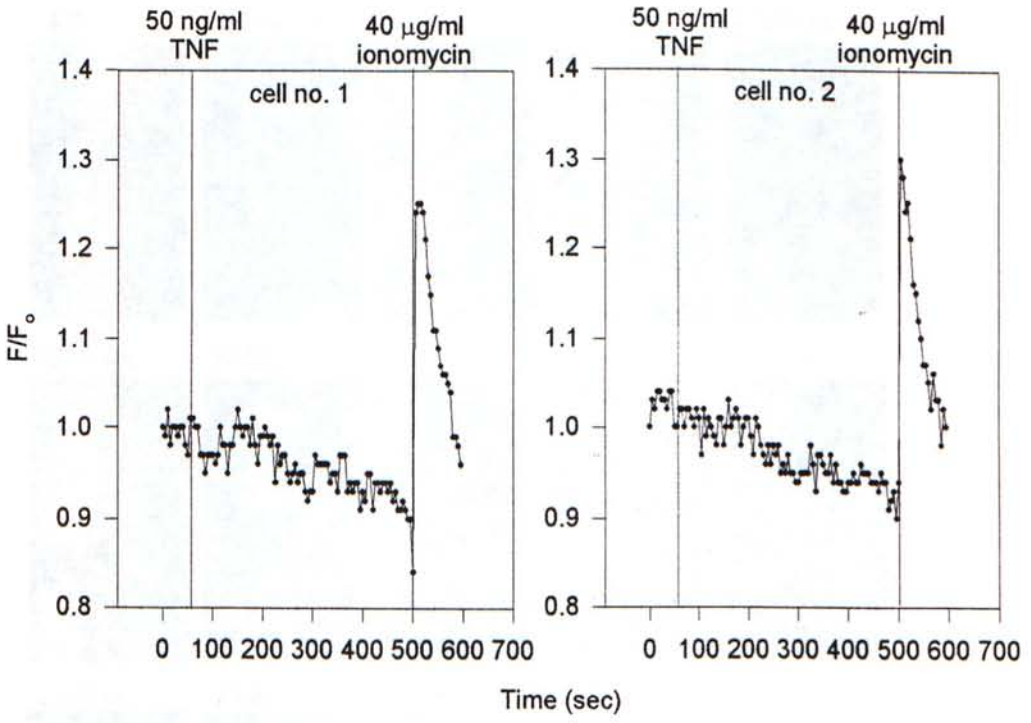

Figure 3.35

Addition of TNF did not cause Ca^{2+} release in a short time assay. This graph summaries quantitatively the results of the confocal images of cell number 1 and 2 from figure 3.34. TNF (50 ng/ml) in Ca^{2+}-free buffer and ionomycin (40μg/ml) were introduced to the cells at the 1st and 2nd hairline, respectively. The initial decrease in fluorescence intensity might be due to the effect of Ca^{2+}-free buffer.

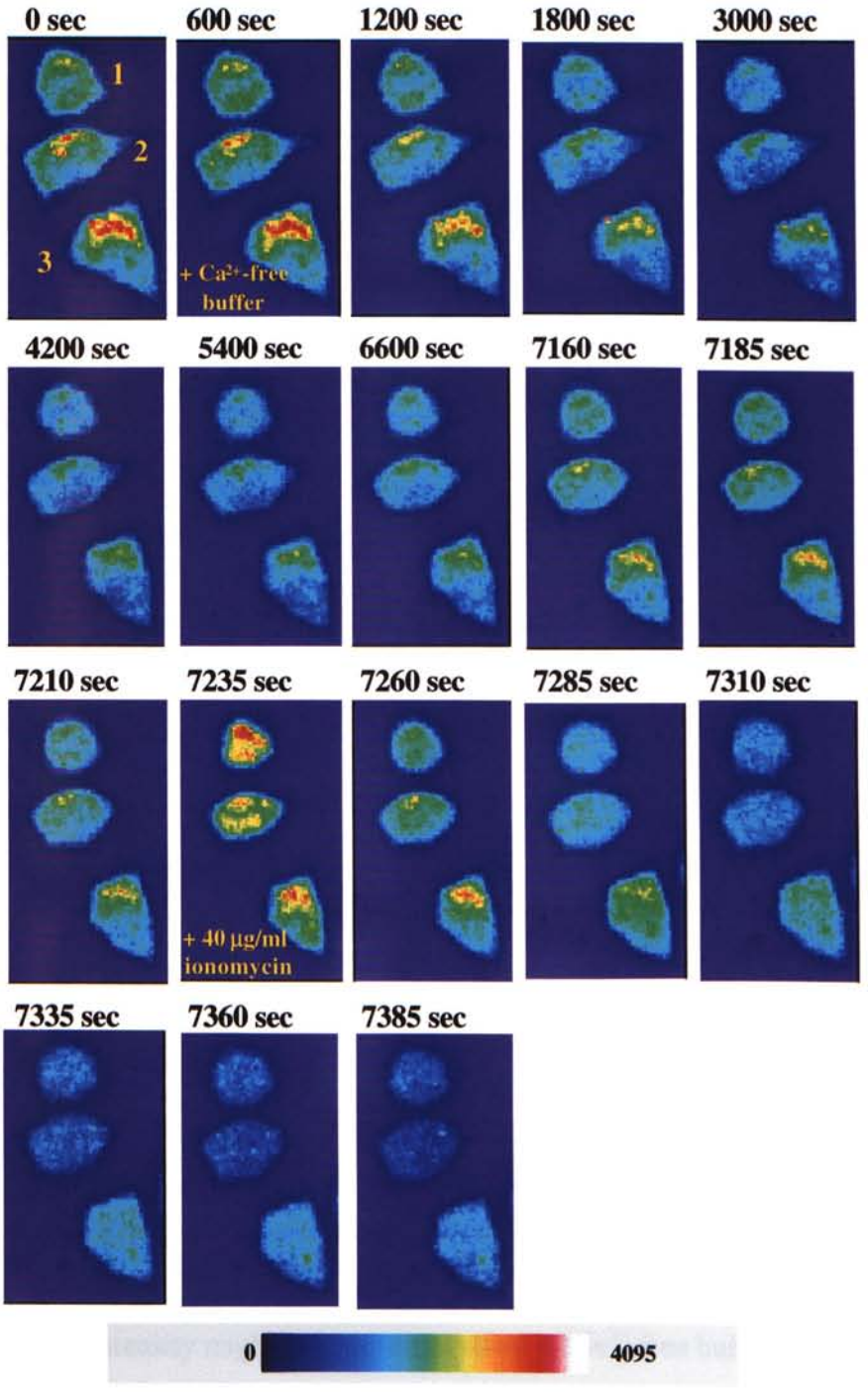

Figure 3.36
The confocal images show that addition of Ca^{2+}-free buffer did not cause Ca^{2+} increase in L929 cells in a long time course. L929 cells (2 x 10^3/ml) were seeded on cover glass and incubated at 37 °C and 5 % CO_2 for 3 days. Cells were mounted on a home-made holder and washed twice by Na^+-HEPES buffer. Cells were loaded with 10 µM fluo-3/AM for 1 hr and then washed twice by Ca^{2+}-free buffer. Confocal scanning was made with a 60-second-interval. Ca^{2+}-free buffer and 40 µg/ml ionomycin were added at the 600th and 6695th sec, respectively (n = 3).

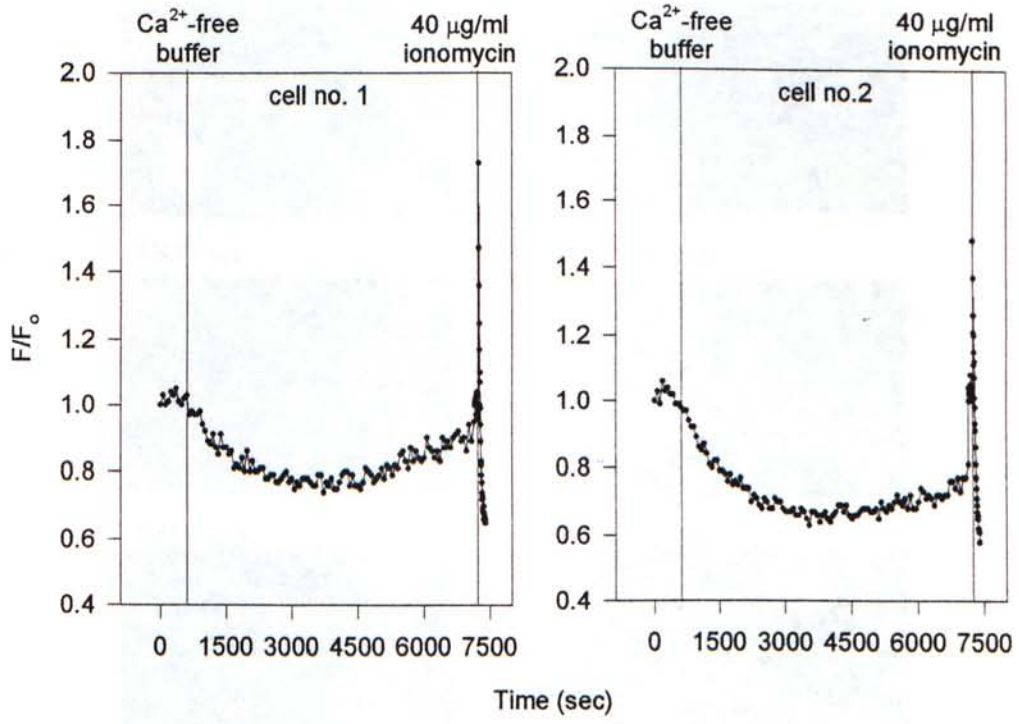

Figure 3.37

Addition of Ca^{2+}-free buffer did not cause Ca^{2+} release in L929 cells in a long time course. This graph summaries quantitatively the results of the confocal images of cell number 1 and 2 from figure 3.36. Ca^{2+}-free buffer and ionomycin (40µg/ml) were introduced to the cells at the 1st and 2nd hairline, respectively. The initial decrease in fluorescence intensity might be due to the effect of Ca^{2+}-free buffer.

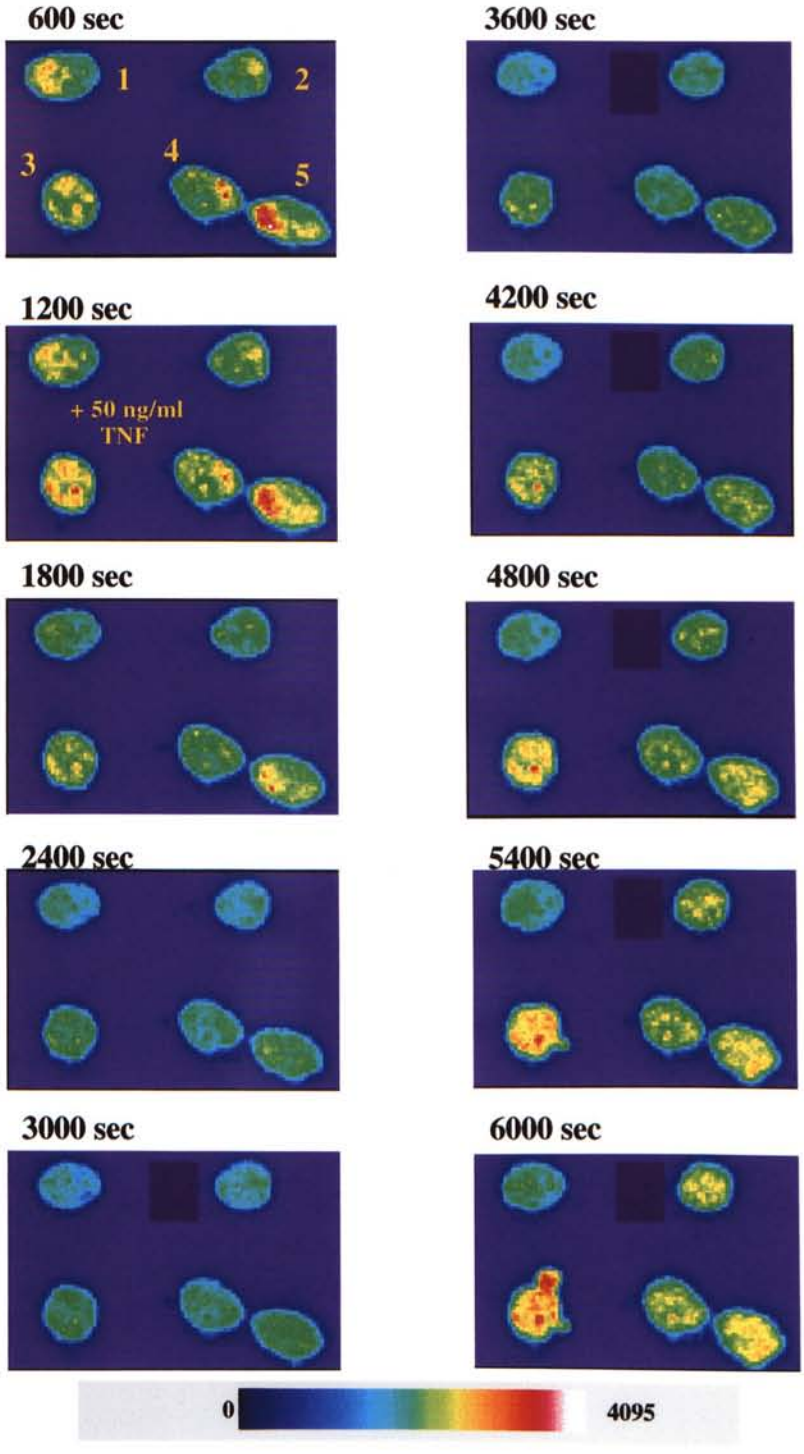

Figure 3.38

The confocal images show that addition of TNF produced a slow rise in $[Ca^{2+}]_i$ in L929 cells in a long time course. L929 cells (2 x 10^3/ml) were seeded on cover glass and incubated at 37 ℃ and 5 % CO_2 for 3 days. Cells were mounted on a home-made holder and washed twice by Na^+-HEPES buffer. Cells were loaded with 10 μM fluo-3/AM for 1 hr and then washed twice by Ca^{2+}-free buffer. Confocal scanning was made with a 60-second-interval. 50 ng/ml TNF was added at the 1200th (n = 5).

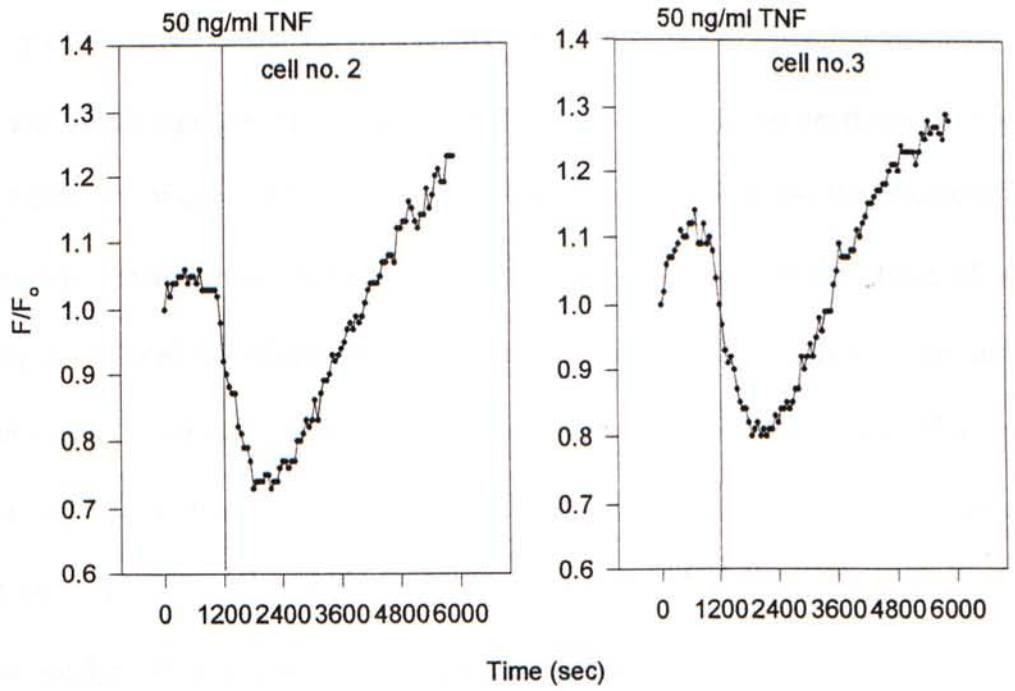

Figure 3.39
Addition of TNF produced the release of Ca^{2+} in a long time assay. This graph summaries quantitatively the results of the confocal images of cell number 2 and 3 from Figure 3.38. 50 ng/ml TNF was added at the 1200th sec and produced a slow rise in $[Ca^{2+}]_i$. The initial decrease in fluorescence intensity might be due to the effect of Ca^{2+}-free buffer.

inside the Ca^{2+} store.

The release of Ca^{2+} in TNF-treated L929 cells was examined by FCM also. Two Ca^{2+} fluorescence dyes, fluo-3/AM and fura-red/AM were loaded into L929 cells simultaneously and the ratio of their fluorescence (fluo-3/fura-red) gave a more accurate and sensitive measurement. Figure 3.40 shows the dot plots from such experiment. The x-axis and y-axis represent the intensity of fluo-3 and fura-red, respectively. It was found that incubation of cells with 50 ng/ml TNF for 3 hr did not increase the release of Ca^{2+} as compare to control group (Figure 3.40a and b). In the control group, addition of 40 μg/ml ionomycin induced the release of Ca^{2+} (Figure 3.40c, Figure 3.41c). In contrast, incubation of cells with 50 ng/ml TNF for 6 hr did produce a significant increase in $[Ca^{2+}]_i$ (Figure 3.41a and b). Addition of ionomycin induced a further release of Ca^{2+}. Furthermore, addition of TNF for 10 hr produced a drastic release of Ca^{2+} (Figure 3.42a and b). To further analyze these results, the cell population was divided into two groups arbitrarily, region 1 (R1) and region 2 (R2) as mentioned in section 2.2.4. Since the $[Ca^{2+}]_i$ level increased, fluorescence of fluo-3 increased whereas fluorescence of fura-red decreased, the cell population shifted anti-clockwisely to the upper-left. If the $[Ca^{2+}]_i$ level was high in L929 cells, more dots should occur in R2 and vice versa in R1. Table 3.1 summarizes the above results, as the incubation time with TNF increased, the release of Ca^{2+} in L929 cells was increased also. It was found that in the incubation of L929 cells with TNF for 3 hr did not cause a significant shift of dots from R1 to R2. However, in 6-hour-incubation of TNF with L929 cells caused a shift of dots from R1 to R2. Furthermore, in 10-hour-inucbation, TNF caused a drastic shift of cells from R1 to R2. In another experiment,

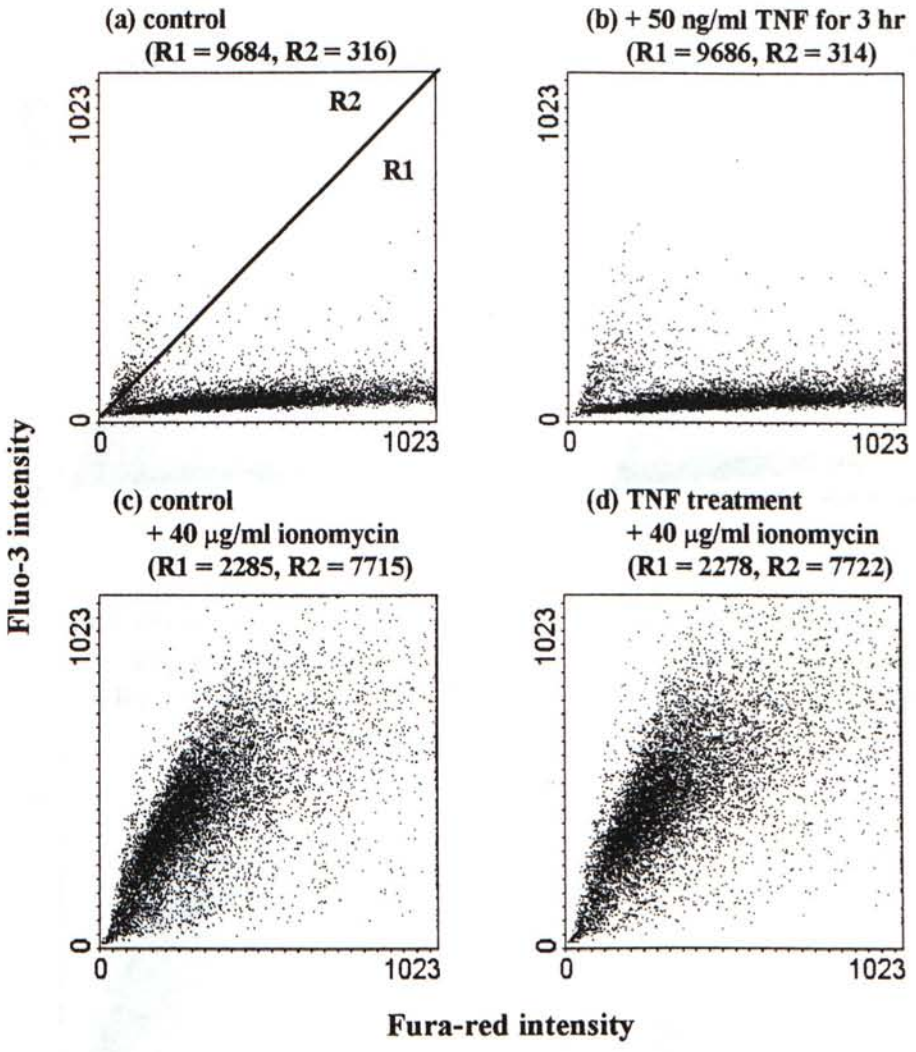

Figure 3.40

Incubation of L929 cells with TNF for 3 hr did not produce a significant change in $[Ca^{2+}]_i$. L929 cells (10^6/ml) were seeded in 6-well plate and were incubated overnight at 37 °C, 5 % CO_2. Subsequently, cells were treated with or without 50 ng/ml TNF at 37 °C for 3 hr and then loaded with 10 μM fluo-3/AM and 10 μM fura-red/AM for another hr. Cells were then trypsinized. After washing, cells were re-suspended in the Na^+-HEPES buffer and the fluorescence of fluo-3 and fura-red were determined by FCM with an argon laser. Y-axis represents the fluorescence intensity of fluo-3 whereas x-axis represents the fluorescence intensity of fura-red. Dots shift to the upper-left, that is, an increase in fluo-3 fluorescence with a decrease in fura-red imply an increase in $[Ca^{2+}]_i$. (a) Control group. (b) L929 cells were incubated with 50 ng/ml TNF. Note that there was no difference in the pattern of dots as compared to the control group. (c) Cells were activated by 40 μg/ml ionomycin 10 min before measurement. (d) Addition of 40 μg/ml ionomycin 10 min before measurement in the TNF-treated group. Note that a shift in the cell population at the upper-left indicates there was no impairment in Ca^{2+} measurement system. The population of cells were divided into two groups (R1 and R2) by the diagonal line arbitrarily and the number of cells in each region was determined.

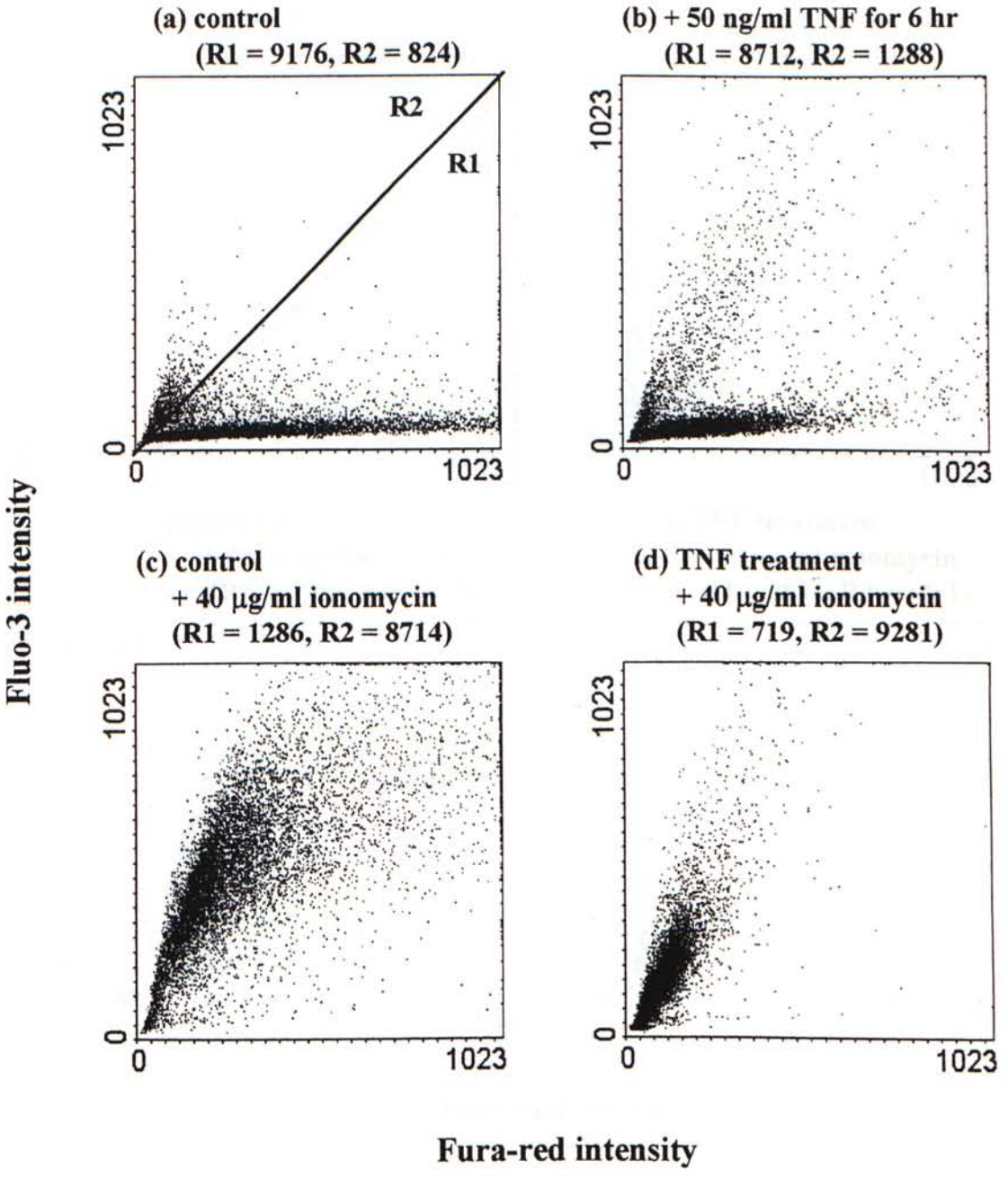

Figure 3.41
Incubation of L929 cells with TNF for 6 hr produced a significant change in $[Ca^{2+}]_i$. (a) Control group. (b) L929 cells were incubated with 50 ng/ml TNF for 6 hr. Note that there was an increase in $[Ca^{2+}]_i$ as compared to the control group. More dots occurred at the upper-left region and there was an decrease in the fluorescence intensity of fura-red. (c) Cells were loaded with 40 μg/ml ionomycin 10 min before measurement. (d) Addition of 40 μg/ml ionomycin in the TNF-treated group caused a shift in the cell population also.

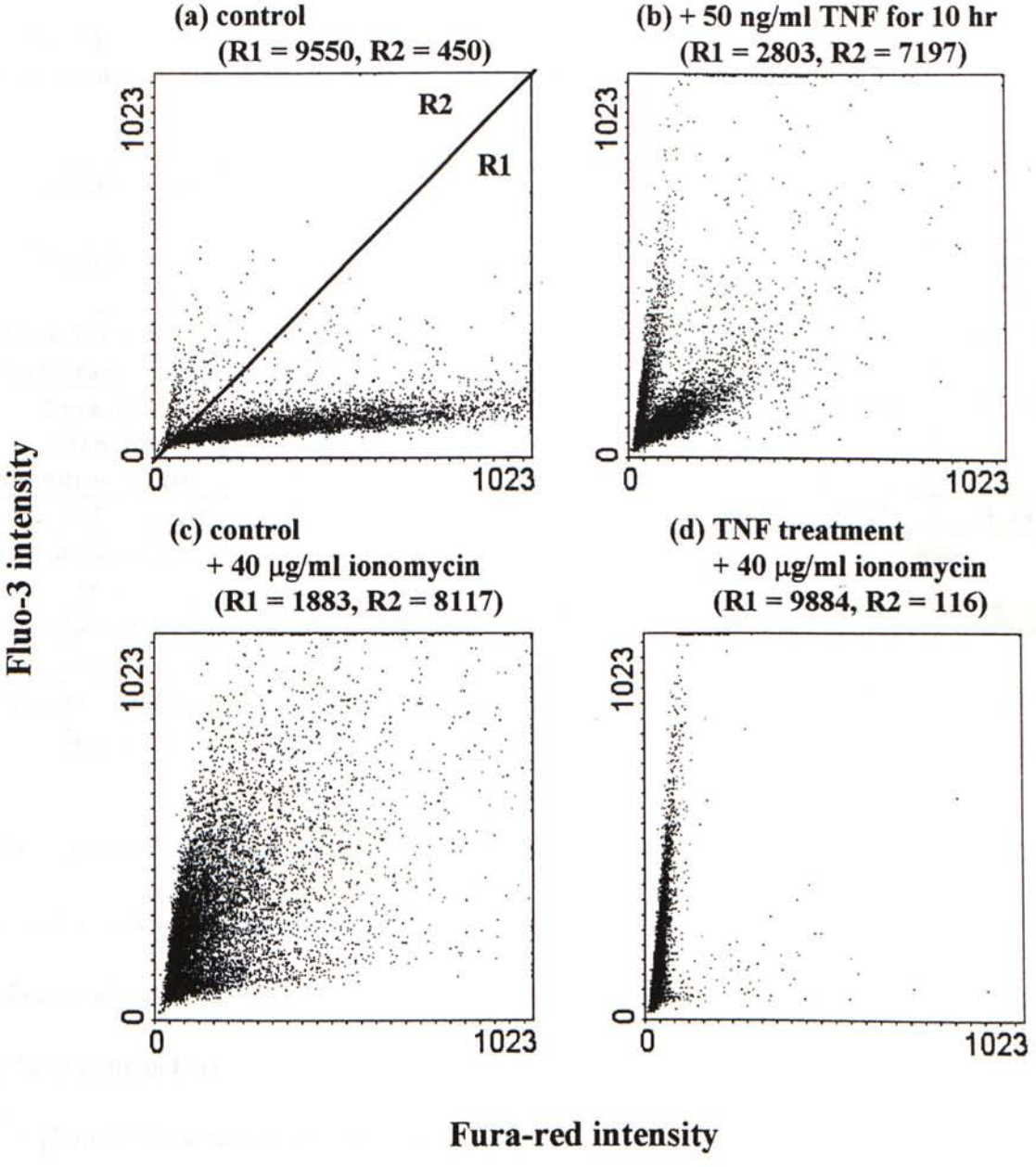

Figure 3.42

Incubation of L929 cells with TNF for 10 hr produced a drastic change in $[Ca^{2+}]_i$. (a) Control group. (b) L929 cells were incubated with 50 ng/ml TNF for 10 hr. Note that there was an increase in $[Ca^{2+}]_i$ as compared to the control group. More dots occurred at the upper-left region and there was an decrease in the fluorescence intensity of fura-red. (c) Cells were loaded with 40 μg/ml ionomycin 10 min before measurement. (d) Addition of 40 μg/ml ionomycin in the TNF-treated group caused a shift in the cell population also.

Table 3.1
TNF-mediated Ca^{2+} release is proportional to the incubation time.

Incubation time	3 hr		6 hr		10 hr	
Treatment	control	50 ng/ml TNF	control	50 ng/ml TNF	control	50 ng/ml TNF
Fluo-3 intensity (arbitrary unit)	74.68	82.83	65.15	81.42	89.49	126.56
Fura-red intensity (arbitrary unit)	406.65	442.00	274.39	214.27	304.80	87.96
Fluo-3 /Fura-red	0.18	0.18	0.24	0.38	0.29	1.44
% of control * (%)	100		158		496	
Number of cells in R1	9684	9686	9176	8712	9550	2803
Number of cells in R2	316	314	824	1288	450	7197

Results from Figure 3.40 - Figure 3.42 were summarized and the peak fluorescences at the x- and y-axis were acquired. The ratio of fluo-3 to fura-red was then calculated and the % of control was obtained according to the following formula:

* % of control (%)

= [fluo-3 / fura-red (TNF treatment)] / [fluo-3 / fura-red (control)] x 100 %

Moreover, the number of dots in R1 and R2 were determined.

addition of large dose of TNF (500 ng/ml) for 3 hr produced a small increase in $[Ca^{2+}]_i$ (Figure 3.43 and Table 3.2). There was a little shift of the cell population from R1 to R2 in 3-hour-incubation of 500 ng/ml TNF with L929 cells. In the ionomycin experiment, the distribution of dots is quite homogeneous as compared to the one with TNF treatment (Figure 3.40 - 3.43). When compared the responses mediated by ionomycin and TNF, it can be seen in Figure 3.41b and Figure 3.42b that cells responded to TNF differently. Basically, two populations of cells can be visualized in terms of the slope of the graph (i.e. the ratio of fluo-3/fura-red). In the upper left population, cells produced a relatively high $[Ca^{2+}]_i$ after TNF addition, while the lower right gave a low $[Ca^{2+}]_i$ rise.

3.4.3 Effect of Calcium-Inducing Agents on TNF-Treated L929 Cells

Thapsigargin is a sesquiterpene lactone originally isolated from the umbrelliferous plant *Thapsia gargancia* (Christensen and Norup, 1985). It acts as an irreversible inhibitor of the Ca^{2+}-ATPase in the endoplasmic reticulum (ER Ca^{2+}-ATPase) (Lytton *et al.*, 1991; Thastrup *et al.*, 1990).When the ER pump is inhibited, for example by thapsigargin, Ca^{2+} can no longer be returned from the cytosol to the ER and therefore, led to a prolonged rise in $[Ca^{2+}]_i$ (Vercesi *et al.*, 1996). However, thapsigargin is not a universal Ca^{2+}-releasing agent in all cell types (Vercesi *et al.*, 1996).

In this experiment, the effect of thapsigargin (2 μM) on TNF-mediated release of Ca^{2+} was examined. Figure 3.44 shows the dot plots from FCM and it indicated that thapsigargin itself did not induce the release of Ca^{2+} after 6-hour-treatment (Figure 3.44a and b). However, incubation of cells with 50 ng/ml TNF together with 2 μM thapsigargin

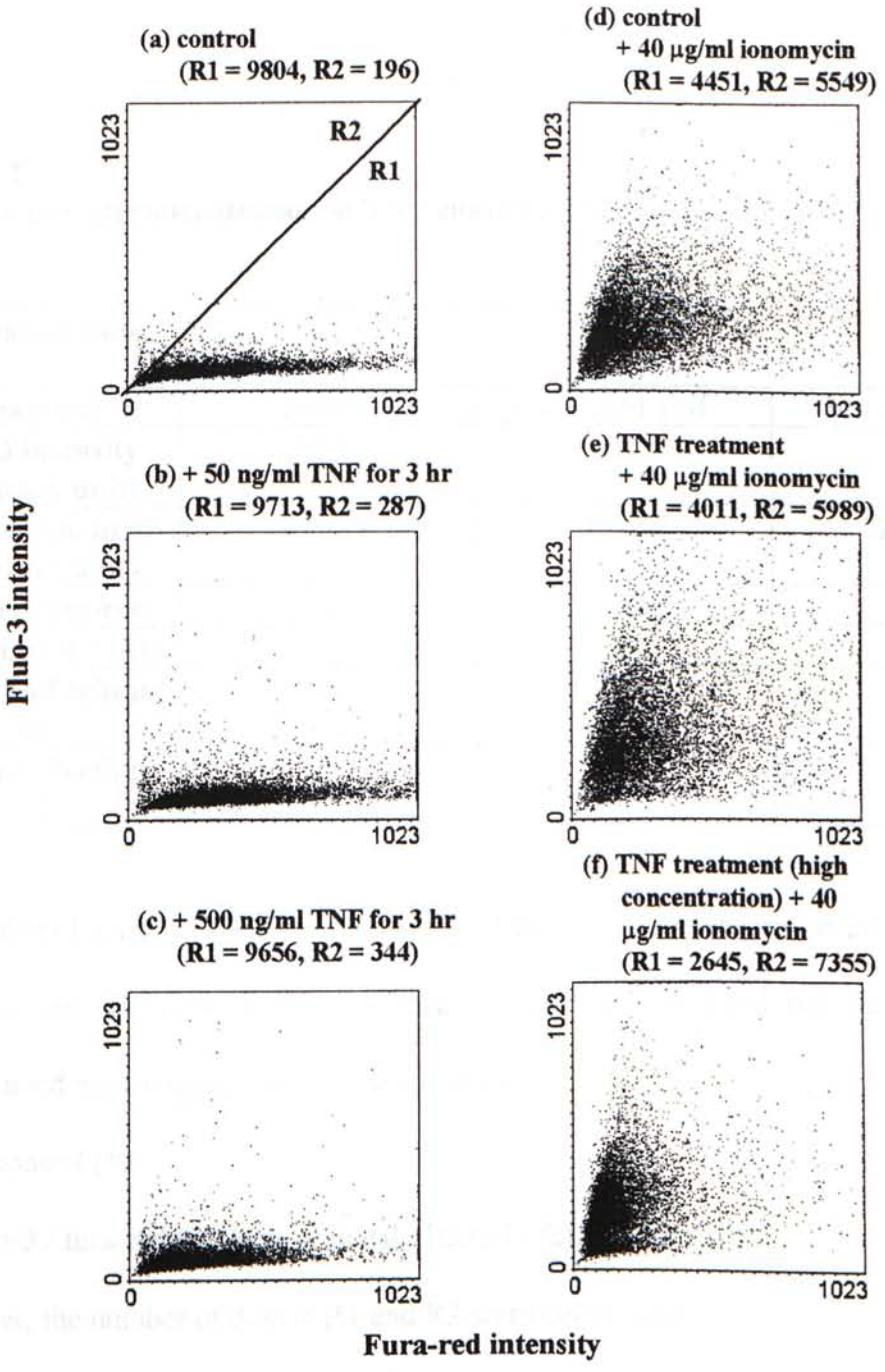

Figure 3.43

Incubation of L929 cells with high concentration of TNF for 3 hr caused a small increase in $[Ca^{2+}]_i$. (a) Control group. (b) L929 cells were incubated with 50 ng/ml TNF for 3 hr. It shows that there was no significant change in $[Ca^{2+}]_i$ as compared to control group. (c) Cells were incubated with 500 ng/ml TNF for 3 hr and it caused a small increase in $[Ca^{2+}]_i$ since the fluorescence intensity of fura-red decreased. Addition of 40 μg/ml ionomycin 10 min before measurement in the (d) control, (e)TNF-treated group, and (f) high concentration of TNF-treated group caused a shift in the cell population also. The number of cells in the region R1 and R2 is also determined.

Table 3.2
Addition of high concentration of TNF caused a small increase in $[Ca^{2+}]_i$.

Incubation time	3 hr		
Treatment	control	50 ng/ml TNF	500 ng/ml TNF
Fluo-3 intensity (arbitrary unit)	78.40	93.55	78.18
Fura-red intensity (arbitrary unit)	273.72	359.50	231.44
Fluo-3 /Fura-red	0.28	0.26	0.34
% of control * (%)	/	92	121
Number of cells in R1	9804	9713	9656
Number of cells in R2	196	287	344

Results from Figure 3.43 were summarized and the peak fluorescences at the x- and y-axis were acquired. The ratio of fluo-3 to fura-red was then calculated and the % of control was obtained according to the following formula:

* % of control (%)

= [fluo-3 / fura-red (TNF treatment)] / [fluo-3 / fura-red (control)] x 100 %

Moreover, the number of dots in R1 and R2 were determined.

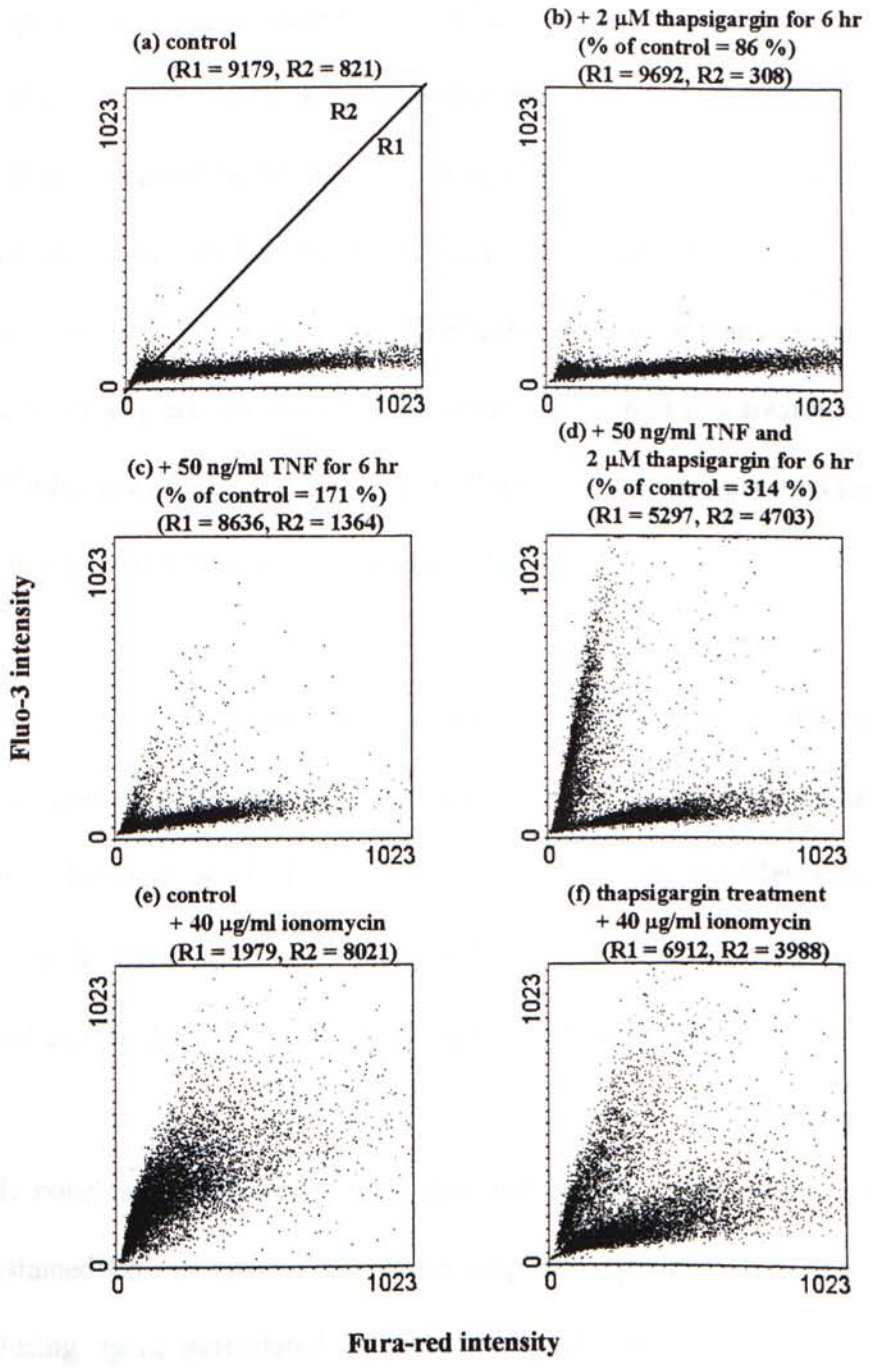

Figure 3.44

Incubation of TNF with thapsigargin produced a drastic increase in $[Ca^{2+}]_i$. (a) Control group. (b) L929 cells were incubated with 2 μM thapsigargin for 6 hr. It shows that there was no significant change in $[Ca^{2+}]_i$ as compared to control group. (c) Cells were incubated with 50 ng/ml TNF for 6 hr and it produced an increase in $[Ca^{2+}]_i$. (d) Addition of 50 ng/ml TNF with 2 μM thapsigargin produced a drastic release of Ca^{2+}. Addition of 40 μg/ml ionomycin 10 min before measurement in the (e) control and (f) thapsigargin-treated group caused a shift in the cell population also. The number of cells in the region R1 and R2 is also determined.

for 6 hr produced a drastic increase in $[Ca^{2+}]_i$ (Figure 3.44a and d) as evidenced by the shifting of cells from R1 to R2 as compared to TNF treatment. This may be due to the fact that the $[Ca^{2+}]_i$ released by TNF could not be uptaken into Ca^{2+} stores as the activity of Ca^{2+}-ATPases were blocked by thapsigargin. Obivously, two populations of cells were also seen when cells were treated with TNF in the presence of thapsigargin (Figure 3.44d). The rise of $[Ca^{2+}]_i$ are also found in the group with ionomycin treatment in the absence (Figure 3.44e) and presence of thapsigargin (Figure 3.44f). These results therefore suggest that TG potentiated TNF-mediated release of Ca^{2+}.

Another Ca^{2+}-inducing agent, thimerosal, was also used. Thimerosal, a thiol-reactive reagent, has been shown to increase the cytosolic Ca^{2+} concentration in a variety of cells (Michelangeli *et al.*, 1995) by sensitizing IP_3 receptors (Berridge, 1991). Figure 3.45 shows the effect of 20 μM thimerosal on TNF-mediated cytotoxicity. Addition of thimerosal increased about 10 % in TNF-mediated cytotoxicity.

In conclusion, TNF produced a slow rise in $[Ca^{2+}]_i$ that may involve in cell death since sustained Ca^{2+} in cytosol may cause apoptosis (Nicotera *et al.*, 1994). Addition of Ca^{2+}-inducing agent potentiated the release of Ca^{2+} and increased the TNF-mediated cytotoxicity.

Since TNF increased the release of ROS and Ca^{2+} in L929 cells, their relationship was examined in the next section.

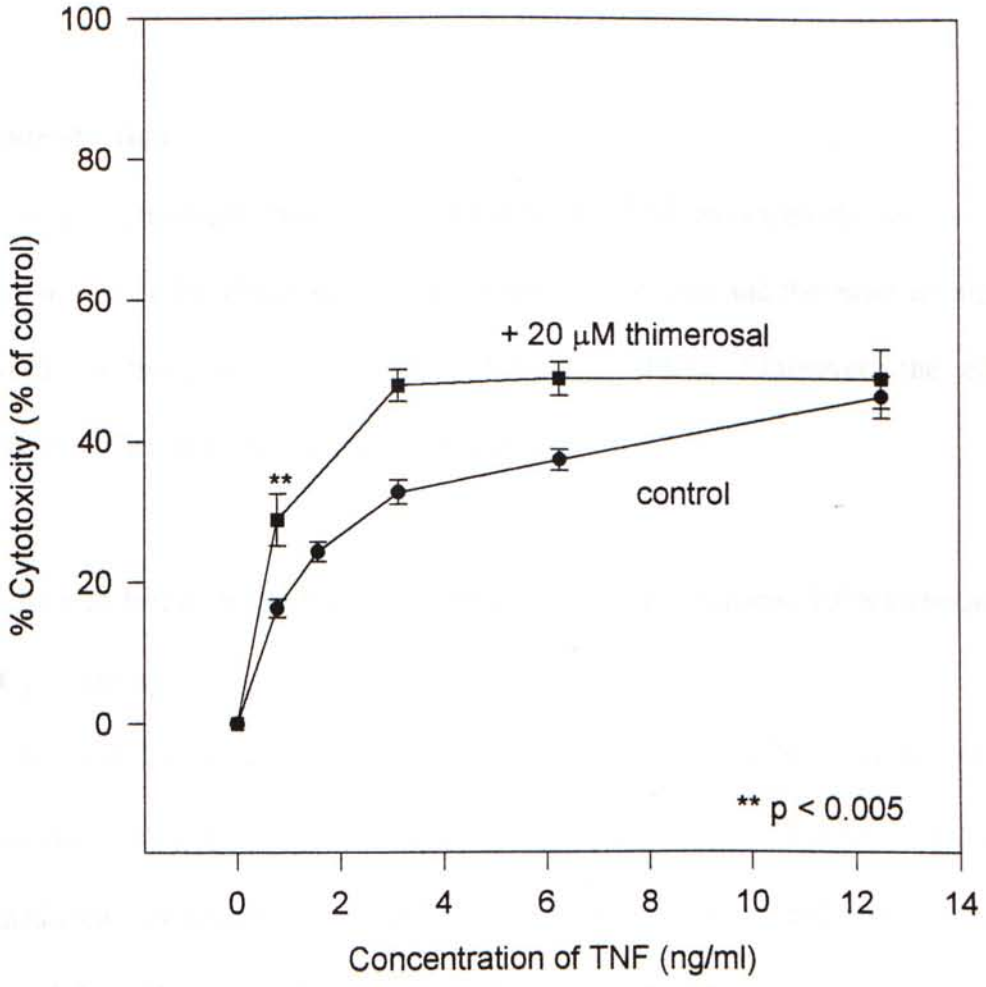

Figure 3.45
Addition of thimerosal enhanced TNF-mediated cytotoxicity. L929 cells were seeded at 3 x 10^4/well in complete medium in a 96-well plate and incubated for 20 hr at 37 °C, 5 % CO_2. 100 μl of TNF of various concentrations in the presence (■) or absence (●) of thimerosal (20 μM) in serum-free medium was added and incubated for 20 hr at 37 °C, 5 % CO_2. Neutral red assay was then applied (n = 7).

3.5 Relationship between Reactive Oxygen Species and Calcium in Tumor Necrosis Factor-Alpha-Mediated Cytotoxicity

3.5.1 Introduction

In previous experiments, we have found that TNF increased the release of ROS and Ca^{2+} in L929 cells. However, their relationship is not clear and therefore we attempted to investigate the possible mechanisms behind by FCM. Moreover, the effect of mitochondrial Ca^{2+} $(Ca^{2+})_m$ was examined also.

3.5.2 Effect of Intracellular Calcium Chelator on TNF-Mediated ROS Release and Cytotoxicity

BAPTA/AM is one of the commonly used Ca^{2+}-chelators (Kong *et al.*, 1996; Pahl and Baeuerle, 1996). In the cytotoxicity assay, application of 10 μM BAPTA/AM reduced TNF-mediated cytotoxicity by about 5 - 10 % (Figure 3.46). Similar to the results in section 3.4.2, challenge of cells with TNF (50 ng/ml) for 3 hr did not produce any change in $[Ca^{2+}]_i$ (Figure 3.47a). However, an increase in the $[Ca^{2+}]_i$ was observed when cells were treated with TNF (50 ng/ml) for 6 hr (Figure 3.47b). As expected, BAPTA/AM could block the rise of Ca^{2+} in the 6-hour-incubation group (Figure 3.47). There was no significant change in the number of dots in R1 and R2 in 3-hour-incubation as compared to control group (Figure 3.47a) whereas addition of BAPTA/AM in the 6-hour TNF treatment reduced the number of dots in R2 as compared to the one with 6-hour TNF treatment alone. Figure 3.48 shows the effect of 10 μM BAPTA/AM on the release of

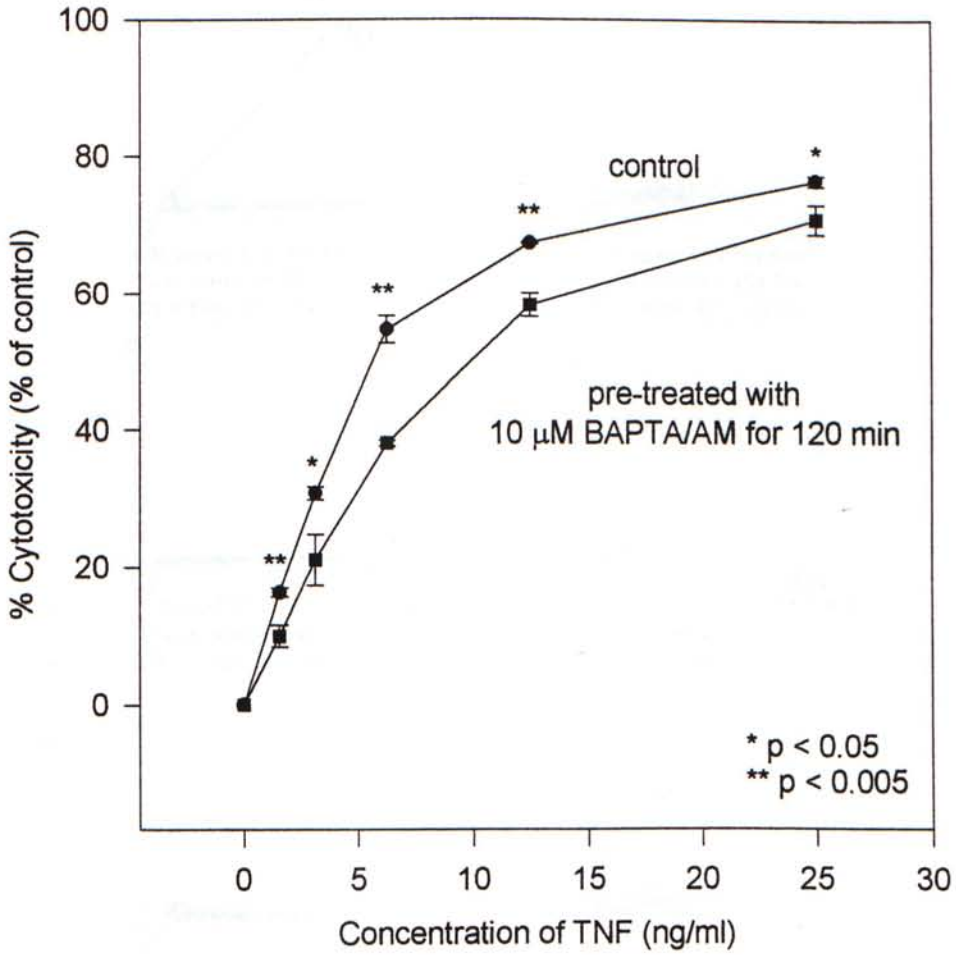

Figure 3.46

Addition of BAPTA/AM reduced TNF-mediated cytotoxicity. L929 cells (3 x 10^4/well) were seeded in a 96-well plate and incubated for 20 hr at 37 °C, 5 % CO_2. In the treatment group, BAPTA/AM (10 μM) in serum-free medium was added to each well and incubated at 37 °C for another 120 min. Subsequently, 100 μl of TNF of various concentrations was added and the cells were incubated for 20 hr at 37 °C, 5 % CO_2. Neutral red assay was then applied (n = 3, expt. = 3).

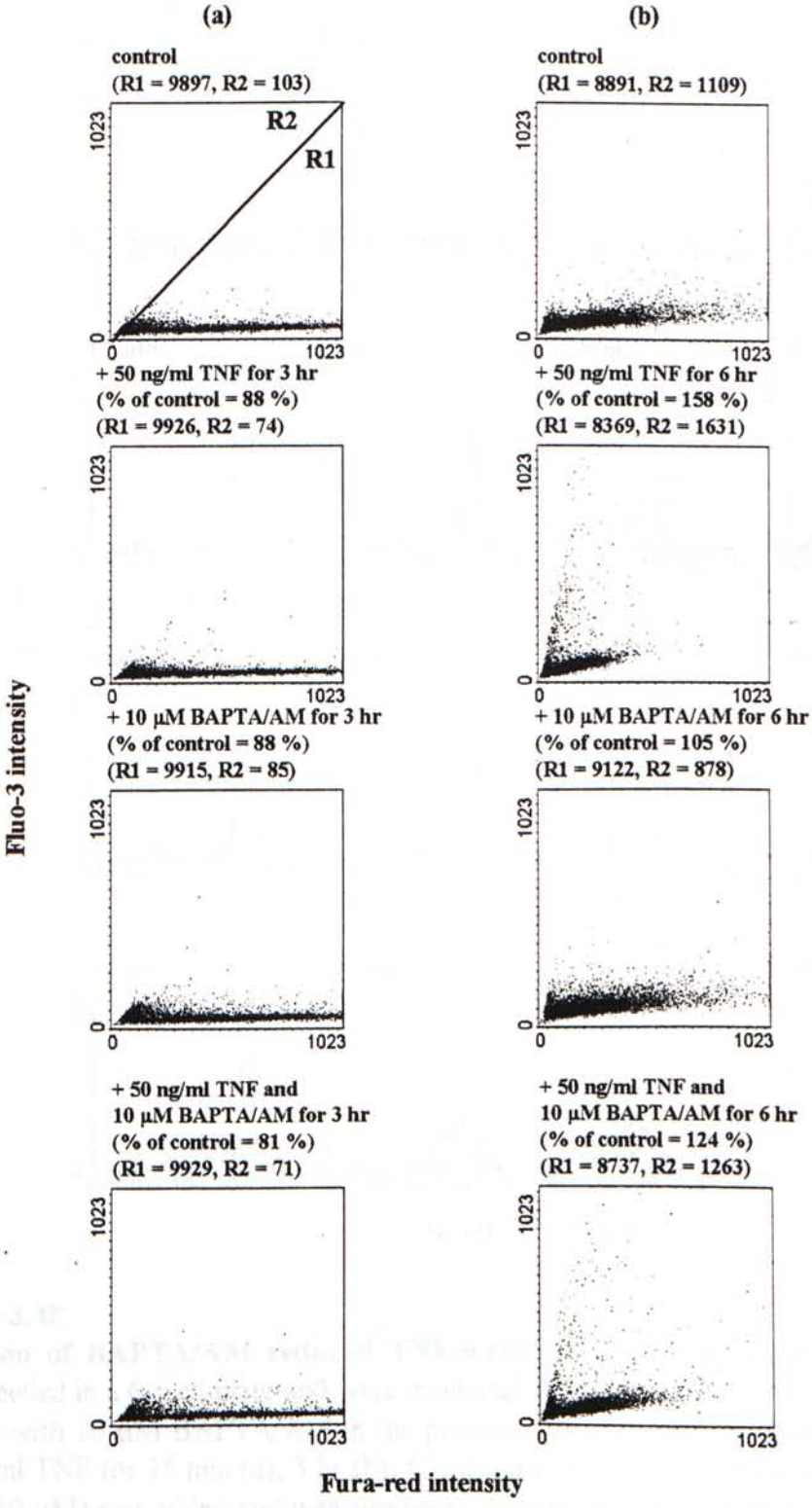

Figure 3.47

Addition of BAPTA/AM chelated TNF-mediated Ca^{2+} release in the 6-hour-incubation but not the 3-hour-treatment. (a) Neither TNF (50 ng/ml) nor BAPTA (10 μM) produced any changes in $[Ca^{2+}]_i$ in L929 cells. (b) Addition of 10 μM BAPTA/AM for 6 hr reduced TNF-mediated Ca^{2+} release.

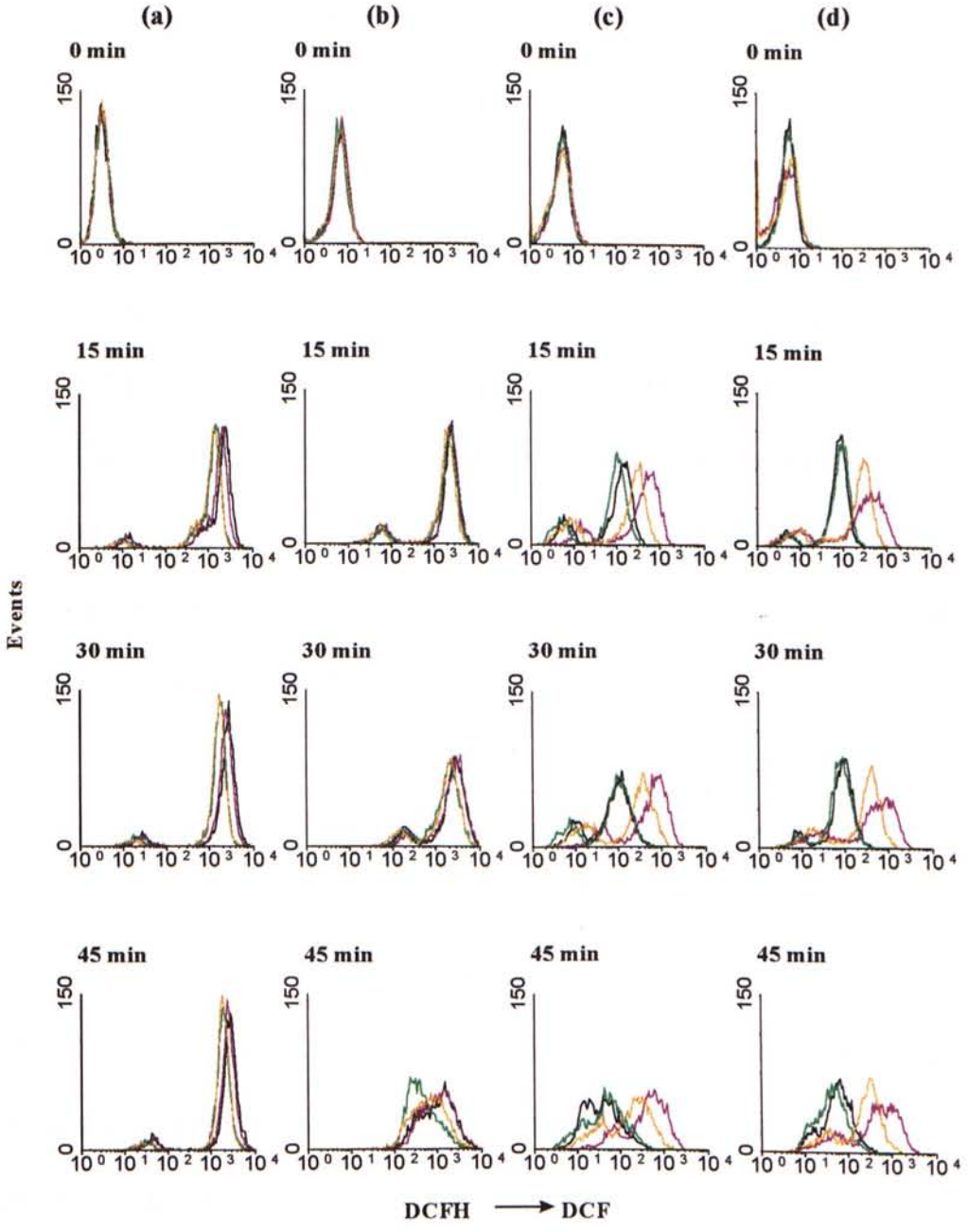

Figure 3.48

Addition of BAPTA/AM reduced TNF-mediated H_2O_2 release. L929 cells (10^6/ml) were seeded in a 6-well plate and were incubated overnight at 37 °C, 5 % CO_2. Cells were treated with 10 μM BAPTA/AM in the presence (orange line) or absence (green line) of 50 ng/ml TNF for 15 min (a), 3 hr (b), 6 hr (c) and 10 hr (d). Cells were then trypsinized. DCF (10 μM) was added and measurements were made with a FCM at the time indicated. The black and the purple lines represent the control and the TNF (50 ng/ml)-treated group, respectively. It was found that cells incubation with BAPTA/AM reduced the release of H_2O_2 in treatment with TNF. These results suggest that the release of Ca^{2+} preceded H_2O_2.

ROS in L929 cells that were incubated for 15 min, 3, 6 and 10 hr. It was found that addition of BAPTA/AM did reduce the release of ROS in TNF-treated cells in the 6- and 10-hour-treatment. Therefore, it seems likely that the release of ROS may be mediated by $[Ca^{2+}]_i$ because if the release of ROS was independent on $[Ca^{2+}]_i$, it would not be inhibited. Figure 3.49 summaries the results from Figure 3.48 quantitatively. On the other hand, addition of 1 mM H_2O_2 did not cause the release of Ca^{2+} at the 3, 6 or 10 hr time point (Figure 3.50). Figure 3.51 shows the confocal images (from CLSM, Meridian) of the early response of TNF on H_2O_2 treatment. Application of 1 or 5 mM H_2O_2 did not cause a spontaneous increase in the level of $[Ca^{2+}]_i$ (Figure 3.52) whereas addition of ionomycin (40 μg/ml) indicates that there was no Ca^{2+} impairment.

However, someone may wonder that there are two possibilities that BAPTA/AM reduced TNF-mediated release of ROS in the long time treatment (i.e. 6- or 10-hour incubation). First, BAPTA/AM reduced the TNF-mediated release of ROS actually by chelating Ca^{2+}. Second, BAPTA/AM induced cell death, thereby reducing the release of ROS from dead cells. From the dot plots of DCF against PI, one may differentiate these possibilities. Cell death was examined simultaneously by applying propidium iodide (PI). PI is one of the DNA chelators that can be used for detecting cell death. PI diffuses into dead cells and chelates DNA. Therefore, dead cells give fluorescence. As the number of dead cells increased, the PI intensity increased also. Figures 3.53 - 3.56 show the dot plots of incubation of TNF for 15 min, 3, 6 and 10 hr, respectively. The x-axis indicates the fluorescence intensity of DCF whereas the y-axis represents the PI intensity. The first column indicates the fluorescence of DCF and PI in the control cells measured at the time

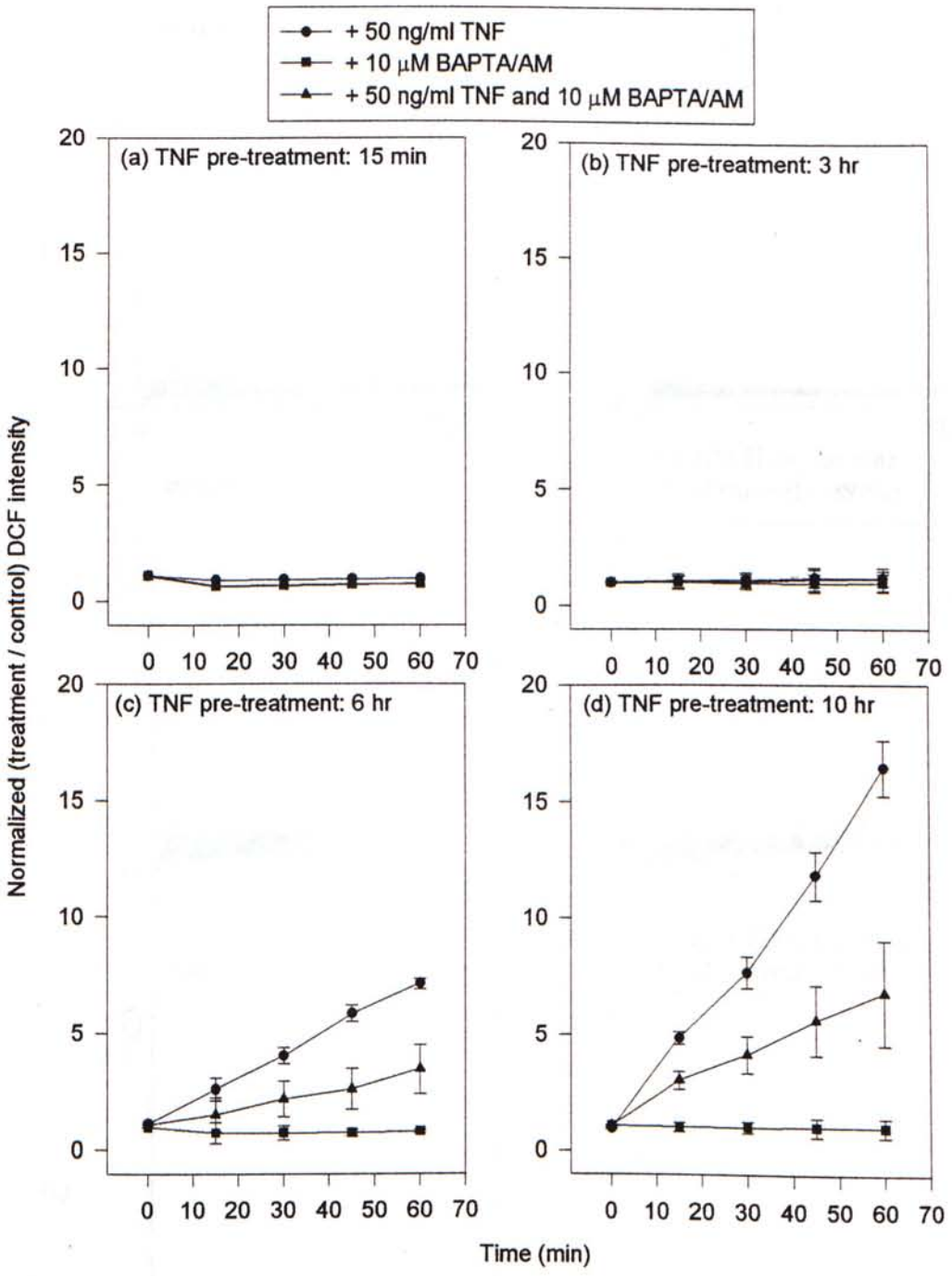

Figure 3.49

Addition of BAPTA/AM caused a reduction in TNF-mediated H_2O_2 release. These graphs summarize the results from Figure 3.48 (mean ± S.D. from 3 expt, except the one with 15 min TNF treatment (1 expt)).

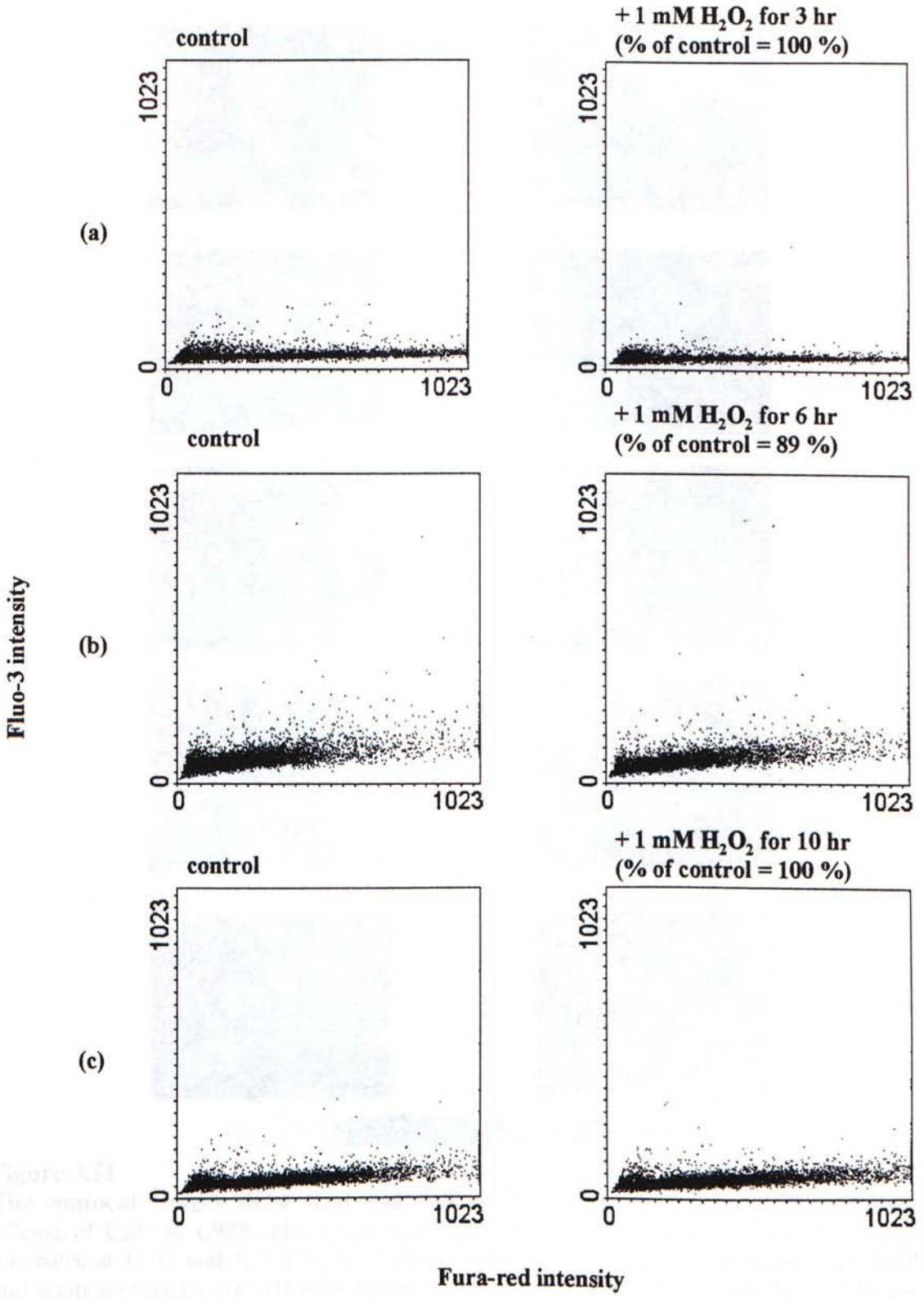

Figure 3.50
Addition of H_2O_2 did not produce Ca^{2+} release in 3, 6 or 10 hr incubation. Addition of 1 mM H_2O_2 for (a) 3 hr, (b) 6 hr or (c) 10 hr did not produce Ca^{2+} release.

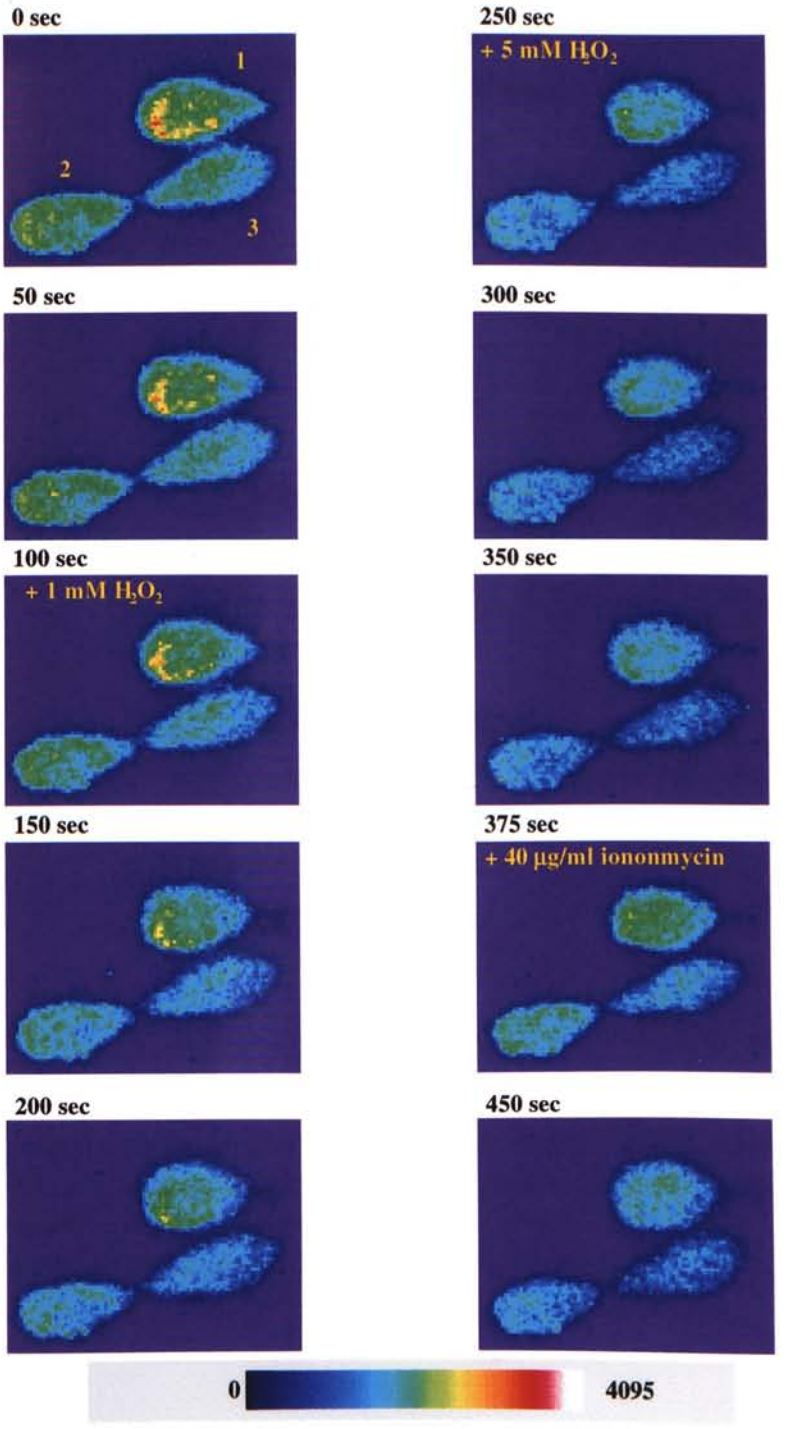

Figure 3.51
The confocal images show that addition of H_2O_2 did not produce a spontaneous release of Ca^{2+} in L929 cells. L929 cells (2 x 10^3/ml) were seeded on cover glass and incubated at 37 ℃ and 5 % CO_2 for 3 days. Cells were mounted on a home-made holder and washed twice by Na^+-HEPES buffer. Cells were loaded with 10 µM fluo-3/AM for 1 hr and then washed twice by Ca^{2+}-free buffer. Confocal scanning was made with a 5-second-interval at room temperature. 1 mM and 5 mM H_2O_2 were added at the 100th and 250th sec, respectively. 40 µg/ml ionomycin was added at the 375th sec (n = 3).

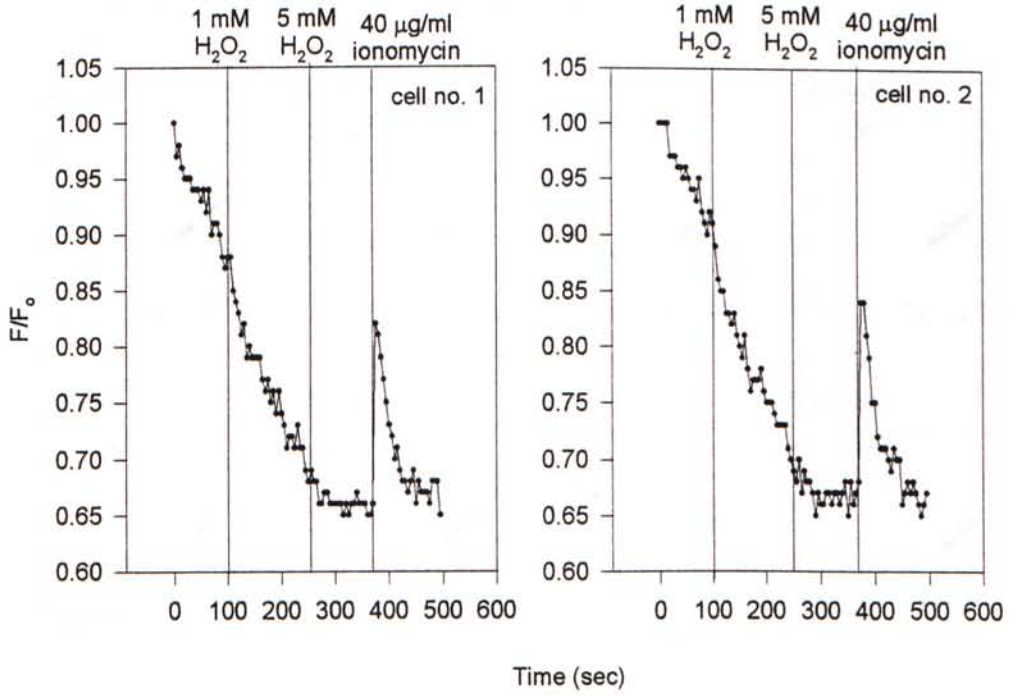

Figure 3.52

H_2O_2 did not cause Ca^{2+} release in L929 cells in a short time course. This graph summaries the results of the confocal images of cell number 1 and 2 from figure 3.51. 1 mM and 5 mM H_2O_2 were introduced to the cells at the 1st and 2nd hairline, respectively. 40 µg/ml ionomycin was introduced to the cells at the 3rd hairline. The y-axis, F/Fo, represented the normalized fluorescence intensity from cells.

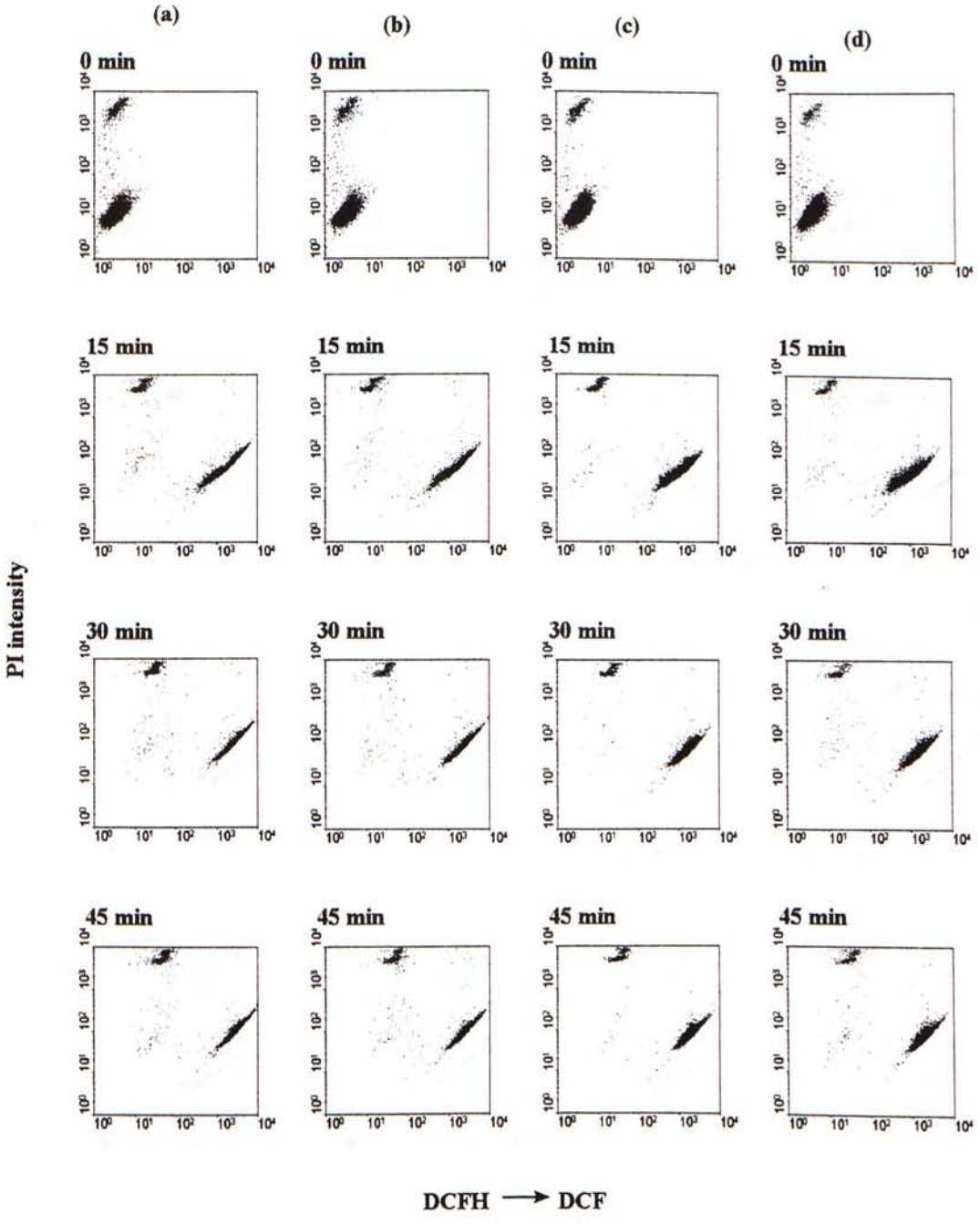

Figure 3.53

Incubation of L929 cells with TNF for 15 min did not produce the release of H_2O_2 and cell death. L929 cells (10^6/ml) were treated with TNF (50 ng/ml) for 15 min at 37 °C, 5 % CO_2. After washing, cells were labelled with DCF (10 μM) and PI (8 μg/ml) and the fluorescences were measured with a FCM at the time indicated. X-axis and y-axis represent the fluorescence intensity of DCF and PI, respectively. (a) It represents the control group. (b) 50 ng/ml TNF was added. (c) 10 μM BAPTA/AM was added. (d) 50 ng/ml TNF and 10 μM BAPTA/AM were added. There was no significant difference among groups.

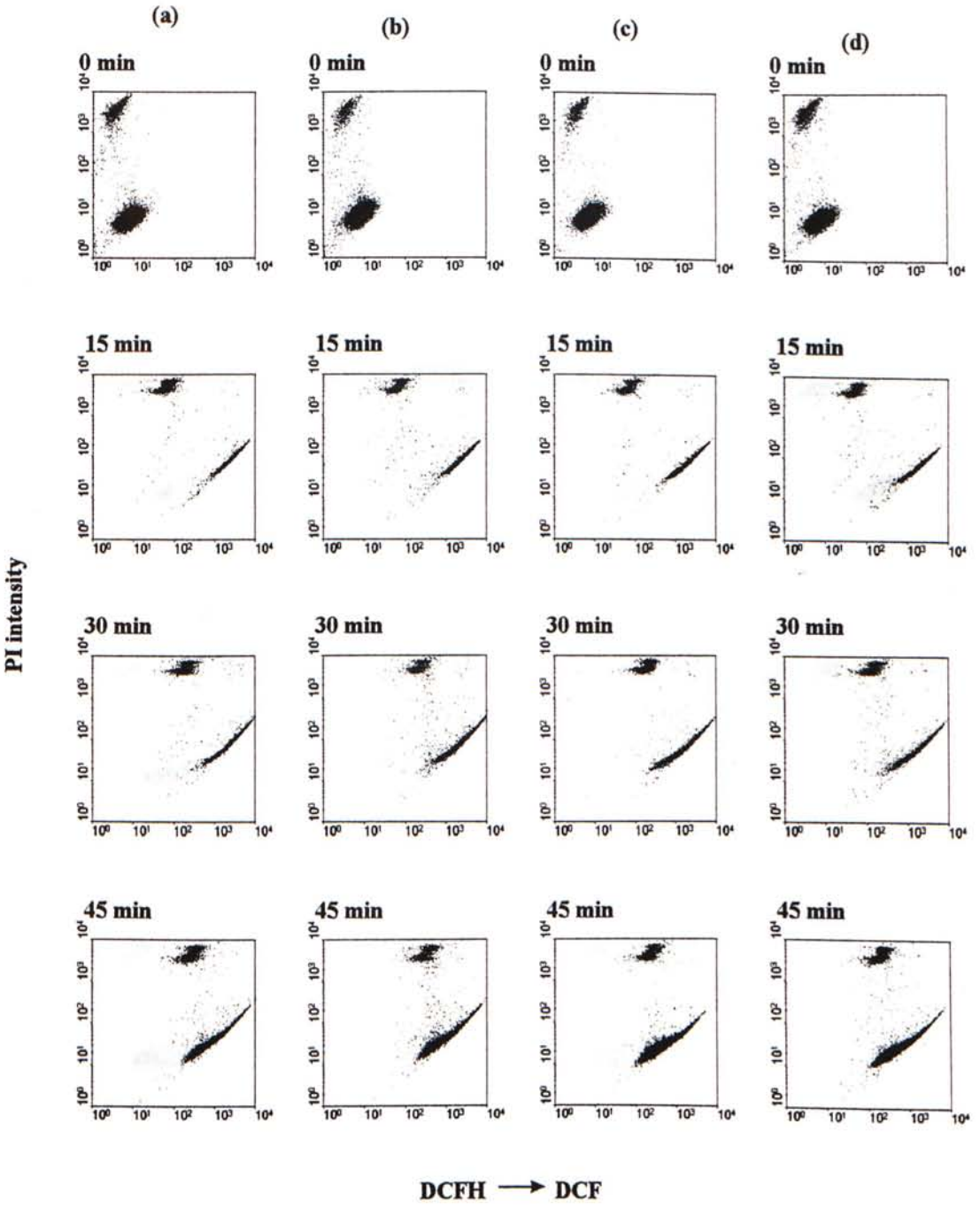

Figure 3.54

Incubation of L929 cells with TNF for 3 hr did not produce the release of H_2O_2 and cell death. L929 cells (10^6/ml) were treated with TNF (50 ng/ml) for 3 hr at 37 °C, 5 % CO_2. After washing, cells were labelled with DCF (10 μM) and PI (8 μg/ml) and the fluorescences were measured with a FCM at the time indicated. X-axis and y-axis represent the fluorescence intensity of DCF and PI, respectively. (a) It represents the control group. (b) 50 ng/ml TNF was added. (c) 10 μM BAPTA/AM was added. (d) 50 ng/ml TNF and 10 μM BAPTA/AM were added. There was no significant difference among groups.

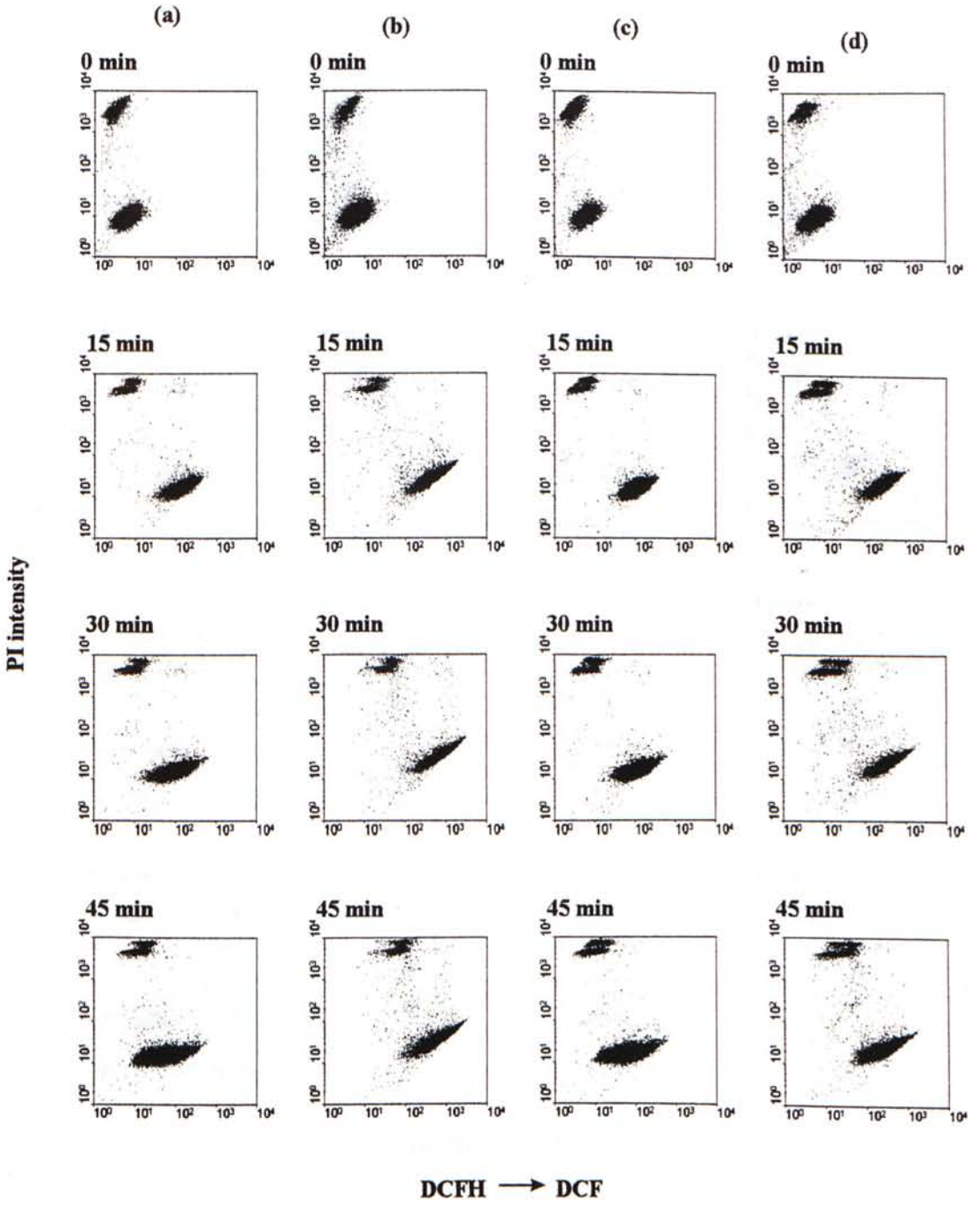

Figure 3.55

Incubation of L929 cells with TNF for 6 hr produced the release of H_2O_2 and cell death. (a) It represents the control group. (b) 50 ng/ml TNF was added. The lower population moved faster to the right than that of the control group (column 1) (c) 10 μM BAPTA/AM was added. No significant difference was found when compared to the control group. (d) 50 ng/ml TNF and 10 μM BAPTA/AM were added. The lower population moved slower to the right than that of the TNF-treated group (column 2). It implied that addition of BAPTA/AM reduced the release of H_2O_2 by chelating Ca^{2+}.

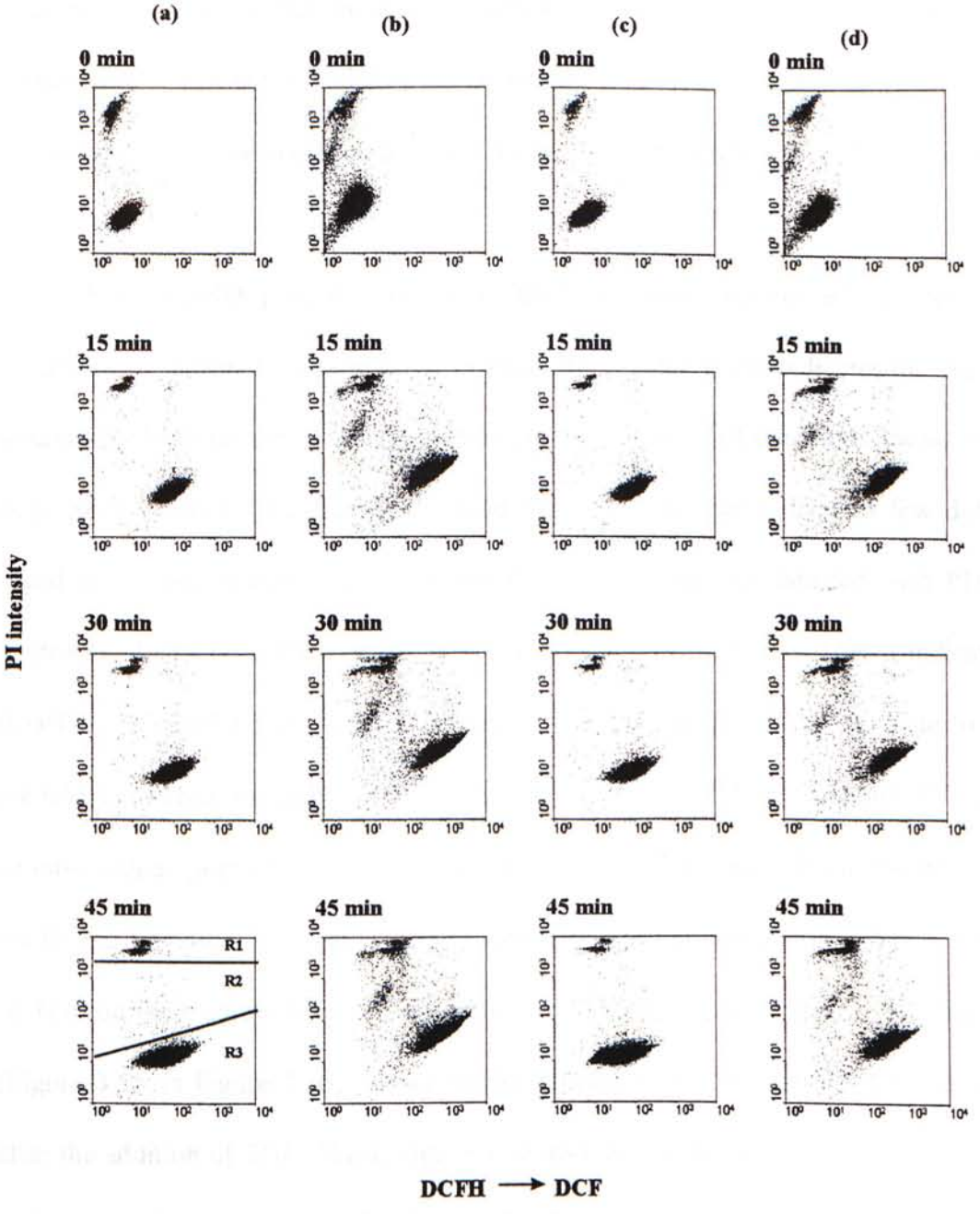

Figure 3.56

Incubation of L929 cells with TNF for 10 hr produced the release of H_2O_2 and cell death. (a) It represents the control group. (b) 50 ng/ml TNF was added. The lower population moved faster to the right than that of the control group (column 1). Moreover, a population in the R2 region was found in the 10 hr treatment but not in the 6 hr group. (c) 10 μM BAPTA/AM was added. (d) 50 ng/ml TNF and 10 μM BAPTA/AM were added. The lower population moved slower to the right than that of the TNF-treated group (column 2). Moreover, addition of BAPTA/AM reduced the population in R2 region as compared to the TNF-treated group. Therefore, it implied that addition of BAPTA/AM reduced the release of H_2O_2 and cell death by chelating Ca^{2+}.

after the addition of the fluorescent indicators. The second column represents the corresponding data in the TNF (50 ng/ml) treated cells. The third and the fourth columns correspond to the one in cells with BAPTA/AM or BAPTA/AM plus TNF, respectively.

For each dot plot, it could be divided into three regions, R1, R2 and R3, as mentioned in section 2.2.4. The lower position (R1) on the y-axis indicates the viable cells whereas the ones on the middle (R2) and upper region (R3) of the y-axis shows the dead cells. Several conclusions can be obtained from these dot plots. First, a few dots were found in the middle region of the y-axis (i.e. only a few cells labelled with PI) in the control and BATPA/AM-treated group (Figure 3.53 - 3.56). These indicate that BAPTA/AM itself did not induce cell death. However, BAPTA/AM was able to reduce the release of H_2O_2 by chelating Ca^{2+} rather than induced cell death. Second, TNF induced an intermediate population (column 2 in Figure 3.55 and Figure 3.56) in the R2 region in the 6- and 10-hour TNF treatment. The appearance of this population is due to the effect of TNF on the membrane lesion. This effect was more obvious in the 10-hour incubation (Figure 3.55 vs Figure 3.56). These results indicate that TNF induced cell death 6-hour after the addition of TNF. Third, Figure 3.56 also shows that addition of BAPTA/AM for 10 hr reduced the number of TNF-induced cell population in R2 region as compared the column 2 with the column 4. These observations suggest that BAPTA/AM may reduce the initiation of cell death by reducing the production of H_2O_2 after 6-hour-treatment of TNF. Fourth, TNF-treated cells gave a higher redox rate in terms of DCF fluorescence in the right-shifting population than the control cells in Figure 3.55 and Figure 3.56 and this implied that the redox rate is higher in the TNF treated group. Finally, addition of

BAPTA/AM reduced TNF-mediated redox rate by comparing the column 2 with column 4 in Figure 3.55 and Figure 3.56. Figure 3.57 further shows that addition of BAPTA/AM reduced PI intensity. It implied that chelation of Ca^{2+} could reduce the cell death mediated by TNF.

Table 3.3 shows the proportion of cells in the 10-hour incubation with TNF (data were from the 45th-minute-plot of each treatment). Only the data from 10-hour incubation were analyzed since they gave a distinct response among these treatments. It was found that addition of TNF induced more cell deaths since the number of cells in R2 and R3 was double as compared to the control group. Addition of BAPTA/AM did not induce cell death since the number of cells in R2 and R3 is fewer than control group. Moreover, TNF with BAPTA/AM reduced the cell number in R2. It indicates that BAPTA/AM may block the cell death mediated by TNF.

In the cytotoxicity assay, it was found that addition of BAPTA (10 μM) in the presence of 4-OH-TEMPO (5 mM) reduced TNF-mediated cytotoxicity to a great extent (Figure 3.58). These results suggest that Ca^{2+}-chelator with antioxidant might have additive effect on the reduction of TNF-mediated cytotoxicity.

3.5.3 Effect of Mitochondrial Calcium on TNF-Mediated ROS Release and Cytotoxicity

It is still controversial that mitochondrion acts as a Ca^{2+} store (Somlyo *et al.*, 1985). The concentration of mitochondrial free Ca^{2+} is found to be low (< 100 nM) in

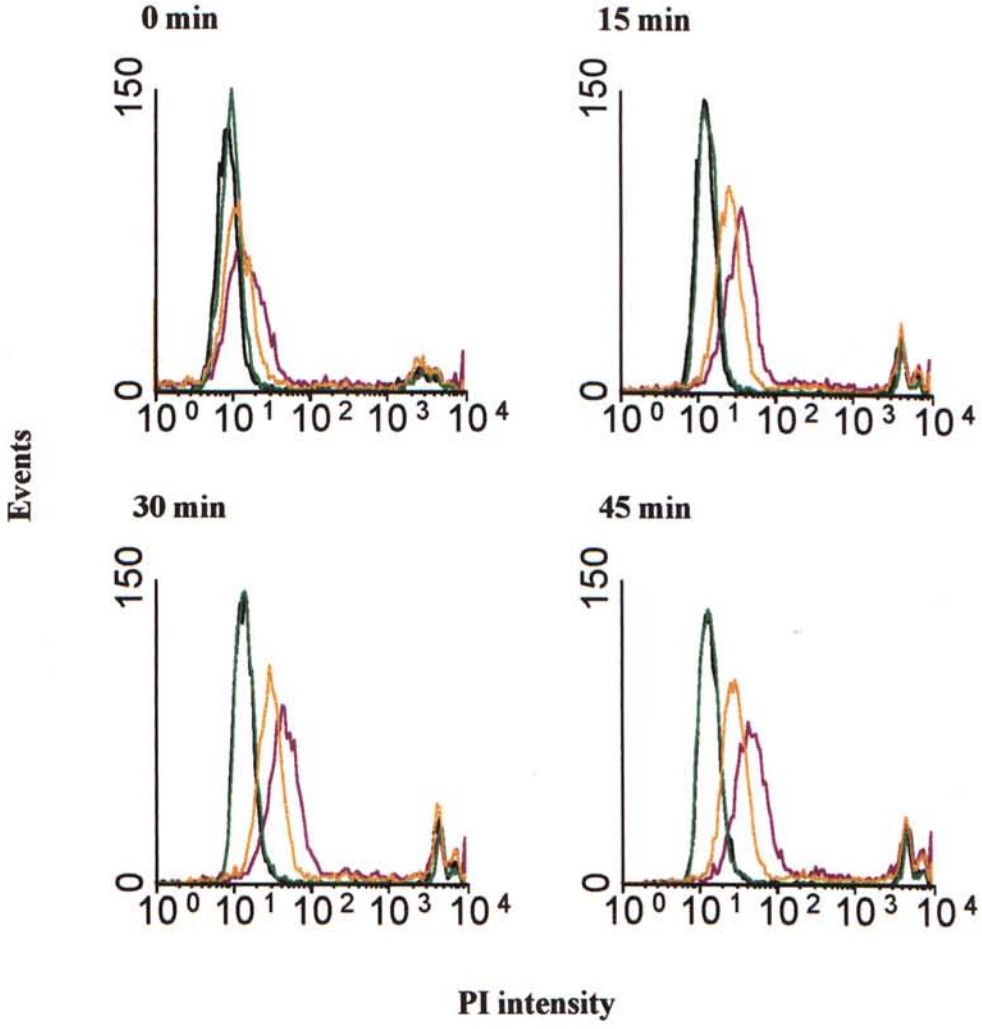

Figure 3.57

Addition of BAPTA/AM reduced cell death in TNF treatment. L929 cells (10^6/ml) were seeded in a 6-well plate and were incubated overnight at 37 °C, 5 % CO_2. Cells were treated with 10 μM BAPTA/AM in the presence (orange line) or absence (green line) of 50 ng/ml TNF 10 hr. Cells were then trypsinized. PI (8 μg/ml) was added and measurement was made with a FCM at the time indicated. The black and the purple lines represent the control and the TNF (50 ng/ml)-treated group, respectively. It was found that cells incubation with BAPTA/AM reduced the cell death.

Table 3.3
Addition of BAPTA/AM reduced TNF-mediated cell death.

Treatment	Number of cells in R1	Number of cells in R2	Number of cells in R3	* % of Cell death (%)
Control	8998	91	911	10.02
50 ng/ml TNF	7618	1161	1221	23.82
10 μM BAPTA/AM	9216	115	669	7.84
50 ng/ml TNF + 10 μM BAPTA/AM	7960	783	1257	20.40

Results were from the 45th-minute-plot of each treatment in Figure 3.56. The number of cells in R1, R2 and R3 were recorded and % of cell death was obtained according to the following formula:

* % of cell death (%)

= [Number of cells in (R2 + R3) ÷ Number of cells in (R1 + R2 + R3)] x 100 %

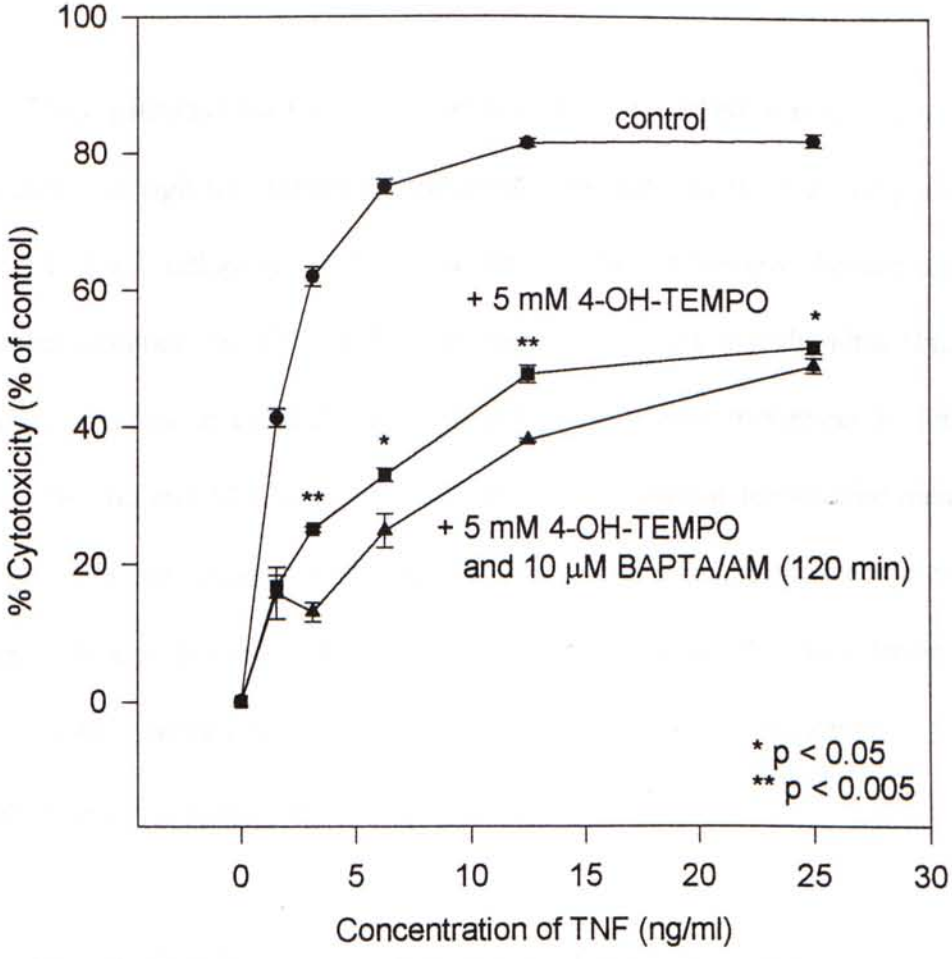

Figure 3.58

Addition of BAPTA/AM and 4-OH-TEMPO further reduced TNF-mediated cytotoxicity. L929 cells (3 x 10^4/well) were seeded in a 96-well plate and incubated for 20 hr at 37 °C, 5 % CO_2. In the treatment group, BAPTA/AM (10 μM) in serum-free medium was added to each well and incubated at 37 °C for another 120 min. Subsequently, 100 μl of 4-OH-TEMPO (5 mM) with TNF of various concentrations in serum-free medium were added and the cells were incubated for 20 hr at 37 °C, 5 % CO_2. Neutral red assay was then applied (n = 3). * $p < 0.05$ and ** $p < 0.005$ indicate that there was a significant difference between 4-OH-TEMPO and BAPTA/AM with 4-OH-TEMPO group.

unstimulated cells (Miyata *et al.*, 1991). The ER, rather than the mitochondria, is the main organelle regulating the $[Ca^{2+}]_i$ (Somlyo *et al.*, 1985).

Three pathways for Ca^{2+} transport have been described in respiring mitochondria that maintain a high transmembrane electrical potential: (1) the Ca^{2+} uniporter; (2) the putative H^+/Ca^{2+} antiporter; and (3) Na^+/Ca^{2+} antiporter (review: Gunter and Pfeiffer, 1990) that maintain the Ca^{2+}-cycling between cytosol and mitochondria (Figure 1.6c). Similar to the role in cytosol, Ca^{2+} also acts as a second messenger in mitochondria (review: Denton and McCormack, 1990). It regulates intra-mitochondrial metabolism by regulating different mitochondrial enzymes such as dehydrogenases (Denton *et al.*, 1980; McCormack and Denton, 1980) thus affecting oxidative phosphorylation (Moreno-Sanchez, 1985). Moreover, the mitochondrial matrix volume is regulated by Ca^{2+} as well (Davidson and Halestrap, 1987).

The mitochondrial Ca^{2+}-cycling can be inhibited by some drugs such as ruthenium red and diltiazem. Ruthenium red, a hexavalent, inorganic dye that prevents mitochondrial Ca^{2+} uptake by inhibiting the mitochondrial Ca^{2+} uniporter (Chacon and Acosta, 1991; Faulk *et al.*, 1995). In contrast, diltiazem prevents the release of Ca^{2+} from mitochondria by inhibiting Na^+-dependent and H^+-dependent pathways (Rizzuto *et al.*, 1987).

In L929 cells, addition of 25 μM ruthenium red reduced TNF-mediated cytotoxicity by about 5 - 10 % (Figure 3.59). Furthermore, addition of 250 μM diltiazem

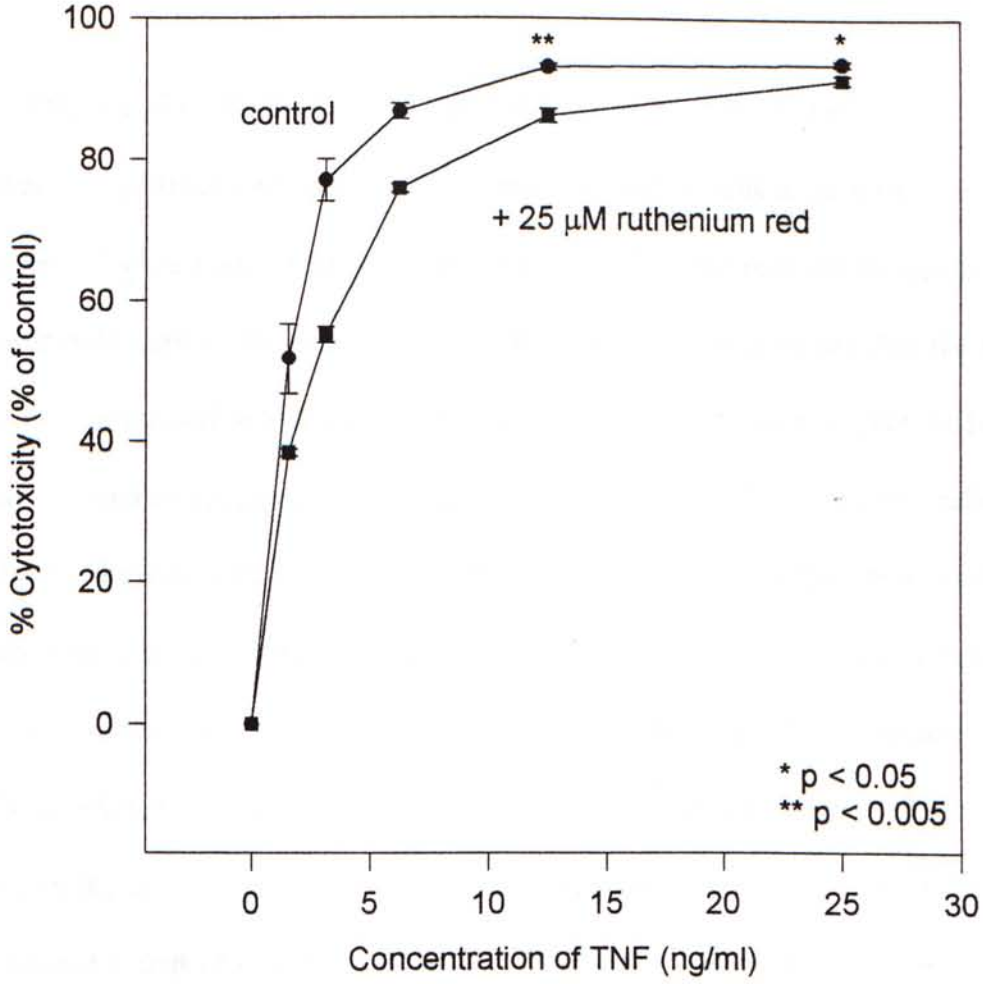

Figure 3.59
Addition of ruthenium red reduced TNF-mediated cytotoxicity. L929 cells were seeded at 3 x 10^4/well in complete medium in a 96-well plate and incubated for 20 hr at 37 °C, 5 % CO_2. 100 μl TNF of various concentrations in the presence (■) or absence (●) of ruthenium red (25 μM) in serum-free medium was added and incubated for 20 hr at 37 °C, 5 % CO_2. MTT assay was then applied (n = 3, expt = 3). Similar results were obtained in neutral red assay (data not shown).

also reduced TNF-mediated cell death (by about 5 - 10 %) (Figure 3.60). It implies that inhibition of Ca^{2+} cycling in the mitochondria inhibited the TNF-mediated cell death.

The dot plots from FCM indicated that addition of ruthenium red (25 μM) or diltiazem (250 μM) for 6 hr without TNF showed a small modification of the $[Ca^{2+}]_i$ level. As shown in Figure 3.61c, treating of cells with ruthenium red reduced the cell number in the lower-right corner. This may be due to the effect of ruthenium red that the Ca^{2+} re-uptake into mitochondria was suppressed. For the effect of diltiazem (Figure 3.61e), more cells were found in the lower right corner indicating a lower $[Ca^{2+}]_i$ in these cells. These may due to the action of diltiazem that the release of Ca^{2+} from the mitochondria was blocked. However, the effect of ruthenium red and diltiazem on the $[Ca^{2+}]_i$ was not so significant. Nevertheless, pre-treatments of cells with ruthenium red and diltiazem reduced the TNF-mediated Ca^{2+} release (Figure 3.61). Furthermore, the number of cells did not increase in R2 (Figure 3.61c - f) as compared to control whereas 6-hour incubation of TNF induced a shift of cells from R1 to R2. These results imply that prevention of Ca^{2+} cycling in mitochondria inhibited the rise of $[Ca^{2+}]_i$ release. Our results also suggest that one of the sources of Ca^{2+} after TNF treatment is from the mitochondria.

The confocal images from CLSM-MD also indicated that addition of 25 μM ruthenium red reduced both H_2O_2 (Figure 3.62) and $O_2\bullet^-$ (Figure 3.64) release. The quantitative measurements from both experiments were summarized in Figure 3.63 and Figure 3.65, respectively. Furthermore, data from FCM also indicated that diltiazem could reduce the TNF-mediated H_2O_2 release (Figure 3.66). These results therefore suggested

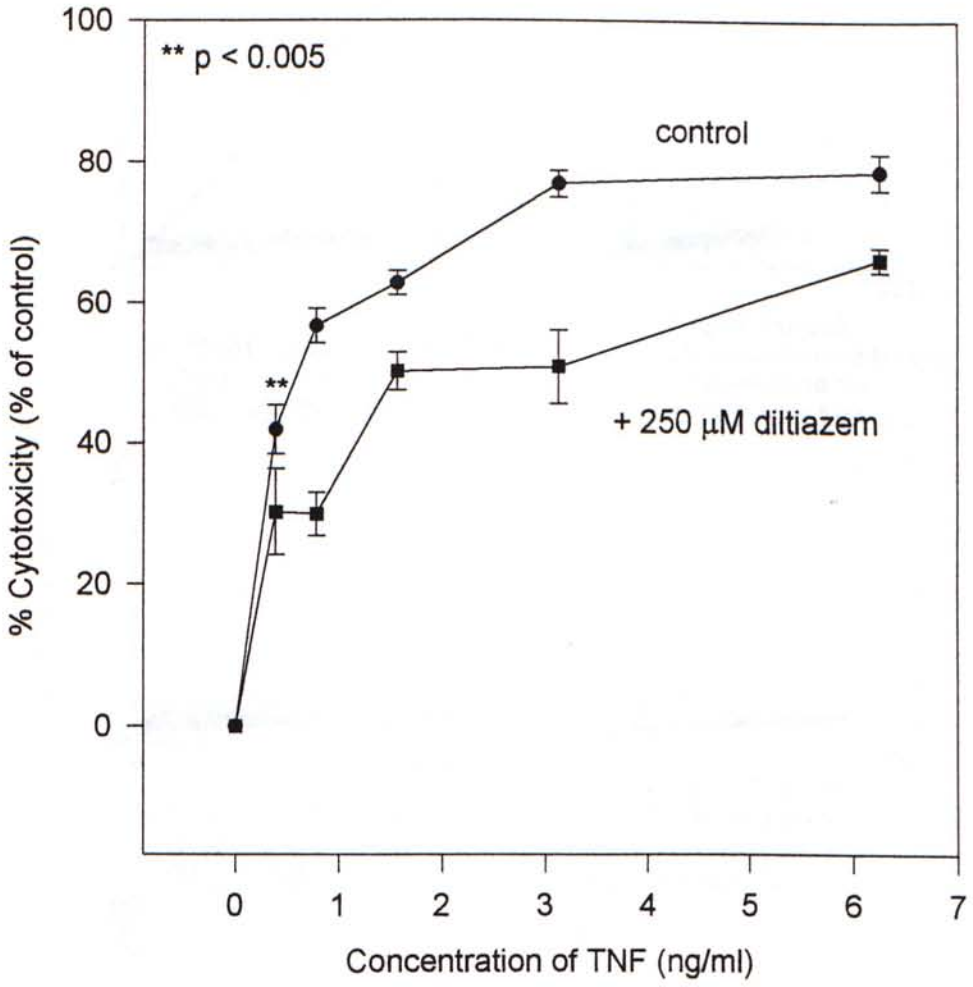

Figure 3.60

Addition of diltiazem reduced TNF-mediated cytotoxicity. L929 cells were seeded at 3 x 10^4/well in complete medium in a 96-well plate and incubated for 20 hr at 37 °C, 5 % CO_2. 100 μl TNF of various concentrations in the presence (■) or absence (●) of diltiazem (250 μM) in serum-free medium was added and incubated for 20 hr at 37 °C, 5 % CO_2. MTT assay was then applied (n = 3, expt = 3). Similar results were obtained in neutral red assay (data not shown).

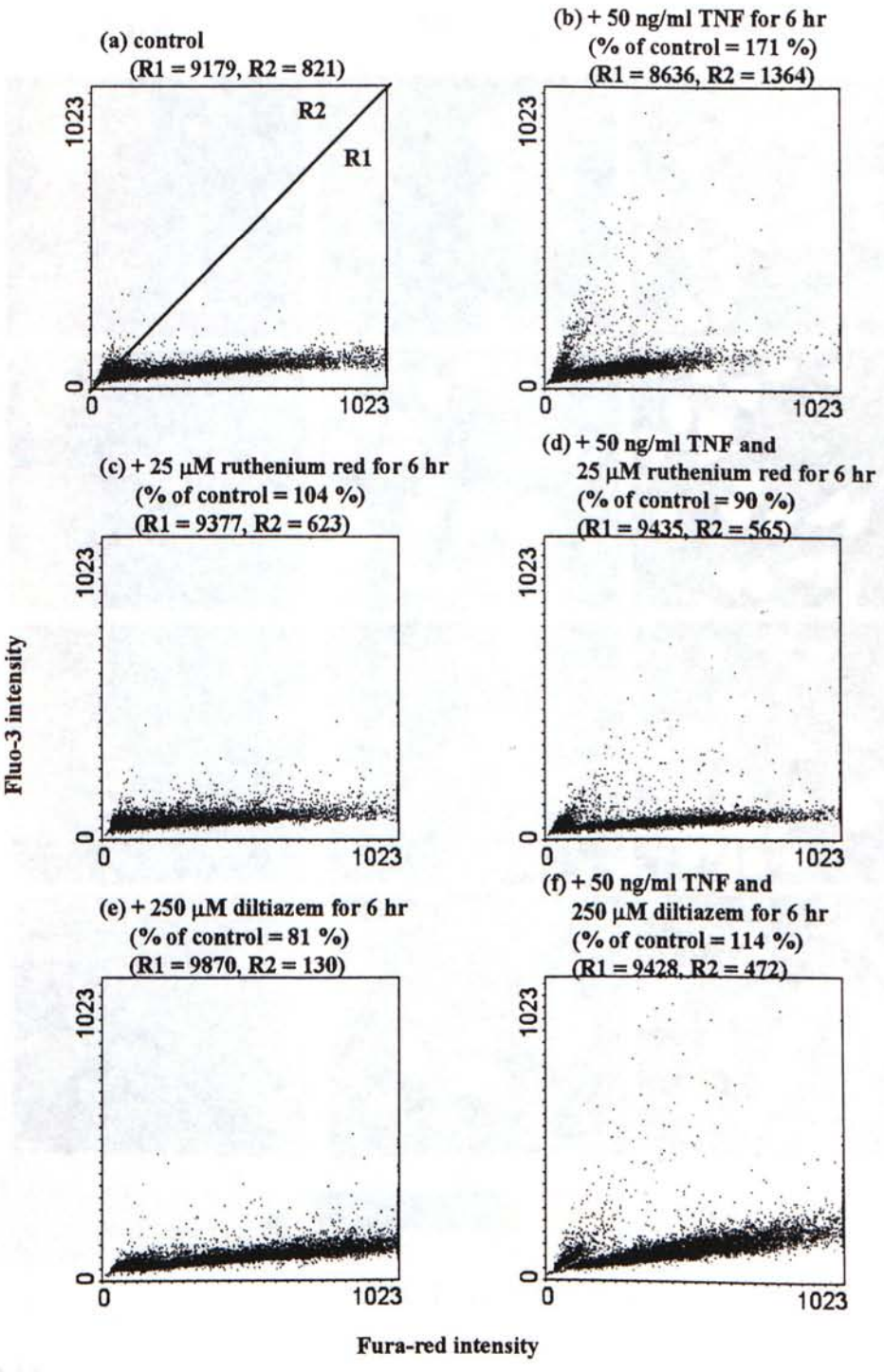

Figure 3.61

Addition of ruthenium red or diltiazem for 6 hr reduced TNF-mediated Ca^{2+} release. (a) Control group. (b) TNF increased the release of Ca^{2+}. (c) Addition of 25 μM ruthenium red did not change the release of $[Ca^{2+}]_i$. (d) Addition of 50 ng/ml TNF with 25 μM ruthenium red reduced TNF-mediated Ca^{2+} release as compare to TNF-treated group. (e) Addition of 250 μM diltiazem did not cause the release of Ca^{2+}. (f) Application of 50 ng/ml TNF and 250 μM diltiazem reduced TNF-mediated Ca^{2+} release.

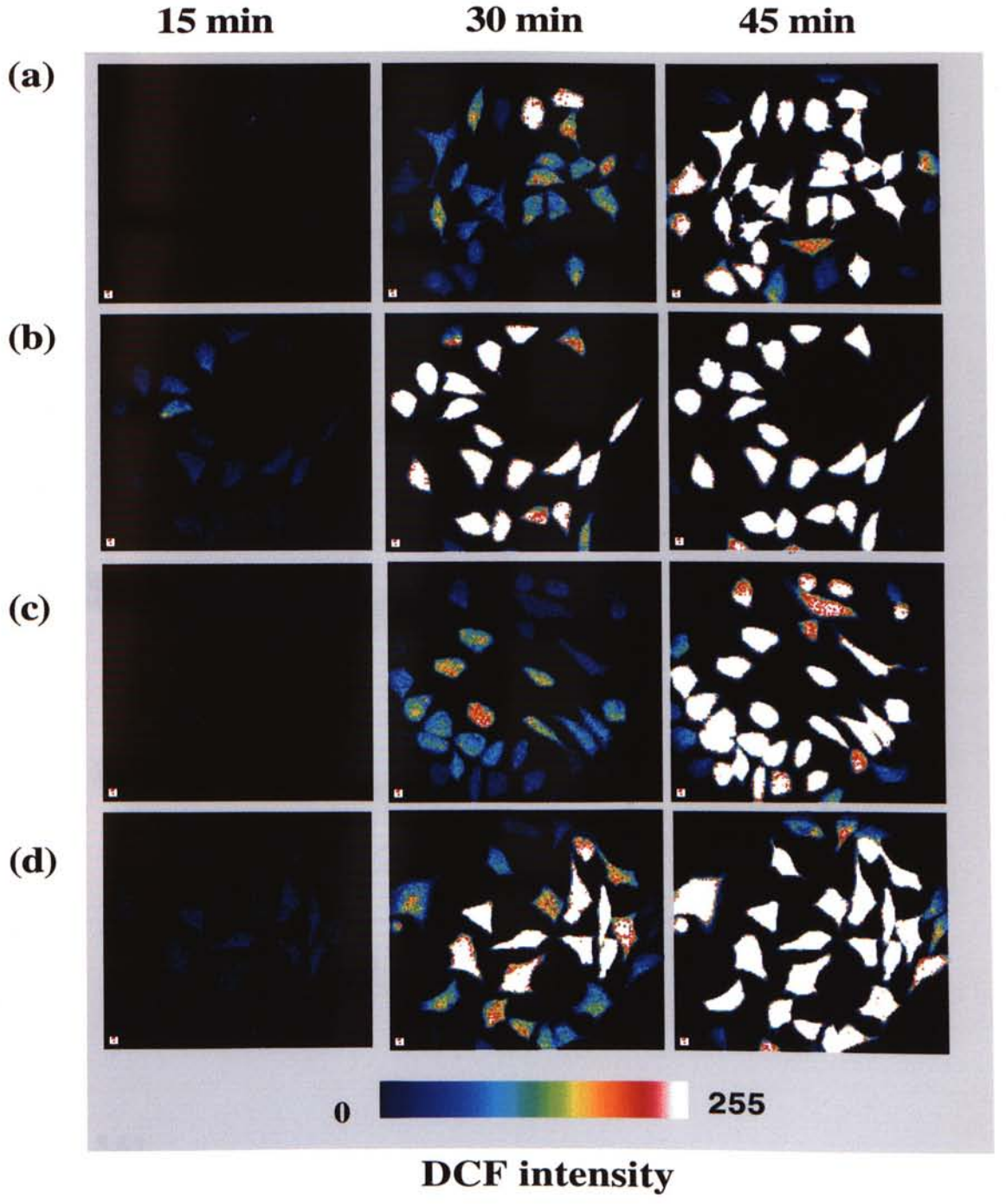

Figure 3.62
The confocal images show that ruthenium red reduced the amount of TNF-mediated H_2O_2 production in L929 cells. L929 cells (2 x 10^3/ml) were seeded on a cover glass and incubated at 37 °C, 5 % CO_2 for 4 days. Cells were then incubated with Na^+-HEPES buffer (a), 50 ng/ml TNF for 15 min (b), 25 µM ruthenium red for 15 min (c), and 50 ng/ml TNF and 25 µM ruthenium red for 15 min (d) at room temperature and the ability of cells to produce H_2O_2 was then detected by DCF (final concentration 10 µM) with a CLSM-MD at time zero.

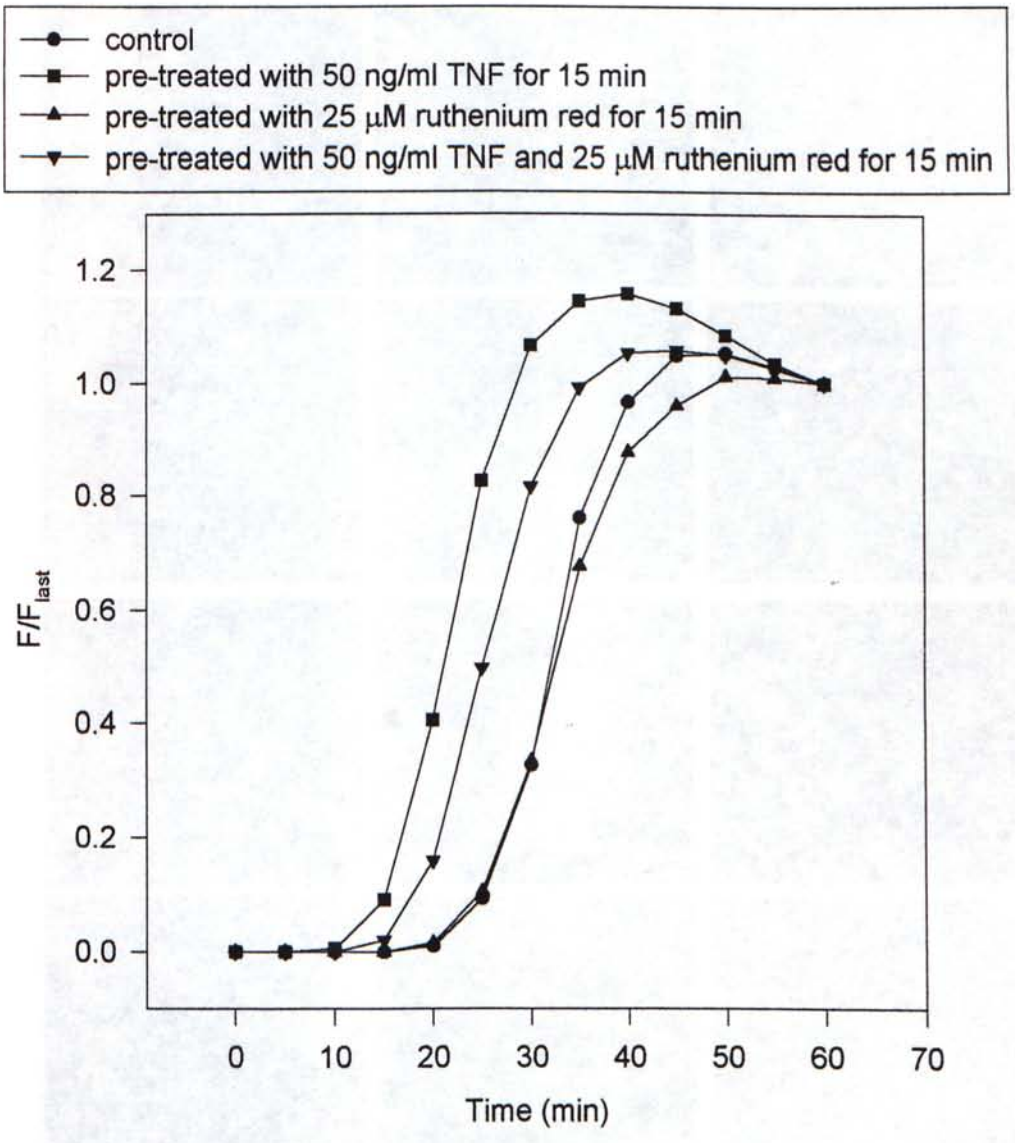

Figure 3.63

Ruthenium red reduced the rate of TNF-mediated H_2O_2 production in L929 cells. This graph summaries the results of the confocal images from figure 3.62. The y-axis, F/F_{last}, represented the summation of fluorescence intensity from all cells at each time interval that was divided by the total fluorescence intensity of the last image.

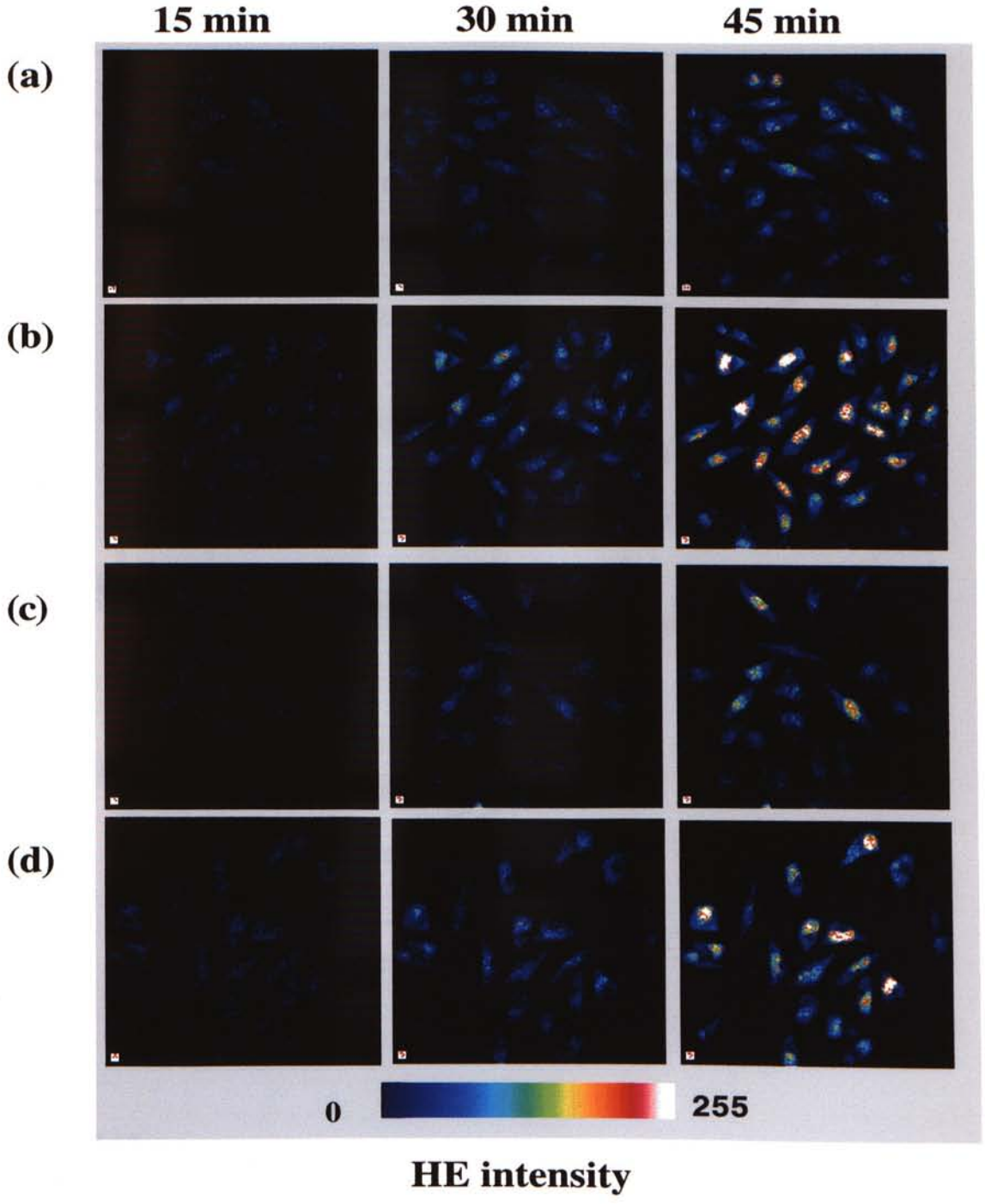

Figure 3.64
The confocal images show that ruthenium red reduced the amount of TNF-mediated $O_2\bullet^-$ production in L929 cells. L929 cells (2 x 10^3/ml) were seeded on a cover glass and incubated at 37 °C, 5 % CO_2 for 4 days. Cells were then incubated with Na^+-HEPES buffer (a), 50 ng/ml TNF for 15 min (b), 25 µM ruthenium red for 15 min (c), and 50 ng/ml TNF and 25 µM ruthenium red for 15 min (d) at room temperature and the ability of cells to produce $O_2\bullet^-$ was then detected by HE (final concentration 10 µM) with a CLSM-MD at time zero.

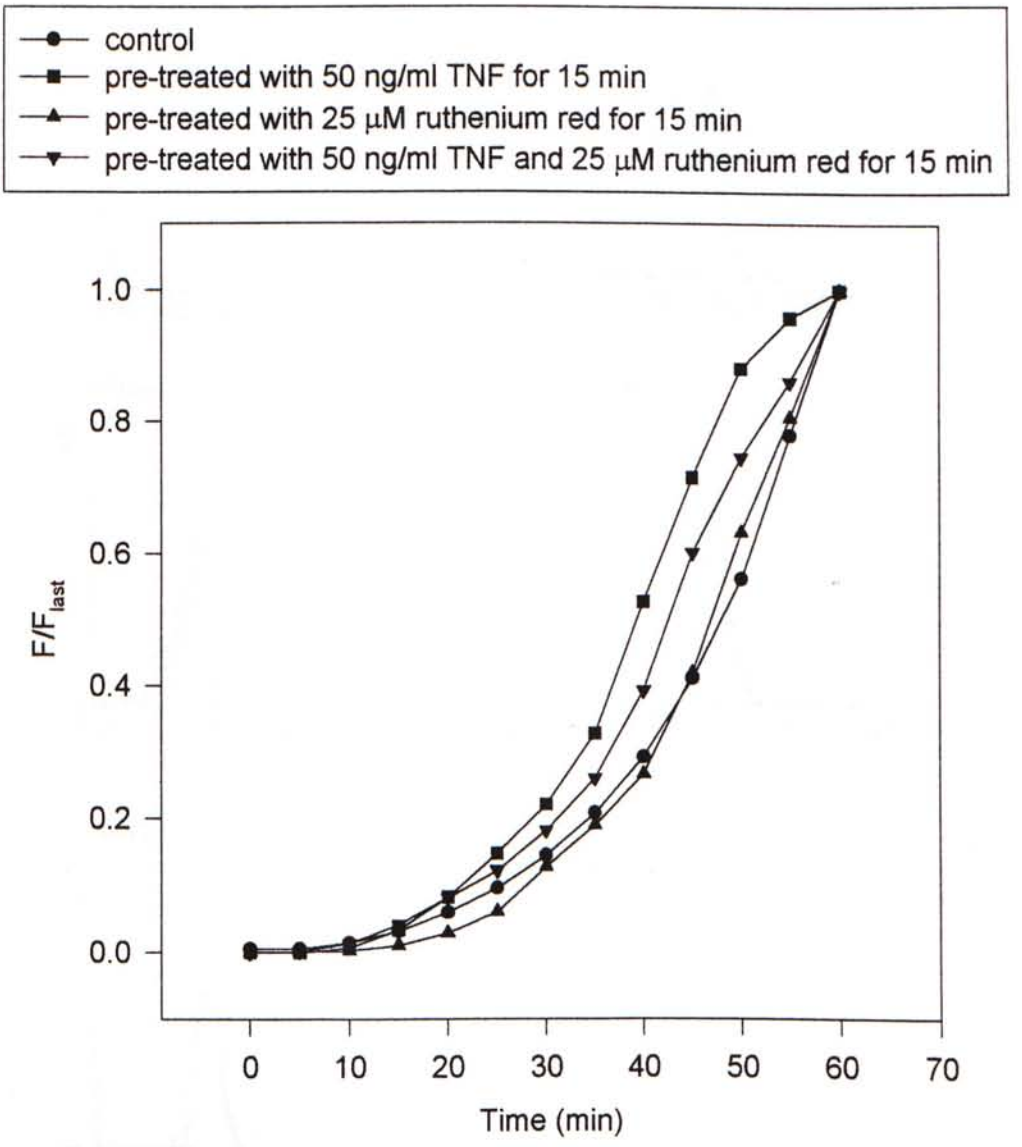

Figure 3.65

Ruthenium red reduced the rate of TNF-mediated $O_2\bullet^-$ production in L929 cells. This graph summaries the results of the confocal images from figure 3.64. The y-axis, F/F_{last}, represented the summation of fluorescence intensity from all cells at each time interval that was divided by the total fluorescence intensity of the last image.

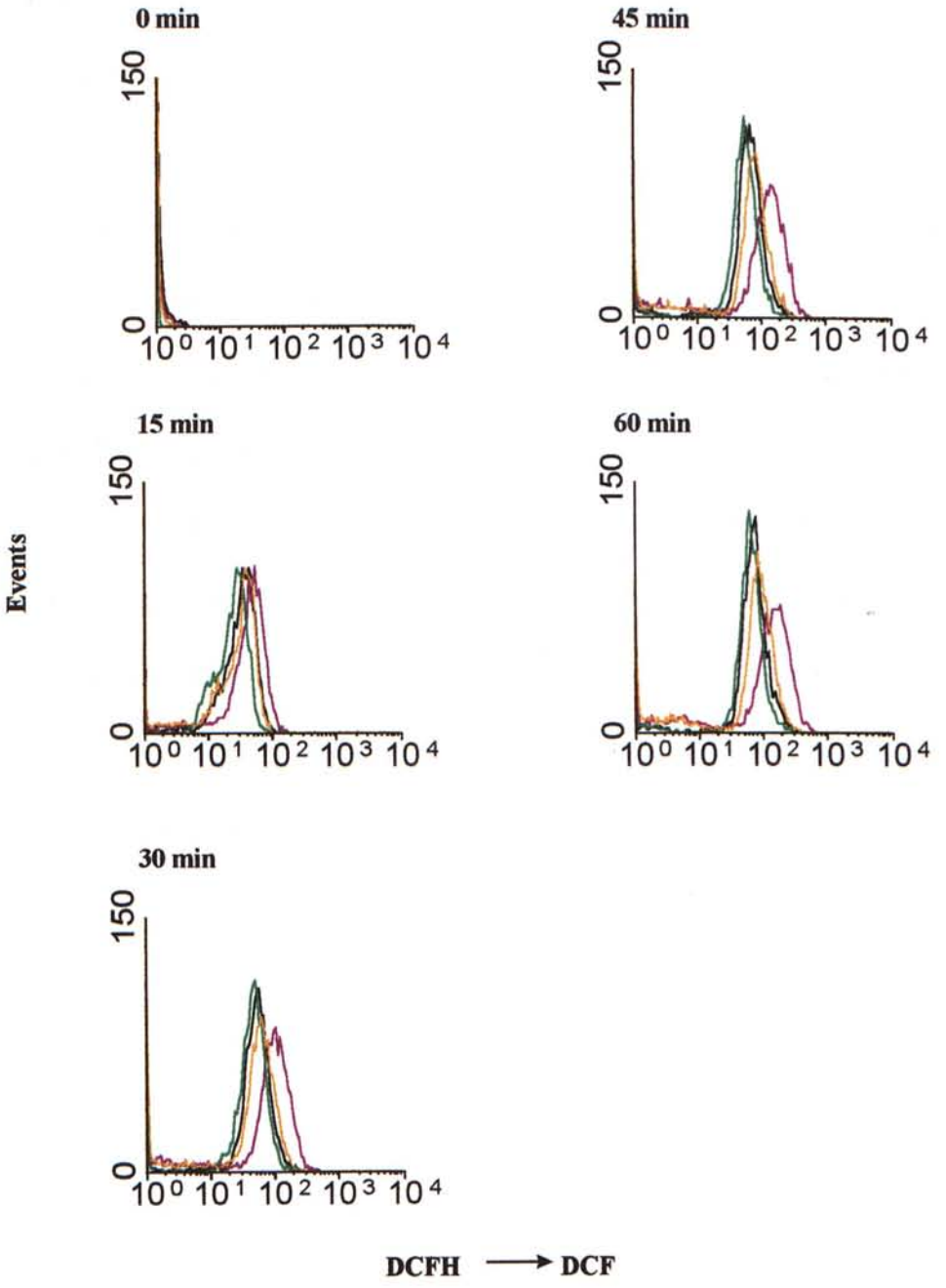

Figure 3.66

Addition of diltiazem reduced TNF-mediated H_2O_2 release. L929 cells (10^6/ml) were seeded in a 6-well plate and were incubated overnight at 37 °C, 5 % CO_2. Cells were treated with 250 μM diltiazem in the presence (orange line) or absence (green line) of 50 ng/ml TNF for 6 hr. Cells were then trypsinized. DCF (10 μM) was added and measurement was made with a FCM at the time indicated. The black and the purple lines represent the control and the TNF (50 ng/ml)-treated group, respectively. It was found that cells incubation with diltiazem reduced the release of H_2O_2 in treatment with TNF.

that both ruthenium red and diltiazem may impair the formation of ROS during the TNF challenge because of theirs inhibitory effect on the mitochondrial Ca^{2+} cycling.

In conclusion, TNF-induced cell death was inhibited by Ca^{2+} chelator such as BAPTA/AM and it implied that Ca^{2+} plays an important role in TNF-mediated cytotoxicity. Moreover, BAPTA/AM was capable of reducing the TNF-mediated H_2O_2 release. This suggested that Ca^{2+} may be one of the mediators for the release of ROS. However, the site of the release of Ca^{2+} is unknown. In the experiments with the use of ruthenium red and diltiazem, the source of Ca^{2+} for the TNF-effect was found to be mitochondria although we could not eliminate the contribution from ER. The ability of BAPTA/AM, ruthenium red and diltiazem in the reduction of TNF-mediated ROS release further suggest that $[Ca^{2+}]_m$ fluxes, probably the $[Ca^{2+}]_m$ cycling, may be responsible for the formation of ROS.

3.6 Effect of Tumor Necrosis Factor-Alpha on pH

3.6.1 Introduction

It was found that intracellular acidification may be involved in apoptosis (Barry and Eastman, 1992). Under the conditions where endonuclease activation occurred in HL-60 cells, Barry and Eastman observed a decrease in cytosolic pH on the order of 0.2 - 0.3 pH units, that may lead to apoptosis. For monitoring pH inside L929 cells, the fluorescence indicator SNARF-1/AM was applied. An increase in the fluorescence intensity indicates that there is an increase in pH.

3.6.2 Effect of TNF on pH

Figure 3.67 shows the confocal images (from CLSM, Meridian) that addition of Na^+-HEPES buffer or 50 ng/ml TNF did not cause a spontaneous change in pH whereas application of 50 mM NH_4Cl induced an increase in the fluorescence intensity. NH_4Cl increased intracellular pH inside the cells, therefore, it was used for the positive control. Figure 3.68 summaries the results form Figure 3.67.

In conclusion, addition of TNF did not change the intracellular pH in L929 cells immediately after the addition of TNF. However, the long-term effect of TNF on intracellular pH remains to be investigated.

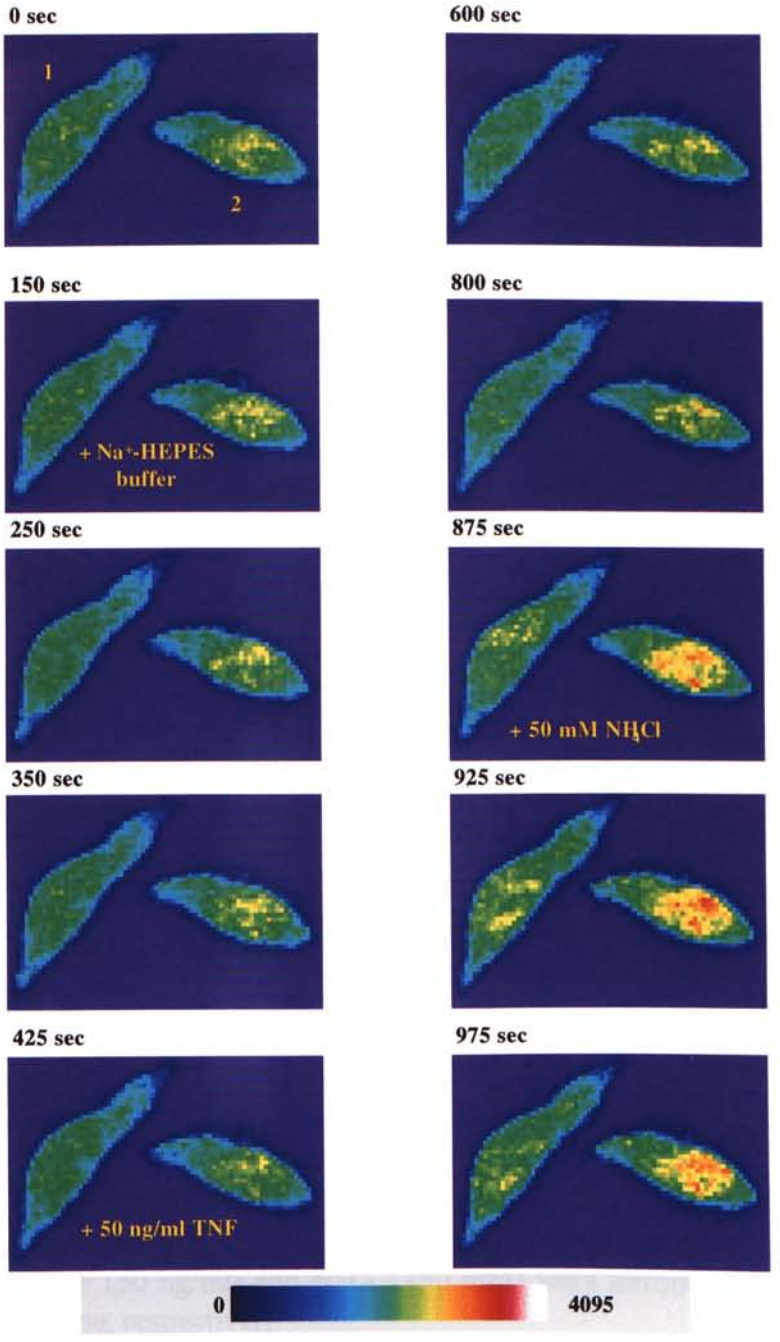

Figure 3.67

The confocal images show that addition of Na^+-HEPES and TNF did not change the pH in L929 cells. L929 cells (2 x 10^3/ml) were seeded on cover glass and incubated at 37 ℃ and 5 % CO_2 for 3 days. Cells were mounted on a home-made holder and washed twice by Na^+-HEPES buffer. Cells were loaded with 10 μM SNARF-1/AM for 1 hr and then washed twice by Na^+-HEPES buffer. Confocal scanning was made with a 5-second-interval. Na^+-HEPES buffer and 50 ng/ml TNF were added at the 150th and 425th sec, respectively. There was no change in the fluorescence intensity. Addition of 50 mM NH_4Cl induced a significant increase in the fluorescence and it indicated the increase in the pH inside L929 cells (n = 2).

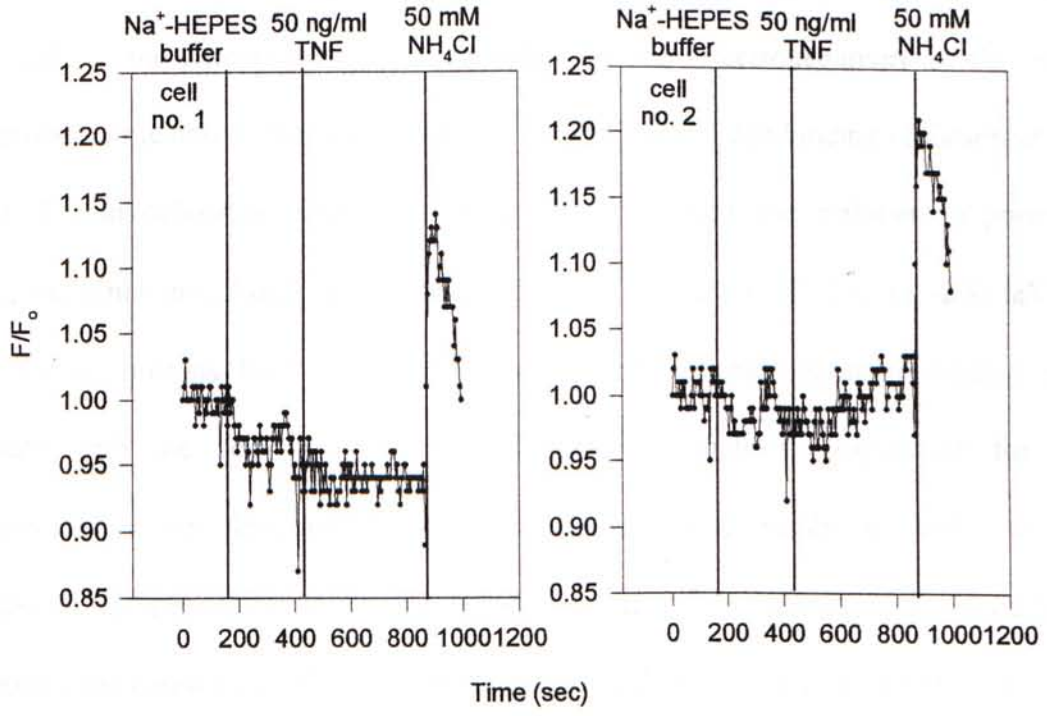

Figure 3.68

Na^+-HEPES buffer and TNF did not change the pH in L929 cells. This graph summaries the results of the confocal images of cell number 1 and 2 from figure 3.67. Na^+-HEPES buffer, TNF (50 ng/ml) and NH_4Cl (50 mM) were introduced to the cells at the 1st, 2nd and 3rd hairline, respectively.

3.7 Effect of Tumor Necrosis Factor-Alpha on Mitochondrial Membrane Potential

3.7.1 Introduction

The positively charged rhodamine analogue rhodamine 123 accumulates specifically in the mitochondria of living cells. The high electronegativity of the intact mitochondrial membrane may be responsible for the specific dye binding (Johnson *et al.*, 1980). The mitochondrial electron transport chain develops and maintains a potential across the inner mitochondrial membrane ($\Delta\psi_m$) of the order of -150 to -200 mV by expulsion of protons from the matrix. The intensity of mitochondrial staining may correlate with the activity of the oxidoreductive complexes responsible for the maintenance of the electronegativity of the mitochondrial membrane, and thus the rhodamine 123 may be a direct marker of the energy-supplying metabolic processes. Moreover, the balance of Ca^{2+} between the cytosol and the mitochondrial matrix ($[Ca^{2+}]_m$ cycling) is determined by the electrochemical potential for Ca^{2+} across the inner mitochondrial membrane, and predominantly by $\Delta\psi_m$. Blockade of electron transport by mitochondrial inhibitors such as rotenone increased rhodamine 123 fluorescence (Duchen and Biscoe, 1992), while fluorescence can be reduced by uncouplers such as DNP (Emaus *et al.*, 1986).

3.7.2 Effect of TNF and Some Drugs on Mitochondrial Membrane Potential

Figure 3.69 shows that addition of TNF (50 ng/ml) for 3, 6 or 10 hr did not

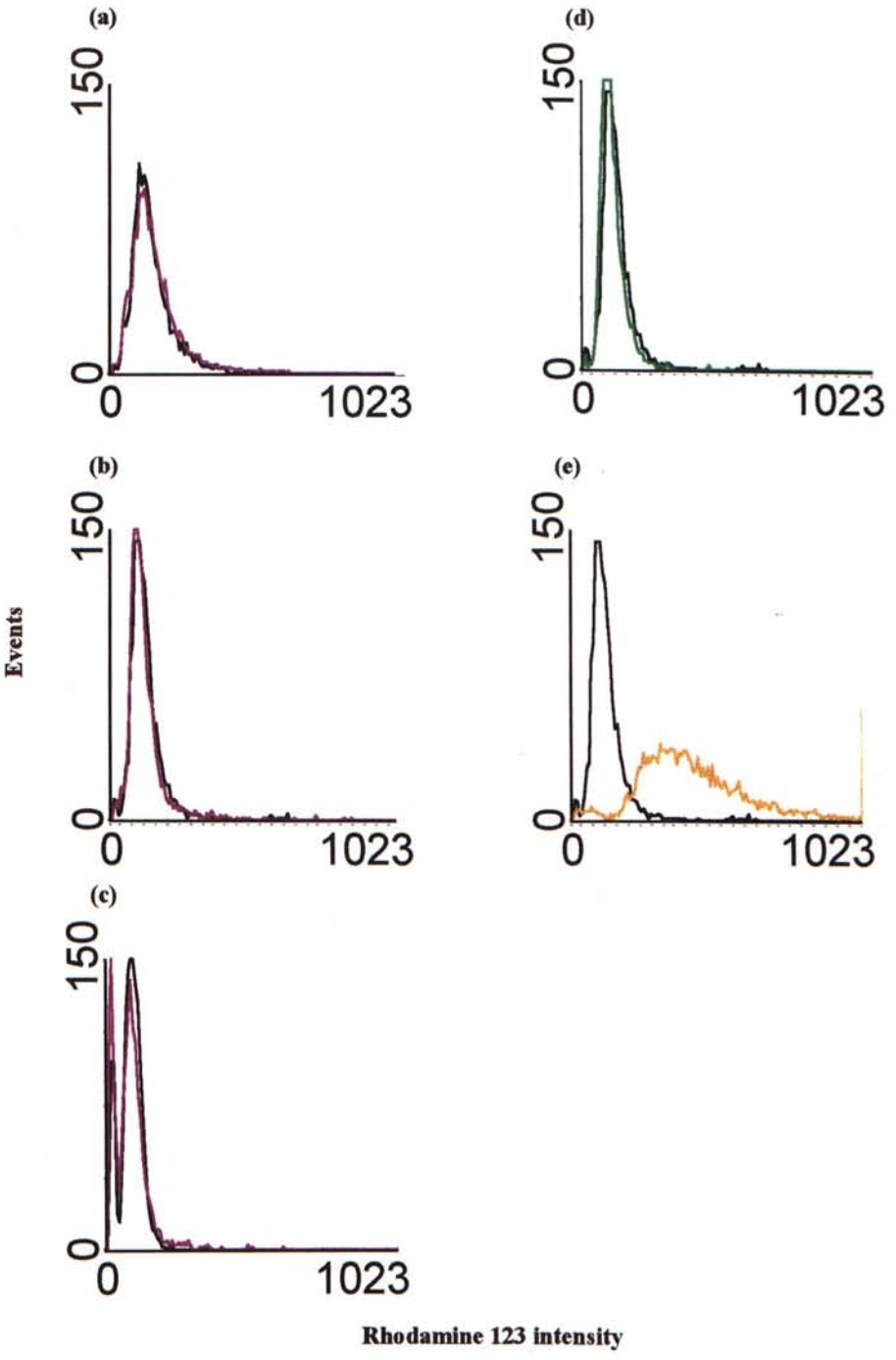

Figure 3.69

Addition of TNF for 3, 6 or 10 hr did not cause any change in rhodamine 123 intensity. L929 cells (10^6/ml) were seeded in a 6-well plate and were incubated overnight at 37 °C, 5 % CO_2. Cells were treated with p-RPMI (black line), 50 ng/ml TNF (purple line) for (a) 3 hr, (b) 6 hr and (c) 10 hr. Moreover, cells were treated with (d) 30 μM DNP (green line) and (e) 50 μM rotenone (orange line). Cells were then trypsinized. After washing, rhodamine 123 (final concentration = 2 μM) was added and incubated at 37 °C for 15 min. Measurement was made by FCM.

cause any change in the $\Delta\psi_m$. Application of DNP (30 μM) induced a small decrease in the fluorescence intensity of rhodamine 123 since it is one of the uncouplers that may depolarize the $\Delta\psi_m$. The depolarization of $\Delta\psi_m$ reduced the binding of positively charged rhodamine 123. In contrast, addition of rotenone (50 μM) induced a drastic increase in the fluorescence intensity of rhodamine 123. It implies that rotenone hyperpolarize the $\Delta\psi_m$. Table 3.4 shows the data from FCM and indicated that addition of 50 ng/ml TNF for 3, 6 or 10 hr did not induce a significant change in the mitochondrial membrane potential. As expected, there was a reduction in the fluorescence intensity in the treatment of cells with DNP or ruthenium red. There was no change in the rhodamine 123 intensity in the treatment of TNF plus DNP or ruthenium red. However, it is interesting that addition of TNF reduced the rhodamine 123 intensity with treatment of rotenone and antimycin A in the 3 and 6 hr incubation. The mechanism of the reduction of rhodamine 123 fluorescence intensity in the treatment of TNF plus rotenone or antimycin A is still unknown.

In conclusion, TNF did not change the $\Delta\psi_m$ but reduced the hyperpolarization of $\Delta\psi_m$ in the treatment of cells with rotenone and antimycin A.

Table 3.4
The effect of TNF and other drugs on $\Delta\psi_m$.

Treatment	Incubation time (hr)	Rhodamine 123 intensity (arbitrary unit)	* % of control (%)
control	3	148.36	/
50 ng/ml TNF	3	160.71	108
50 μM rotenone	3	600.81	404
50 μM antimycin A	3	449.73	303
30 μM DNP	3	128.43	86
25 μM ruthenium red	3	139.53	94
50 ng/ml TNF + 50 μM rotenone	3	473.20	318
50 ng/ml TNF + 50 μM antimycin A	3	224.23	151
50 ng/ml TNF + 30 μM DNP	3	129.31	89
50 ng/ml TNF + 25 μM ruthenium red	3	140.25	94
control	6	127.16	/
50 ng/ml TNF	6	125.58	98
50 μM rotenone	6	415.23	326
50 μM antimycin A	6	234.11	184
30 μM DNP	6	112.36	88
25 μM ruthenium red	6	101.64	80
50 ng/ml TNF + 50 μM rotenone	6	316.41	248
50 ng/ml TNF + 50 μM antimycin A	6	156.25	122
50 ng/ml TNF + 30 μM DNP	6	110.74	88
50 ng/ml TNF + 25 μM ruthenium red	6	99.91	78
control	10	93.53	/
50 ng/ml TNF	10	89.65	96

% of control was obtained according to the following formula:

* % of control (%)

= [rhodamine 123 (TNF treatment)] ÷ [rhodamine (control)] x 100 %

3.8 Comparison of Effects of Tumor Necrosis Factor-Alpha on Susceptible Cell Line, L929 and Resistant Cell Lines, rL929, rL929-11E and rL929-4F

3.8.1 Introduction

The resistant cell lines, rL929, rL929-11E and rL929-4F were developed by Prof. K. P. Fung and H. K. Cheng (Department of Biochemistry, CUHK). The resistant cell line was defined by their inert response to TNF cytotoxicity and was developed by Kwan as mentioned in section 2.1.4.2 (Kwan, 1995). Kwan concluded that there was no distinctive morphological change in TNF-resistant cells (rL929, rL929-11E and rL929-4F) as compared to the parental cells (Kwan, 1995). Moreover, several conclusions are obtained from his study: (1) There is no difference in growth rate between L929 and rL929 cells; (2) Expression of TNFR1 in rL929 cells is the same as L929 (the expression of TNFR1 in rL929-11E and rL929-4F was not identified); (3) the resistance to TNF in rL929 cells is not due to a higher capacity of scavenging of TNF-generated free radicals. The actual mechanism is still unknown and may be due to a lack of the ability of rL929 cells to generate free radicals.

In light of this, the differences between TNF-sensitive and resistant cell lines and the possible mechanisms account for the resistance to TNF were examined in this project. The effect of TNF on the (1) cytotoxicity, (2) release of ROS, (3) release of Ca^{2+}, and (4)

cell cycle were investigated and the responses to TNF in both sensitive and resistant L929 cells were compared.

3.8.2 Effect of TNF on the Cytotoxicity of Resistant Cell Lines

Figure 3.70 shows that TNF did not induce a significant cell death in rL929 cells as compared with the parental line, L929 cells. Moreover, rL929-11E (Figure 3.71) and rL929-4F (Figure 3.72) did not show a distinct cytotoxicity after TNF treatment.

3.8.3 Effect of TNF on the Release of ROS in Resistant Cell Lines

Figure 3.73 shows that addition of 50 ng/ml TNF for 6 hr caused an increase in the H_2O_2 release in the TNF-sensitive L929 cell line whereas there was no increase in the rate of production of H_2O_2 in resistant cell lines. Figure 3.74 and Figure 3.75 show the dot plots of TNF-treated sensitive and resistant cells. It is obvious that treatment of resistant cells with TNF did not show any difference from the one without TNF treatment. At the same time, TNF increased the production of H_2O_2 and cell death in sensitive cell lines (Figure 3.74b). Table 3.5 shows the population of cell of TNF-sensitive and resistant cell lines in R1, R2 and R3 as described previously (Figure 2.4) after the TNF treatment. As shown in the Table 3.5, an increase in the cell number in the R2 region in the group with 6-hour-incubation of TNF was observed. This indicates that dead cells were formed after TNF treatment in the parental cell line, L929. In contrast, only a few number of cells in region R2 was observed in the resistant cell lines, rL929 (Figure 3.74d), rL929-11E (Figure 3.75b) and rL929-4F (Figure 3.75d) (Table 3.5) after 6-hour TNF treatment.

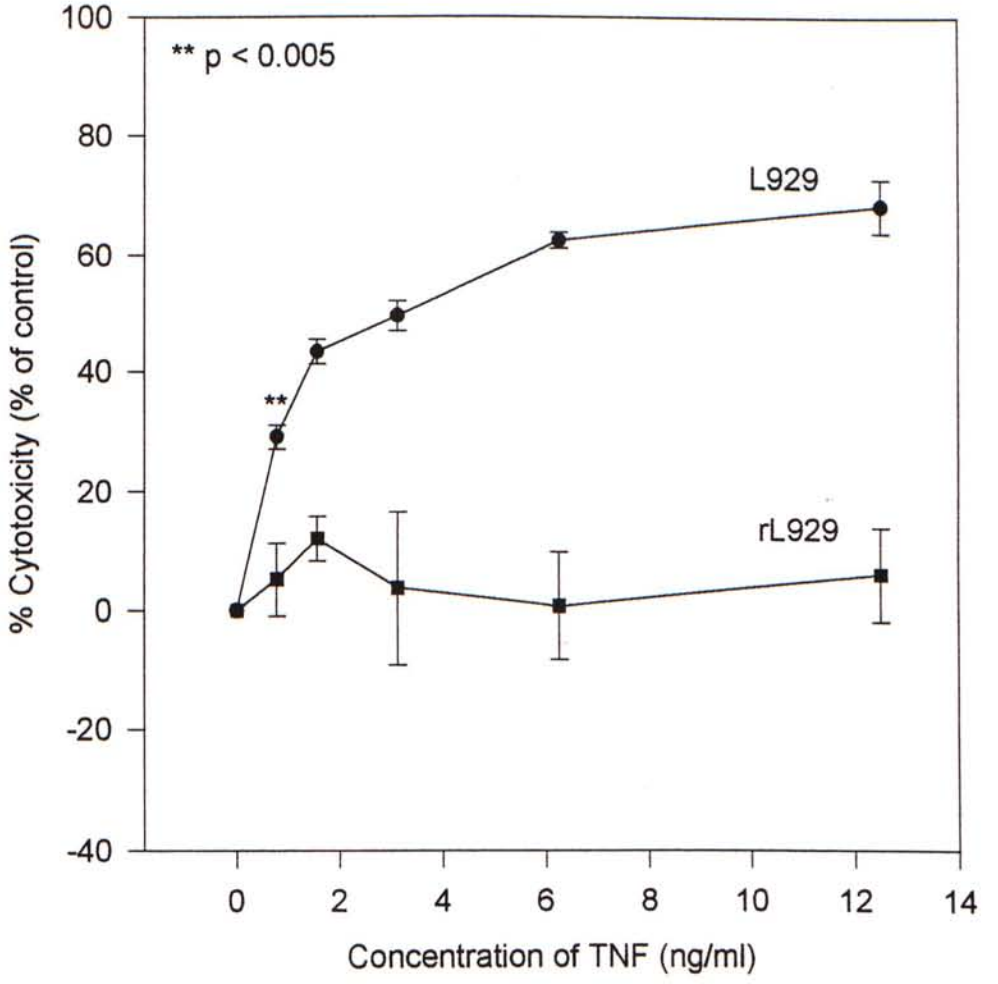

Figure 3.70

TNF did not induce a significant cell death in rL929. L929 and rL929 cells were seeded at 3 x 10^4/well in complete RPMI 1640 medium and incubated for 20 hr at 37 °C, 5 % CO_2. After incubation, spent medium was discarded and washed twice by serum-free medium. 100 µl of serum-free medium with various concentrations of TNF was added to each well and incubated for 20 hr at 37 °C, 5 % CO_2. MTT assay was applied (n = 7).

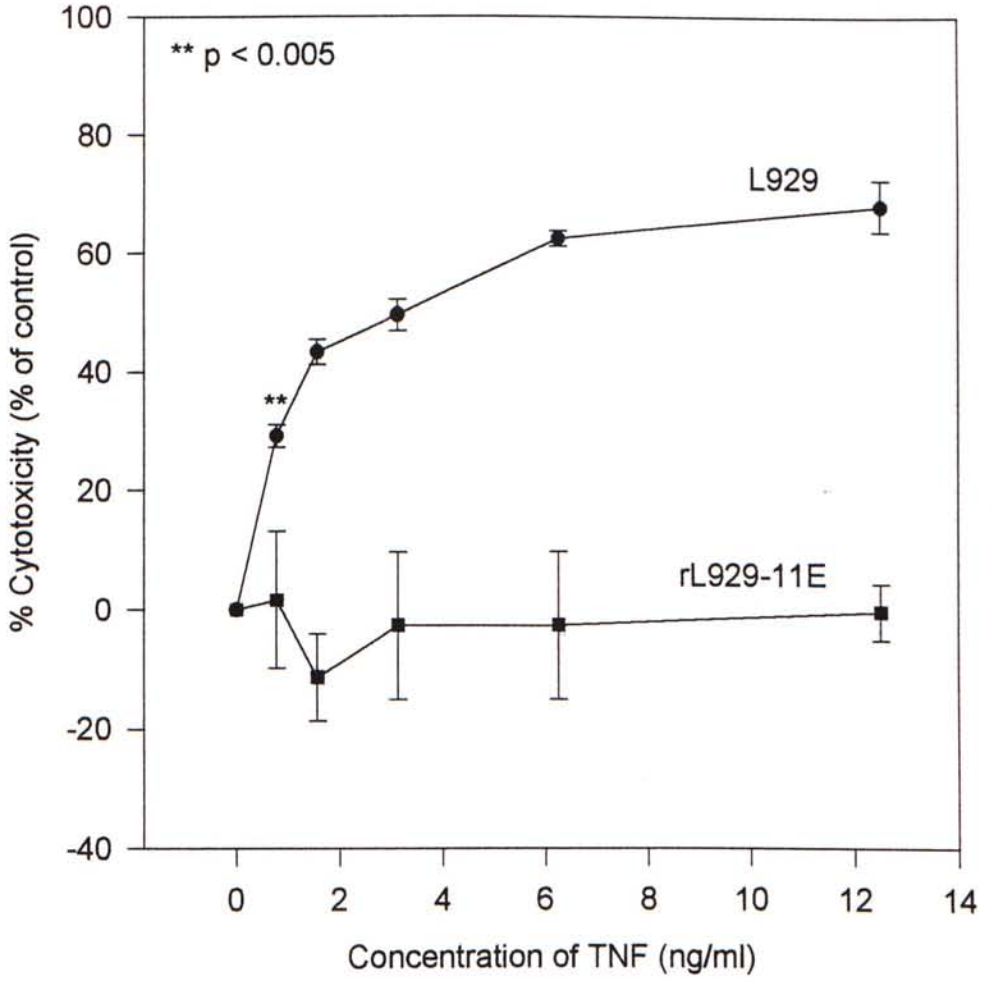

Figure 3.71
TNF did not induce a significant cell death in rL929-11E. L929 and rL929-11E cells were seeded at 3 x 10^4/well in complete RPMI 1640 medium and incubated for 20 hr at 37 °C, 5 % CO_2. After incubation, spent medium was discarded and washed twice by serum-free medium. 100 µl of serum-free medium with various concentrations of TNF was added to each well and incubated for 20 hr at 37 °C, 5 % CO_2. MTT assay was applied (n = 7).

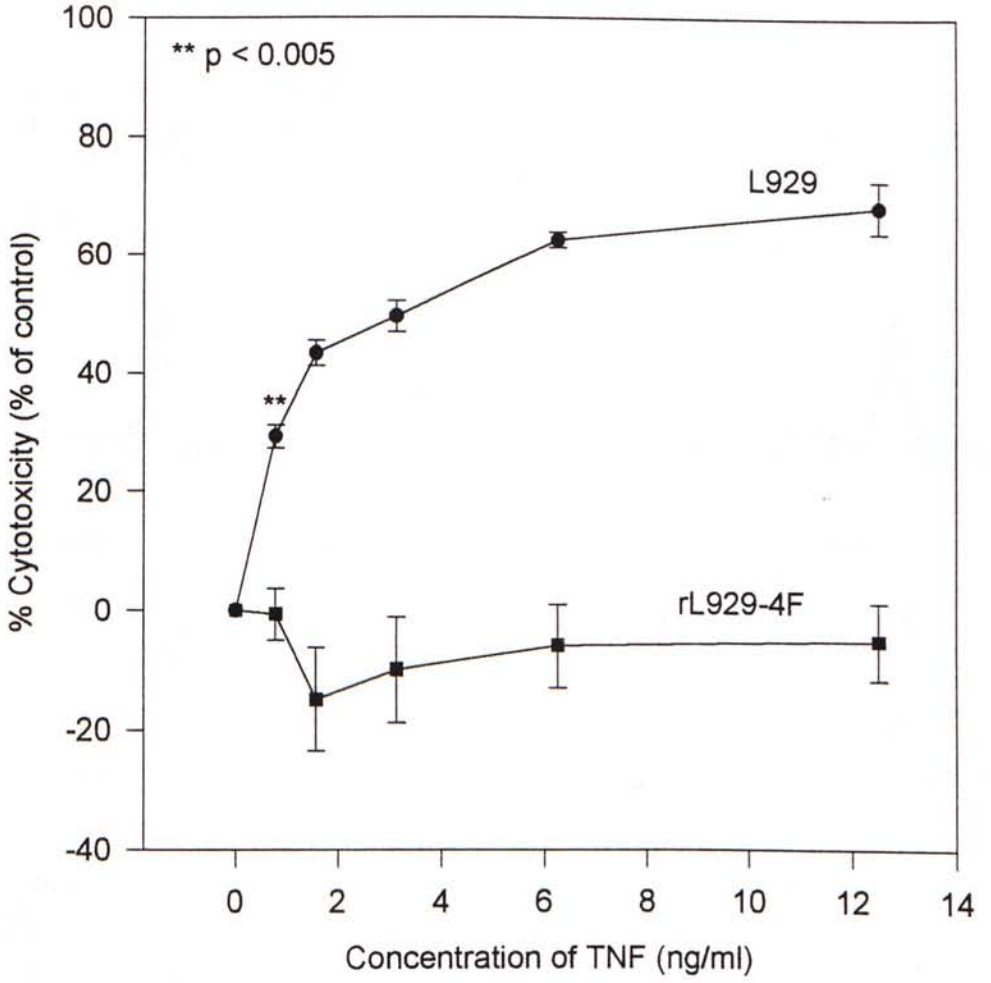

Figure 3.72
TNF did not induce a significant cell death in rL929-4F. L929 and rL929-4F cells were seeded at 3 x 10^4/well in complete RPMI 1640 medium and incubated for 20 hr at 37 °C, 5 % CO_2. After incubation, spent medium was discarded and washed twice by serum-free medium. 100 µl of serum-free medium with various concentrations of TNF was added to each well and incubated for 20 hr at 37 °C, 5 % CO_2. MTT assay was applied (n = 7).

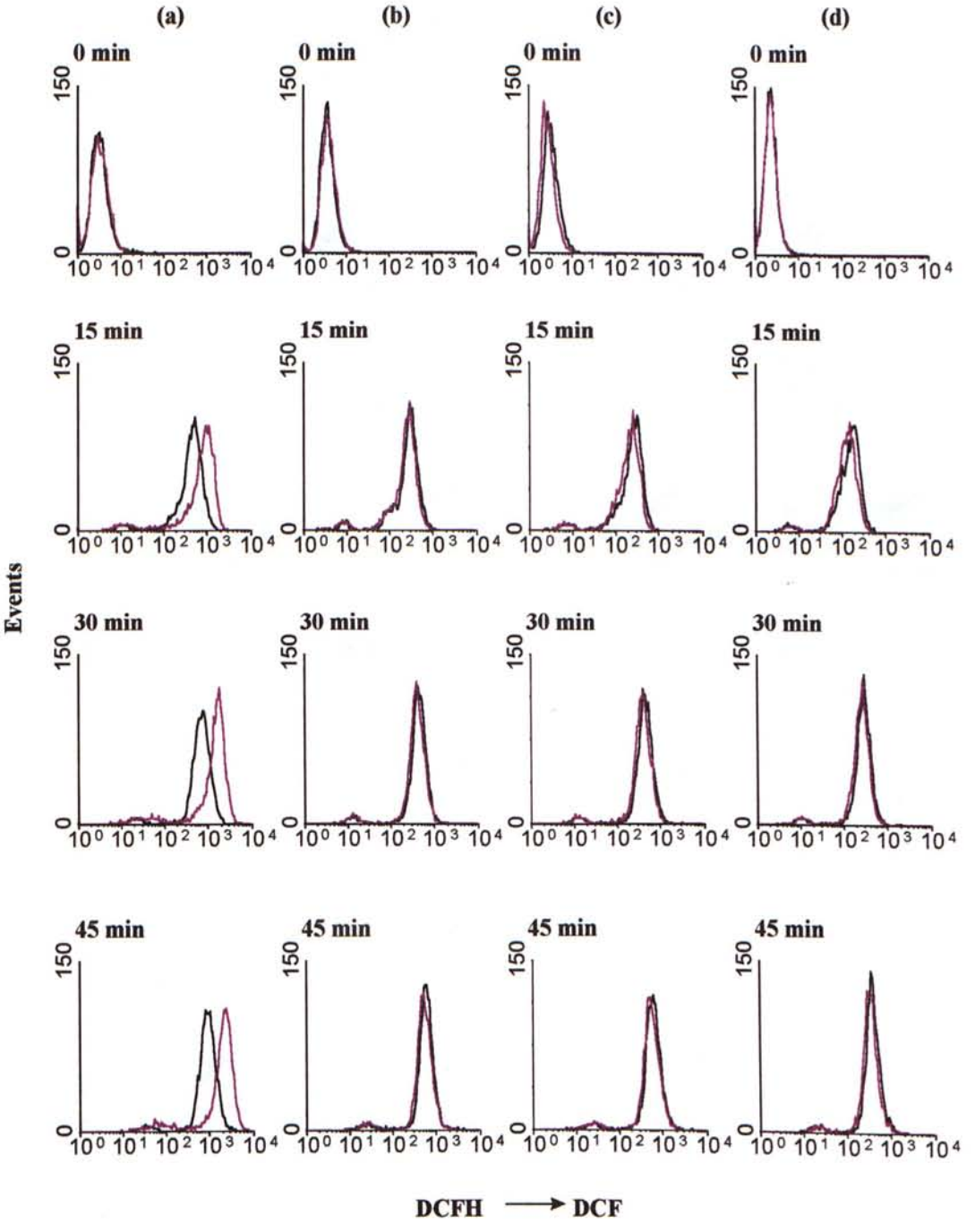

Figure 3.73

Addition of TNF for 6 hr did not increase the release of H_2O_2 from resistant cell lines, rL929, rL929-11E and rL929-4F cells. (a) Application of 50 ng/ml TNF (purple line) for 6 hr in L929 cells increased the release of H_2O_2. However, addition of 50 ng/ml TNF for 6 hr in (b) rL929, (c) rL929-11E and (d) rL929-4F did not increase the production of H_2O_2 as compared to control group (black line). The time on the left indicates the incubation period of cells with DCF.

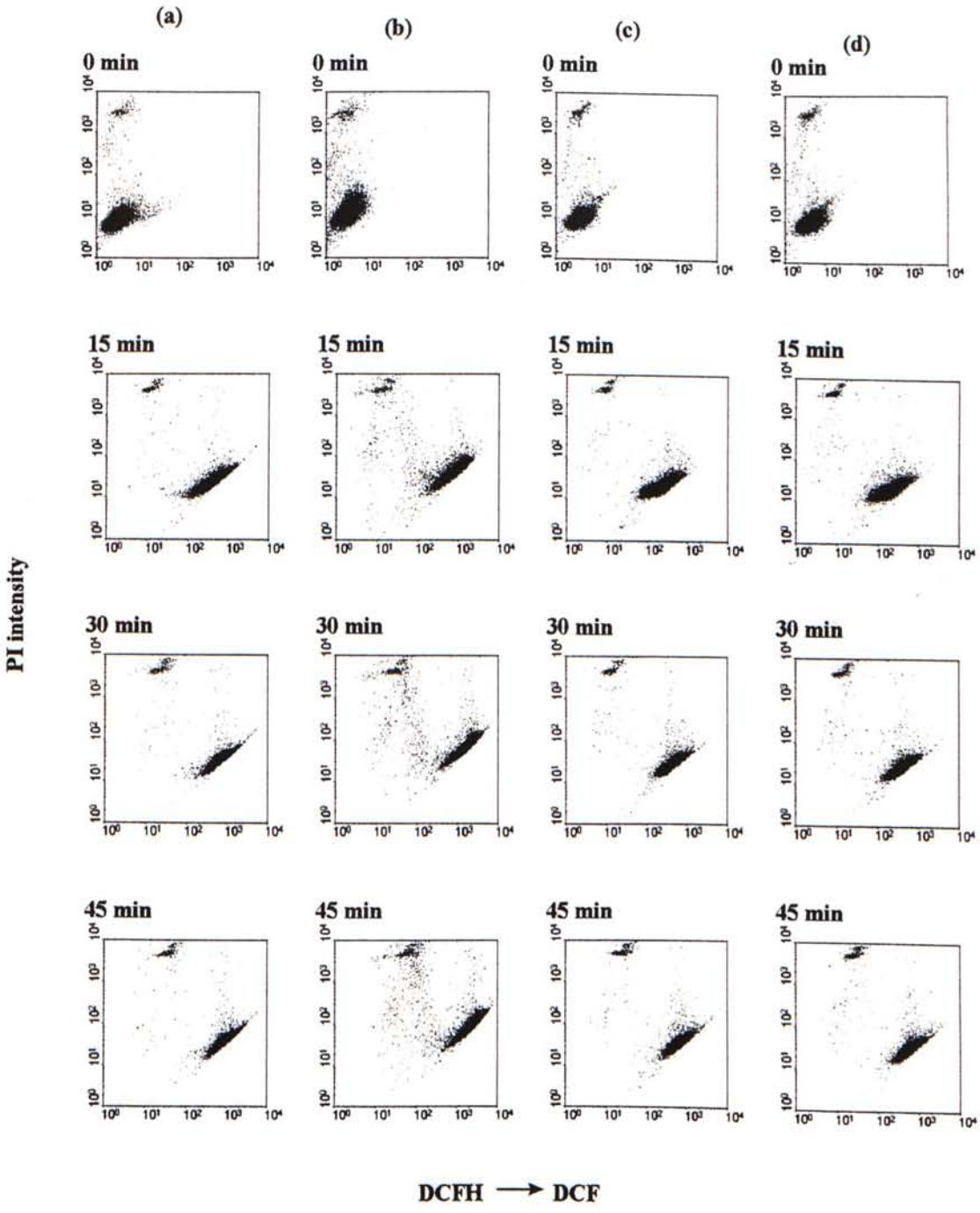

Figure 3.74

Incubation of L929 cells with TNF for 6 hr produced the release of H_2O_2 and cell death in L929 cells but not in rL929 cells. (a) It represents the L929 control group. (b) 50 ng/ml TNF was added with L929 cells. The lower population moved faster to the right than that of the L929 control group (column 1) (c) It represents the rL929 control group. (d) 50 ng/ml TNF was added with rL929 cells. There was no increase in the rate of right-shifting of lower population in rL929 cells (column 4) as compared to rL929 control group (column 3). Little intermediate population was obtained in the rL929 control and TNF-treated rL929 group.

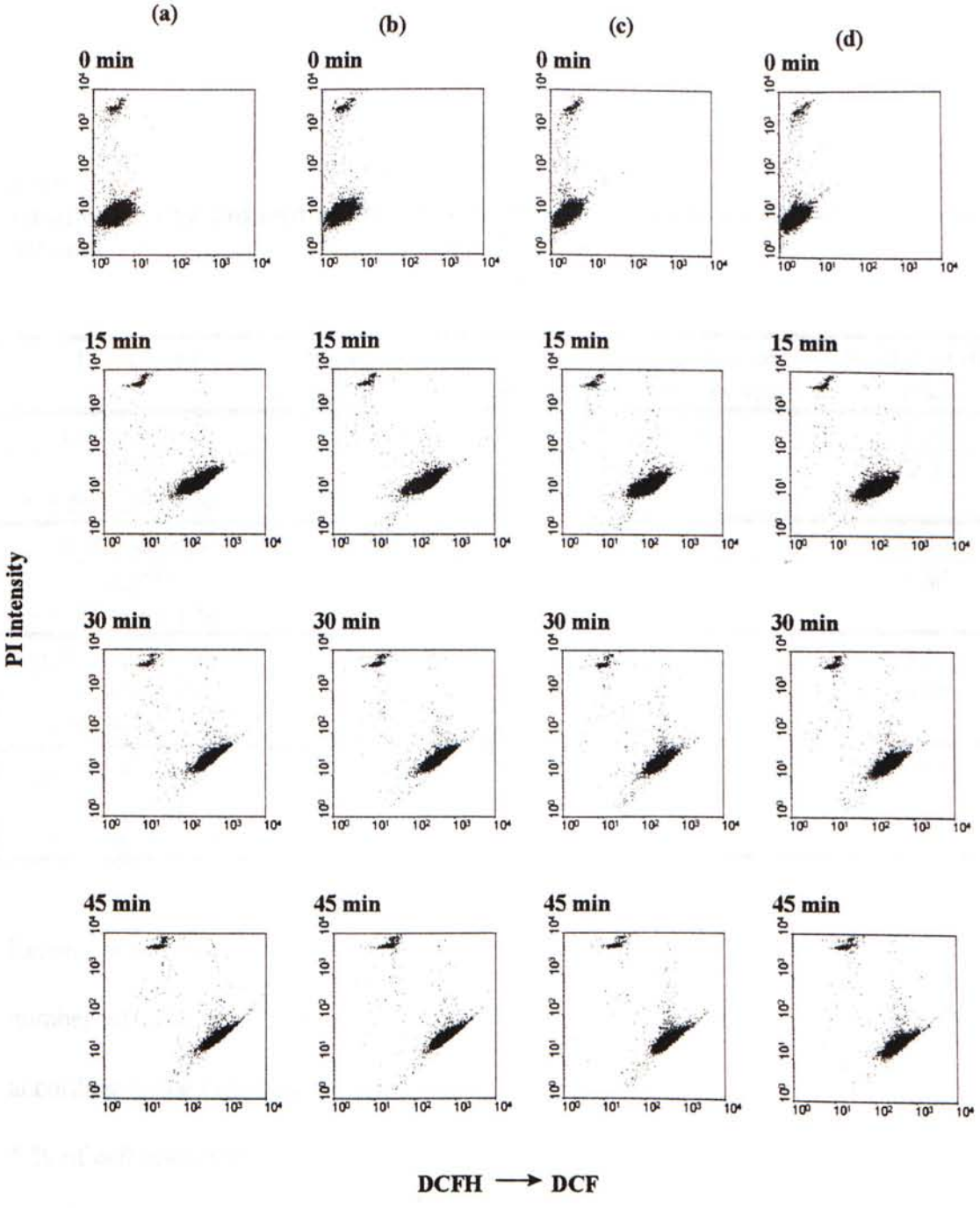

Figure 3.75

Incubation of L929 cells with TNF for 6 hr did not produce the release of H_2O_2 and cell death in rL929-11E and rL929-4F cells. (a) It represents the rL929-11E control group. (b) 50 ng/ml TNF was added with rL929-11E cells. (c) It represents the rL929-4F control group. (d) 50 ng/ml TNF was added with rL929-4F cells. There was no increase in the rate of right-shifting of lower population in rL929-11E and rL929-4F cells (column 2 and column 4, respectively) as compared to rL929-11E and rL929-4F control group, respectively (column 1 and column 3). Little intermediate population was obtained in the all four columns.

Table 3.5
Addition of TNF induced cell death in L929 whereas there was no effect on resistant cell line.

Treatment	Number of cells in R1	Number of cells in R2	Number of cells in R3	* % of Cell death (%)
L929 control	9636	91	273	3.64
L929 + 50 ng/ml TNF	8769	788	443	12.31
rL929 control	9556	141	303	4.44
rL929 + 50 ng/ml TNF	9518	138	344	4.82
rL929-11E control	9639	88	273	3.61
rL929-11E + 50 ng/ml TNF	9544	94	362	4.56
rL929-4F control	9604	104	292	3.96
rL929-4F + 50 ng/ml TNF	9627	96	277	3.73

Results were from the 45th-minute-plot of each treatment in Figure 3.74 - 3.75. The number of cells in R1, R2 and R3 were recorded and % of cell death was obtained according to the following formula:

* % of cell death (%)

= [Number of cells in (R2 + R3) ÷ Number of cells in (R1 + R2 + R3)] x 100 %

From the assay in measuring the release of $O_2\bullet^-$, it was found that challenge of the L929, rL929, rL929-11E and rL929-4F cells for 6 hr with TNF (50 ng/ml) did not increase the rate of $O_2\bullet^-$ release (Figure 3.76). However, addition of 2 μg/ml AMD produced more $O_2\bullet^-$ release in rL929-11E and rL929-4F cells (Figure 3.77c and Figure 3.77d). This might be due to the inhibition of SOD production by AMD and therefore, TNF could potentiate the release of $O_2\bullet^-$. In contrast, addition of AMD did not change the rate of the release of $O_2\bullet^-$ in the TNF resistant line, rL929 cells (Figure 3.77b). In L929 cells, addition of TNF with AMD induced cell death (Figure 3.78a) and therefore, there was no shift in the peak (Figure 3.77a). These results suggest that rL929 cells were the most resistant to TNF action even in the presence of TNF plus AMD. Figure 3.78 shows the PI intensity in L929, rL929, rL929-11E and rL929-4F cells after the treatment with TNF plus AMD that elicited an extent of cell death in L929, rL929-11E and rL929-4F but not in rL929 cells. The release of $O_2\bullet^-$ in L929, rL929-11E and rL929-4F might act on plasma membrane and change the membrane permeability. Therefore, PI diffused into the cells and the PI intensity was high in L929, rL929-11E and rL929-4F cells (Figure 3.78).

3.8.4 Effect of TNF on the Release of Calcium in Resistant Cell Lines

Figure 3.79 shows that addition of 50 ng/ml TNF for 10 hr produced a drastic increase in $[Ca^{2+}]_i$ level in L929 cells while it only caused a small change in rL929 cells. It was found that the population of L929 cells shifted from R1 to R2 whereas no distinct migration of rL929 cells from R1 to R2. Figure 3.80 and Figure 3.81 indicate that application of 50 ng/ml TNF for 10 hr did not produced an increase in $[Ca^{2+}]_i$ level in rL929-11E cells and it caused a little increase in rL929-4F cells. Moreover, there was still

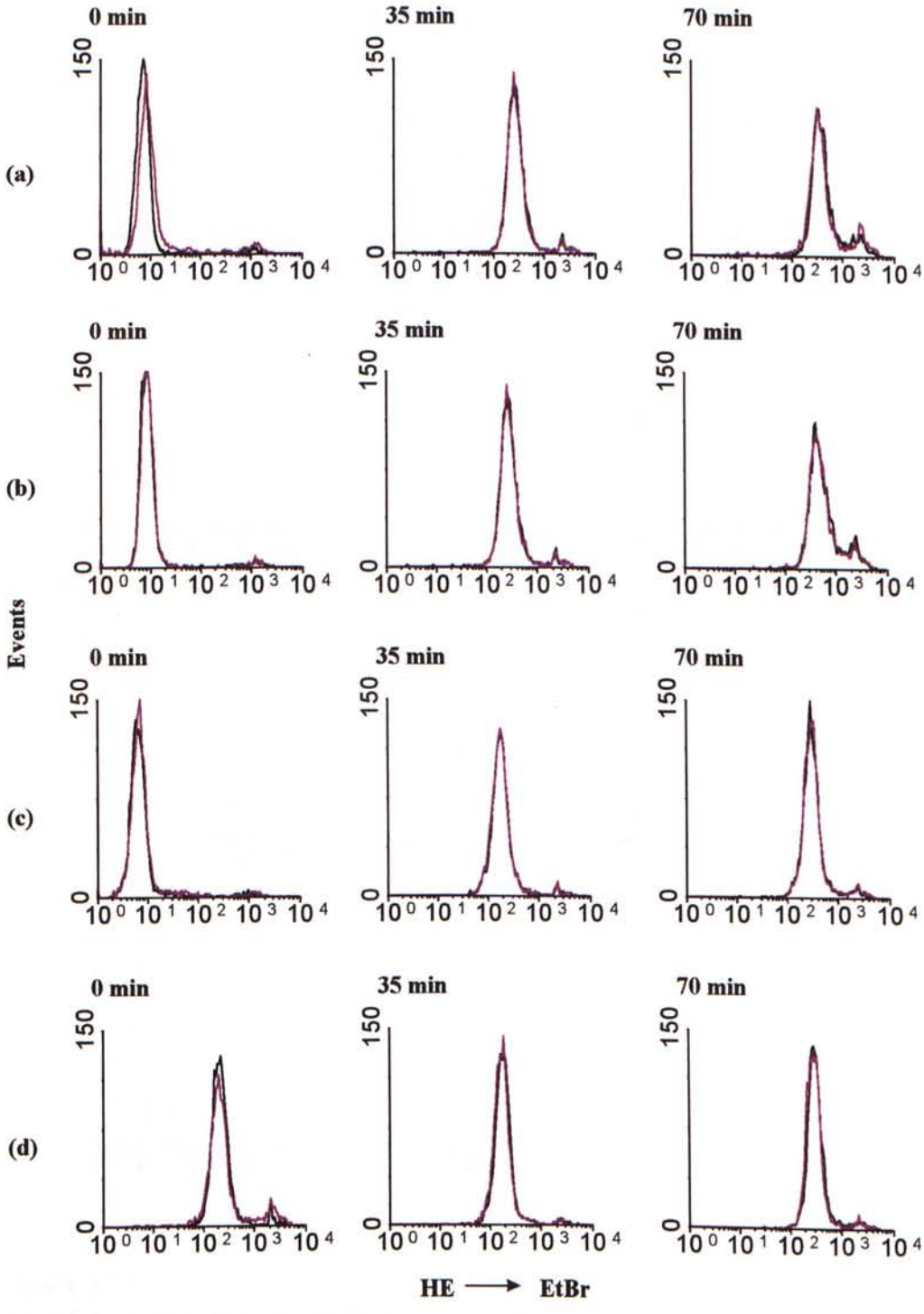

Figure 3.76

Addition of TNF for 6 hr did not produce the release of $O_2\bullet^-$ from L929, rL929, rL929-11E and rL929-4F cells. Application of 50 ng/ml TNF (purple line) for 6 hr in (a) L929 cells, (b) rL929, (c) rL929-11E and (d) rL929-4F did not increase the production of $O_2\bullet^-$ as compared to control (black line). The time on the left indicates the incubation period of cells with DCF.

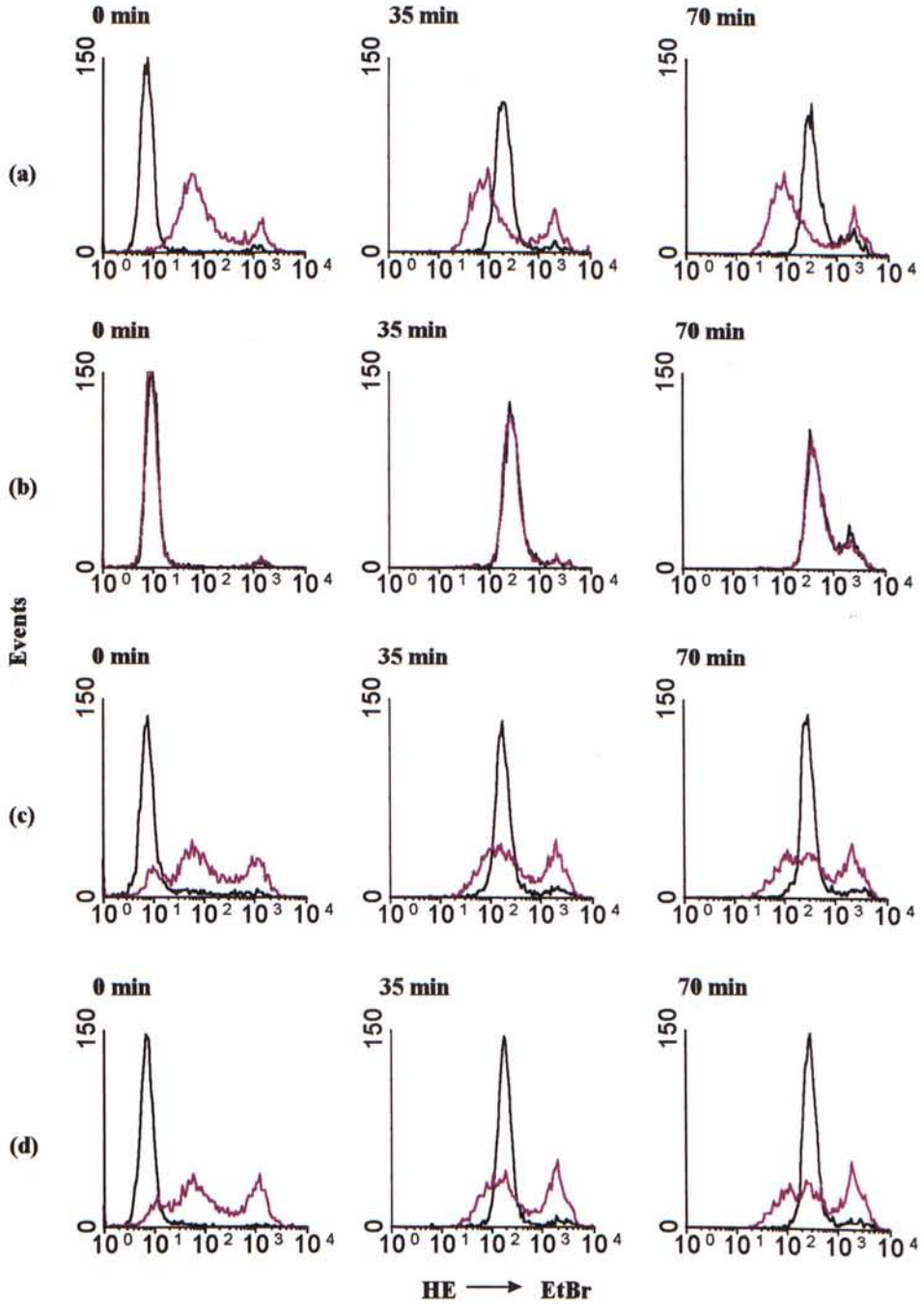

Figure 3.77

Addition of TNF plus AMD for 6 hr produced the release of $O_2\bullet^-$ from L929, rL929-11E and rL929-4F but not in rL929 cells. (a) Application of 50 ng/ml TNF plus AMD (purple line) for 6 hr in L929 cells increased the production of $O_2\bullet^-$ as compared to the control group (AMD only, black line). (b) rL929 cells treated with TNF plus AMD did not produce an increase in the production of $O_2\bullet^-$. Addition of TNF plus AMD with (c) rL929-11E and (d) rL929-4F increased the production of $O_2\bullet^-$. The time on the left indicates the incubation period of cells with DCF.

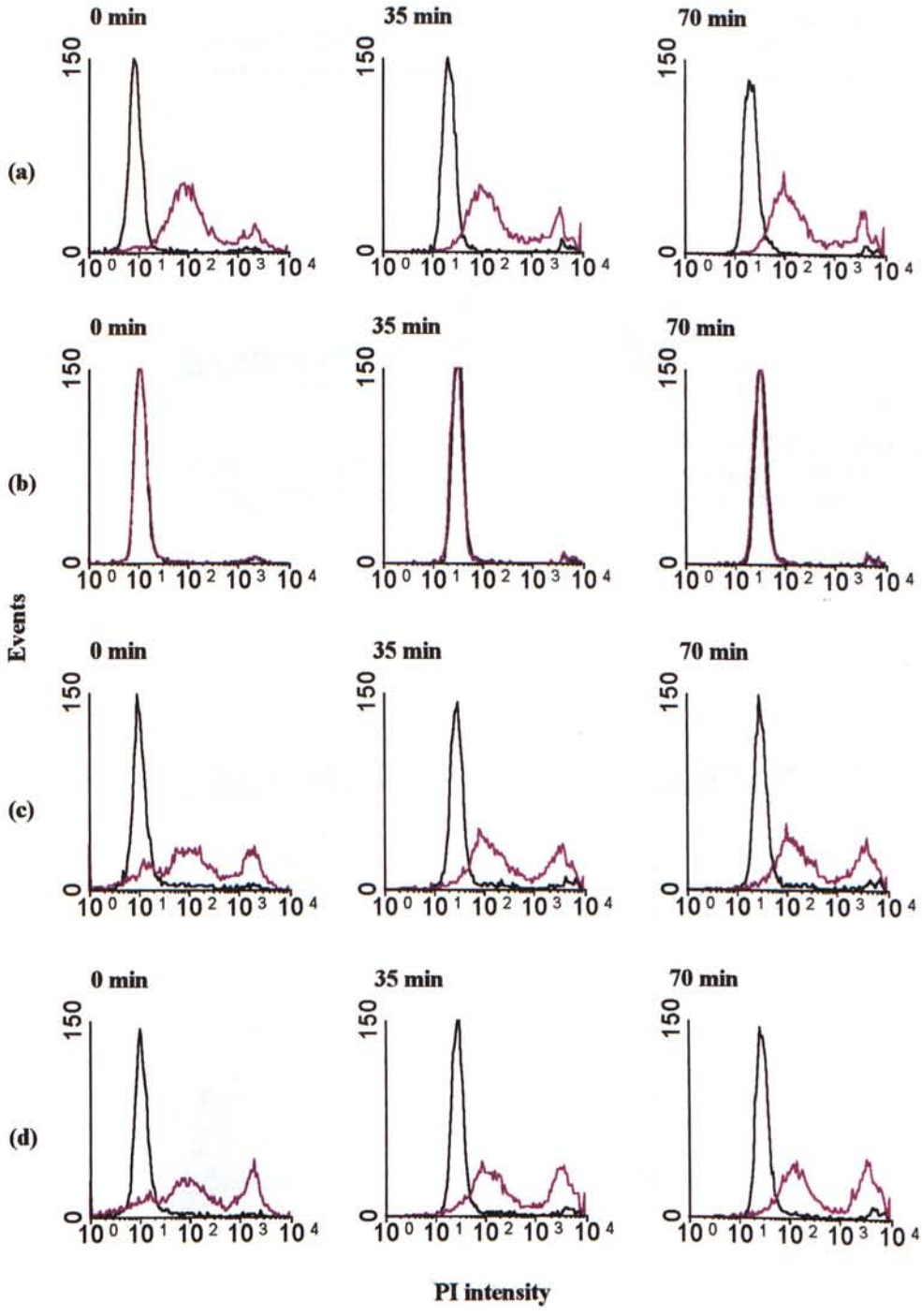

Figure 3.78

Addition of TNF plus AMD for 6 hr induced cell death in L929, rL929-11E and rL929-4F but not in rL929 cells. The results show the PI intensity in (a) L929, (b) rL929, (c) rL929-11E and (d) rL929-4F. It was found that addition of TNF plus AMD (purple line) induced cell death in L929, rL929-11E and rL929-4F cells as compared to their control group (AMD only, black line) but not in rL929 cells. The time on the left indicates the incubation period of cells with DCF.

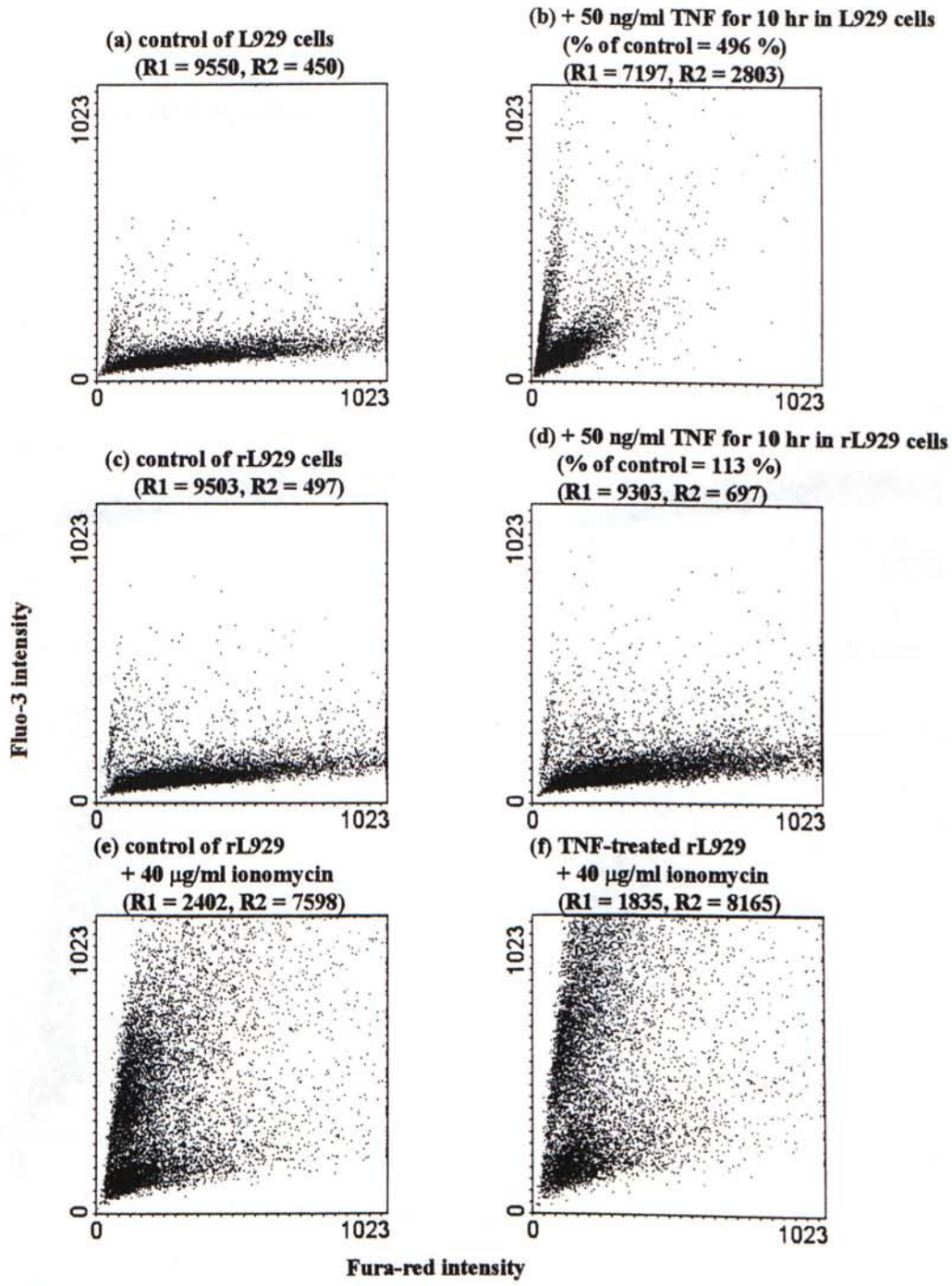

Figure 3.79

Addition of TNF for 10 hr did not produce a significant change in $[Ca^{2+}]_i$ level in rL929. (a) It shows the control group of L929 cells. (b) L929 cells were incubated with 50 ng/ml TNF for 10 hr. It shows that there was a drastic change in $[Ca^{2+}]_i$ level as compared to control group. (c) It shows the control of rL929 cells. (d) rL929 cells were treated with 50 ng/ml TNF for 10 hr did not produce a drastic change in $[Ca^{2+}]_i$ level. (e) and (f) show that addition of 40 μg/ml ionomycin (10 min before measurement) induce the release of Ca^{2+} in control and TNF-treated rL929 cells.

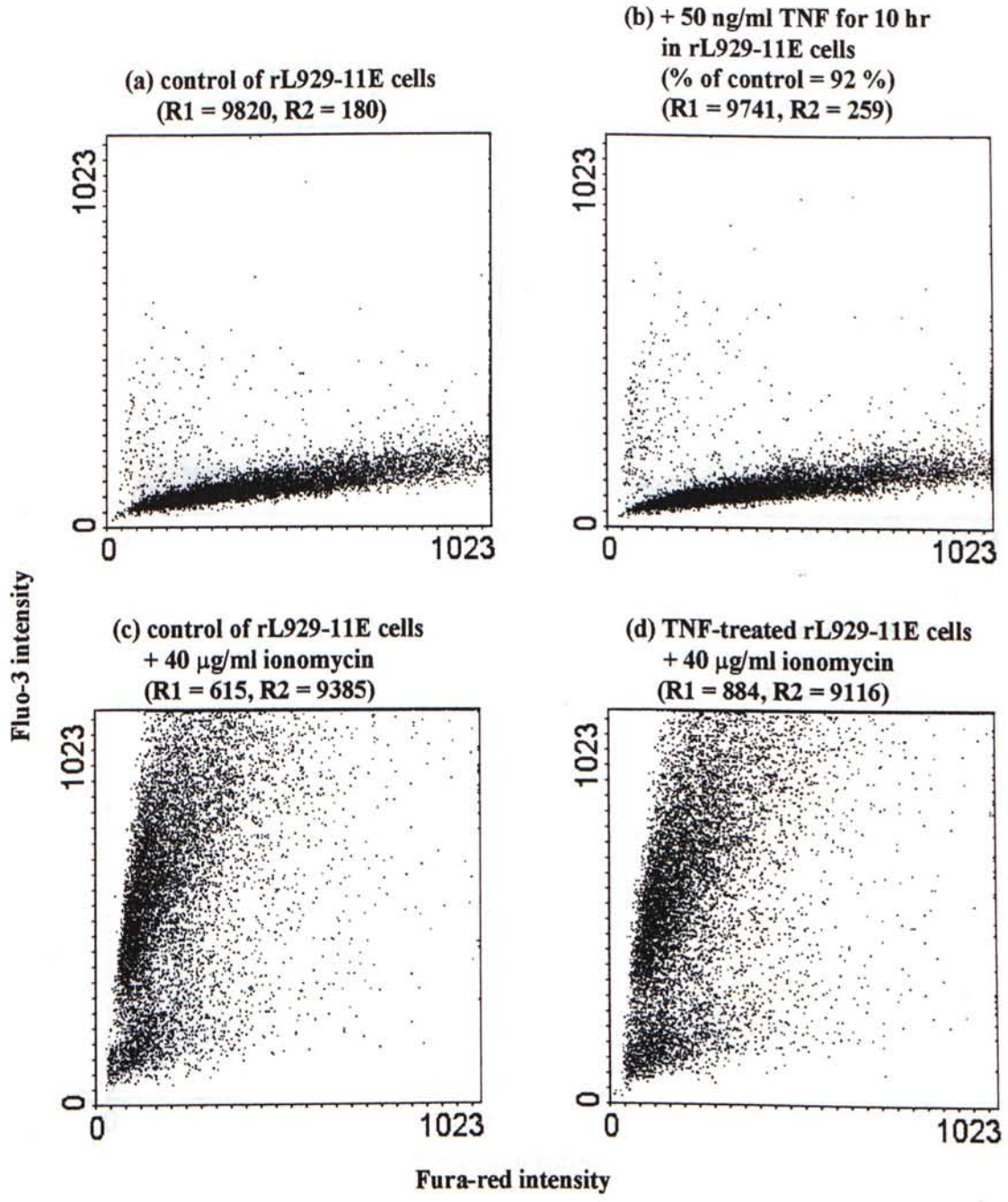

Figure 3.80
Addition of TNF for 10 hr did not cause a significant change in $[Ca^{2+}]_i$ level in rL929-11E. (a) It shows the control group of rL929-11E cells. (b) rL929-11E cells were incubated with 50 ng/ml TNF for 10 hr. It shows that there was no change in $[Ca^{2+}]_i$ level as compared to control group. (c) and (d) show that addition of 40 μg/ml ionomycin (10 min before measurement) induce the release of Ca^{2+} in control and TNF-treated rL929-11E cells.

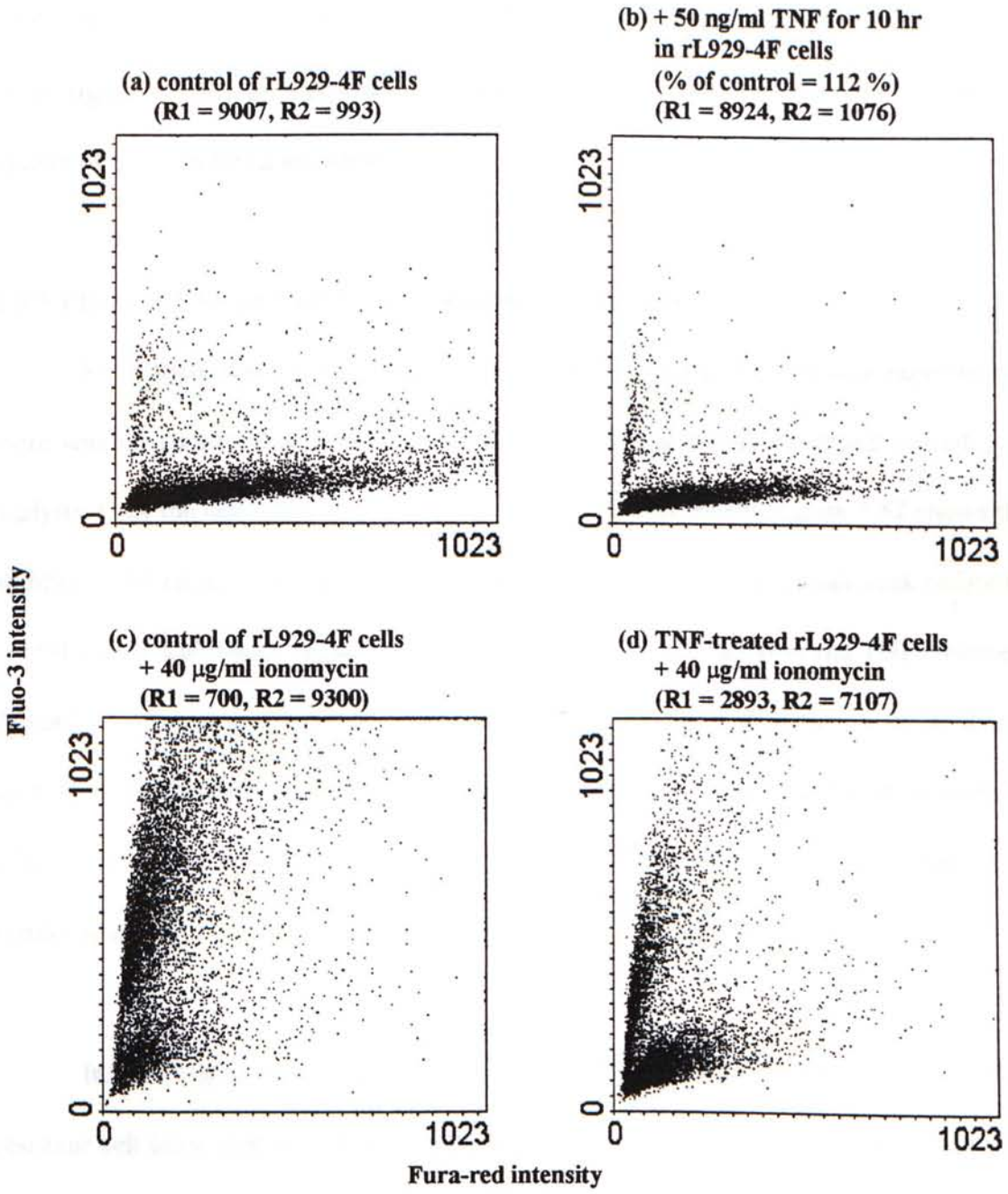

Figure 3.81

Addition of TNF for 10 hr did not cause a significant change in $[Ca^{2+}]_i$ level in rL929-4F. (a) It shows the control group of rL929-4F cells. (b) rL929-4F cells were incubated with 50 ng/ml TNF for 10 hr. It shows that there a small change in $[Ca^{2+}]_i$ level as compared to control group. (c) and (d) show that addition of 40 μg/ml ionomycin (10 min before measurement) induce the release of Ca^{2+} in the control and TNF-treated rL929-4F cells.

no distinct shifting of population of rL929-11E or rL929-4F cells from R1 to R2. Addition of 40 μg/ml ionomycin was used to confirm that there was no impairment in the Ca^{2+} system of the cells being investigated.

3.8.5 Effect of TNF on Cell Cycle in Resistant Cell Lines

Since there was no increase in the release of ROS and Ca^{2+}, it was expected that there was no apoptosis in TNF-treated resistant cells and it was examined by cell cycle analysis. Only the cell cycle of resistant cell line rL929 was shown. Figure 3.82 shows that addition of 50 ng/ml TNF with rL929 cells for 10 hr did not induce a small peak before the G0/G1 phase. This result implied that there was no apoptotic cell after the TNF treatment. Actually, by the observation, there was no non-adherent cells after the 10 hr incubation with TNF. Furthermore, in the presence of serum, it induced more accumulation of rL929 cells in the S phase as compared with the serum-free condition, that was similar to the results in section 3.2.2.

In conclusion, the differences between TNF-sensitive cell line L929 and TNF-resistant cell lines, rL929, rL929-11E and rL929-4F were (1) TNF increased cytotoxicity in sensitive cell line but not in resistant cell lines; (2) TNF increased the release of ROS and Ca^{2+} in sensitive cell line whereas there was no response in resistant cell lines; (3) TNF plus AMD produced more $O_2\bullet^-$ release and cell death in L929, rL929-11E and rL929-4F but not in rL929 cells; (4) TNF induced apoptosis in L929 cells but not in rL929 by cell cycle analysis.

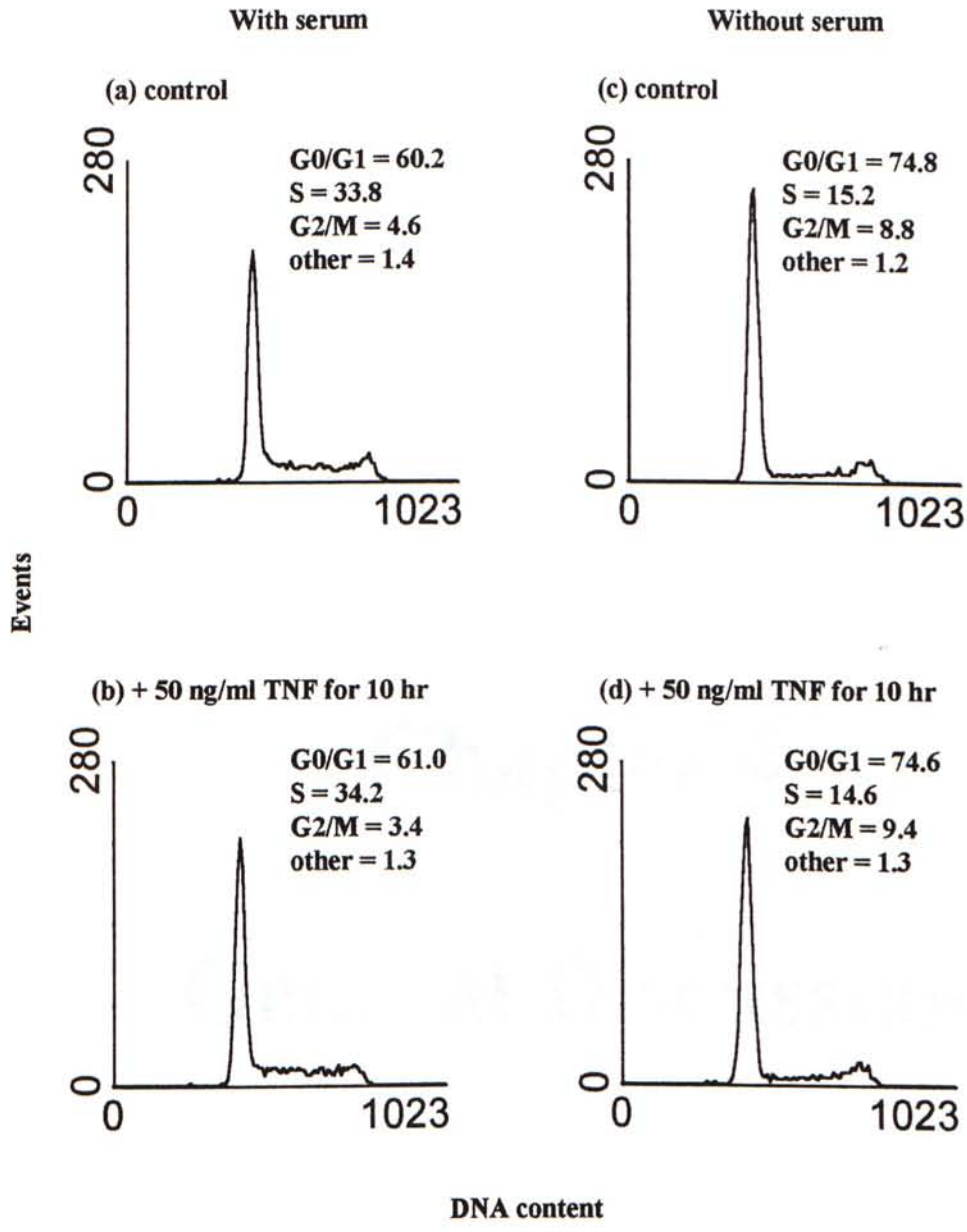

Figure 3.82
DNA histograms of TNF-treated rL929 cells in the presence and absence of serum. (a) rL929 cells were treated with complete RPMI. (b) rL929 cells were treated with complete RPMI plus 50 ng/ml TNF for 10 hr. (c) In addition, rL929 cells were treated with serum-free RPMI. (d) rL929 cells were treated with serum-free RPMI plus 50 ng/ml TNF for 10 hr.

Chapter 4

General Discussion

Chapter 4. General Discussion

Several biochemical pathways have been suggested for the cell death. These include the activation of proteases and phospholipases (Orrenius *et al.*, 1989), the generation of ROS (Tsujimoto *et al.*, 1986), and/or the degradation of DNA (Jones *et al.*, 1989). However, the exact mechanism of TNF cytotoxicity is still largely unknown.

4.1 Tumor Necrosis Factor Induced Apoptosis in L929 Cells

TNF can induce both apopotic and necrotic forms of cell lysis (Laster *et al.*, 1988). Our study showed that rMuTNF-α induced DNA fragmentation in murine fibroblast cell line L929 (Figure 3.4). It was found that addition of TNF (50 ng/ml) for 3 hr did not induce cell death whereas in the 6- or 10-hr incubation, some of them become DNA fragmented cells. These results strongly indicate that TNF caused apoptosis in L929 cells, although necrosis was found in the same cell line after incubation with TNF in other laboratories (Vercammen *et al.*, 1997; Grooteen *et al.*, 1993). Our conclusion that TNF elicits apoptosis in L929 cells was further confirmed by the analysis of cell cycle (Figure 3.6). It was found that in the 10-hr TNF treatment, a small peak occurred before the G0/G1 phase (Figure 3.6e). This hypodiploid peak was the cells with fragmented DNA. Moreover, these apoptotic activities arose as a rather late event after the addition of TNF to L929 cells further indicate the requirement of time to initiate the apoptotic pathway.

After TNF treatment, two types of cells were found, the adherent cells attached to the bottom of plate, and the non-adherent cells. Our results show that the non-adherent cells were mainly the DNA fragmented cells whereas the adherent cells were viable cells even they were treated with TNF for 10 hr. These observations can be found in the agarose gel electrophoresis (Figure 3.4) and the flow cytometric assay (Figure 3.7). At present, we do not know the role of matrix adherence on the TNF-mediated cytotoxicity. However, recent reports indicate that surface adherence is an important factor to keep cell survival and the disruption of extracellular matrix results in apoptosis (Chen *et al.*, 1998).

4.2 Tumor Necrosis Factor Increased the Release of Reactive Oxygen Species in L929 Cells

Our study showed that treatment of L929 cells with TNF produced an increase in the level of intracellular ROS. ROS is produced continuously inside the cells in respiring cells. However, about 1 - 3 % of electrons leak out from the inner mitochondrial membrane and react with molecular oxygen directly to form ROS (Figure 1.5). In the experiment of flow cytometry, TNF increased the release of H_2O_2 and was in a time dependent manner (Figure 3.14). For a short time course such as 15-min or 3-hr incubation of L929 cells with TNF (50 ng/ml), the rate of H_2O_2 production did not increase as compared to control group in the flow cytometry study (Figure 3.12). However, the incubation of L929 cells with TNF for a longer time (e.g. 6 or 10 hr) produced a significant increase in the rate of H_2O_2 release (Figure 3.13). This indicates that TNF produced a slow rise in the H_2O_2 level.

On the other hand, addition of TNF (50 ng/ml) for 15 min, 3 or 6 hr did not cause an increase in the rate of $O_2\bullet^-$ release (Figure 3.15a - c). For the 10-hr incubation, there was only a small increase in the rate of $O_2\bullet^-$ release (Figure 3.15d). Addition of metabolic inhibitor, AMD, with TNF for 15 min did not cause more $O_2\bullet^-$ production in L929 cells (Figure 3.16). However, incubation of TNF with AMD for 3 or 6 hr produced more intracellular $O_2\bullet^-$ production (Figure 3.17).

It is interesting to note in the experiments of CLSM that incubation of cells with TNF (50 ng/ml) for 15 min could increase the rate of intracellular H_2O_2 production as compared to control (Figure 3.9) whereas in that of FCM, no such increase was observed at 15 min. However, the production of H_2O_2 was found when cells were incubated with TNF for 6 and 10 hr. These discrepancies in responses may be due to the difference in the number of cells in the assay. Therefore, application of the same concentration of TNF may exert a greater effect on the cells in CLSM. In fact, when cells were treated with a high dose of TNF (500 ng/ml) for 3 hr, Ca^{2+} rise was observed (Figure 3.43c) and no such effect was found when cells were challenged with a lower dose of TNF (50 ng/ml) (Figure 3.43b). Moreover, similar results were obtained in the case of detection of $O_2\bullet^-$. In the assay from CLSM, incubation of TNF for 15 min could increase the rate of $O_2\bullet^-$ production but not in the FCM assay.

As indicated in Figure 1.5, $O_2\bullet^-$ is converted into H_2O_2 by MnSOD inside mitochondria. It was shown previously that TNF induced the production of MnSOD mRNA in all cell lines (Wong and Goeddel, 1988). Wong and Goeddel (1988) further

indicated that one hr of TNF treatment was sufficient to induce substantial level of transcript of MnSOD that remained high for 24 hr. This explains why addition of TNF did not increase the release of $O_2\bullet^-$ in the 3- or 6- hr TNF treatment in the FCM assay. In this connection, AMD, a transcriptase blocker (Ostrove and Gifford, 1979) was found to block the expression of MnSOD mRNA (Wong and Goeddel, 1988). Therefore, addition of TNF with AMD should produce more $O_2\bullet^-$ release. In fact, our results have indicated this point and our results thus illustrated that release of ROS is one of the mechanisms of TNF-mediated cytotoxicity.

The effect of antioxidants on TNF-mediated cytotoxicity was investigated in this study. It was found that antioxidants such as catalase, MnSOD, NAc and 4-OH-TEMPO reduced TNF-mediated cytotoxicity (Figure 3.19 - Figure 3.22). Both catalase and MnSOD are not cell-permeable (Mitchell *et al.*, 1990). The reduction of cytotoxicity is probably due to an extracellular removal of H_2O_2 and $O_2\bullet^-$ by catalase and MnSOD, respectively, from the culture medium that promotes the efflux of H_2O_2 and $O_2\bullet^-$ from the cellular cytoplasm to the external environment. When NAc was added to TNF-treated cells, a marked reduction in cytotoxicity was observed. Since the actions of NAc involve the replenishment of GSH stores, scavenging ROS and prevention of mitochondrial membrane depolarization (Cossarizza et al., 1995), it is very possible that NAc removes the ROS thereby reducing the TNF-mediated cytotoxicity. Antioxidant 4-OH-TEMPO also produced a lower TNF-mediated cytotoxicity. A likely sequence of reactions (1 - 4) shown below explains the possible protective effect of 4-OH-TEMPO on the TNF elicited ROS (Mitchell *et al.*, 1991).

$$H_2O_2 + Fe^{2+} \rightarrow OH\bullet + OH^- + Fe^{3+} \quad (1)$$

$$Fe^{3+} + O_2\bullet^- \rightarrow Fe^{2+} + O_2 \quad (2)$$

$$O_2\bullet^- + \text{>N—O}\bullet \xrightarrow{H^+} O_2 + \text{>N—OH} \quad (3)$$

$$\text{>N—OH} + O_2\bullet^- \xrightarrow{H^+} H_2O_2 + \text{>N—O}\bullet \quad (4)$$

The first two reactions are the Haber-Weiss reaction for the iron-catalyzed production of OH•. $O_2\bullet^-$ acts to recycle the iron from Fe^{3+} to Fe^{2+} and it is therefore critical to the production of the OH•. In reactions (3) and (4), $O_2\bullet^-$ is converted to H_2O_2 and O_2 by the catalytic reaction with 4-OH-TEMPO.

The first oxygen reduction product generated in mitochondria under both physiological and pathological conditions appears to be the $O_2\bullet^-$, which can subsequently be converted into H_2O_2 (Figure 1.5). Dismutation of $O_2\bullet^-$ and H_2O_2 can result in the production of the OH•. Conversion of $O_2\bullet^-$ and H_2O_2 into OH• is catalyzed by transition metals such as iron ions in the Haber-Weiss reaction (Dawson and Dawson, 1996). Oxygen radicals escaping detoxifying enzymes are capable of inducing various damage. Attack by radicals can result in lipid peroxidation and DNA degradation. Results from our study indicate that ROS induced membrane lesion and therefore, the influx of PI into the cells was observed (Figure 3.57).

Inhibition of mitochondrial electron transport at specific sites can differentially interfere with TNF-mediated cytotoxicity. Inhibition of the electron transport at complex I

with rotenone or at complex II with TTFA significantly protected the cells against TNF (Figure 3.24 and Figure 3.25). On the other hand, inhibition of the electron transport at the site behind the ubiquinone region with antimycin A potentiated TNF cytotoxicity (Figure 3.26). These results suggest that oxidative events generated in mitochondria are crucial in TNF-mediated cytotoxicity. The enhancement of TNF cytotoxicity with antimycin A and the inhibition with rotenone and TTFA, strongly indicate that TNF activates radical production in mitochondria at the ubiquinone site. However, it remains unclear from our results in what way TNF affects the mitochondrial electron transport. Similar results were obtained from Schulze-Osthoff *et al.* (Schulze-Osthoff *et al.*, 1992). However, O'Donnell *et al.* (1995) demonstrated in rMuTNF-treated L929 cells that mitochondrial-derived radicals or respiratory chain did not involve in the lytic pathway. They even show that significant ROS generation was not observed in TNF-treated L929 cells using other assays such as DCF assay for H_2O_2 in a 96-well plate measured by Cytofluor 2300 plate reader and cytochrome c reduction assay. On the other hand, they suggest a central role of lipoxygenase in the TNF-mediated cell lysis. The differences between our data and theirs were that in their DCF assay, they treated the cells with 250 pg/ml TNF and incubated for about 140 min only. The low concentration of TNF and short incubation time may not increase the release of H_2O_2 in L929 cells. On the other hand, they did not show the result of cytochrome c reduction assay and therefore, we cannot compare our results with theirs.

Furthermore, addition of the protonophorous uncoupler DNP allows electron transport in mitochondria to occur but prevents the phosphorylation of ADP to ATP and

therefore, the supply of energy was limited. Depletion of intracellular ATP blocked apoptosis since apoptosis is ATP-dependent (review: Nicotera and Leist, 1997). Therefore, addition of uncoupler DNP may block apoptosis and reduced TNF-mediated cytotoxicity (Figure 3.31). However, Schulze-Osthoff *et al.* (1992) found that DNP did not exert effect on TNF-elicited cytotoxicity. Moreover, they demonstrated that oligomycin, which directly blocks the ATP synthesis by inhibiting the F_1-ATPase subunit, did not influence the activity of TNF on L929 cells. These imply that ATP did not involve in the TNF-mediated cell death.

4.3 Tumor Necrosis Factor Increased the Release of Calcium in L929 Cells

In this study, we also found that TNF caused a slow rise in $[Ca^{2+}]_i$. In the experiment of FCM, it was found that application of TNF (50 ng/ml) for 3 hr did not change $[Ca^{2+}]_i$ in L929 cells (Figure 3.40). Contrary to these observations, data from CLSM shows a faster (30 min after TNF application) release of $[Ca^{2+}]_i$ (Figure 3.38). Again, the number of cells in the assay may account for this discrepancy. In fact, application of higher dose of TNF (500 ng/ml) for 3 hr in the assay from FCM did produce a small increase in the level of $[Ca^{2+}]_i$ (Figure 3.43). However, in the 6- or 10-hr incubation of L929 cells with TNF, a significant increase in the $[Ca^{2+}]_i$ was visualized (Figure 3.41 and Figure 3.42). Therefore, TNF caused a slow release of Ca^{2+}. Similar conclusion was obtained in BT-20 cells (Bellomo *et al.*, 1992) and glial cells (Koller *et al.*,

1996) after TNF treatment. In contrast, TNF causes a rapid release of $[Ca^{2+}]_i$ in human neutrophils (Schumann *et al.*, 1993).

It seems that in L929 cells, the release of Ca^{2+} is not due to the IP_3 system. Stored Ca^{2+} within intracellular pools is released to the cytotsol when IP_3 binds to its receptor. When embedded in a lipid membrane, the IP_3 receptor responds like a conventional channel, displaying an increase in open frequency in response to IP_3. The mean open time was less than 10 msec (review: Berridge, 1993). Since TNF caused a slow rise in Ca^{2+}, we concluded that the release of Ca^{2+} in TNF-treated L929 cells was not due to the transient activation of IP_3 system.

Since Ca^{2+} cannot be generated or degraded, the level of Ca^{2+} is tightly regulated (Figure 1.6). However, the site of TNF-mediated Ca^{2+} release is still poorly understood. The data from the study with Ca^{2+}-free buffer suggests that the source of Ca^{2+} released by TNF should be intracellular. Our results further indicate that the Ca^{2+} may come from mitochondria since addition of ruthenium red or diltiazem reduced the TNF-mediated Ca^{2+} release (Figure 3.61) and at the same time, cells were viable. As mitochondrial Ca^{2+}-cyclings can be inhibited by ruthenium red and diltiazem, it is possible that ruthenium red prevents mitochondrial Ca^{2+} uptake by inhibiting mitochondrial Ca^{2+} uniporter (Chacon and Acosta, 1991; Faulk *et al.*, 1995) and diltiazem prevents the release of Ca^{2+} from mitochondria by inhibiting Na^+-dependent and H^+-dependent pathways (Rizzuto *et al.*, 1987). It implies that prevention of Ca^{2+} cycling in mitochondria inhibited the rise of $[Ca^{2+}]_i$ and therefore reduced TNF-mediated cytotoxicity (Figure 3.59 and Figure 3.60).

Another line of evidence shows that addition of Ca^{2+}-inducing agent such as thimerosal produced a higher TNF-mediated cell death (Figure 3.45). Thimerosal has been shown to increase the cytosolic [Ca^{2+}] (Michelangeli *et al.*, 1995) by sensitizing IP_3 receptors. On the other hand, application of Ca^{2+}-chelator BAPTA/AM reduced the TNF-mediated cytotoxicity (Figure 3.46).

These results suggest that an elevation of $[Ca^{2+}]_i$ level, that may come from mitochondria or ER, may induce TNF-mediated cell death. It has long been demonstrated that sustained increase in the $[Ca^{2+}]_i$ induces the activation of Ca^{2+}-dependent proteases, phospholipases and endonucleases (review: Orrenius *et al.*, 1989). All these enzymes induce cell death. The major target for proteases are the cytoskeletal proteins such as α-actinin and actin-binding protein. A stimulation of intracellular proteolysis and the appearance of plasma membrane blebs (Nicotera *et al.*, 1986) is one of the characteristics of apoptosis. PLA_2 catalyzes the hydrolysis of membrane phospholipids that requires Ca^{2+} for activation, which could cause cell damage (Chien *et al.*, 1979). Ca^{2+} activates endonucleases that cleaves cell chromatin into oligonucleosomal fragments. Accumulation of [Ca^{2+}] induced DNA fragmentation in rat liver nuclei (Jones *et al.*, 1989). Since there were some DNA fragments observed in L929 cells 6 or 10 hr after the addition of TNF and the $[Ca^{2+}]_i$ was very high at that time, it is very possible that Ca^{2+} played a role in the TNF-mediated cytotoxicity. With the use of BAPTA/AM, a Ca^{2+} chelator, the TNF-meidated cytotoxicity was really reduced.

Apart from the release of Ca^{2+} from intracellular store, Ca^{2+} may entry from the extracellular environment. Ca^{2+} entry into cells can be regulated by a number of mechanisms, for example through channels operated by voltage or by receptors (review: Berridge, 1993). In L929 cells, TNF was able to open Ca^{2+} channels on the cell surface (Kong *et al.*, 1997). Our results also indicate that in the absence of external Ca^{2+}, the release of intracellular Ca^{2+} still occurred in TNF-treated L929 cells.

4.4 Calcium Induced Reactive Oxygen Species Release in TNF-Treated L929 Cells

A sustained level of ROS and/or Ca^{2+} can induce cell death. Our study indicates that TNF increased both ROS and Ca^{2+} release in L929 cells but their relationship is still unknown. It was found that H_2O_2 did not induce Ca^{2+} release (Figure 3.50 and Figure 3.51). On the other hand, in the assay from FCM, application of Ca^{2+}-chelator BAPTA/AM reduced the rate of TNF-mediated H_2O_2 release (Figure 3.48). A reduction in cell death in the 10-hr incubation with TNF was also observed (Figure 3.57). Moreover, addition of diltiazem, that prevents the release of Ca^{2+} from mitochondria, reduced the rate of H_2O_2 release in TNF-treated cells (Figure 3.66). In the assay from CLSM, application of ruthenium red reduced the rate of both H_2O_2 and $O_2\bullet^-$ release too (Figure 3.62 and Figure 3.64). Therefore, TNF-mediated ROS production requires mitochondrial Ca^{2+} cycling because they are suppressed by the omission of Ca^{2+} in the presence of ruthenium red and diltiazem. These observations imply that TNF may cause the release of Ca^{2+} from

mitochondria firstly and then somehow induces the release of ROS. Our findings provide evidence for the correlation between the elevation of $[Ca^{2+}]_i$ and the formation of ROS in response to TNF. Both elevation of $[Ca^{2+}]_i$ and ROS have been shown to be messengers in the initiation of process such as apoptosis. Several findings indicate that disruption in Ca^{2+} homeostasis may be involved in the release of ROS (Goldman *et al.*, 1998; Chacon and Acosta, 1991; Malis and Bonventre, 1986). Chacon and Acosta (1991) suggested that in doxorubicin-treated myocardial cells, Ca^{2+} fluxes through the mitochondrial membrane may be linked to the formation of ROS which results in the permeabilization of the membrane of a Ca^{2+}-induced permeabilization which then allows the release of $O_2\bullet^-$ to the cytosolic side of the membrane. In contrast, Richter (1993) suggested that pro-oxidants induce Ca^{2+} release from mitochondria, which may be followed by Ca^{2+} cycling, collapse of $\Delta\Psi_m$, and ATP depletion. Under these conditions the cellular Ca^{2+} homeostasis cannot be maintained, the cytosolic Ca^{2+} level rises, and cells go into apoptosis. Moreover, recent study found that TNF-mediated ROS release may relate to ceramide (Garcia-Ruiz *et al.*, 1997). The enzyme PC-PLC appears to be involved in the activation of acidic SMase through 1,2-DAG. This enzyme generates a functional distinct pool of ceramide, that acts on mitochondria, enhancing the production of ROS (review: Fernandez-Checa *et al.*, 1997) and therefore, induces apoptosis (Hartfield *et al.*, 1997).

4.5 Tumor Necrosis Factor Did Not Change the pH and Mitochondrial Membrane Potential in TNF-Treated L929 Cells

A decrease in cytosolic pH on the order of 0.2 - 0.3 pH unit may lead to apoptosis by endonuclease activation (Barry and Eastman, 1992). In this study, it was found that TNF did not change the pH in L929 cells immediately after the addition of TNF to cells (Figure 3.67). In addition, collapse of $\Delta\Psi_m$ induces Ca^{2+} release from mitochondria (review: Vercesi, 1993). However, our study shows that TNF did not change the $\Delta\Psi_m$ in the 6- and 10-hr assay (Table 3.4). This implies that in L929 cells, TNF-mediated Ca^{2+} release from mitochondria is independent on the collapse of $\Delta\Psi_m$. However, recent finding indicates that L929 cells treated with TNF and AMD resulted in the loss of 80 % of rhodamine 123 fluorescence within 6 hr (Pastorino *et al.*, 1996). As mentioned before, AMD inhibits the expression of MnSOD and therefore, increases the release of $O_2\bullet^-$, that may cause damage on mitochondrial membrane in TNF-treated cells. In our experiments, L929 cells were treated with TNF alone. Therefore, the discrepancy between our result and theirs may be due to the additive effect of AMD on the TNF-induced change of $\Delta\Psi_m$. Another finding in human hepatoma-derived HuH-7 cells indicates that geranylgeranoic acid induced a rapid loss of the mitochondrial inner membrane potential that finally led to apoptosis (Shidoji *et al.*, 1997). It seems that dysfunction of $\Delta\Psi_m$ is one of the most likely candidates to induce apoptosis. Moreover, using the lipophilic dye JC-1 to determine $\Delta\Psi_m$, Polla *et al.* (1996) showed that TNF induces time-dependent alterations in $\Delta\Psi_m$ in L929 cells.

Figure 4.1 shows the proposed mechanism of TNF-mediated cytotoxicity in L929 cells. At first, TNF binds to TNFR1 and stimulates the unknown messenger(s) in the cytosol. The unknown messenger(s) then stimulates the Ca^{2+} release from mitochondria. In consequence, the level of $[Ca^{2+}]_i$ increases. The increase in the $[Ca^{2+}]_i$ level induces more ROS release from mitochondria and the site of action may be on the ubiquinone site (complex III). It is still unknown how the cytoplasmic or mitochondrial Ca^{2+} acts on electron transport chain. The release of ROS can be prevented by the application of BAPTA/AM, ruthenium red, diltiazem, MnSOD, catalase, NAc or 4-OH-TEMPO. In contrast, applicaction of AMD enhances the release of $O_2\bullet^-$ by inhibiting the MnSOD expression. This causes an increase in the level of intracellular ROS. A sustained increase in $[Ca^{2+}]_i$ level induces the activation of proteases, phospholipases or endonucleases that leads to cell death. On the other hand, an increase in intracelllular ROS leads to lipid peroxidation and base damage on DNA or RNA (Park *et al.*, 1998; Wiseman and Halliwell, 1996), that results in cell death also. This model is based on the findings from this project. Of course, TNF may utilize some other signal molecules to execute its cytotoxicity in L929 cells. In fact, the use of blockers, or inhibitors to block the Ca^{2+} and/or ROS activity could not totally eliminate the killing effect of TNF. These suggest that some other biochemical pathways may involve in the TNF-mediated cytotoxicity.

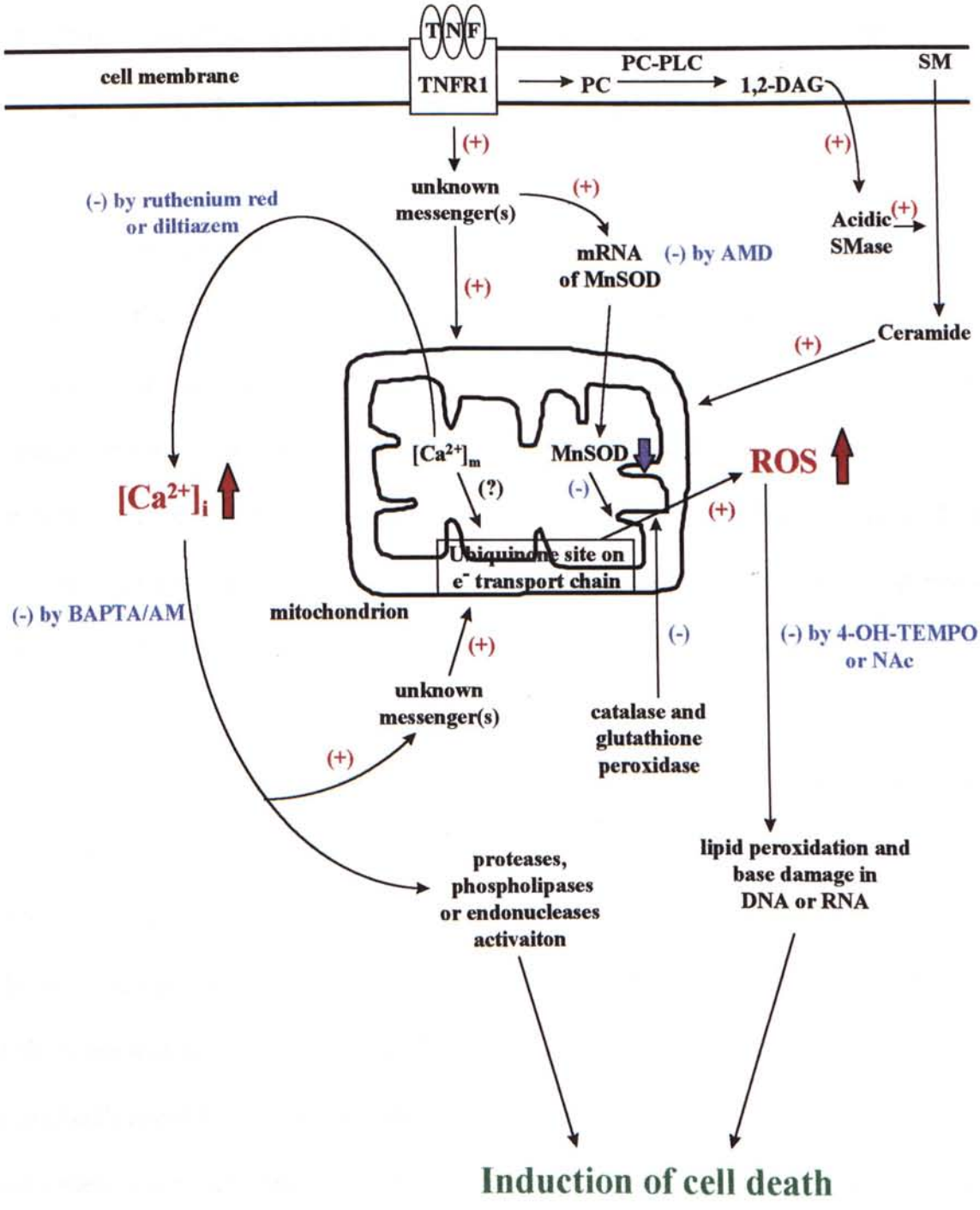

Figure 4.1
A proposed model for TNF-mediated cell death in L929 cells. Note that TNF increased the release of both Ca^{2+} and ROS that eventually lead to cell death.

4.6 Tumor Necrosis Factor Did Not Increase the Release of Reactive Oxygen Species or Calcium in Resistant Cell Lines

TNF resistant cell lines such as rL929, rL929-11E and rL929-4F gave an inert response to TNF cytotoxicity. To produce resistant L929 cells, parental L929 cells were subcultured in the presence of TNF (20 units/ml). The cells were maintained in this medium for two weeks with a change of fresh medium every 3 days. Dead cells were washed away and living cells were allowed to grow to confluence again. TNF concentration was then increased to 50, 100, 200, 1000, and 2000 units/ml in a stepwise manner. Finally, three cell clones, rL929, rL929-11E and rL929-4F, were isolated.

Someone may wonder that the absence of TNFR1 in resistant cell lines may make them resistant to TNF action. Although the expression of TNFR1 in rL929-11E and rL929-4F was not identified, Kwan found that the expression of TNFR1 in rL929 cells is the same as parental cell line (Kwan, 1995). Therefore, the characteristic of resistant to TNF is not due to the absence of TNFR1. Moreover, Kwan found that TNF resistant of rL929 cells is not due to a higher capacity of the cell to scavenge ROS generated by TNF since there was no difference between the expression of rescue genes (such as glutathione reductase) in L929 and rL929 cells. The actual mechanism is currently unknown and may be due to a lack of the ability of rL929 cells to generate ROS.

Cell cycle analysis indicates that there was no DNA fragmentation in the 10-hr TNF treatment in rL929 cell (Figure 3.82). Moreover, the 6 hr treatment of all resistant

cell lines with TNF (50 ng/ml) did not cause a higher rate in the release of H_2O_2 as compared to the parental cell line (Figure 3.73b - d). However, when rL929-11E and rL929-4F were treated with TNF with AMD, more $O_2\bullet^-$ release was observed whereas no response was found in rL929 cells (Figure 3.77b - d). These results suggest that rL929 cells were the most resistant line to TNF action. Moreover, addition of TNF for 10 hr did not cause the release of Ca^{2+} in rL929 and rL929-11E cells, whereas there was a small increase in rL929-4F cells (Figure 3.80 and Figure 3.81). Since there was no sustained increase in $[Ca^{2+}]_i$ and ROS in the resistant cell lines, TNF did not produce cytotoxicity in these cell lines (Figure 3.70 - Figure 3.72). According to our proposed model, TNF should not increase the release of ROS without the rise of $[Ca^{2+}]_i$. To our surprise, TNF, together with AMD, produced more $O_2\bullet^-$ release in rL929-11E and rL929-4F but not accompanied with a significant increase in $[Ca^{2+}]_i$. These imply that the rise of $[Ca^{2+}]_i$ is not the only inducer to produce ROS. Therefore, the cytotoxic mechanism mediated by TNF in resistent L929 cells remains to be elucidated.

Chapter 5

Future Perspective

Chapter 5. Future Perspective

This study found that TNF increased the release of Ca^{2+} and ROS from mitochondria thus induced cell death. However, the connection among TNF-TNFR1 complex, mitochondria and $[Ca^{2+}]_i$ is still unknown. Further information about their relationship should be investigated. Moreover, the mechanism of resistant cell lines on TNF is still unknown. To decode this unknown mechanism of resistant cell lines may be one of the best ways to understand why some tumor cell lines are resistant to TNF. Actually, to study the mechanisms of TNF-mediated cell death is virtually unlimited and is under exploration by several groups of research.

5.1 The Relationship Between Tumor Necrosis Factor and Cytochrome c

Recently, it was found that the migration of cytochrome c from mitochondria to cytosol may involve in cell apoptosis (Yang *et al.*, 1997; Kluck *et al.*, 1997). Cytochrome c is localized on the outer surface of the inner mitochondrial membrane (review: Skulachev, 1998). Cells undergoing apoptosis were found to have an elevation of cytochrome c in the cytosol and a corresponding decrease in the mitochondria. It is interesting to investigate whether there is a relationship among TNF, cytochrome c and apoptosis. By the application of the antibody technique, the localization of cytochrome c can be traced after the application of TNF on sensitive cell line such as L929.

5.2 The Relationship Between Tumor Necrosis Factor and Mitochondrial DNA Damage

The mitochondrial respiratory system is the major intracellular source of the ROS. The mitochondrial DNA (mtDNA), while not protected by histones or DNA-binding proteins, is continually exposed to a high steady state level of ROS in the matrix of the mitochondria (Wei, 1998). The oxidative modification and mutation of mtDNA occur with great ease. The respiratory enzymes containing the defective mtDNA-encoded protein subunits exhibit impaired electron transport function and thereby increase the electron leak and ROS production, which in turn elevate the oxidative stress and oxidative damage to mitochondria. Therefore, the effect of TNF on mtDNA damage should be investigated, to see whether there is another mechanism on TNF-mediated ROS release from mitochondria.

5.3 Clinical studies with Tumor Necrosis Factor

The *in vivo* antitumor effects of TNF may be related to direct cytotoxicity, immunomodulatory effects or endothelial effects on tumor vasculature (Spriggs *et al.*, 1987). The clinical trials of rHuTNF are under way in Japan and the USA as early as 1992 (Taguchi *et al.*, 1992; Spriggs and Yates, 1992). rHuTNF is directly cytotoxic to some but not all human tumor cell lines (Old, 1985). This cytotoxicity is dose-dependent. Moreover,

TNF is much less toxic to normal cells, suggesting that this agent could have a high therapeutic index.

Since there is about 79 % homology between rHuTNF and rMuTNF, application of rMuTNF is possible for clinical studies. At first, the effect of rMuTNF on human cell line such as human breast carcinoma MCF-7 should be investigated. It was found that MCF-7 is sensitive to rHuTNF (Sugarman *et al.*, 1985) and therefore, rMuTNF is expected to give similar effect on MCF-7 (Kramer *et al.*, 1988).

On the other hand, the effect of rHuTNF on human cell lines can also be studied by similar methods that are mentioned in this study. The investigation of the release of Ca^{2+} and ROS should be examined. Combination studies have been initiated utilizing rHuTNF with γ-interferon, in an attempt to exploit the synergy seen in the pre-clinical tumor studies (Williamson *et al.*, 1983). Combination studies with established antitumor agents such as metabolic inhibitor (AMD), Ca^{2+}-inducing agent (thapsigargin or thimerosal) can also be expected.

References

References

Aderka, D., Engelmann, H., Moor, Y., Brakebush, C., and Wallach, D. (1992) Stabilization of the bioactivity of tumor necrosis factor by its soluble receptors. *J. Exp. Med.* **175**:323-329

Agarwal, S., Drysdale, B. and Shin, H. S. (1988) Tumor necrosis factor-mediated cytotoxicity involves ADP-ribosylation. *J. Immunol.* **140**:4187-4192

Aggarwal, B. B. (1992) Comparative analysis of the structure and function of TNF-α and TNF-β. In: *Tumor necrosis factors: structure, function, and mechanism of action*, (edited by Aggarwal, B. B. and Vilcek, J.) Marcel Dekker, Inc.:61-78

Aggarwal, B. B., and Eessalu, T. E. (1987) Effect of phorbol esters on down-regulation and redistribution of cell surface receptors for tumor necrosis factor-α. *J. Biol. Chem.* **262**:16450-16455

Aggarwal, B. B., Moffat, B., and Harkins, R. N. (1984) Human lymphotoxin. *J. Biol. Chem.* **259**:686-691

Aggarwal, B. B., Traquina, P. R., and Eessalu, T. E. (1986) Modulation of receptors and cytotoxic response of tumor necrosis factor-α by various lectins. *J. Biol. Chem.* **261**:13652-13656

Bachs, O., Agell, N., and Carafoli, E. (1994) Calmodulin and calmodulin-binding proteins in the nucleus. *Cell Calcium* **16:**289-296

Barry, M., A., and Eastman, A. (1992) Endonuclease activation during apoptosis: the role of cytosolic Ca^{2+} and pH. *Biochem. Biophys. Res. Comm.* **186**:782-789

Bauldry, S. A., McCall, C. E., Cousart, S. L., and Bass D. A. (1991) Tumor necrosis factor-α priming of phospholipase A_2 activation in human neutrophils: An alternative mechanism of priming. *J. Immuno.* **146**:1277-1285

Bellomo, G., Perotti, M., Taddei, F., Mirabelli, F., Finardi, G., Nicotera, P., and Orrenius, S. (1992) Tumor necrosis factor α induces apoptosis in mammary adenocarcinoma cells by an increase in intranuclear free Ca^{2+} concentration and DNA fragmentation. *Cancer Res.* **52**:1342-1346

Berridge, M. J. (1985) The molecular basis of communication within the cell. *Scientific American* **October:**124-134

Berridge, M. J. (1991) Cytoplasmic calcium oscillations: a two pool model. *Cell Calcium* **12**:63-72

Berridge, M. J. (1993) Inositol trisphosphate and calcium signalling. *Nature* **361**:315-325

Beutler, B. and Cerami, A. (1986) Cachectin and tumor necrosis factor as two sides of the same biological coin. *Nature* **320**:584-588

Beutler, B., and Cerami, A. (1989) The biology of cachectin/TNF-a primary mediator of the host response. *Ann. Rev. Immunol.* 7:625-655

Beutler, B., Mahoney, J., Le Trang, N., Pekala, P., and Cerami, A., (1985a) Purification of cachectin, a lipoprotein lipase suppressing hormone secreted by endotoxin induced RAW 264.7 cells. *J. Exp. Med.* **161**:984-995

Beutler, B., Milsark, I. W., Cerami, A. (1985b) Cachectin/tumor necrosis factor: production, distribution, and metabolic fate *in vivo*. *J. Immunol.* **135**:3972-3977

Beyaert, R., Heyninck, D., De Valck, D., Boeykens, F., Van Roy, F., and Fiers W. (1993) Enhancement of tumor necrosis factor cytotoxicity by lithium chloride is associated with increased inositol phosphate accumulation. *J. Immuno.* **151**:291-300

Bonavida, B. (1992) TNF as immunomodulatory agent. In: *Tumor necrosis factors: structure, function, and mechanism of action*, (edited by Aggarwal, B. B. and Vilcek, J.) Marcel Dekker, Inc.:315-329

Brakebusch, C., Nophar, Y., Kemper, O., Engelmann, H., and Wallach, D. (1992) Cytoplasmic truncation of the p55 tumor necrosis factor (TNF) receptor abolishes signalling, but not induced shedding of the receptor. *EMBO J.* **11**:943-950

Briehl, M. M., and Baker, A. F. (1996) Modulation of the antioxidant defence as a factor in apoptosis. *Cell Death and Differ.* **3**:63-70

Brouckaert, P. G. G., Leroux-Roels, G. G., Guisez, Y., Tavernier, J., and Fiers, W. (1986) *In vivo* anti-tumor activity of recombinant human and murine TNF, alone and in combination with murine IFN-gamma, on a syngeneic murine melanoma. *Int. J. Cancer* **38**:763-769

Brouckaert, P., Libert, C. Everaerdt, B., and Fiers, W. (1992) Selective species specificity of tumor necrosis factor for toxicity in the mouse. *Lymphokine Cytokine Res.* **11**:193-196

Carswell, E. A., Old, L. J., Kassel, R. L., Green, S., Fiore, N., and Williamson, B. (1975) An endotoxin-induced serum factor that causes necrosis of tumors. *Proc. Natl. Acad. Sci. USA* **72**:3666-3670

Cathcart, R., Schwiers, E., and Ames, B. N. (1983) Detection of picomole levels of hydroperoxides using a fluorescent dichlorofluorescein assay. *Ana. Biochem.* **134**:111-116

Chacon, E., and Acosta, D. (1991) Mitochondrial regulation of superoxide by Ca^{2+}: an alternate mechanism for the cardiotoxicity of doxorubicin. *Toxicol. App. Pharmacol.* **107**:117-128

Chen, C. S., Mrksich, M., Huang, S., Whitesides, G. M., and Ingber, D. E. (1998) Geometric control of cell life and death *Science* **276**:1425-1428

Chien, K. R., Pfau, R. G., and Farber, J. L. (1979) Ischemic myocardial injury: prevention by chlorpromazine of an accelerated phospholipid degradation and associated membrane dysfunction. *Am. J. Pathol.* **97**:505-530

Christensen, S. B., and Norup, E. (1985) Absolute configurations of the histamine liberating sesquiterpene lactones thapsigargin and trilobolide. *Tetrahedron Lett.* **26**:107-110

Coley, W. B. (1891) Contribution to the knowledge of Sarcoma. *Ann. Surg.* **14**:199-220

Cossarizza, A., Franceschi, C., Monti, D., Salvioli, S., Bellesia, E., Rivabene, R., Biondo, L., Rainaldi, G., Tinari, A., and Malorni, W. (1995) Protective effect of N-Acetylcysteine in tumor necrosis factor-α-induced apoptosis in U937 cells: the role of mitochondria. *Exp. Cell Res.* **220**:232-240

Davidson, A. M., and Halestrap, A. P. (1987) Liver mitochondrial pyrophosphate concentration is increased by Ca^{2+} and regulates the intramitochondrial volume and adenine nucleotide content. *Biochem. J.* **246**:715-723

Dawson, V. L., and Dawson, T. M. (1996) Free radicals and neuronal cell death. *Cell Death and Differ.* **3**:71-78

Denton, R. M. and McCormack, J. G. (1990) Ca^{2+} as a second messenger within mitochondria of the heart and other tissues. *Annu. Rev. Physiol.* **52**:451-466

Denton, R. M., McCormack, J. G., and Edgell, N. J. (1980) Role of calcium ions in the regulation of intramitochondrial metabolism: effects of Na^{+}, Mg^{2+} and ruthenium red on the Ca^{2+}-stimulated oxidation of oxoglutarate and on pyruvate dehydrogenase activity in intact rat heart mitochondria. *Biochem. J.* **190**:107-117

Ding, A. H., Sanchez, E., Srimal, S., and Nathan, C. F. (1989) Macrophage rapidly internalize their tumor necrosis factor receptors in response to bacterial lipopolysaccharide. *J. Biol. Chem.* **264**:3924-3929

Dressler, K. A., Mathias, S., and Kolesnick R. N. (1992) Tumor necrosis factor-α activates the sphingomyelin signal transduction pathway in a cell-free system. *Science* **255**:1715-1718

Dubois, M. F., Ferrieus, C., and Lebon, P. (1989) Synergistic cytotoxic effects of recombinant human necrosis factor, interferons, and heat stress. *Cancer Res.* **49**:5618-5622

Duchen, M., R., and Biscoe, T., J. (1992) Relative mitochondrial membrane potential and $[Ca^{2+}]_i$ in type I cells isolated from the rabbit carotid body. *J. Physiol.* **450**:33-61

Emaus, R., K., Grunwald, R., and Lemasters, J. J. (1986) Rhodamine 123 as a probe of transmembrane potential in isolated rat-liver mitochondria: spectral and metabolic properties. *Biochim Biophys Acta* **850**:436-448

Engelmann, H., Holtmann, H., Brakebusch, C., Avni, Y. S., Sarovt, I., Nophar, Y., Hadas, E., Leitner, O., and Wallach, D. (1990a) Antibodies to a soluble form of a tumor necrosis factor (TNF) receptor have TNF-like activity. *J. Biol. Chem.* **265**:14497-14504

Engelmann, H., Novick, D., and Wallach, D. (1990b) Two tumor necrosis factor binding proteins purified from human urine. *J. Biol. Chem.* **265**:1531-1536

Espevik, T., Brockhaus, M., Loetscher, H., Nonstad, U., and Shalaby, R. (1990) Characterization of binding and biological effects of monoclonal antibodies against a human tumor necrosis factor receptor. *J. Exp. Med.* **171**:415-426

Faulk, E. A., McCully, J. D., Tsukube, T., Hadlow, N. C., Krukenkamp, I. B., and Levitsky, S. (1995) Myocardial mitochondrial calcium accumulation modulates nuclear calcium accumulation and DNA fragmentation. *Ann. Thorac. Surg.* **60**:338-344

Fernandez-Checa, J. C., Kaplowitz, N., Garcia-Ruiz, C, Colell, A., Miranda, M., Mari, M., Ardite, E., and Morales, A. (1997) GSH transport in mitochondria: defense against TNF-induced oxidative stress and alcohol-induced defect. *Am. J. Physiol.* **273**:G7-G17

Flick, D. A., and Gifford, G. E. (1984) Comparison of *in vitro* cell cytotoxic assays for tumor necrosis factor. *J. Immunol. Methods* **68**:167-175

Fransen, L., Van der Heyden, J., Ruysschaert, R., and Fiers, W. (1986) Recombinant tumor necrosis factor: its effect and its synergism with interferon-gamma on a variety of normal and transformed human cell lines. *Eur. J. Cancer. Clin. Oncol.* **4**:419-424

Gamble, J. R., Harlan, J. M., Klebanoff, S. J., and Vadas, M. A. (1985) Stimulation of the adherence of neutrophils to umbilical vein endothelium by human recombinant tumor necrosis factor. *Proc. Natl. Acad. Sci. USA* **83**:8667-8671

Garcia-Ruiz, C., Colell, A., Mari, M., Morales, A., and Fernandez-Checa, J. C. (1997) Direct effect of ceramide on the mitochondrial electron transport chain leads to generation of reactive oxygen species: Role of mitochondrial glutathione. *J. Biol. Chem.* **272**:11369-11377

Gardner, A. M., Xu, F. H., Fady, C., Jacoby, F. J., Duffey, D. C., Tu, Y. and Lichtenstein, A. (1997a) Apoptotic vs. Nonapoptotic cytotoxicity induced by hydrogen peroxide. *Free Rad. Biol. Med.* **22**:73-83

Gardner, A., Xu, F. H., Fady, C., Sarafian, T., Tu, Y., and Lichtenstein, A. (1997b) Evidence against the hypothesis that Bcl-2 inhibits apoptosis through an anti-oxidant effect. *Cell Death and Differ.* **4**:487-496

Garrett, I. R., Durie, B. G. M., Nedwin, G. E., Gillespie, A., Bringman, T., Sabatini, M., Bertolini, D. R., and Mundy, G. R. (1987) Production of lymphotoxin, a bone-resorbing cytokine, by cultured human myeloma cells. *N. Engl. J. Med.*, **317**:526-532

Gearing, A. J. H., Beckett, P., Christodoulou, M., Churchill, M., Clements, J., Davidson, A. H., Drummond, A. H., Galloway, W. A., Gilbert, R., and Gordon, J. L. (1994) Processing of tumor necrosis factor-α precursor by metalloproteinases. *Nature* **370**:555-557

Goldman, R., Moshonov, S., and Zor, U. (1998) Generation of reactive oxygen species in a human keratinocyte cell line: role of calcium. *Arch. Biochem. Biophys.* **350**:10-18

Goppelt-Struebe, M., and Rehfeldt, W. (1992) Glucocorticoids inhibit TNFα-induced cytosolic phospholipase A_2 activity. *Biochim. Biophys. Acta* **1127**:163-167

Gorman, A, McGowan, A., and Cotter, T. G. (1997) Role of peroxide and superoxide anion during tumor cell apoptosis. *FEBS Lett.* **404**:27-33

Granger, G. A. and Williams, T. W. (1968) Lymphocyte cytotoxicity *in vitro*: activation and release of a cytotoxic factor. *Nature* **218**:1253-1254

Gratia, A. and Linz, R. (1931) Le Phenomene de Shwartzman dans le sarcoma du Cobaye. *C. R. Soc. Biol.(Paris)* **108**:427-428

Grooten, J., Goossens, V., Vanhaesebroeck, B., and Fiers, W. (1993) Cell membrane permeabilization and cellular collapse, followed by loss of dehydrogenase acitivity: early events in tumor necrosis factor-induced cytotoxicity. Cytokine 5:546-555

Gunter, T. E., and Pfeiffer, D. R. (1990) Mechainisms by which mitochondria transport calcium. *Am. J. Physiol.* **258**:C755-C786

Gustafson-Svard, C., Tagesson, C., Boll, R. M., and Kald, B. (1993) Tumor necrosis factor-α potentiates phosphlipase A_2-stimulated release and metabolism of arachidonic acid in cultured interstinal epithelial cells (INT 407). *Scand. J. Gastroenterol.* **28**:323-330

Haliday, E. M., Ramesha, S., and Ringold, G. (1991) TNF induces c-fos via a novel pathway requiring conversion of arachidonic acid to a lipoxygenase metabolite. *EMBO J.* **10**:109-115

Hartfield, P. J., Mayne, G. C., and Murray, A. W. (1997) Ceramide induces apoptosis in PC12 cells. *FEBS Lett.* **401**:148-152

Hasegawa, Y. and Bonavida, B. (1989) Calcium-independent pathway of tumor necrosis factor-mediated lysis of target cells. *J. Immunol.* **142**:2670-2676

Hawkins, H. K., Ericsson, J. L. E., Biberfeld, P., and Trump, B. F. (1972) Lysosome and phagosome stability in lethal cell injury: morphologic tracer studies in cell injury due to inhibition of energy metabolism, immune cytolysis and photosensitization. *Am. J. Pathol.* **68**:255-258

Hayakawa, M., Ishida, N., Takeuchi, K., Shibamoto, S., Hori, T., Oku, N., Ito, F., and Tsujimoto, M. (1993) Arachidonic acid-selective cytosolic phospholipase A_2 is crucial in the cytotoxic action of tumor necrosis factor. *J. Biol. Chem.* **268**:11290-11295

Hayakawa, M., Jayadev, S., Tsujimoto, M., Hannun, Y. A., and Ito, F. (1996) Role of ceramide in stimulation of the transcription of cytosolic phsopholipase A_2 and cyclooxygenase 2. *Biochem. Biophys. Res. Commun.* **220**:681-686

Hennager, D. J., Welsh, M. J., and DeLisle, S. (1995) Changes in either cytosolic or nucleoplasmic inositol 1,4,5-trisphosphate levels can control nuclear Ca^{2+} concentration. J. *Biol. Chem.* **270:**4959-4962.

Hockenbery, D., Nunez, G., Milliman, C., Schreiber, R. D., and Korsmeyer, S. J. (1990) Bcl-2 is an inner mitochondrial membrane protein that blocks programmed cell death. *Nature* **348**:334-336

Hohmann, H., Brockhaus, M., Baeuerlet, P. A., Remy, R., Kolbeck, R., and van Loon, A. P. G. M. (1990) Expression of the types A and B tumor necrosis factor (TNF) receptors is independently regulated, and both receptors mediated activation of the transcription factor NF-κB. *J. Biol. Chem.* **265**:22409-22417

Holtmann, H., and Wallach, D. (1987) Down regulation of the receptors for tumor necrosis factor by interleukin 1 and 4β-phorbol-12-myristate-13-acetate. *J. Immunol.* **139**:1161-1167

Hsu, H., Huang, J., Shu, H. B., Baichwal, V., and Goeddel, D. V. (1996a) TNF-dependent recruitment of the protein kinase RIP to the TNF receptor-1 signaling complex. *Immunity* **4**:387-396

Hsu, H., Shu, H. B., Pan, M. G., and Goeddel, D. V. (1996b) TRADD-TRAF2 and TRADD-FADD interactions define two distinct TNF receptor 1 signal transcription pathways. *Cell* **84**:299-308

Hsu, H., Xiong, J., and Goeddel, D. V. (1995) The TNF receptor 1-associated protein TRADD signals cell death and NF-κB activation. *Cell* **81**:495-504

Jacobson, M. D., Weil, M. and Raff, M. C. (1997) Programmed cell death in animal development. *Cell* **88**:347-354

Jarvis, W. D., Kolesnick, R. N., Fornari, F. A., Traylor, R. S., Gewirtz, D. A., and Grant, S. (1994) Induction of apoptotic DNA damage and cell death by activation of the sphingomyelin pathway. *Proc. Natl. Acad. Sci. USA* **91**:73-77

Jindal, H. K., Chaney, W. G., Anderson, C. W., Davis, R. G., and Vishwanatha, J. K. (1991) The protein-tyrosine kinase substrate, calpactin I heavy chain (p36), is part of the primer recognition protein complex that interacts with DNA polymerase α. *J. Biol. Chem.* **266:**5169-5176

Johnson, L., V., Walsh, M., L., and Chen, L., B. (1980) Localization of mitochondria in living cells with rhodamine 123. *Proc. Natl. Acad. Sci. USA* **77**:990-994

Jones, D. P., McConkey, D. J., Nicotera, P., and Orrenius S. (1989) Calcium-activated DNA fragmentation in rat liver nuclei. *J. Biol. Chem.* **264:**6398-6403

Kerr, J. F. R., Gobe, G. C., Winterford, C. M., and Harmon, B. V. (1995) Anatomical methods in cell death. In: *Methods in cell biology* (edited by) Academic press, Inc. **vol. 46**:1-27

Kerr, J. F. R., Wyllie, A. H., and Currie, A. R. (1972) Apoptosis: a basic biological phenomenon with wide-ranging implications in tissue kinetics. *Br. J. Cancer* **26**:239-257

Kim, M. Y., Linardic, C., Obeid, L., and Hannun, Y. (1991) Identification of sphingomyelin turnover as an effector mechanism for the action of tumor necrosis factor α and κ-interferon. *J. Biol. Chem.* **266**:484-489

Kitahara-Tanabe, N., Tanabe, Y., Morioka, A., Mizuno, D., and Soma G. I. (1991) Post-translational processing of tumor necrosis factor production. *Chem. Pharm. Bull.* **39**:417-420

Kluck, R. M., Bossy-Wetzel, E., Green, D. R., and Newmeyer, D. D. (1997) The release of cytochrome c from mitochondria: a primary site for Bcl-2 regulation of apoptosis. *Science* **275**:1132-1136

Kohno, T., Brewer, M. T., Baker, S. L., Schwartz, P. E., King, M. W., Hale, K. K., Squires, C. H., and Vannice, J. L. (1990) A second tumor necrosis factor gene product can shed a naturally occurring tumor necrosis factor inhibitor. *Proc. Natl. Acad. Sci. USA* **87**:8331-8335

Kolesnick, R. N. (1987) 1,2-Diacylglycerols but not phorbol ester stimulate sphingomyelin hydrolysis in GH3 pituitary cells. *J. Biol. Chem.* **262**:16759-16762

Kolesnick, R., and Golde, D. W. (1994) The sphingomyelin pathway in tumor necrosis factor and interleukin-1 signaling. *Cell* **77**:325-328

Koller, H., Thiem, K., and Siebler, M. (1996) Tumor necrosis factor-α increases intracellular Ca^{2+} and induces a depolarization in cultured astroglial cells. *Brain* **119**:2021-2027

Kong, S. K., Fung, K. P., Choy, Y. M., and Lee, C. Y. (1997) Slow increase in intranuclear and cytoxolic free calcium concentrations in L929 cells is important in tumor necrosis factor-alpha-mediated cell death. *Oncology* **54**:55-62

Kong, S. K., Suen, Y. K., Chan, Y. M., Chan, C. W., Choy, Y. M., Fung, K. P., and Lee, C. Y. (1996) Concanavalin A-induced apoptosis in murine macrophages through a Ca^{2+}-independent pathway. *Cell Death Differ.* **3**:307-314

Kramer, S. M., Aggarwal, B. B., Eessalu, T. E., McCabe, S. M., Ferraiolo, B. L., Figari, I. S., and Palladino, M. A. (1988) Characterization of the *in vitro* and *in vivo* species preference of human and murine tumor necrosis factoer-α *Cancer Res.* **48**:920-925

Kriegler, M., Perez, C., DeFray, K., Albert, I., and Lu. S. D. (1988) A novel form of TNF/cachectin is a cell surface cytotoxic transmembrane protein: Ramifications for the complex physiology of TNF. *Cell* **53**:45-53

Kruppa, G., Thoma, B., Machleidt, T., Wiegmann, K., and Kronke, M. (1992) Inhibition of tumor necrosis factor (TNF)-mediated NF-κB activation by selective blockade of the human 55-kDa TNF receptor. *J. Immunol.* **148**:3152-3157

Kull, F. C. (1988) Reduction in tumor necrosis factor receptor affinity and cytotoxicity by glucocorticoids. *Biochem. Biophys. Res. Commun.* **153**:402-409

Kwan, L. (1995) Murine L929 cell and its tumor necrosis factor (TNF)-resistant variants: biochemical characterization with respect to mechanism of TNF action. *In: M. Phil. Thesis* The Chinese University of Hong Kong

Laster, S. M., Wood, J. G., and Gooding, L. R. (1988) Tumor necrosis factor can induce both apoptic and necrotic forms of cell lysis. *J. Immunol.* **141**:2629-2634

Lewit-Bentley, A., Fourme, R., Kahn, R., Prange, T., Vachette, P., Tavernier, J., Hauquier, G., and Fiers, W. (1988) Structure of tumor necrosis factor by x-ray solution scattering and preliminary studies by single crystal x-ray diffraction. *J. Mol. Biol.* **199**:389-392

Lichtman, J. W. (1994) Confocal microscopy. *Scientific American* **August** 30-35

Liu, Z. G., Hsu, H., Goeddel, D., and Karin, M (1996b) Dissection of TNF receptor 1 effector functions: JNK activation is not linked to apoptosis while NF-κB activation prevents cell death. *Cell* **87**:565-576

Liu, X., Kim, C. N., Yang, J., Jemmerson, R., and Wang, X. (1996a) Induction of apoptotic program in cell-free extracts: requirement for dATP and cytochrome c. *Cell* **86**:147-157

Lin, J. X., and Vilcek, J. (1987) TNF and IL 1 causes a rapid and transient stimulation of c-fos and c-myc mRNA levels in human fibroblasts. *J. Biol. Chem.* **262**:11908-11911

Loetscher, H., Pan, Y. C. E., Lahm, H. W., Gentz, R., Brockhaus, M., Tabuchi, H., and Lesslauer, W. (1990) Molecular cloning and expression of the human 55 kDa TNF receptor. *Cell* **61**:351-359

Lui, P. P. Y., Lee, M. M. F., Ko, S., Lee, C. Y., and Kong, S. K. (1997) Practical considerations in acquiring biological signals from confocal microscope: II. Laser-induced rise of fluorescence and effect of agonist droplet application. *Biol. Signals* **6**:45-51

Lytton, J., Westlin, M., and Hanley, M. R. (1991) Thapsigargin inhibits the sarcoplasmic or endoplasmic reticulum Ca-ATPase family of calcium pumps. *J. Biol. Chem.* **266**:17067-17071

Malis, C. D., and Bonventre, J. V. (1986) Mechanism of calcium potentiation of oxygen free radical injury to renal mitochondria: a model for post-ischemic and toxic mitochondrial damage. *J. Biol. Chem.* **261**:14201-14208

Malviya, A. N. (1994) The nuclear inositol 1,4,5-trisphosphate and inositol 1,3,4,5-tetrakisphosphate receptors. *Cell Calcium* **16:**301-313

Mathias, S., Dressler, K. A., and Kolesnick, R. N. (1991) Characterization of a ceramide-activated protein kinase: stimulation by tumor necrosis factor α. *Proc. Natl. Acad. Sci. USA* **88**:10009-10013

McCormack, J. G., and Denton, R. M. (1980) Role of calcium ions in the regulation of intramitochondrial metabolism: properties of the Ca^{2+}-sensitive dehydrogenases within intact uncoupled mitochondria from the white and brown adipose tissue of the rat. *Biochem. J.* **190**:95-105

Merritt, J. E., McCarthy, S. A., Davies, M. P. A., and Moores, K. E. (1990) Use of fluo-3 to measure cytosolic Ca^{2+} in platelets and neutrophils: loading cells with the dye, calibration of traces, measurements in the presence of plasma, and buffering of cytosolic Ca^{2+}. *Biochem. J.* **269**:513-519

Michelangeli, F., Mezna, M., Tovey, S., and Sayers, L. G. (1995) Pharmacological modulators of the inositol 1,4,5-trisphosphate receptor. *Neuropharmacology* **34**:1111-1122

Mitchell, J. B., DeGraff, W., Kaufmann, D., Drishna, M. C., Samuni, A., Finkelstein, E., Ahn, M. S., Hahn, S. M., Gamson, J., and Russo, A. (1991) Inhibition of oxygen dependent radiation-induced damage by the nitroxide superoxide dismutase mimic, tempol. *Arch. Biochem. Biophys.* **289**:62-70

Mitchell, J. B., Samuni, A., Krishna, M. C., DeGraff, W. G., Ahn, M. S., Samuni, U., and Russo, A. (1990) Biologically active metal-independent superoxide dismutase mimics. *Biochemistry* **29**:2802-2807

Miyata, H., Silverman, H. S., Sollott, S. J., Lakatta, E. G., Stern, M. D., and Hansford, R. G. (1991) Measurement of mitochondrial free Ca^{2+} concentration in living single rat cardiac myocytes. *Am. J. Physiol.* **261**:H1123-H1134

Moreno-Sanchez, R. (1985) Regulation of oxidative phosphorylation in mitochondria by external free Ca^{2+} concentrations. *J. Biol. Chem.* **260**:4028-4034

Morgan, J. L., and Curran, T. (1986) Role of ion flux in the control of c-fos expression. *Nature* **322:**552-555

Mosmann, T. (1983) Rapid colorimetric assay for cellular growth and survival: application to proliferation and cytotoxicity assays. *J. Immunol. Methods* **65**:55-63

Murakami, K., and Routtenberg, A. (1985) Direct activation of purified protein kinase C by unsaturated fatty acids (oleate and arachidonate) in the absence of phospholipids and Ca^{2+}. *FEBS Lett.* **192**:189-193

Nagata, S. (1997) Apoptosis by death factor. *Cell* **88**:355-365

Naume, B., Shalaby, R., Lesslauer, W., and Espevik, T. (1991) Involvement of the 55- and 75-kDa tumor necrosis factor receptors in the generation of lymphokine-activted killer cell activity and proliferation of natural killer cells. *J. Immunol.* **146**:3045-3048

Neale, M. l., Fiera, R. A., and Matthews, N. (1988) Involvement of phospholipase A_2 activation in tumor cell killing by tumor necrosis factor. *Immunology* **64**:81-85

Nicotera, P., Hartzell, P., Davis, G., and Orrenius, S. (1986) The formation of plasma membrane blebs in hepatocytes expose to agents that increase cytosolic Ca^{2+} is mediated by the activation of a non-lysosomal proteolytic system. *FEBS Lett.* **209**:139-144

Nicotera, P., and Leist, M. (1997) Energy supply and the shape of death in neurons and lymphoid cells. *Cell Death and Differ.* **4**:435-442

Nicotera, P., Zhivotovsky, B., and Orrenius, S. (1994) Nuclear calcium transport and the role of calcium in apoptosis. *Cell Calcium* **16:**279-288

Nophar, Y., Kemper, O., Brakebusch, C., Engelmann, H., Zwang, R., Aderka, D., Holtmann, H., and Wallach, D. (1990) Soluble forms of tumor necrosis factor receptors (TNF-Rs). The cDNA for type I TNF-R, cloned using amino acid sequence data of its soluble form, encodes both the cell surface and a soluble form of the receptor. *EMBO J.* **9**:3269-3278

Obeid, L. M., Linardic, C. M., Karolak, L. A., and Hannun, Y. A. (1993) Programmed cell death induced by ceramide. *Science* **259**:1769-1771

O'Donnell, V. B., Spycher, S., and Azzi, A. (1995) Involvement of oxidants and oxidant-generating enzyme(s) in tumor-necrosis-factor-α-mediated apoptosis: role for lipoxygenase pathway but not mitochondrial respiratory chain. Biochem. J. 310:133-141

Old, L. J. (1985) Tumor necrosis factor. *Science* **230**:630-632

Ormerod, M. G. (1994) *Flow Cytometry*. BIOS Scientific Publishers Limited.

Orrenius, S., McConkey, D. J., Bellomo, G., and Nicotera, P. (1989) Role of Ca^{2+} in toxic cell killing. *TiPS* **10**:281-285

Ostrove, J. M., and Gifford, G. E. (1979) Stimulation of RNA synthesis in L929 cells by rabbit tumor necrosis factor. *Proc. Soc. Exp. Biol. Med.* **160**:354-358

Owen-Schaub, L. B., Crump, W. L., Morin, G. I., and Grimm, E. A. (1989) Regulation of lymphocyte TNF receptors by IL 2. *J. Immunol.* **143**:2236-2241

Pagliacci, M. C., Spinozzi, F., Migliorati, G., Fumi, G., Smacchia, M., Grignani, F., Riccardi, C., and Nicoletti, I. (1993) Genistein inhibits tumor cell growth *in vitro* but enhances mitochondrial reduction of tetrazolium salts: a further pitfall in the use of the MTT assay for evaluating cell growth and survival. *Eur. J. Cancer* **29A**:1573-1577

Pahl, H. L., and Baeuerle, P. A. (1996) Activation of NF-κB by ER stress requires both Ca^{2+} and reactive oxygen intermediates as messengers. *FEBS Lett.* **392**:129-136

Palladino, M. A., Patton, J. S., Figari, I. S., and Shalaby M. R. (1987) Possible relationships between *in vivo* antitumor activity and toxicity of tumor necrosis factor-α.. In: *Tumor necrosis factor and related cytotoxins,* Wiley, Chichester **Ciba Foundation Symposium 131**:21-30

Park, H. J., Makepeace, C. M., Lyons, J. C. and Song, C. W. (1996) Effect of intracellular acidity and ionomycin on apoptosis in HL-60 cells. *Eur. J. Cancer* **32A**:540-546

Park, Y. M., Han, M. Y., Blackburn, R. V., and Lee Y. J. (1998) Overexpression of HSP25 reduces the level of TNFα-induced oxidative DNA damage biomarker, 8-hydroxy-2'-deoxyguanosine, in L929 cells. *J Cell. Physiol.* **174**:27-34

Pastorino, J. G., Simbula, G., Yamamoto, K., Glascott, P. A., Rothman, R. J., and Farber, J. L. (1996) The cytotoxicity of tumor necrosis factor depends on inducation of the mitochondrial permeability transition. *J. Biol. Chem.* **271**:29792-29798

Pennica, D., Hayflick, J. S., Bringman, T., Palladino, M., and Goeddel, D. V. (1985) Cloning and expression in *Escherichia coli* of the cDNA for murine tumor necrosis factor. *Proc. Natl. Acad. Sci. USA* **82**:6060-6064

Pennica, D., Nedwin, G. E., Hayflick, J. S., Seeburg, P. H., Derynck, R., Palladino, M. A., Kohr, W. J., Aggarwal, B. B., and Goeddel, D. V. (1984) Human tumor necrosis factor: precursor structure, cDNA cloning, expression, and homology to lymphotoxin. *Nature* **312**:724-729

Pennica, D., Shalaby, M. R. and Palladino, M. A. (1987) Tumor necrosis factors alpha and beta. In: *Recombinant lymphokines and their receptors*, (edited by Gillis, S.) Marcel Dekker, Inc.:301-317

Playfair, J. H. L., and Taverne, J. (1987) Antiparasitic effects of tumor necrosis factor in vivo and in vitro. In: *Tumor necrosis factor and related cytotoxins,* Wiley, Chichester **Ciba Foundation Symposium 131**:192-198

Polla, B. S., Jacquier-Sarlin, M. R., Kantengwa, S., Mariethoz, E., Hennet, T., Fusso-Marie, F., and Cossarizza, A. (1996) TNFα alters mitochondrial membrane potential in L929 but not in TNFα-resistant L929.12 cells: relationship with the expression of stress proteins, annexin 1 and superoxide dismutase activity. *Free Rad. Res.* **25**:125-131

Quintern, L. E., Weitz, G., Nehrkorn, H., Tager, J. M., Schramm, A. W., and Sandhoff, K. (1987) Acid sphingomyelinase from human urine: purification and characterization. *Biochim. Biophys. Acta* **992**:323-336

Radi, R., Beckman, J. S., Bush, K. M., and Freeman, B. A. (1991) Peroxynitrite induced membrane lipid peroxidation: the cytotoxic potential of superoxide and nitric oxide. *Arch. Biochem. Biophys.* **288**:481-487

Ranges, G. E., Zlotnik, A., Espevik, T., Dinarello, C. A., Cerami, A., and Palladino, M. A., (1988) Tumor necrosis factor alpha/cachectin is a growth factor for thymocytes: synergistic interactions with other cytokines. *J. Exp. Med.* **167**:1472-1478

Reddan, J. R., Sevilla, M. D., Giblin, F. J., Padgaonkar, V., Dziedzic, D. C., Leverenz, V., Misra, I. C., and Peters, J. L. (1993) The superoxide dismutase mimic TEMPOL protects cultured rabbit lens epithelial cells from hydrogen peroxide insult. *Exp. Eye Res.* **56**:543-554

Reed, J. (1994) Bcl-2 and the regulation of programmed cell death. *J. Cell. Biol.* **124**:1-6

Richter, C. (1993) Pro-oxidants and mitochondrial Ca^{2+}: their relationship to apoptosis and oncogenesis. *FEBS Lett.* **325**:104-107

Rizzuto, R., Bernardi, P., Favaron, M., and Azzone, G. F. (1987) Pathways for Ca^{2+} efflux in heart and liver mitochondria. *Biochem. J.* **246**:271-277

Robaye, B., and Dumont J. E. (1992) Phospholipase A_2 activity is not involved in the tumor necrosis factor-triggered apoptotic DNA fragmentation in bovine aortic endothelial cells. *Biochem. Biophys. Res. Commun.* **188**:1312-1317

Ruddle, N. H., Li, C. B., Tang, W. L., Gray, P. W., and McGrath, K. M. (1987) Lymphotoxin: cloning, regulation and mechanism of killing. In: *Tumor necrosis factor and related cytotoxins,* Wiley, Chichester **Ciba Foundation Symposium 131**:64-79

Ruddle, N. H. and Waksman, B. H. (1967) Cytotoxic effect of lymphocyte-antigen interaction in delayed hypersensitivity. *Science* **157**: 1060-1062

Sanchez-Alcazar, J. A., Hernandez, I., De la Torre, M. P., Garcia, I., Santiago, E., Munoz-Yague, M. T., and Solis-Herruzo, J. A. (1995) Down-regulation of tumor necrosis factor receptors by blockade of mitochondrial respiration. *J. Biol. Chem.* **270**:23944-23950

Schall, T. J., Lewis, M., Koller, K. J., Lee, A., Rice, G. C., Wong, G. H. W., Gatanaga, T., Granger, G. A., Lentz, R., Raab, H., Kohr, W. J., and Goeddel, D. V. (1990). Molecular cloning and expression of a receptor for human tumor necrosis factor. *Cell* **61**:361-370

Scheurich, P., Kobrich, G., and Pfizenmaier, K. (1989) Antagonistic control of tumor necrosis factor receptors by protein kinases A and C: enhancement of TNF receptor synthesis by protein kinase A and transmodulation of receptors by protein kinase C. *J. Exp. Med.* **170**:947-958

Schild, D. (1996) Laser scanning microscopy and calcium imaging. *Cell Calcium* **19**:281-296

Schulze-Osthoff, K., Bakker, A. C., Vanhaesebroeck, B., Beyaert, R, Jacob, W. A., and Fiers, W. (1992) Cytotoxic activity of tumor necrosis factor is mediated by early damage of mitochondrial functions. *J. Biol. Chem.* **267**:5317-5353

Schumann, M. A., Gardner, P., and Raffin, T. A. (1993) Recombinant human tumor necrosis factor α induces calcium oscillation and calcium-activated chloride current in human neutrophils: the role of calcium/calmodulin-dependent protein kinase. *J. Biol. Chem.* **268**:2134-2140

Schutze, S., Berkovic, D., Tomsing, O., Unger, C., and Kronke, M. (1992a) Tumor necrosis factor induces rapid production of 1'2'diacylglycerol by a phosphatidylcholine-specific phospholipase C. *J. Exp. Med.* **174**:975-988

Schutze, S., Nottrott, S., Pfizenmaier, K., and Kronke, M. (1990) Tumor necrosis factor signal transduction: cell-type-specific activation and translocation of protein kinase C. *J. Immunol.* **144**:2604-2608

Schutze, S., Potthoff, K., Machleidt, T., Berkovic, D., and Wiegmann, K. (1992b) TNF activates NF-κB by phosphatidylcholine-specific phospholipase C-induced "acidic" sphingomyelin breakdown. *Cell* **71**:765-776

Shalaby, M. R., Sundan, A., Loetscher, H., Brockhaus, M. Lesslauer, W., and Espevik, T. (1990) Binding and regulation of cellular functions by monoclonal antibodies against human tumor necrosis factor receptors. *J. Exp. Med.* **172**:1517-1520

Shear, M. J., Turner, F. C., Perrault, A., and Shovelton, T. (1943) Chemical treatment of tumors. V. Isolation of the hemorrhage-producing fraction from *Serratia marcescens* (*Bacillus prodigiosus*) culture filtrates. *J. Natl. Cancer Inst.* **4**:81-97

Sherwood, S. W., and Schimke, R. T. (1995) Cell cycle analysis of apoptosis using flow cytometry. In: *Methods in cell biology* (edited by) Academic press, Inc. **vol. 46**:77-97

Shidoji, Y., Nakamura, N., Moriwake, H., and Muto, Y. (1997) Rapid loss in the mitochondrial membrane potential during geranylgeranoic acid-induced apoptosis. *Biochem. Biophys. Res. Commun.* **230**:58-96

Silk, S. T., Clejan, S., and Witkom, K. (1989) Evidence of TNF-binding protein regulation of phospholipase A_2 activity in isolated human platelet membranes. *J. Biol. Chem.* **264**:21466-21469

Skulachev, V. P. (1998) Cytochrome c in the apoptotic and antioxidant cascades. *FEBS Lett.* **423**:275-280

Smith, C. A., Davis, T., Anderson, D., Solam, L., Beckmann, M. P., Jerzy, R., Dower, S. K., Cosman, D., and Goodwin, R. G. (1990a) A receptor for tumor necrosis factor defines an unusual family of cellular and viral proteins. *Science* **248**:1019-1023

Smith, M. R., Munger, W. E., Kung, H. F., Takacs, L., and Durum, S. K. (1990b) Direct evidence for an intracellular role for tumor necrosis factor-α: microinjection of tumor necrosis factor kills target cells. *J. Immunol.* **144**:162-169

Smith, R. A., and Baglioni, C. (1987) The active form of tumor necrosis factor is a trimer. *J. Biol. Chem.* **262**:6951-6954

Somlyo, A. P., Bond, M., and Somlyo, A. V. (1985) Calcium content of mitochondria and endoplasmic reticulum in liver frozen rapidly *in vivo*. *Nature* **314**:622-625

Spriggs, D. R., Sherman, M. L., Frei III, E., and Kufe, D. W. (1987) Clinical studies with tumor necrosis factor. In: *Tumor necrosis factor and related cytotoxins,* Wiley, Chichester **Ciba Foundation Symposium 131**:206-227

Spriggs, D. R., and Yates, S. W. (1992) Clinical studies of tumor necrosis factor in the USA. In: *Tumor necrosis factor: structure-function relationship and clinical application*, (edited by Osawa, T., and Bonavida, B.) Karger:275-284

Suffys, P., Beyaert, R., Van Roy, F., and Fiers, W. (1987) Reduced tumor necrosis factor-induced cytotoxicity by inhibitors of the arachidonic acid metabolism. *Biochem. Biophys. Res. Commun.* **149**:735-743

Sugarman, B. J., Aggarwal, B. B., Hass, P. E., Figari, I. S., Palladino, M. A., and Shepard, H. M. (1985) Recombinant human tumor necrosis factor α: effects on proliferation of normal and transformed cells *in vitro*. *Science* **230**:943-945

Taguchi, T., Ikeda, S., and Ishihara, K. (1992) Recent clinical studies of recombinant human tumor necrosis factor in Japan. In: *Tumor necrosis factor: structure-function relationship and clinical application*, (edited by Osawa, T., and Bonavida, B.) Karger:269-274

Tartaglia, L. A., Ayres, T. M., Wong, G. H. W., and Goeddel, D. V. (1993) A novel domain within the 55 kd TNF receptor signals cell death. *Cell* **74**:845-853

Tartaglia, L. A., and Goeddel, D. V. (1992) Two TNF receptors. *Immunol. Today* **13**:151-153

Tartaglia, L. A., Weber, R. F., Figari, I. S., Reynolds, C., Palladino, M. A., and Goeddel, D. V. (1991) The two different receptors for tumor necrosis factor mediate distinct cellular responses. *Proc. Natl. Acad. Sci. USA* **88**:9292-9296

Thastrup, O., Cullen, P. J., Drobak, B., Hanley, M. R., and Dawson, A. P. (1990) Thapsigargin, a tumor promoter, discharges intracellular Ca^{2+} stores by specific inhibition of the endoplasmic reticulum Ca^{2+}-ATPase. *Proc. Natl. Acad. Sci. USA* **87**:2466-2470

Thoma, B., Grell, M., Pfizenmaier, K., and Scheurich, P. (1990) Identification of a 60-kD tumor necrosis factor (TNF) receptor as the major signal transducing component in TNF responses. *J. Exp. Med.* **172**:1019-1023

Torti, F. M., Dreckmann, B., Beutler, B., Cerami, A., and Ringold, G. M. (1985) A macrophage factor inhibits adipocyte gene expression: an *in vitro* model of cachexia. *Science* **229**:867-869

Trinchieri, G. (1992) Effects of TNF and lymphotoxin on the hematopoietic system. In: *Tumor necrosis factors: structure, function, and mechanism of action*, (edited by Aggarwal, B. B. and Vilcek, J.) Marcel Dekker, Inc.:289-313

Tsujimoto, M., Oku, N. (1992) Regulation of TNF receptors. In: *Tumor necrosis factors: structure, function, and mechanism of action*, (edited by Aggarwal, B. B. and Vilcek, J.) Marcel Dekker, Inc.:149-160

Tsujimoto, M., and Vilcek, J. (1987) Tumor necrosis factor-induced down-regulation of its receptors in HeLa cells. *J. Biochem.* **102**:1571-1577

Tsujimoto, M., Yip, Y. K., and Vilcek, J. (1985) Tumor necrosis factor: Specific binding and internalization in sensitive and resistant cells. *Proc. Natl. Acad. Sci. USA* **82**:7626-7630

Tsujimoto, M., Yip, Y. K., and Vilcek, J. (1986a) Interferon-γ enhances expression of cellular receptors for tumor necrosis factor. *J. Immunol.* **136**:2441-2444

Tsujimoto, M., Yokota, S., Vilcek, J. and Weissmann, Gerald (1986b) Tumor necrosis factor provokes superoxide anion generation from neutrophils. *Biochem. Biophys. Res. Commun.* **137**:1094-1100

Tsujimoto, Y. (1997) Apoptosis and necrosis: intracellular ATP level as a determinant for cell death modes. *Cell Death and Differ.* **4**:429-434

Utsugi, T., Mattern, M. R., Mirabelli, C. K., and Hanna, N. (1990) Potentiation of topoisomerase inhibitor-induced DNA strand breakage and cytotoxicity by tumor necrosis factor: enhancement of topoisomerase activity as a mechanism of potentiation. *Cancer Res.* **50**:2636-2640

Van Lint., J., Agostinis, P., Vandevoorde, V., Haegeman, G., Fiers, W., Merlevede, W, and Vandenheede, J. R. (1992) Tumor necrosis factor stimulates multiple sering/threonine protein kinases in Swiss 3T3 and L929 cells: implication of casein kinase-2 and extracellular signal-regulated kinases in the tumor necrosis factor signal transduction pathway. *J. Biol. Chem.* **267**:25196-25921

Vercammen, D., Vandenabeele, P., Beyaert, R., Declercq, W., and Fiers, W. (1997) Tumor necrosis factor-induced necrosis versus anti-Fas-induced apoptosis in L929 cells. Cytokine 9:801-808

Vercesi, A. E. (1993) Ca^{2+} transport and oxidative damage of mitochondria. *Brazilian J. Med. Biol. Res.* **26**:441-457

Vercesi, A. E., Moreno, S. N. J., Bernardes, C. F., Meinicke, A. R., Fernandes, E. C., and Docampo, R. (1996) Thapsigargin causes Ca^{2+} release and collapse of the membrane potential of *Trypanosoma brucei* mitochondria *in situ* and of isolated rat liver mitochondria. *J. Biol. Chem.* **268**:8564-8568

Waterman, W. H., and Sha'afi, R. I. (1995) A mitogen-activated protein kinase independent pathway involved in the phosphorylation and activation of cytosolic phospholipase A_2 in human neutrophils stimulated with tumor necrosis factor-α. *Biochem. Biophys. Res. Commun.* **209**:271-278

Wei, Y. H. (1998) Oxidative stress and mitochondrial DNA mutations in human aging. *Proc. Soc. Exp. Biol. Med.* **217**:53-63

Weilckens, K., Schmidt, A., Georg, E., Bredehorst, R., and Hilz, H. (1982) DNA fragmentation and NAD depletion: their relation to the turnover of endogenous mono(ADP-ribosyl) and poly(ADP-ribose)polymerase. *Proc. Natl. Acad. Sci. USA* **83**:4908-4912

Williamson, B. D., Carswell, E. A., Rubin, B. Y., Prendergast, J. S., and Old, L. J. (1983) Human tumor necrosis factor produced by human B-cell lines: Synergistic cytotoxic interaction with human interferon. *Proc. Natl. Acad. Sci. USA* **80**:5397-5401

Wiseman, H., and Halliwell, B. (1996) Damage to DNA by reactive oxygen and nitrogen species: role in inflammatory disease and progression to cancer. *Biochem. J.* **313**:17-29

Wissing, D., Moruitzen, H., Egeblad, M., Poirier, G. G., and Jaattela, M. (1997) Involvement of caspase-dependent activation of cytoxolic phospholipase A_2 in tumor necrosis factor-induced apoptosis. *Proc. Natl. Acad. Sci. USA* **94**:5073-5077

Wong, G. H. W., and Goeddel, D. V. (1986) Tumor necrosis factors α and β inhibit virus replication and synergize with interferons. *Nature* **323**:819-822

Wong, G. H. W., and Goeddel, D. V. (1988) Induction of manganous superoxide dismutase by tumor necrosis factor: possible protective mechanism. *Science* **242**:941-944

Wu, T., Ikezono, T., Angus, C. W., and Shelhamer J. H. (1996) Tumor necrosis factor-α induces the 85-kDa cytosolic phospholipase A_2 gene expression in human bronchial epithelial cells. *Biochim. Biophys. Acta* **1310**: 175-184

Wyllie, A. H., Kerr, J. F. R. and Currie (1980) Cell death: the significance of apoptosis. *Int. Rev. Cytol.* **68**:251-306

Yang, J., Liu, X., Bhalla, K., Kim, C. N., Ibrado, A. M., Cai, J., Peng, T., Jones, D. P., and Wang, X. (1997) Prevention of apoptosis by Bcl-2: release of cytochrome c from mitochondria blocked. *Science* **275**:1129-1132

Zhang, Y., Lin, J. X., Yip, Y. K., and Vilcek, J. (1988) Enhancement of cAMP levels and of protein kinase activity by tumor necrosis factor and interleukin 1 in human fibroblasts: role in the induction of interleukin 6. *Proc. Natl. Acad. Sci. USA* **85**:6802-6805

Zimmerman, R. J., Chan A., and Leadon, S. A. (1989) Oxidative damage in murine tumor cells treated *in vitro* by recombinant human tumor necrosis factor. *Cancer Res.* **49**:1644-1648